Biophysical Analysis of Binding Interactions between Clathrin and its Adaptor Proteins

by

Mary Halebian

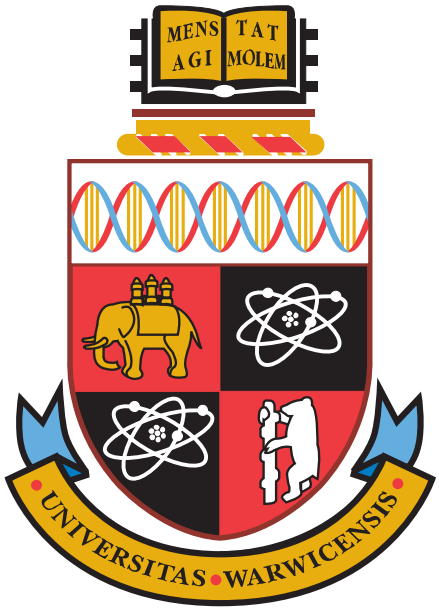

A thesis submitted to the University of Warwick for the degree of Doctor of Philosophy

Medical Research Council Doctoral Training Partnership

University of Warwick, Warwick Medical School

September 2017

I. Table of Content

I. List of Figures and Tables

i. Acknowledgements

I would like to give my biggest thanks to Corinne, my supervisor for her great support, advice and guidance throughout this journey. I would like to give my sincere thanks to Frances, who was very supportive of my work and gave very valuable suggestions at every meeting. I would like to thank the MRC and the MRC DTP program for giving me the opportunity to pursue this PhD project. I would also thank my review panel members; Steve Royle for the valuable discussions and suggestions and Richard Napier for his suggestions on SPR optimization as well as guidance and support for my project. I would like to give a massive thank you to Dr. Veselina Uzunova for her time training me on the SPR and the assistance in the optimization stages.

A very special thank you is to all the past and present Smith's group members who lived with me through this PhD, especially Michael who was always so helpful, supportive and the person to whom I could easily tell my concerns too. He truly has lived through my ups and downs during this 3-year PhD adventure and I whole heartily wish him the best of luck in his future. To Sarah, whom I only met in my final year of PhD, I consider a friend close to my heart who always gave me sound advice, helped and encouraged me during my final year and in my social life. I will miss our Diamond visits, and best of luck with cryo. Thank you to Kyle, who was very supportive and taught me microscopy and image processing during my first year and Joe who was my supervisor during my MSc mini project and made me love clathrin. I would like to thank past and present C10 members, I could not have asked for a better lab group and I would like to thank each and every one of you. I will really miss our lab outings – especially the Christmas meals.

I would like to thank all my close friends in Cyprus, always providing me with comforting words when I felt homesick. I would like to thank the friends I made during my PhD journey in UK, in particular Georgia who, as a co-

scientist, was always very understanding of my scientific challenges. To Hamdi, who has been a wonderful friend from day one when we started our MSc together – and massively supportive with reassurance. To Patrick and Raman, whom even though I met at the beginning of my last PhD year, have been wonderful lab colleagues during my hardest times. I would like to give special thanks to Patrick, for all those late nights doing lab experiments in the lab and all your comforting words when SPR did not work. And for all those weekends that you brought me coffee to keep me awake and do all my SPR experiments. I whole-heartedly wish him the best of luck for his PhD. Thank you to Christina, who has been the most caring and emotionally supportive friend during all my hectic time when I wrote my thesis. I also thank Alex who has been very supportive, patient and understanding, especially when I prioritised my work over my social life.

And finally, to my incredible parents, Rebecca and Garabet, and my godmother, Rita who even from distance have always been the most supportive and understanding, always providing me with constant encouragement in my life especially during my hardest times. I cherish the faith they had in me to follow my dreams, even if that meant that I would be many miles away from them for 7 years. Words cannot describe how thankful I am for their continued love. I would not be able to achieve my goals if it were not for their emotional and economical support.

Thank you

ii. Declaration

The work conducted and presented in this thesis is original and was conducted by the author (unless otherwise stated in the thesis) under the supervision of Dr. Corinne Smith and Prof. Frances Brodsky.

None of this work has been submitted previously for another degree at the University of Warwick or any other institution, apart from Chapter 7, Figure 7.6.2 and Figure 7.8.2, which have been previously submitted for the Doctor of Philosophy degree of Dr. Michael Baker (Baker Michael, 2016) for the University of Warwick, and the figures presented were with his permission. These figures have been included to support the data in this thesis and subsequent conclusions made and their relation to the original analysis made by the author.

Collaborative work has been conducted in this thesis, but only original work conducted by the author has been presented in this thesis from these collaborations. In summary, these collaborations are with:

Dr. Veselina Uzunova with assisting in the development and the optimization of the surface plasmon resonance in Chapter 5 and advice on the relevant work in Chapters 6 and 7.

This research was funded by the Medical Research Council (MRC) through the MRC doctoral training partnership in Interdisciplinary Biomedical Research.

All sources of information have been acknowledged by means of reference and any information, which has been included through personal discussions, has been noted in the relevant chapters.

iii. Summary

Clathrin-mediated endocytosis (CME) plays a central role in fundamental processes such as synaptic vesicle recycling, receptor recycling, signaling and development. CME begins with clathrin assembly on the plasma membrane, facilitated by adaptor proteins. This process forms an endocytic vesicle that allows transport of cargo into the cell, and is followed by clathrin disassembly through the action of different adaptor/accessory proteins. A large number of different adaptor and accessory proteins are recruited during CME, in a spatially and temporally ordered manner. Although our understanding is growing as to the roles of individual adaptor proteins, we still do not understand the way in which some adaptors interact with clathrin or the molecular details of their interactions with one another in the presence of clathrin. Clathrin adaptor proteins contain short, linear clathrin-binding motifs, which form the basis of their interaction with the four distinct sites on the clathrin N-terminal domain (TD). An adaptor protein with tighter binding or more numerous clathrin binding sequences could displace one with weaker or fewer binding elements. This raises the question of whether adaptor proteins compete for binding to clathrin or whether they can bind simultaneously.

Using certain biochemical and biophysical techniques *in vitro* and purified WT and mutant adaptor proteins, I have shown the complex 'multiple TD linking effect' of epsin 1 via the cooperative action of its two clathrin box motifs and unstructured region. Using the newly developed SPR/IAC (2-injection) method, I explored competition between five purified structurally and functionally diverse adaptor proteins when simultaneously binding to clathrin TD. I have shown how the complex structure of epsin 1 causes competition with β-arrestin 1 for clathrin TD binding. Such competition is observed between espin 1 and auxilin 1 as well, which reveals information about the mechanism of disassembly. However, β2-adaptin and auxilin 1 demonstrate no such competition.

iv. Abbreviations

ADP - Adenosine Diphosphate

AEBSF - 4-(2-Aminoethyl) benzenesulfonyl fluoride hydrochloride

ANTH - AP180 N-Terminal Homology domain

AP(1-5) - Adaptor Protein complex (1-5)

AP180 - Adaptor Protein 180

APS - Ammonium per sulphate

Arf6 - ADP-ribosylation factor 6

ATP - Adenosine Triphosphate

β2HA - β2 adaptin Hinge Appendage domain

BAR - Bin/Amphiphysin/Rvs domain

βME - Beta-2-Mercaptoethanol

BSA – Bovine Serum Albumin

CALM - Clathrin Assembly Lymphoid Myeloid leukemia protein

CBox - Clathrin box

CC - Coiled Coil domain

CCP - Clathrin Coated Pit

CCV - Clathrin Coated Vesicle

CD - Circular Dichroism

CHC - Clathrin Heavy Chain

CLASP - Cytoplasmic Linker Associated Protein

CLC - Clathrin Light Chain

CME - Clathrin Mediated Endocytosis

Cryo - cryogenic

DEPOL - Depolymerisation buffer

DLS - Dynamic Light Scattering

DMSO - Dimethyl Sulphoxide

DNA - Deoxyribonucleic Acid

DTT - Dithiothreitol

EDTA - ethylene-diamine-tetraacetic acid

EGFR - Endothelial Growth Factor Receptor

EGTA - ethylene-glycol-bis(β aminoethyl ether)-tetraacetic acid

ELISA - Enzyme Linked Immuno Sorbent Assay

EM - Electron Microscopy

ENTH - Epsin N-Terminal Homology domain

Eps15 - Epidermal growth factor receptor substrate 15

Fab - Functional antibody

FCHo - Fer/CIP4 Homology domain only

FPLC – Fast protein liquid chromatography

GAK - cyclin-G-Associated Kinase

GLUT4 – glucose transporter 4

GPCR - G-Protein Coupled Receptor

gp64 – glucoprotein precursor 64

GSH - Glutathione

GST - Glutathione S-Transferase

GTP - Guanosine Triphosphate

Hip1 - Huntingtin Interacting Protein 1

Hip1R - Huntingtin Interacting Protein 1 Related

HKM - Hepes, Potassium acetate, Magnesium Acetate buffer

Hsc70 - Heat Shock Cognate protein 70 kDa

IMAC- gravity immobilized metal affinity chromatography

IgG – Immunoglobulin G

IPTG - Isopropyl β-D-1-thiogalactopyranoside

ITC - Isothermal Titration Calorimetry

LB - Lysogeny broth

MOPS - 3-*N*-morpholinopropanesulfonic acid

MES - 2-(N-morpholino)ethanesulfonic acid

PBS - Phosphate Buffered Saline

PIP - Phosphatidylinositol Phosphate

POL - Polymerisation buffer

PTB - Phsophotyrosine Binding domain

PRD - Proline Rich Domain

SBD - Substrate Binding Domain

SCK – single cycle kinetics

SDS - Sodium Dodecyl Sulphate

SDS PAGE - Sodium Dodecyl Sulphate Poly Acrylamide Gel Electrophoresis

SNARE - Soluble NSF Attachment Protein Receptor

SOC – Super Optimal Broth

SP1-2 – signal protein 1-2

SPR - Surface Plasmon Resonance

TBS – Tris Buffered Saline

TD – clathrin N- Terminal Domain

TEA - Triethanolamine

TEMED - Tetramethylethylenediamine

TFB - Transformation Buffer

TIR – Total Internal Reflection

TGN - Trans-Golgi Network

THATCH – Talin-Hip1/R/Slap2 Actin Tethering C-terminal Homology domain

UIM - Ubiquitin Interacting Motif

VEGFR2 - Vascular Endothelial Growth Factor Receptor 2

WT- wild type

3D- three dimensional

Chapter 1: Introduction

1.0.0 Overview

In this chapter I introduce the topic of my PhD project, emphasizing the structures and functions of a variety of different proteins that are involved in the clathrin mediated endocytosis (CME) process, with a focus on the proteins used in this thesis. The aims and objectives of this thesis are stated in section 1.11.0.

1.1.0 Endocytosis

Endocytosis is a fundamental process involved in engulfing and selective packing of cell-surface proteins in cytoplasmic vesicles in order to be internalized into the cell to be targeted to the appropriate organelle. Any alterations into this fundamental process could lead to serious implications to variety of disease states such as for cancer cell development (Mellman and Yosef, 2013).

Endocytosis can be categorised into three major types: phagocytosis (cell cargo eating); pinocytosis (cell drinking of small fluids) and 'receptor mediated endocytosis' (Doherty and Mcmahon, 2009). Mechanisms of endocytosis have been classified into (I) caveolae-dependent (II) clathrin-independent and (III) clathrin-dependent (Doherty and Mcmahon, 2009; McMahon and Boucrot, 2011; Mayor *et al.,* 2014). The caveolae-dependent mechanism utilises caveolae, which are ~ 60 nm lipid and protein rafts that are released into the cell response to stimuli (Parton and Del Pozo, 2013; Kovtun *et al.,* 2015). Clathrin independent endocytosis (CIE) is involved in internalization of specific cargo without the use of clathrin. An example of this is the Arf6-associated pathway where histocompatibility complex class I proteins (MHCI), β-integrin, and the GPI-anchored protein CD59 are internalized (Karnik *et al.,* 2013; Mayor *et al.,* 2014). Clathrin-mediated endocytosis (CME) is one of the earliest endocytic pathways to be

discovered for receptor-mediated endocytosis with the aid of clathrin. It is the best studied and characterised up till now and is the main pathway focused in this thesis.

1.2.0 Clathrin mediated endocytosis

The assembly and disassembly of clathrin structure *in vitro* provides a model system in order to further understand how proteins can contribute mechanically in concert to perform CME. Brown and Goldstein were the first to demonstrate the uptate of the low-density lipoproteins (LDL) via CME, which was not observed in patients with Familiar Hypercholesterolemia (FH) (Goldstein *et al.,* 1985). Through the years, CME has shown to underpin important processes, such as nutrient uptake, synaptic vesicle recycling, viral and bacteria entry, signaling mechanisms and determination of cell polarity (Goldstein *et al.,* 1985; Pizarro-Cerda *et al.,* 2010; Young *et al.,* 2013).

The stages of CME begin with clathrin forming interactions with different adaptor/accessory proteins during its assembly for the construction of a coat around the newly developing endocytic vesicle. This coat engages with cargo on the cell surface and facilitates the inclusion of the cargo into the vesicle. Once the vesicle has budded from the plasma membrane, the clathrin coat disassembles using different adaptor/accessory proteins e.g. Hsc70/auxilin, allowing the endocytic machinery to be recycled, and the vesicle goes on to deliver cargo in the cell (McMahon & Boucrot, 2011; Young *et al.,* 2013) (Figure 1.2.0 (A)).

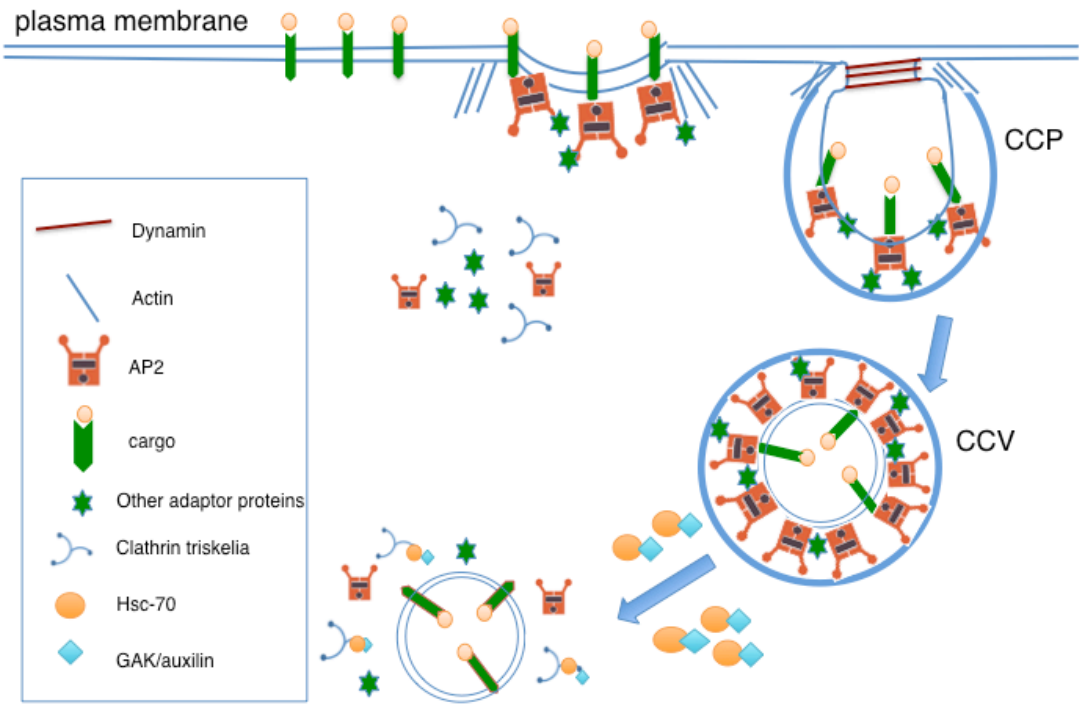

Figure 1.2.0: The general steps of clathrin mediated endocytosis (CME) with the addition of key adaptor and accessory proteins involved. *The endocytic cargo is detected by adaptor proteins such as AP2 or β-arrestin at the plasma membrane and recruitment of other adaptor proteins, e.g. epsin, causes curvature of plasma membrane. Further recruitment of other adaptor proteins along with cytoskeletal components e.g. actin, results in membrane invagination and the formation of a clathrin coated pit (CCP) after the clathrin assembly completition. The maturation of the CCP continues until scission begins with the activation of the GTPase dynamin causing the CCP to "pinch off" forming a clathrin coated vesicle (CCV). The clathrin coat is disassembled by the coordinated function of ATP hydrolysis by Hsc70 mediated by GAK (cyclin-G associated kinase)/auxilin. Once clathrin disassembly is complete, the vesicle is able to fuse with its target compartment in the cell. The endocytic components are then recycled ready for the next round of endocytosis.*

1.3.0 The stages of clathrin mediated endocytosis

1.3.1 Assembly: adaptor protein recruitment

A number of studies have monitored the activity and recruitment of adaptor proteins at the plasma membrane to promote coordinated clathrin assembly (Mettlen *et al.,* 2009; Saffarian *et al.,* 2009; Mettheyses *et al.,* 2011; Taylor *et al.,* 2011; Avinoam *et al.,* 2015). At least 25 adaptor proteins are recruited at specific times to the plasma membrane according to their role in clathrin assembly and nucleation process (Traub, 2011; Taylor *et al.,* 2011).

In certain situations, during low membrane curvature and depending on the cell type and cargo, FCHo proteins, which are BAR domains (Bin–Amphiphysin–Rvs) are initially recruited at the surface causing activation of the adaptor protein, AP2, which is the primary adaptor protein for clathrin assembly (Godlee and Kaksonen, 2013; Liu *et al.,* 2015; Hollopeter *et al.,* 2014). The AP2 complex interacts with the plasma membrane, clathrin, cargo and other adaptors to promote the initiation of the clathrin coat assembly. This is carried out with AP2 binding to cytoplasmic motifs on cargo (e.g. receptors bound to ligands- such as transferrin receptors) (Traub, 2009), enabling clathrin to assemble around the vesicle. This process progresses with the aid of multiple endocytic proteins, which have been previously identified to be recruited at the surface. Additionally, β-arrestins are used for receptor internalization and detect changes in cargo such as G-protein coupled receptors (GPCR) serine/threonine phosphorylated tail (Lefkowitz *et al.,* 2006). These classes of adaptor proteins will bind to clathrin and AP2 and recruit them to the surface for progression of the internalisation of the GPCR via CME (Laporte *et al.,* 2000; Burtey *et al.,* 2007). Overall, a variety of different adaptor proteins are recruited at the surface during the initiation of the clathrin assembly around the outer layer of the newly forming coated vesicle (Ungewickell and Hinrichsen, 2007; Traub, 2009) enabling the formation of the characteristic, continuously remodeling clathrin lattice (Ungewickell and Hinrichsen, 2007; Avinoam *et al.,* 2015).

1.3.2 Clathrin coat vesicle (CCV) maturation

In the lattice, clathrin is essential for driving coated pit invagination, where the coated surface remains constant and the engagement of clathrin with multiple binding partners at the surface promotes its maturation and increases the clathrin coat curvature. Each adaptor protein performs their targeted role and change conformation to induce the clathrin coated pits (CCPs) formation (Hinrichsen *et al.,* 2006). Bending of the dynamic clathrin lattice coat is involved in the budding of the CCV (Avinoam *et al.,* 2015). Hence, following the clathrin assembly initiation process, clathrin a

flat-to-curved lattice transition takes place to form the clathrin-coated pits (CCPs) (Ungewickell and Hinrichsen, 2007; Burtey *et al.,* 2007). This transition initiates with the clathrin assembly growing as a flat structure, which then begins to bend when clathrin has reached 70% final content, a change in clathrin/adaptor (AP2) ratio occurs prior to the completion of coat assembly (Bucher *et al.,* 2017). The bending process is carried out with the help of specific adaptor proteins, which maintain a constant surface area (Traub, 2009; Bucher *et al.,* 2017). Such adaptor proteins are epsin and eps15 (Cocucci *et al,* 2012; Hollopeter *et al.,* 2014; Ma *et al.,* 2016) which bind to ubiquitinated proteins via its ubiquitin interacting motifs (UIM) (Traub, 2005). AP180/CALM and epsin 1 use their ANTH/ENTH domains to bind to phosphatidyl-inositol 4,5 bis-phosphate (PI(4,5)P2) (Ford *et al.,* 2001; Ford *et al.,* 2002). The ENTH domain of epsin changes the membrane fluidity promoting bending for invagination (Hom *et al.,* 2007; Lai *et al.,* 2012; Busch *et al.,* 2015), and the unstructured C-terminal domains of both AP180 and epsin are hypothesized to control the clathrin coated vesicle (CCV) size to a uniform size distribution (Kalthoff *et al.,* 2002; Jakobsso *et al.,* 2008; Holkar *et al.,* 2015).

1.3.3 Elongation and Scission of CCPs

Once the CCP has been fully formed, amphiphysin and endophilin, which are BAR domain containing proteins, recruit the GTPase dynamin, which wraps around the narrow neck of the CCP (Verstreken *et al.,* 2003; Loerke *et al.,* 2009; Mettlen *et al.,* 2010; Neumann and Schmid, 2013). These ring-like dynamin layers contract in a GTP-hydrolysis dependent manner, causing stretching of the neck until the CCP is pinched off (scission) (Loerke *et al.,* 2009). In certain cases, the elongation and scission process is actin-dependent, depending on specific cargo and membrane tension, especially in yeast (Saffarian *et al.,* 2009; Mishra *et al.,* 2014). Actin assembles at the neck of the CCP by the help of cortactin (Le Clainche *et al.,* 2007), however the plasma membrane remains flat (Picco *et al.,* 2017). Epsin and Hip1/Hip1R act cooperatively to couple actin and the plasma membrane and

drive membrane bending and the subsequent growth of the plasma membrane, invagination and the elongation of the CCP neck (Fujimoto *et al.,* 2000; Wilbur *et al.,* 2008; Picco *et al.,* 2017). Thus, the changes to the plasma membrane are physically linked to the actin network, which has been identified to have a 'two phase' mechanism to drive the membrane reshaping process (Picco *et al.,* 2017). Once scission of the CCP is completed, myosin II and myosin IV have been suggested to facilitate the closure of the neck before the CCP enters into the cell (Buss *et al.,* 2001; Chandrasekar *et al.,* 2014).

1.3.4 Un-coating of the CCVs

Once the CCV enters the cell the clathrin coat disassembly process initiates, where the clathrin cage will dismantle, allowing the vesicle to fuse with the target organelle and recycling of the adaptor proteins and clathrin to prepare for further endocytic events (Xing *et al.,* 2010; Sousa *et al.,* 2016). It has been suggested that clathrin disassembly onset could be based on competition of auxilin with AP2 for clathrin binding, due to similarities in clathrin binding motifs (Scheele *et al.,* 2003; Smith *et al.,* 2004), as well as the recruitment of the phosphatase synaptojanin prior the completion of scission (Taylor *et al.,* 2011) via interactions with the BAR domain of endophilin (Milosevic *et al.,* 2011). PI(4,5)P2 is dephosphorylated to PI(4)P by phosphatases such as synaptojanin, releasing many adaptors from the membrane due to reducing their affinity (Stefan *et al.,* 2002; Verstreken *et al.,* 2003; Stefan *et al.,* 2005). This disassembly mechanism of clathrin is mediated by the interactions of different adaptors proteins/chaperones such as Hsc70, which interact with the J- domain of auxilin/GAK in an ATP-dependent manner (Greener *et al.,* 2000; Umeda *et al.,* 2000; Kirchhausen *et al.,* 2014; Xing *et al.,* 2010; Sousa *et al.,* 2016). This occurs when the auxilin binds to the clathrin cage which recruits the Hsc70 to bind under the vertex of the clathrin triskelia trimerisation domain where it binds to a QLMLT motif on the clathrin C-terminus, (Rappoport *et al.,* 2006; Xing *et al.,* 2010; Sousa *et al.,* 2016). The final process involves the vesicle being targeted to the

appropriate organelle via the interaction CALM and EpsinR (Miller *et al.,* 2011; Hirst *et al.,* 2004).

1.4.0 Clathrin structure and function

1.4.1 Overview of clathrin

In 1975, Barbara Pearse first purified clathrin from clathrin-coated vesicles. The name clathrin arose from its ability to form lattice structures, enclosing a protein-lipid cargo in a cage (Pearse, 1975). Clathrin has a distinct three-legged structure, called triskelion, which was confirmed as the basic building block for clathrin assembly to form a cage structure (Ungewickell and Branton, 1981). Each triskelion trimer is composed of three ~190 kDa long and thin heavy chain (CHC) subunits which connect at the trimerisation hub, each of which associates with three ~25 kDa light chain (CLC) subunit (Figure 1.4.1 (A) and (B)), forming heterogeneous (according to its transporting cargo) cage sizes (Fotin *et al.,* 2004).

Figure 1.4.1: The structural features of a clathrin triskelion extracted from the alpha carbon model. *(**A**) The alpha carbon model used was from Fotin et al., 2004. View from above with domains labelled as follows. Terminal domain (orange); distal domain (pink); proximal domain (red); trimerisation domain (green) and light chain (cyan). (**B**) Side view of a clathrin triskelion. The images is constructed using 3iyv.pdb in UCSF Chimera (Pettersen et al. 2004) and adapted from (Halebian et al., 2017)*

1.4.1.1 The role of clathrin in disease

Defects in clathrin assembly or disassembly are associated with neurodegenerative disease e.g. Alzheimer's disease (Wu and Yao, 2009), as clathrin has a major role in synaptic vesicle recycling. Additionally, CME is a major means of viral entry into the cell, for example in recent studies by Huang *et al.,* 2017; where the main nervous necrosis virus (betanodavirus) enters the cell via CME pathway (Huang *et al.,* 2017). Therefore, understanding the mechanism by which clathrin functions in CME are extremely important for therapeutical use.

1.4.2 Clathrin Structure

1.4.3 Clathrin heavy chain (CHC)

The proximal leg consists of CHC repeats (CHCRs) comprising 10 helices of 10–12 residues each connected by loops, creating two helical and two loop faces to the triskelion leg (Ybe *et al.,* 1999). The CHC is divided up into 8 distinct regions (CHCR0-CHCR7), which begin from the trimerisation domain until the N-terminal domain at the end of the clathrin leg (Ybe *et al.,* 1999; Fotin *et al.,* 2004). Clathrin triskelion can self-assemble into a polyhedral lattice facilitated by a pH change (~ pH 6.4) *in vitro* (Ybe *et al.,* 1998; Chen and Brodsky, 2005). This is due to interactions between the proximal and distal regions of the CHC, which facilitate interactions between triskelia, by salt bridges of histidines with glutamates in neighboring triskelia legs (Ybe *et al.,* 1998; Bocking *et al.,* 2014). There are two isoforms of CHC in humans; the CHC17 and CHC22 from the two genes located on chromosome 17 and 22. The CHC17 is the most abundant isoform, whereas the major role of the CHC22 is trafficking of the insulin-responsive glucose transporter (GLUT4) in skeletal muscle (Vassilopoulos *et al.,* 2009). However, the biochemical properties of CHC22 have yet to be elucidated (Brodsky, 2012). Thus, in this thesis the CHC17 isoform has been used.

1.4.3.1 Clathrin N-terminal Domain (TD)

An essential component of clathrin heavy chain (CHC), the N- terminal domain (TD) (residues 1-330) consists of a β-propeller structure formed by seven ‘‘WD40 repeats’’, with tryptophans and aspartic acids at the canonical positions in most of its seven blades (ter Haar *et al.,* 2000), (Lemmon and Traub, 2012; Willox and Royle, 2012). The TD is the major binding site for most endocytic adaptor proteins, which is considered an ideal position, as it is the positioned closest to the membrane surface in the clathrin lattice (Willox and Royle, 2012). In 1998, ter Harr *et al.,* showed the 2.6 Å crystal structure of the 55 kDa N-terminal domain suggesting that this region in the CHC could bind to multiple adaptor proteins in its packing of the β-sheets (ter Haar *et al.,* 1998). Acidic and bulky hydrophobic residues, L(L, I)(D, E, N)(L, F)(D, E) (Dell'Angelica *et al.,* 1998); Drake and Traub, 2000), termed the ‘clathrin box’ motif (ter Haar *et al.,* 2000), which are highly-conserved in many proteins for example epsin’s two clathrin binding motifs (LMDLADV and LVDLD) (Darke *et al.,* 2000; Drake and Traub, 2001), which could occupy the same TD sites and aid in the membrane bending (Hom *et al.,* 2007; Lai *et al.,* 2012; Busch *et al.,* 2015).

Despite its relatively small size, the TD has four distinct binding sites for adaptor proteins, as seen in Figure 1.4.3.1. Certain adaptor proteins are hypothesized to interact with multiple of these TD sites, which are essential for assembly and disassembly of clathrin function *in vivo* (Zhuo *et al.,* 2015; Muezner *et al.,* 2017). These four sites/motifs are: CBox (LΦXΦ[DE]), the ‘W-box’ motifs (PWXXW), ‘Arrestin box’ (LI][LI]GXL) and the Royle box, as shown in Figure 1.4.3.1 (ter Harr *et al.,* 2000; Lemmon and Traub, 2012; Willox and Royle, 2012; Zhuo *et al.,* 2015; Muenzner *et al.,* 2017). The major site for the adaptor-TD interaction is via the conserved ‘CBox (LΦXΦ[DE])’ TD site located in the blades 1 and 2 in the TD structure (Drake *et al*., 2000; Lemmon and Traub 2012; Willox and Royle 2012; Zhuo *et al.,* 2015; Muezner *et al.,* 2017). A 2.3 Å crystal structure of amphiphysin 1 peptide bound to clathrin TD reveled the site 2 on TD, the ‘W-box’ with a sequence of

PWXXW which is located in the middle of the TD structure (Miele *et al.,* 2004). The TD site 3, 'ArrestinBox' was shown by Kang *et al.,* 2009 where β-arrestin 1L (longer isoform) bound to blades 4 and 5 on the TD, via the extended 8-amino acid loop on the N-terminal domain (Kang *et al.,* 2009). The newly discovered site 4 named "Royle box" was initially described by Willox and Royle, 2012, where they showed how clathrin/AP2 mediated endocytosis in HEK293 cells was successful even when mutating three TD sites (CBM, W-box, ArrestinBox). The location of the "RoyleBox" was revealed to be between blades 6 and 7 of the TD, but a consensus sequence has not yet been discovered (Muenzner *et al.,* 2017).

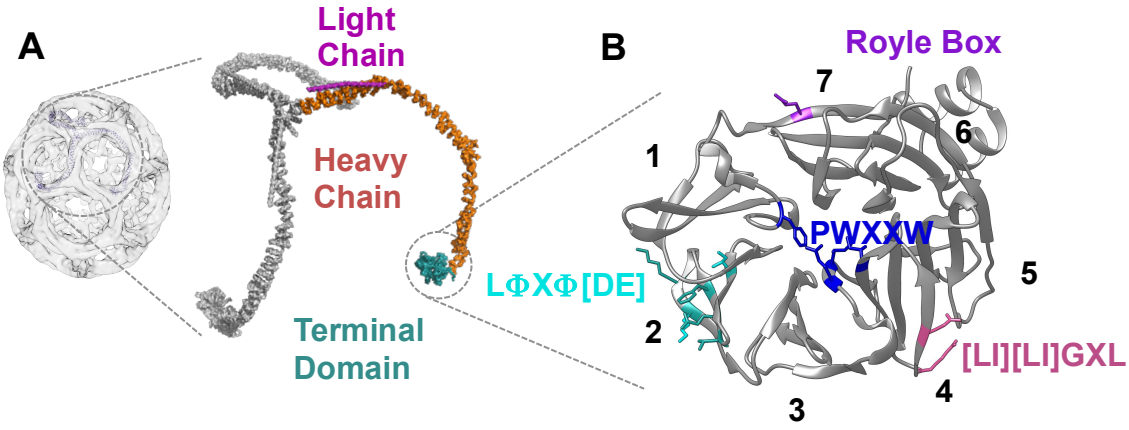

Figure 1.4.3.1: The location of the N-terminal domain and illustrating the four adaptor binding sites on the TD. (A) *Clathrin cages are formed by triskelia monomers, formed of trimer of CHC (orange) and their equivalent CLC (pink). The TD (cyan) is the primary binding location for adaptor proteins and is located at the inner layer of the cage closest to the plasma membrane.* ***(B)*** *The TD consists of four sites, which interact though binding motifs on adaptor proteins. Site 1 is situated in blades 1 and 2 and it is the conserved clathrin box site (LFXF[DE]) (turquoise). Site 2 situated in the center of the propeller, the W-box (PWXXW) (blue). Site 3 is the Arrestin-box ([LI][LI]GXL) (Pink) which is situated in blades 4 and 5; and Site 4 is the Royle Box (purple), which located at blades 6 and 7 with no interaction sequence yet. Image adapted from (Smith et al., 2017) (in press). The* structures adapted from PDB code: 3IYV (A) (Fotin *et al.,* 2004), 5M5R (B) (Muenzner *et al.,* 2017).

1.4.4 Clathrin light chain (CLC)

CLC are tightly associated at 1:1 ratio with CHC, which require strong denaturants, such as sodium isothiocyanate, to achieve dissociation (Winkler and Stanley, 1983; Girard *et al.,* 2005). The biological role of the light chains has not yet been fully established (Brodsky, 2012). The light chains are categorized into light chain types α and b, and neuronal splice variants have been identified for each type (Brodsky, 2012). The consensus region shared by both light chains has been shown to bind to the Hip1 protein family, which interact with actin and actin-associated proteins (Chen and Brodsky, 2005), however light chains which interact with the Hip1/R family reduce their affinity to interact with actin (Wilbu *et al.,* 2008; Wilbur *et al.,* 2010). Both types of CLC but more specifically type b have been shown to be necessary for the endocytosis of some G-protein coupled receptors (Ferreira *et al.,* 2012). Both light chains are able to negatively regulate clathrin assembly *in vitro* and play a significant role in stabilizing the trimerisation domain (Ybe *et al.,* 2007; Chen *et al.,* 2002). They may also regulate the degree of bending that the triskelion legs adopt (Wilbur *et al.,* 2010). Interestingly, CLC have been shown to influence the 'stiffness' of clathrin lattices (Dannhauser *et al.,* 2015). The difference between light chain α and b is that CLCa contains Hsc70 site but not CLCb (De Luca-Flaherty *et al.,* 1990). In addition, there is a negative regulator assembly effect through interactions with calcium and magnesium on CLCb as well as a phosphorylation site (Brodsky *et al.,* 1991; Liu *et al.,* 1995).

1.4.5 Clathrin cage structures

Clathrin-coated vesicles in cells can vary in size within a range of 50 to 80 nm depending on the cargo they internalize, however *in vitro* clathrin triskelia assemble (pH sensitive) to form heterogeneous cage structures (Fotin *et al.,* 2004). Some of these have symmetry, e.g. D6 hexagonal barrel (Fotin *et al.,* 2004). To obtain clathrin cage structures, X-ray crystallography has been unfeasible for entire cages due to the large cage size, but vital information

has been gained through crystallographic analysis of fragments of CHC. Therefore, single particle cryogenic electron microscopy (cryo-EM) was used to investigate the large heterogeneous sized clathrin cages. Using a combination of the information derived from X-ray crystallography of CHC regions and cryo-EM data has given us our current picture and knowledge of the structure of the clathrin cage.

In 1986, the first cryoEM map of a clathrin cage was published by Vigers, Crowther and Pearse indicating how clathrin forms an outer layer around the vesicle with adaptor proteins located inside the cage between clathrin and the membrane (Vigers *et al.,* 1986). Most interestingly, the next clathrin cage structure was obtained from Smith *et al.*, a 21 Å clathrin hexagonal barrel confirming the arrangement and interaction of triskelions in the cage and the location of AP2 in the center of the clathrin cage structure (Smith *et al.,* 1998). The most current cryoEM map of 7.9 Å from Fotin *et al.,* revealed detail of the trimerisation domain secondary structure (ankle and terminal domain), showing key points of interaction between the legs supporting the cage structure, and the location of the clathrin light chain (CLCs) (Fotin *et al.,* 2004). The highest resolution structures revealed have been obtained bound to regulatory adaptors Hsc70 and auxilin, revealing how Hsc70 and the auxilin J-domain bound beneath the clathrin vertex where they disrupt multiple leg contacts (Young *et al.,* 2013; Xing *et al.,* 2010). Identifying location of adaptor proteins in the clathrin cage has proved informative but the mode of interaction of the clathrin cage with its other adaptor proteins still remains unclear.

1.5.0 Structure, function and role of adaptor proteins

In CME, a large number of different proteins, are required to recruit, assemble and disassemble clathrin at the plasma membrane. Therefore, CME is considered a tremendously complex mechanism with a combination of at least 25 different adaptor proteins recruited to the plasma membrane

during CME in an ordered sequence and with different roles (Figure 1.5.0) (Merrifield and Kaksonen, 2014; Traub, 2011; Taylor *et al*., 2011). The pivotal study of Taylor *et al*., 2011 enabled these proteins according to their proposed functions and time of recruitment to the surface at different stages (assembly, maturation, disassembly). There are still unanswered questions as to the precise organisation of these proteins together during CME stages to facilitate efficient endocytosis. It is of great interest to understand how adaptor proteins co-exist and whether they function cooperatively or competitively for clathrin binding, promoting successful assembly and disassembly. In this section, I introduce the structure, function and role of certain adaptor proteins, from different stages of endocytosis, which are further used in this thesis. These adaptor proteins are AP2, epsin 1, β-arrestin 1L, auxilin 1 and Hip1/Hip1R.

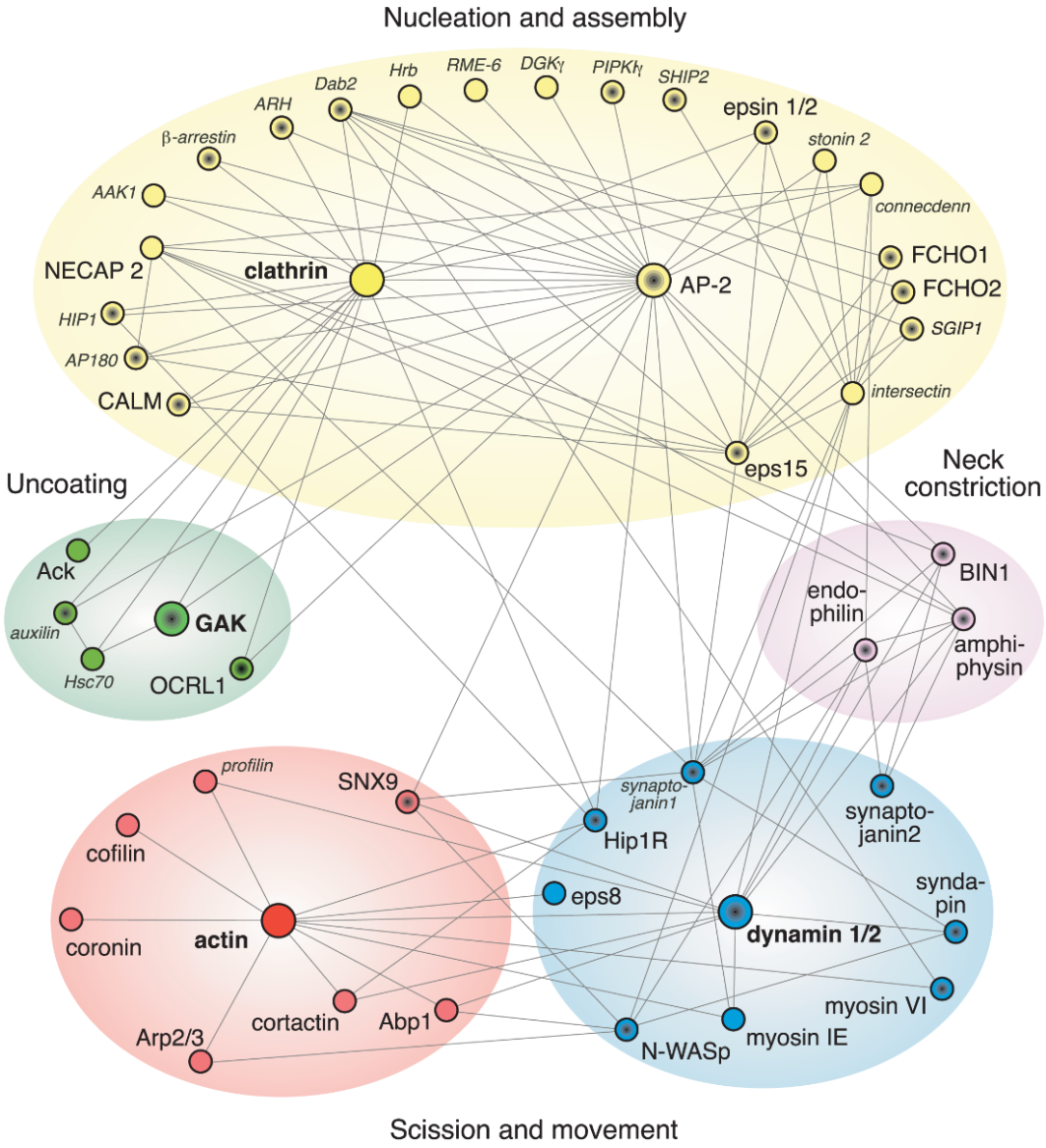

Figure 1.5.0: The huge complex of adaptor protein network involved in different stages of CME. *A large number of proteins involved in CME grouped according to their proposed functionality and recruitment timings during endocytosis, separated in hubs in the spider diagram. Hubs with dark circles indicate proteins that bind to phospholipids. Image adapted from (Traub, 2011).*

1.5.1 Assembly adaptor proteins

1.5.2 Structure of Adaptor Protein 2 (AP2)

The primary adaptor proteins are AP1, AP2, AP3 and AP4, from which AP1, AP2 and AP3 are involved in the CME by interacting with clathrin, and AP4 doesn't bind to clathrin at all (Collins et al., 2002; Edeling *et al.,* 2006a). The main AP used in this thesis is the AP2 complex, which is found at the plasma membrane instead of localized in the endosomes like AP1, AP3, AP4 (Edeling *et al.,* 2006a). The heterotrimeric adaptor protein, AP2, has two large subunits corresponding to the 100–110kD, called adaptins (β2-adaptin and γ2- or α-adaptin), together with a medium-sized (μ2) subunit of ~50 kD and a small (σ2) subunit of ~20 kD (Collins *et al.,* 2002; Edeling *et al.,* 2006a; Jackson *et al.,* 2010, Paczkowski *et al.,* 2015) (Figure 1.5.2). AP2 interacts with two canonical internalization motifs found in the cytoplasmic domains of endocytic cargo proteins; YXX Ø (X-amino acids, Ø-bulky hydrophobic amino acid), which binds to the μ2 subunit; and the [DE]XXXL[LI} motif in the cytoplasmic domain of the receptors (Owen and Evans, 1998; Kelly *et al.,* 2008; Jackson *et al.,* 2010; Traub and Bonifacino, 2013). The AP2 complex also interacts with phosphatidylinositol 4,5-bisphosphate (PIP_2), clathrin, several endocytic accessory and adaptor proteins (Traub, 2009; Jackson *et al.,* 2010).

'Redacted due to copyright. See (Paczkowski et al., 2015)'

Figure 1.5.2: The heterotrimeric AP2 complex. *The complex is made up of two large subunits corresponding to the 100–110kD, called adaptins (β2-adaptin in green and γ2- or α-adaptin in blue), A medium-sized (μ2) subunit in purple of ~50 kD and a small (σ2) subunit of ~20 kD in cyan. A clathrin box is situated at the long flexible linker region of the large β2-adaptin subunit. This diagram illustrates the open conformation of AP2 with the 'clathrin box' accessible. Image adapted from Paczkowski et al. 2015.*

1.5.3 AP2 structure conformational changes

In the cytoplasm, AP2 'clathrin binding box' (LLNLD) is located on the long flexible unstructured linker of the large β2 subunit, which is hidden in the core of the AP2 structure when in its locked/closed conformation (Shih *et al.,* 1995; Owen *et al.,* 2000; Collins *et al.,* 2002; Paczkowski *et al.,* 2015). The cargo binding sites on the AP2 complex are obscured when free in the cytosol (Figure 1.5.3 (A)), but when AP2 is recruited onto the appropriate membrane surface, phosphorylation of Thr156 by AAK1 (Olusanya *et al.,* 2001; Ricotta *et al.,* 2002) or even GAK (Umeda *et al.,* 2000) triggers the release of μ2 subunit of the AP2 complex and other sites for its interaction with PIP2 (Owen *et al.,* 2000; Kelly *et al.,* 2014; Paczkowski *et al.,* 2015). This releases the long flexible loop, which in turn exposes the clathrin binding box motifs. This conformational change of the AP2 complex allows its interaction with clathrin, cargo proteins and other adaptor proteins (Figure 1.5.3 (B)) (Paczkowski *et al.,* 2015).

AP2 and FCHo are both essential CCV initiators, at the early stages of endocytosis (Henne *et al.,* 2010; Godlee and Kaksonen, 2013). However, AP2 is not essential for the initiation of endocytosis in yeast (Owen and Evans, 1998; Collins *et al.* 2002). Interestingly, the closed- AP2 conformation could still bind weakly to clathrin via its α-ear domain, which is always exposed, however there are no know motifs for this interaction yet (Smith et al., 1998; Fotin *et al.,* 2004; Boecking *et al.,* 2011; Kelly *et al.,* 2014).

Figure 1.5.3: Conformational change of the AP2 complex by its interaction with cargo, adaptors and plasma membrane, and its interaction with clathrin. ***(A)*** *In the closed conformation of AP2, the clathrin box in the flexible linker region but once the μ subunit (purple) of the AP2 complex interacts with PIP2 and cargo (navy red), the flexible linker region causes the release forming an open conformation of the AP2 complex* ***(B)****, which can now interact with clathrin (red star) via the clathrin box (LLNLD) (orange box)* ***(C).*** *Image adapted from Paczkowski et al. 2015.*

1.5.4 AP2/clathrin and other adaptor proteins

The ear domains (also referred to as the appendage domains) and the hinge regions of α and β2-adaptin (residues 619–944) are important for the interaction of AP2 with other adaptors (Paczkowski *et al.,* 2015). There are two modes of binding between AP2 and clathrin: (i) The β2-ear of AP2 binds to the clathrin heavy chain ankle, (ii) the β2 hinge which contains a clathrin box motif (LLNLD) in its unstructured region interacts with the clathrin N-terminal domain (TD) (Shih *et al.,* 1995; Clairmont *et al.,* 1997; Owen *et al.,* 2000) with a stoichiometry of 3:1 (Zhuo *et al.,* 2015). The 'clathrin box motif' peptides of AP180, another assembly adaptor protein, and AP2 peptides interaction with clathrin TD could simultaneously bind not only to TD site 1

(CBM) sites 2 (the “W-box”) and site 3 (Arrestin box) on a single TD with low affinity of 800-900 μM K_D (Zhuo *et al.,* 2015), which are common TD sites with variety clathrin adaptor proteins.

The multiple interactions of AP2 with clathrin suggests a cooperative action, which stabilises cage polymerization (Knuehl *et al.,* 2006). More interestingly, a change in the clathrin:AP2 ratio takes place when changing from flat-to-curved transition of the clathrin lattice *in vivo.* This transition occurs when the content of clathrin is around 70% indicating the completion of the coat assembly (Bucher *et al.,* 2017). This flat-to-curved transition is hypothesised to be controlled by biophysical properties of the plasma membrane (e.g. tension) (Bucher *et al.,* 2017). It has been suggested that there is a cooperative interaction between certain endocytic adaptors proteins with AP2 for clathrin recruitment and assembly around the budding vesicle. This is due to the fact that, AP2 may be preferentially present at different stages during endocytosis, and the α and β2 appendages are a common location for interaction with a variety of adaptor proteins (Traub, 2011; Praefcke *et al.,* 2004).

1.6.0 Epsin

Epsin is a key CLASP (Cytoplasmic Linker Associated Protein) protein, discovered in 1998 by Chen *et al*., (Chen *et al.,* 1998) highly expressed in the brain (Rosenthal *et al.,* 1999). Epsin is an important clathrin assembly adaptor protein at the early stages of CME, but it is also important in the later stages of CME, as loss of epsin interferes with the recruitment of HipR (Brady *et al.,* 2010) and results in a reduction in the maturation of CCPs (Mettlen *et al.,* 2009). Epsin reduces its affinity for AP2 when phosphorylated, which allows it to fulfill separate roles in mitosis (Kariya *et al.,* 2000).

1.6.1 The structure of epsin

Epsin 1 is a membrane binding protein that binds to the clathrin coat components, clathrin, Eps15 and the AP2 complex to promote clathrin assembly (Drake *et al.,* 2000). Epsin has an ENTH domain (N-terminal homology domain) that binds to PI(4,5)P2 and contains an amphipathic helix which modifies the membrane curvature (Ford *et al.* 2002; Hawryluk et al., 2006; Hom *et al.,* 2007; Busch *et al.,* 2015; Skruzny *et al.,* 2015) by the insertion of this helix into the membrane and increasing its fluidity (Lai *et al.,* 2012; Holkar *et al*. 2015). This domain also facilitates interactions with other adaptors such as Hip1R for its recruitment to the plasma membrane during CME (Brady *et al*., 2010; Lai *et al*., 2012; Messa *et al.,* 2014; Holkar *et al*. 2015). Following the ENTH domain, epsin has 3 ubiquitin-interacting motifs (UIM) (Hawryluk *et al.,* 2006) used for internalisation of ubiquitinated receptors such as VEGFR2 (Dong *et al.,* 2015) and EGFR (Fortian *et al.,* 2015).

The middle region of the epsin structure contains two clathrin box motifs (LMDLA (starting residue 257) and LVDLD (starting residue 480)) at the C-terminal end, which have been shown to bind to clathrin heavy chain (CHC) and more specifically to the clathrin N-terminal domain (TD) (Drake *et al.,* 2000). The unstructured central region in between these two boxes contains tripeptide motif aspartic acid-proline-tryptophan (DPW) motifs, which have also been hypothesized to bind to clathrin independently (Drake *et al.* 2000; Brett *et al.,* 2002; Kalthoff *et al*., 2002) (Figure 1.6.1). Additionally, the central region of epsin with the eight DPW motif structure bind to the a-ear of the AP2 and at the β2 –ear with a lower affinity (Drake *et al.* 2002; Brett *et al.* 2002; Dafforn and Smith, 2004; Edeling *et al.,* 2006a).

These two chemically distinct motifs are hypothesized to bind to different sites on the clathrin N-terminal domain (Drake *et al.,* 2000). The hypothesized sites are: 1(CBM), 2 (W box) and 3 (Arrestin box) and

additional binding is likely provided by the multiple DPW motifs (Drake *et al.,* 2000; Drake and Traub, 2001; Kalthoff *et al*., 2002; (Collette *et al.,* 2009). Therefore, considering the location of the two clathrin binding boxes and the unstructured flexible large region in between; it has been hypothesized that epsin 1 could be interacting with multiple clathrin triskelia to facilitate efficient clathrin assembly (Kalthoff *et al*., 2002; Dannhauser and Ungewickell, 2012; Holkar *et al*. 2015), which has yet to be confirmed. Following the clathrin box motif in the epsin structure, three NPF repeats exist, which are known to interact with Eps15 homology domains (Chen *et al.,* 1998; Rosenthal *et al.,* 1999).

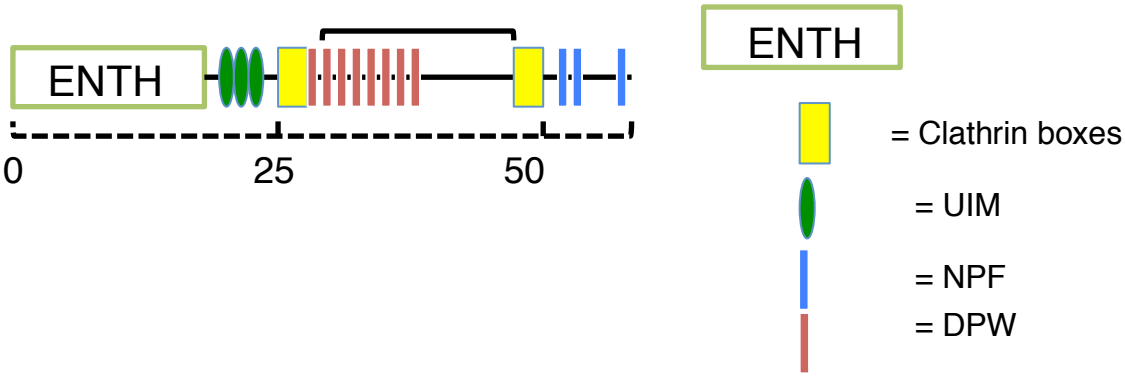

Figure 1.6.5: Linear representation of the structure of epsin. *At the N-terminal there is the ENTH domain (green/white) which interacts with PI(4,5)P2 to promote membrane binding and promote membrane curvature and recruits Hip1R; following with three ubiquitin-interacting motifs (UIM) (dark green). There are two clathrin box motifs at starting residue 257 and 480 (two yellow boxes), which are separated by a long and unstructured region, which contains eight DPW motifs (red). At the C-terminal there are three NPF motifs (blue), which interact with Eps15 homology domains.*

1.6.2 The role of epsin in CME

Epsin has been shown to have a fundamental role in endocytosis, as well as influencing the size of clathrin-coated vesicles, promoting small cage structures *in vitro* (Kalthoff *et al.,* 2002). This property of epsin has been attributed to the location of the two clathrin binding boxes on epsin in combination with the flexible unstructured region in between, which could stretch and allow binding to different multiple triskelia (Drake *et al*., 2000; Drake and Traub, 2001; Miele *et al.,* 2004). This hypothesis was supported

when one of the two clathrin box motifs were mutated and clathrin was unable to assemble on liposomes (Holkar *et al.,* 2015). This led to the suggestion that clathrin assembly was successful with the action of both epsin clathrin box motifs, but also via this unstructured region between the two clathrin binding boxes which facilitates membrane curvature especially (Busch *et al.,* 2015).

At the later stages of CME, epsin accumulates at the neck of the CCP (Saffarian *et al.,* 2009) and any loss of epsin function, potentially at the ENTH domain, results in defects in actin recruitment and Hip1R recruitment (Brady *et al.,* 2010), and thus reduction in the maturation of CCPs (Mettlen *et al.* 2009), (Messa *et al.,* 2014). Epsin has also an important role in mitosis, where knocking down three epsins in mice resulted in severe division defects leading to death of the mice after 4 weeks (Smith and Chircop, 2012; Messa *et al.,* 2014). This resulted in accumulation of early U-shaped pits (Messa *et al.,* 2014). Epsin is also involved in the synaptic development and plasticity (Vanlandingham *et al.,* 2013).

However, the precise location or fate of epsin after completing its role in endocytosis and during cage disassembly is still unknown and debatable (Chen *et al*., 1998; Edeling *et al.,* 2006a; Hawryluk *et al*., 2006; Saffarian *et al*. 2009). It has been suggested that during CCP maturation, epsin would migrate to the neck of the CCP as it's involved with Hip1R functionality to elongate the CCP neck (Jakobsson *et al*., 2008; Mettlen *et al*., 2009). Although, it has been also suggested that epsin could localize at the edges and be excluded from the budded clathrin coated vesicle/pit (Drake *et al.,* 2000; Praefcke *et al*., 2004; Saffarian *et al*., 2009), based on observations of competition between AP2/clathrin complex and epsin (Edeling *et al.,* 2006a; Schmid *et al.,* 2006).

1.7.0 Huntingtin-interacting protein 1 (Hip1/Hip1R)

1.7.1 Structure of Hip1/Hip1R

Another class of endocytic adaptor homodimer proteins Huntingtin-interacting protein 1 (HIP1 and HIP1R), yeast homolog of Slap2 which contribute to the budding of clathrin-coated vesicles (CCVs), at the later stages of CME (Engqvist-Goldstein *et al.,* 2001; Legendre-Guillemin *et al.,* 2004; Brett *et al.,* 2006; Le Clainche *et al.,* 2007; Wilbur *et al.,* 2008; Gottfried *et al.,* 2010). They are associated with other cellular processes such as tumorigenesis (e.g. prostate cancer) with the associating of Hip1 with EGF receptor, transcription regulation and cell death (Hyun *et al.,* 2004; Niu and Ybe, 2008; Gottfried *et al.,* 2010; Boettner *et al.,* 2011).

The structures of Hip1 and Hip1R are very similar, with an ANTH domain, a coil-coil domain and a talin-like domain. The membrane ANTH binding domain at the N terminus binds phospholipids e.g. PI(3,4)P2 (Legendre-Guillemin *et al*., 2004; Gottfried *et al.,* 2010). A 2.8 Å structure of the helical central domain of the Hip1/Hip1R structure the coiled-coil (CC) domain has been shown to promote dimerization of the protein and it has been identified to interact with clathrin light chain (CLC), which promotes the formation of the clathrin cages in vitro (Ybe *et al.,* 2007; Niu and Ybe, 2008; Ybe *et al.,* 2009). This allows the recruitment of Hip1 to the membrane (Hyun *et al*. 2004; Ybe *et al.,* 2009; Gottfried *et al.,* 2010). On the N-terminal domain of Hip1/R, talin-like domain (THATCH) binds to the F-actin, however this interaction is blocked and regulated by the C-terminus of upstream helix (USH) when the Hip1/R CC interacts with the CLC (Brett *et al.,* 2006). This caused the regions to fold back forming ‘dumbbell’ (Engqvist-Goldstein *et al.,* 2001; Brodsky, 2012).

1.7.2 Major differences between Hip1 and Hip1R

Hip1 has a clathrin box motif (LMDMD), which binds to clathrin N-terminal domain, and FXDXF and DPF motifs (X denotes any amino acid) bind to the AP2 complex (α-adaptin) (Mishra *et al.,* 2001; Legendre-Guillemin *et al.,* 2002; Chen and Brodsky, 2005; Hyun *et al.,* 2004; Ybe *et al.,* 2009). More interestingly, Hip1 CC was demonstrated to interact with CHC via a proposed motif of VDLE, which was suggested by Waelter *et al.,* 2001 (Waelter *et al.,* 2001). Whereas Hip1R has been shown to bind weakly to clathrin N-terminal domain compared to Hip1 (Legendre- Guillemin *et al.,* 2002; Hyun *et al.,* 2004). The role of Hip1R is the control of actin polymerization and organization as it interacts with cortactin via a C-terminal proline rich domain (PRD) in the talin-like domain (Le Clainche *et al.,* 2007).

1.8.0 β -arrestin

There are four small gene families in vertebrates, which have multifunctional roles. These are visual arrestins (arrestin 1 and 4) expressed in rods and cones, non-visual arrestins (β-arrestin 1/arrestin 2 and β-arrestin 2/arrestin 3) which are ubiquitously expressed in mammalian cells, cone arrestins (X-arrestins), α-arrestins (Gurevich, 2014). However, for the purpose of this project, I focused on the β-arrestin 1 (non-visual).

1.8.1 Structure of β-arrestin 1

A 1.9 Å resolution crystal structure of inactive β-arrestin 1 by Han *et al.,* 2001 and Milano *et al.,* 2002 revealed that the unbound/inactive β-arrestin 1 has a ribbon–like elongated structure divided into two domains; the C-terminus and the N-terminus composed entirely of anti-parallel β-sheets connected by a 12-residue linker (hinge) region (Han *et al.,* 2001; Milano *et al.,* 2002) These two domains are separated by a polar core (hydrogen bonded network of charged residues) at its' centre and has one short α-helix at the back of the N-terminal domain. β-arrestin 1 has two concave pocket sites for receptor interaction at a cationic amphipathic helix and allows high-affinity binding (N-

terminus site) with the ligand activated- GPCR. Phosphatidylinositol 4,5-bisphosphate (PIP2) also play an important role in delivering the receptor–arrestin complex to CCPs (Figure 1.8.1) (Han *et al.,* 2001; Milano *et al.,* 2002) The high-affinity phosphoinositide-binding site is located in the C-terminal domain (Gurevich, 2014).

The convex sides allow docking of other proteins such as clathrin and β2-adaptin required for endocytic receptor internalization. Both β-arrestin 1S (shorter isoform) and β-arrestin 1L (longer isoform) bind to the to clathrin terminal domain (TD) β-propeller blades 1 and 2 by hydrophobic interactions via a LIELD (LØXØ[DE]) single letter amino acid code where Ø represents a hydrophobic residue) clathrin-box motif (residues 357-383) with a K_D of 10-60 nM (Goodman *et al.,* 1997; Kang *et al.,* 2009). The β-arrestin 1L LIELD clathrin box motif deleted still binds to clathrin TD (N-terminal domain, residues 1-363) regions upon agonist treatment (Lefkowitz *et al.* 2006; Kang *et al.,* 2009; Lemmon and Traub, 2012; Kang *et al.,* 2015; Gurevich, 2014). The eight-amino acid β-arrestin 1L splice loop has also been proposed to bind to a shallow hydrophobic groove in blades 4 and 5 of clathrin TD at a different clathrin box motif ([LI][LI]GXL) (Kang et al., 2009). Kang *et al.,* 2009 proposed that β-arrestin 1L effectively localizes to CCPs even in the absence of the conserved clathrin box motif, thus demonstrating that the eight- amino acid splice loop can mediate arrestin redistribution to CCPs (Kang *et al.,* 2009). Each clathrin box motif is independent and that is functionally relevant in CCPs, but the second clathrin box motif having a low affinity for clathrin (Kang *et al*., 2009). A 2:1 β-arrestin 1L to clathrin stoichiometry was observed in the crystal structure but this was hypothesized to be different in cells as a number of loops on opposing β-arrestin 1L domains are disordered and were not clearly defined (Kang *et al.,* 2009).

It has also been shown that β2-adaptin, a subunit of AP2 complex, also binds to β-arrestins (Ferguson, 2001; (Keyel *et al.,* 2008). In 2000, Laporte *et al.,* proved the binding of specific arginine residues (Arg 394 and Arg 396) in

the C-terminus of β-arrestin 1L *in vitro* to AP2 was independent of clathrin binding (Laporte *et al.,* 2000), and residues Glu 849 and Glu 902 in β2-adaptin (AP2) interact with β-arrestin (Laporte *et al.,* 2002). More specifically, the isoleucine-valine-phenylalanine (IVF) motif of the C-terminal tail of β-arrestin has been confirmed to be the key motif for its interaction with AP2 (Burtey *et al.,* 2007). The F residue of the IVF motif is stated to be responsible for the AP2 binding, with the I and V residues, enhancing the affinity for AP2 (Edeling *et al.,* 2006; Burtey *et al.,* 2007).

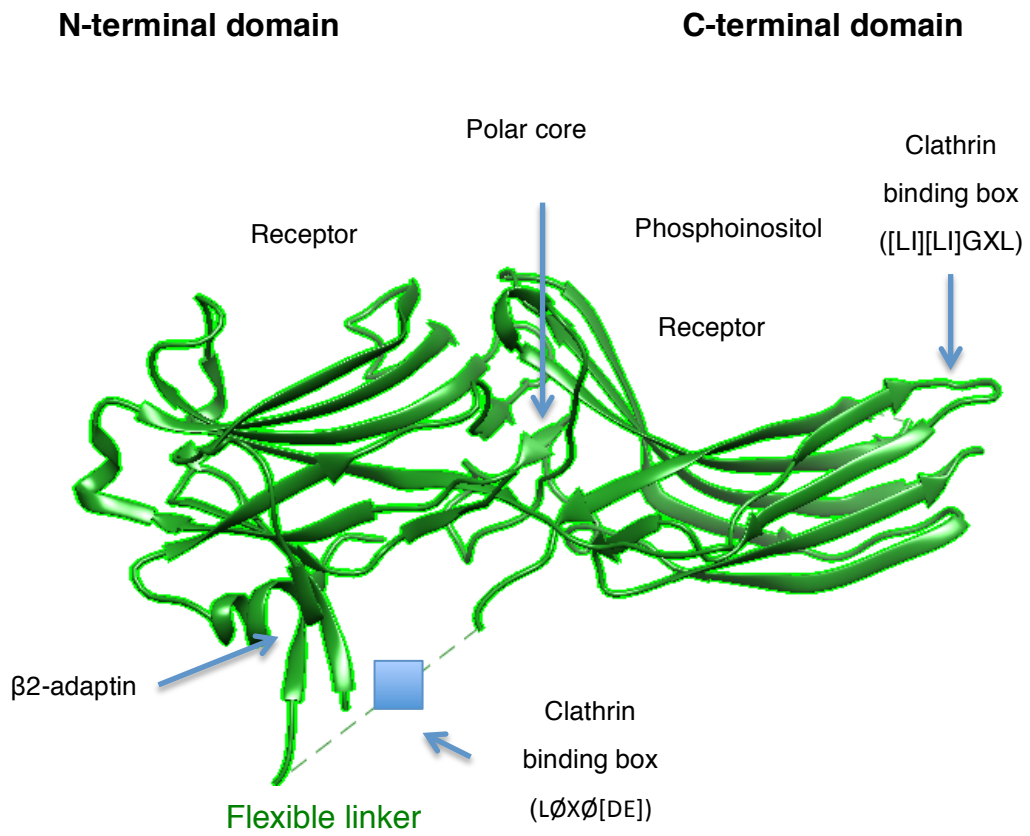

Figure 1.8.1: Structure of inactive β-arrestin 1L. *The structure illustrates the N- and C- domains, the polar core, the two GPCR receptor binding sites (concave sites) with high affinity binding at the C-terminal end, phosphoinositol (PIP2, PIP3, IP6) binding site, two clathrin binding sites which are exposed for binding when the ribbon-like shape of inactive β-arrestin 1 becomes active clamp-shell structure (not shown here) and β2- adaptin binding site on the N-domain. Protein structure was produced using the PDB 1G4M (Han et al., 2001) and displayed using UCSF Chimera (Chimera (Pettersen et al., 2004).*

1.8.2 Function of β -arrestin 1 in endocytosis

β-arrestin 1 is a multifunctional protein involved in the "turning-off" (desensitization) and uncoupling of GPCRs from G-proteins causing loss of responsiveness of the receptor to ongoing stimulus (Lefkowitz *et al.,* 2006; (Kang *et al.,* 2009; Lemmon and Traub, 2012; Kang *et al.,* 2015; Gurevich, 2014). The desensitized receptor is then recycled through the process of receptor internalization. β-arrestin 1 internalization involves the interaction with both cargo and clathrin. Initially, β-arrestin 1 binds to the phosphorylated GPCR (Kang *et al.,* 2009; Lemmon & Traub, 2012; Shukla *et al.,* 2013; Shukla *et al.*, 2014). This interaction allows the β-arrestin 1 conformational to change to an "open" conformation exposing clathrin binding sites, which are hidden in a "closed" β-arrestin 1 conformation. This internalization occurs via clathrin coated pit (CCP) machinery (Figure 1.8.2). Its main role in CME is to recruit clathrin and other vital adaptors, such as β2-adaptin (AP2), to the plasma membrane to facilitate receptor internalization (Kang *et al.,* 2009; Gurevich, 2014; Goodman *et al.,* 1997). However, AP2 and clathrin are not sufficient individually for CCP targeting and thus both need to be present and cooperate for this function (Burtey *et al.,* 2007). Lastly, it acts as scaffold protein (signaling intermediates) to initiate a signaling cascade by the mitogen-activated signaling pathways (MAPK 1/3, ERK 1/2, Src etc) for downstream signaling and generation of endocytic vesicles ("signalosomes"), which result in ERK1/2 activation via the β-arrestin 1 scaffolding action (Lefkowitz *et al.,* 2006; Shenoy and Lefkowitz, 2011; Smith and Rajagopal, 2016; Kumari *et al.,* 2016).

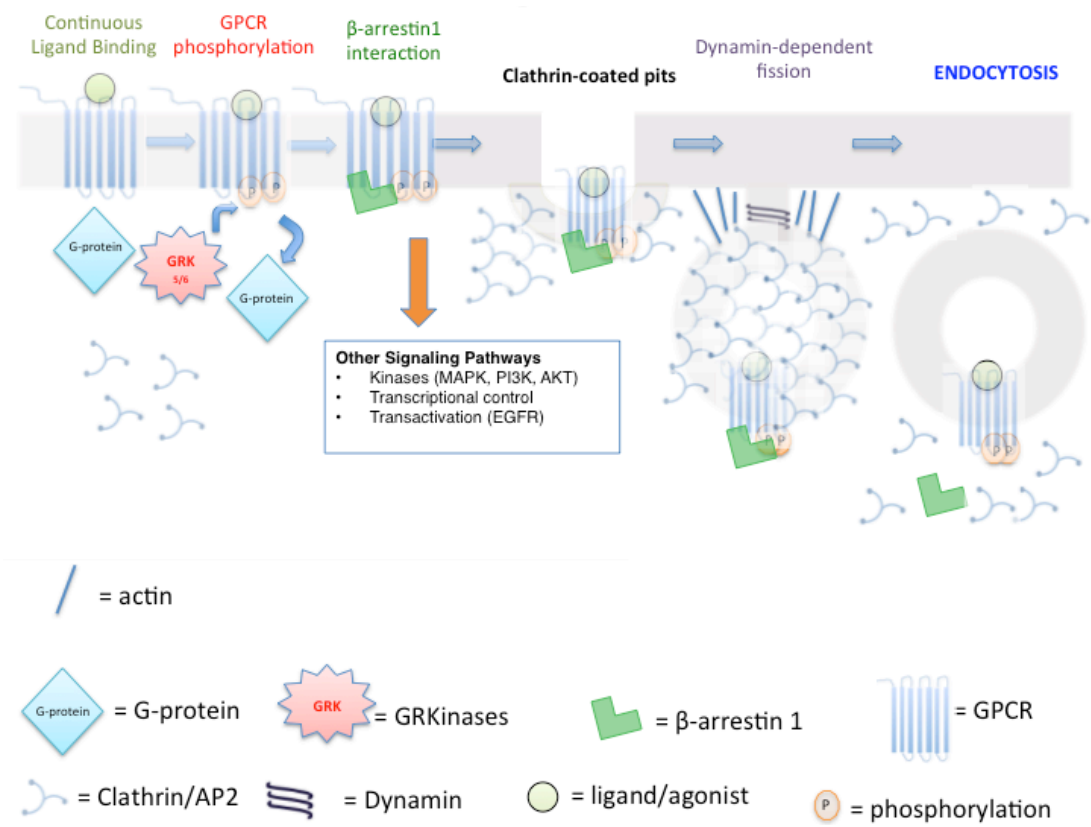

Figure 1.8.2: Diagram representing GPCR internalization via CME with the aid of β-arrestin. *Ligand binds to the GPCR causing G-protein binding to the receptor resulting to G_{α} and $G_{\beta\gamma}$ dissociation. The receptor activation promotes GRKinases (GRK) binding to mediate phosphorylation within the third intracellular loop domain or the C-terminal tail of the GPCR. The β-arrestin 1L will then localize near the plasma surface and associate with the 'receptor tail and core' causing its conformational change into active/open conformation, exposing/unmasking its LIELD clathrin binding site (loop) and β2-adaptin site in the N-terminal end for binding, which would allow recruitment of clathrin at the plasma surface and assembly to clathrin cages (action of β2-adaptin and other accessory proteins) to form GPCR-β-arrestin 1L complex and promote receptor internalization.*

1.8.3 Transition: "inactive" to "active" β-arrestin 1 state

β-arrestin 1 adopts an inactive (ribbon shape) 'closed' cytoplasmic form in the cytoplasm with its polar core stabilized by an extended C-terminal tail. This tail locks β-arrestin 1 into an inactive state (Laporte *et al.,* 2000). Upon agonist-GPCR interaction, G-protein association with the receptor triggers GRKinase recruitment to the plasma membrane for phosphorylation of the receptor C-tail. This recruits β-arrestin 1 to the surface allowing it to bind in a biphasic manner, at the tail and the core of the GPCR (class A and B GPCRs) (Shukla *et al.,* 2014). After β-arrestin 1 binds to these sites it

changes its conformation (polar region rotation, residues Arg169 and Asp290) to an active 'open' state (clam-shell shape) upon binding to those phosphate group regions, with a ~ 20 ^{o} inter-domain rotation between the amino and carboxyl domains (Yang *et al.,* 2015; Kang *et al.,* 2015) and the breakage of the polar core (Scheerer and Sommer, 2017). The β-arrestin 1 remains active and at the cell surface performing other independent cell signaling/trafficking roles after dissociation from the receptor (Nuber *et al.,* 2016).

1.8.4 GPCR

GPCRs are composed of seven-transmembrane helices in the plasma membrane and represent by far the largest, most versatile family of plasma membrane due to their importance in drug development (~ 60% of prescribed drugs targeted to these receptors) (Ladds *et al.,* 2005).

1.8.5 Vasopressin type 2 GPCR

The structural organisation of type 2 Vasopressin GPCR is currently undetermined and has been of great interest in the GPCR community due to its role in renal kidney homeostasis and diabetes insipidus (Birnbaumer, 2000). There are over 150 mutations of the V2R, which have been identified resulting in congenital nephrogenic diabetes insipidus (cNDI) (Birnbaumer, 2000). This condition causes improper water reabsorption by kidneys, as the mutated V2R does not respond to vasopressin appropriately because the miss-folded receptor limits its expression on the cell membrane. This disorder has extensive complications such as dehydration, and the drugs available are considered toxic (Gastrointestinal NSAID toxicity) causing gastric bleeding (Birnbaumer, 2000). Class B GPCRs, such as V2R, form a complex with β- arrestin and remain tightly bound to β- arrestin upon internalisation with a slower recycling rate (60 minutes) compared to other GPCRs (Terrillon *et al.,* 2004; Lefkowitz *et al.,* 2006; Thomsen *et al.,* 2016; Suleymanova *et al.,* 2017). Additionally, GRK- mediated phosphorylation of

V2R and consequent β–arrestin recruitment are due to GRK 2 and GRK 3 (Ren *et al.,* 2005; Yang *et al.,* 2015).

Shukla *et al.,* 2013 obtained a 2.6 Å crystal structure of activated β-arrestin 1-human V2Rpp (29-amino acid C-terminal peptide)-Fab30 (antigen binding fragments) complex, which provides novel insight into the mechanism of the receptor-mediated β-arrestin 1 activation (Shukla *et al.,* 2013). The following year, Shukla *et al.,* 2014 visualized β-arrestin recruitment by β2-adrenergic receptor with its C terminus replaced with that of arginine vasopressin 2 receptor (AVV_2) using the single particle negative stain EM imaging technique. They published a 29 Å model of β_2V_2R –β-arrestin 1-Fab30 complex, from 3D negative stain computational reconstruction (Shukla *et al.* 2014). According to Shukla *et al.,* 2014, this model confirms that β_2V_2R can activate β-arrestin 1 entirely (confirmation with clathrin pull-down assays) and suggested the biophasic mechanism of β- arrestin to engage with the receptor (Shukla *et al.,* 2014). The biphasic interaction of β-arrestin 1 with the 'receptor tail and core' causes the formation of two GPCR/ β-arrestin 1 conformations, which have been shown to perform distinct functionality (Shukla *et al.,* 2014), (Ranjan *et al*., 2017). The biphasic mechanism is divided into two steps, the 'low-affinity pre-complex' formation between the β-arrestin 1 and the receptor C-tail, and then a high affinity complex if formed once the β-arrestin 1 binds to the receptor core (Shukla *et al.,* 2014; Ranjan *et al*., 2017; Scheerer and Sommer, 2017). The complex with 'receptor tail' formed can internalize the GPCR but does not 'turn off' the G-protein signaling pathway (Thomsen *et al.,* 2016; Cahill *et al.,* 2017).

1.9.0 Clathrin disassembly adaptor proteins

Separation of the clathrin-adaptor coat is important in order to allow the clathrin and adaptors to be recycled and be used for the next endocytosis process. The vesicle can then be targeted to the appropriate organelle. This process in CME is mediated by the interactions of different adaptor proteins/chaperones such as Hsc70 chaperone, which interacts with its co-chaperone auxilin or GAK (auxilin2) (Greener *et al.,* 2000; Umeda *et al*. 2000; Zhang *et al.,* 2005). Auxilin/GAK bind to clathrin and recruits the Hsc70 under the clathrin hub domain where it binds to a QLMLT motif on the clathrin C-terminus (Ahle and Ungewickell, 1990; Ungewickell *et al.,* 1995; Rapoport *et al.,* 2008; Xing *et al*. 2010). ATP hydrolysis to ADP in Hsc70 stimulated by the J-domain of auxilin/GAK induces tight binding to clathrin, which destabilises triskelia interactions through a collision-induced mechanism (Sousa *et al.,* 2016) (Figure 1.9.0).

Figure 1.9.0: Diagram illustrating the steps of clathrin cage disassembly by the action of auxilin and Hsc70 recruited to the clathrin trimerisation domain. *Auxilin (red) is recruited through the terminal domain-leg interactions (blue) under the hub, which contains the unstructured C-terminal tails containing the Hsc70 binding motif (orange), which allows the recruitment of Hsc70 (green). Hsc70 is tightly bound to the clathrin due to the ATP hydrolysis carried out by the J-domain. This causes the disassembly of the clathrin to be recycled, and once the ATP regenerated ADP+Pi, auxilin is removed from clathrin and recycled as well. Image adapted from (Xing et al., 2010).*

1.9.1 Structure and function of auxilin 1

The auxilin 1 adaptor protein has a unique structure of 100 kDa that allows the interaction of chaperones, assembled clathrin and lipids, and is involved in the clathrin disassembly process along with Hsc70 chaperone (Fotin *et al.* 2004; Young *et al.,* 2013; Xing *et al.,* 2010). The J-domain allows auxilin 1 to interact with Hsc70 and recruit it to clathrin. The N-terminal domain of auxilin 1 has a phosphopeptide phosphatase homology domain (PTEN) that binds to lipids (e.g. PIP2) (Massol *et al.,* 2006). Importantly, auxilin 1 interacts with AP1 and AP2 complex (μ2 subunit), dynamin and clathrin (Umeda *et al*., 2000). Auxilin has several binding sites for clathrin via a range of motifs including DLL and DPF (Scheele *et al.,* 2001; Scheele *et al.,* 2003). More specifically, the DPF motifs bind to both the CHC and the ear domain of α-adaptin in AP2 and DLL motifs bind to clathrin (Scheele *et al.,* 2001).

In addition, auxilin contains a clathrin binding box 'LLGLE' motif (residues 495-500), which allows the interaction with the clathrin N-terminal domain and the clathrin 'leg' (Smith *et al.,* 2004). One auxilin molecule per triskelion is optimal for Hsc70 ATP hydrolysis and for the maximal rate of cage disassembly (Holstein *et al.,* 1996) Clathrin/auxilin binding causes the N-terminal domains on clathrin to twist outwards, thus causing change in the position of the 'ankle' (Fotin *et al.,* 2004). This causes an increase in the diameter of the entire lattice leading to a global distortion of the clathrin coat (Popova and Petrenko, 2013). But, assembled clathrin can be disassembled even when auxilin does not bind to the clathrin N-terminal domain directly (Ungewickell *et al*., 1995), as auxilin binds to multiple sites on the clathrin leg (Edeling *et al.,* 2006b; Young *et al.,* 2013) (Figure 1.9.1). However, auxilin alone is not sufficient to initiate clathrin coat disassembly, it needs the aid of Hsc70 ATP hydrolysis, as auxilin alone can in fact promote clathrin assembly *in vitro* (Holstein *et al*., 1996; Scheele *et al*., 2003). On the other hand, the role of auxilin as a disassembly adaptor protein has an additional important aspect, which involves the ability of auxilin to discriminate between free and polymerized clathrin triskelia via its multiple low affinity interactions with the

clathrin TD and α-appendage domain of AP2 complex, which are hypothesized to have competition for auxilin 1 binding (Scheele *et al*., 2001).

Figure 1.9.1: Representing auxilin: CHC domain interaction locations. *An α-carbon map of a single CHC leg with the colours representing each segment individually in the box below the figure. A linear representation of auxilin structure, demonstrating the auxilin clathrin box motif (LLGLE) at a starting residue 495. The clathrin binging domain (CBD) of auxilin binds at the distal region, with other clathrin binding domains (e.g. DLL motifs). The PTEN domain binds to the membrane and the J-domain interacts with the Hsc70 chaperone (linear representation in green). The Hsc70 substrate binding domain motif on clathrin (QLMLT) found under the trimerisation domain at clathrin C-terminus. Abbreviations: nucleotide-binding domain (NBD), substrate-binding domain (SBD) and C-terminal domain (CTD). Image adapted from (Edeling et al., 2006b).*

Whilst CHC are very important in the disassembly process, CLC have been stated to be important for the dissociation and recycling of auxilin after the completion of the disassembly process, as removal of CLCs has been shown to affect the catalytic mechanism (Young *et al.,* 2013). In yeast, the CCVs accumulate more when in an auxilin depleted environment *in vivo* (Pichvaee *et al.,* 2000). Therefore, the onset of uncoating is based on the timing of auxilin burst, but Hannan *et al.,* 1998 stated that the uncoating process (clathrin, auxilin/GAK and Hsc70) does not remove adaptor proteins, AP2 from coated vesicles *in vitro* (Hannan *et al.,* 1998). Interestingly, auxilin is recruited transiently in small amounts during the endocytosis process with the larger burst occurring after the peak of dynamin signal in vesicle budding, where the PTEN domain interacts with PIP(4) recruiting auxilin to the coat to begin uncoating (Massol et al., 2006; Taylor *et al.,* 2011).

1.11.0 Overall aim and objectives of this investigation

Despite the large amount of research dedicated to understand the roles that some adaptor proteins play at different stages of endocytosis, we still do not understand the manner in which some adaptors interact with clathrin or the molecular details of their interactions with one another. Therefore, using purified adaptor proteins, clathrin cages/clathrin TD, I tried to address the above questions using variety of biophysical and structural techniques, *in vitro*:

1. To carry out optimization to obtain optimal buffer/pH conditions for the binding interaction between whole clathrin cages and clathrin TD with active β-arrestin 1L *in vitro.* Furthermore, explore the buffer/pH conditions for clathrin cages assembled with epsin 1 and β-arrestin 1L individually and in combination with SDS-PAGE binding assays and negative stain electron microscopy (EM).

2. β-arrestin 1L mutagenesis studies, SDS-PAGE binding assays and surface plasmon resonance (SPR) were used to investigate:

    I. Whether the two clathrin box motifs on β-arrestin 1L act synergistically or antagonistically. This will enhance our knowledge from the work of Kang *et al.,* 2009 (Kang et al., 2009).
    II. To confirm the functionality of the optimized SPR/IAC system relative to aim number 3.
    III. How the second clathrin box of β-arrestin 1L and the hypothesised linking effect of multiple TDs that active β-arrestin 1L could promote, could interfere with the interaction of other adaptor proteins for clathrin TD binding.

3. Despite the large amount of research dedicated to understand the CME, we are still unclear how clathrin assembly and disassembly

adaptor protein sequence takes place and how the adaptors co-exist. Therefore, I aimed to further understand how the unique structure of epsin 1, one of the main assembly proteins, binds to clathrin forming uniform clathrin cages (Kalthoff *et al.,* 2002). In order to address this aim I used mutagenesis studies of the whole protein epsin 1 (clathrin box motifs and unstructured/DPW region). To explore the binding events between clathrin TD and epsin 1 mutants, I used the SPR/IAC method, which I optimized for epsin 1 whole proteins in this thesis.

4. As there are numerous potential clathrin-adaptor protein interactions during the different stages of the endocytosis, this raises the question of whether some adaptor proteins compete for binding to clathrin or whether some adaptor proteins can bind to clathrin simultaneously. I aimed to address these questions using ultracentrifugation/GST-pulldown binding assays and a newly developed SPR/IAC (2-injection) method. Intially, well-characterised adaptor proteins known to play a significant role in clathrin-mediated endocytosis would be investgated. These are β2-adaptin, epsin 1, auxilin 1 and β-arrestin 1L, Hip1CC/Hip1RCC. It was hypothesised that these adaptor proteins bind to multiple sites on the clathrin TD, as they have one or more similar clathrin box motifs. Different adaptor protein peptide ligands have been shown to bind to one or more of these sites simultaneously (Muenzner *et al.,* 2017). Alternatively, the affinity and number of clathrin binding sites could allow one adaptor protein to displace another from the clathrin TD, influencing the progress of clathrin CCV (Zhuo *et al.,* 2015). Therefore, our hypothesis was that both competition and simultaneous binding play a role in the engagement of different adaptor protein combinations to clathrin TD. This hypothesis was investigated using the SPR/IAC (2-injection) system.

Chapter 2:

Materials and Methods

2.0.0 Overview

This is an overview chapter including the methods and materials used in each experiment carried out in my project. Any changes to protocols, that are specific to a particular chapter will be documented in the relevant chapters.

2.1.0 Materials and Reagents

All the companies that supplied the chemicals, reagents and materials are listed below:

Abcam (UK): Prism Ultra Protein Ladder (10-245 kDa)

Affymetrix (USA): 2-(N-morpholino)ethanesulfonic acid monohydrate (MES)

Agar Scientific (UK): Formvar/Carbon 300 mesh copper grids

AGTC Alfa Aesar (USA): Manganese chloride

AMRESCO (USA): Hepes free acid

Applichem Lifesciences (USA): Dithiothreitol (DTT), sodium dodecyl sulphate (SDS)

Biological Industries (USA): EZ-ECL Chemiluminescence Detection Kit for HRP

Biacore (Slovakia): Surface Plasmon Resonance 2000 instrument

Bioproducts Ltd. (UK): Agarose

Bio-Rad (USA): Hydroxyapatite Bio-Gel HG Ge

Cell Signaling (USA): His-Tag (27E8) Mouse mAb, GST (26H1) Mouse mAb,Anti-mouse IgG HRP-linked Antibody.

Expedeon (UK): Instant Blue

First Link Ltd. (UK): Porcine brain

Fisher Scientific (UK): Ammonium sulphate, glycerol, magnesium acetate

tetrahydrate, nitric acid, potassium acetate, potassium chloride, potassium phosphate dihydrate, potassium phosphate monohydrate, sodium chloride, sodium hydroxide

GE Healthcare (USA): ECL Western Blotting Detection Reagents, Ficoll™ PM70, Glutathione sepharose 4B, GSTrap™ FF column, HiLoad 26/600 Superdex 200 pg column, HiPrep 26/60 Sephacryl S-500 HR, HWM-SDS Marker Kit, Hybond TM-P PVDF membrane, L WM-SDS Marker Kit, PreScission Protease, XK 16/100 Superdex 75 column, Sensor Chip CM5, Rubber Caps and Plastic Vials, o.d. 7 mm, amine coupling kit.

Life Technologies (USA): NuPAGE Transfer Buffer (x20)

Melford Laboratories Ltd. (UK): Isopropyl β-D-1-thiogalactopyranoside (IPTG)

Medicell Membranes Ltd. (UK): visking dialysis tubing 19 mm 12-14 kDa cut-off

National Diagnostics (USA): 30% w/v Accugel acrylamide (acrylamide 29:1 bis- acrylamide)

New England Bioscience (USA): 10x NEB buffer, Gel loading dye (6x)

PanReac AppliChem (USA): 4-(2-Aminoethyl) benzenesulfonyl fluoride hydrochloride (AEBSF), Color Protein Standard Broad Range (P77125)

Parr Instrument Company (USA): Nitrogen Cavitation Vessel

Premier International Foods (UK): Marvel Milk Powder

Qiagen (Germany): QIAprep Spin Miniprep Kit

Roche Diagnostics Ltd. (Switzerland): c0mplete HisTrap, c0mplete Protease Inhibitor Tablets

Sartorius Stedim (Germany): Vivaspin 20 centrifugal concentrators

Sigma-Aldrich (UK): Ammonium per sulphate (APS), ampicilin, β2-mercaptoethanol (βME), bovine serum albumin (BSA), chloramphenicol, dimethyl sulphoxide (DMSO), ethylene-diamine-tetraacetic acid (EDTA), ethylene-glycol-bis(β aminoethyl ether)-tetraacetic acid (EGTA), glutathione (GSH), glycine, hydrochloric acid, imidazole, kanamycin, magnesium chloride hexahydrate, rubidium chloride, sucrose, triethylamine (TEA), tetra-methyl-

ethylene-diamine (TEMED), thrombin, Tris-HCl, Monoclonal Anti-Glutathione-S-Transferase (GST) antibody produced in mouse (G1160), Tris(2-carboxyethyl) phosphine hydrochloride (TCEP)

SPI-Supplies (USA): Uranyl acetate

Thermo Scientific (USA): Pierce BCA Protein Assay Reagents, Slide-A-Lyzer MINI Dialysis Units 7000 MWCO

VWR Chemicals (UK): bromophenol blue, ethanol, methanol

Whatmann (UK): 3 mm filter paper 0.2 ìm, blotting paper

2.2.0 Buffers and gel compositions

Buffer Name	Ingredients	pH
β-arrestin 1L WT and mutants purification and GST-TD		
CB1	10mM Tris-HCL, 150 mM NaCl, 1 mM EDTA, 2mM DTT	8.0
GSH elution buffer CB1	20 mM Tsi-HCL, 150 mM NaCl, 1mM EDTA, 2mM DTT, 10 mM GSH	7.2
Analytical experiments		
HKM	25 mM Hepes, 125 mM Potassium acetate, 5 mM Magnesium acetate	6.4 7.0 7.2
Surface plasmon resonance experiments		
Antibody immobilization buffer	10mM Sodium Acetate	5.5
SPR Buffer 1	10mM HEPES, 150mM NaCl, 1mM TCEP, 3 mM EDTA, 0.05% Tween 20	7.4

SPR Buffer 2	10mM HEPES, 500mM NaCl, 1mM TCEP, 3 mM EDTA, 0.05% Tween 20	7.4

For GST- auxilin$_{401-910}$ and GST-β2 adaptin$_{695-983}$ purification

Buffer A	20 mM Hepes, 200 mM NaCl	7.2
GSH elution buffer A	20 mM Hepes, 200 mM NaCl, 10 mM GSH	7.0

His$_6$ -epsin1 WT/mutants and Hip1/R purification

Buffer B	50 mM Tris, 500 mM NaCl	7.9
Imidazole washing buffer	50 mM Tris, 500 mM NaCl, 20 mM imidazole	7.9
Imidazole elution buffer	50 mM Tris, 500 mM NaCl, 200 mM imidazole	7.9

SDS PAGE gel

4% SDS PAGE stacking mix	150 mM Tris, 4% acrylamide - 29% acylamide, 1%bis-acrylamide, 0.12% SDS	6.8
12% SDS PAGE resolving mix	250 mM Tris HCl, 12% acylamide - 29% acylamide, 1%bis-acrylamide, 0.12% SDS	8.8
Loading dye	250 mM Tris-HCl, 5 % w/v SDS, 25 % w/v glycerol, 50 mM DTT, 4 % w/v β-	6.8

	mercaptoethanol, 0.05 % w/v Bromophenol blue	

clathrin purification

Depolymerisation buffer (DEPOL)	20 mM TEA, 1 mM EDTA, 1 mM DTT	8.0
Saturated Ammonium Sulphate	770g ammonium sulphate, 10mM Tris, 0.1 mM EDTA	7.1
2 x 1M Tris	0.1 M Tris base, 1.9M Tris-HCL, 2mM EDTA, 2mM DTT	7.1
6.25% Ficoll/6.25% sucrose	0.0625 g/ml Ficoll PM70, 0.0625 g/ml sucrose, 25 mM Hepes, 125 mM Potassium acetate, 5 mM Magnesium acetate	
Polymerisation buffer (POL)	100 mM MES, 1.5 mM $MgCl_2$, 200 mM EGTA	6.4

competent cells

TFB1	30 mM potassium acetate, 10 mM calcium chloride, 50 mM manganese chloride, 100 mM rubidium chloride, 15 % w/v glycerol	5.8
TFB2	10 mM MOPS, 75 mM calcium chloride, 10 mM rubidium chloride, 15 % w/v glycerol	5.8

Western Blot

Transfer Buffer	25 mM Tris 190 mM glycine and 20% methanol	-

TBS-Tween	20 mM Tris and 150 mM NaCl and 0.1% Tween 20	-
5% milk	5g Milk powder in 100ml of TBS-Tween	-

Table 1.0.0: Buffer components and gel mixture components used in this thesis

2.3.0 Expression DNA constructs

The Table 1.1.0 below documents all the DNA constructs used in this thesis for expression of recombinant proteins in *E.coli* or insect cells.

Construct	Description	Source	Reference
pGEX4T2- β2 adaptinHA	pGEX4T2 + GST-$\beta2_{695-983}$	David Owen (Bristol)	Owen *et al.,* 2000
pGEX6P3-β-arrestin 1L	pGEX6P3 + GST- β -arrestin $1L_{1-418}$	-	Keyel *et al.,* 2008
pGEX4T2- TD	pGEX4T2 + GST-TD_{1-363}	Owen (MRC)	Smith *et al.,* 2004
pET32c-epsin 1	pET32c + thioredoxin-His_6 - $epsin1_{1-575}$	Ernst Ungewickell (Hannover Medical School)	Kalthoff *et al.,* 2002
pGEX4T2- auxilin	pGEX4T2 GST- $auxilin_{401-910}$	Helen Kent (MRC LMB)	Smith *et al.* 2004
pETDuet-1-mHip1RCC	pETDuet-1 + His_6-$mHip1RCC_{346-655}$	Frances Brodsky (UCL)	Wilbur *et al.,* 2008
pETDuet-1- Hip1cc	pETDuet-1 + His_6-$Hip1_{346-637}$	Frances Brodsky (UCL)	Wilbur *et al.,* 2008
GST tag	pGEX6P3	-	-

Table 1.1.0 Details of DNA constructs for expression of recombinant proteins in E.coli.

2.4.0 Generation of β-arrestin 1L and epsin 1 mutants

The mutagenesis described in this section was conducted by GenScript (NJ, USA) who provide a commercial cloning and mutagenisis service.

2.4.1 β-arrestin 1L

Design of the mutations to β-arrestin 1L clathrin-binding motifs was conducted with reference to Keyel *et al.,* 2008. The following mutants were designed using a pGEX6P3 plasmid with numbers indicating the first residue of each motif:

Name	***Original motif -> mutated motif and/or deletions***
Active (IVF)	^{386}IVF->AAF
IVF-ΔCB	^{386}IVF -> AAF + ^{376}clathrin box deleted
WT-ΔCB	WT + ^{376}clathrin box deleted
IVF-AAEA	^{386}IVF + ^{376}clathrin box (LIEL->AAEA)
WT-AAEA	WT + ^{376}clathrin box (LIEL ->AAEA)

Table 1.2.0: Description of all the GST-β-arrestin 1L mutants.

2.4.2 Epsin 1

Generation of epsin 1 clathrin box motif mutants (257, 480 and DKO) were conducted in line with reference to Drake *et al.,* 2000. The ½ DPW, ¼ DPW and ΔDPW mutants were generated by the Smith's Group. The following mutants were generated from the base pET32c-epsin 1 construct with numbers indicating the first residue of each motif in epsin 1.

1) Alaline substitution of the clathrin box motifs in epsin 1	
Name	***Original motif-> mutated to***
257	LMDLA **->** AAAAA
480	LVDLD **->** AAAAA
DKO	LMDLA -> AAAAA and LVDLD -> AAAAA
2) Shortening/Deletion of unstructured region (containing DPW motifs) of epsin 1	
Name	***Residue deletions***
½ DPW	At 123rd residue we cut out 93 AAs – approx. half of the DPW unstructured region
1/4th DPW	At 63rd residue – cut out 60 AAs- approximately 1/4th of the DPW unstructured region
ΔDPW	deletion of the whole unstructured region keeping 7 AAs between the two clathrin box motifs

Table 1.3.0: Description of all His$_6$-epsin 1 mutants. *These mutations are carried out in reference from Drake et al., 2000 and the mutagenisis was conducted from GenScript (NJ, USA).*

2.5.0 Cell lines

2.5.1 *E.coli* cell lines for protein expression

Strain	Genomic information
BL21 (DE3)	huA2 [lon], ompT gal, (λ DE3) [dcm], ΔhsdSλ DE3 = λ sBamHIo, ΔEcoRI-B int::(lacI::PlacUV5::T7 gene1), i21 Δnin5
MAX Efficiency® DH10Bac™	F- *mcr*A Δ(*mrr-hsd*RMS-*mcr*BC) ϕ80d*lac*ZΔM15 *lac*X74 *rec*A1 *end*A1 *ara*D139 Δ(*ara- leu*)7697 *gal*U *gal*K *rps*L *nup*G λ- *ton*A (confers resistance to phage T1)

Table 1.4.0: The E.coli strains and their genetic propertied which have been used in this thesis

2.5.2 Generation of chemically competent *E.coli cells*

The chemically competent BL21 (DE3) cells were transformed on LB-agar plate and a single colony was inoculate 5 ml of LB (10 g/l NaCl, 10 g/L bactotryptone and 5 g/l yeast extract) which was in turn grown overnight at 37°C. The 5 ml culture was then used to inoculate 250 ml of LB supplemented with 20 mM $MgSO_4$ and grown whilst shaking at 180 rpm at 37°C until OD_{600} reached 0.4-0.6. Cells were harvested at 4500 x g for 5 minutes at 4°C. 100 ml of TFB1 buffer was then used to re-suspend the cell pellet chilled on ice, with a further incubation of the cell suspension on ice for 5 minutes. The cells were then pelleted again as described previously. 10 ml of TFB2 was used to re-suspend the final cell pellet on ice and incubated for 1 hour. Finally, the cells were aliquoted into 50-100 µl aliquots and snap frozen in dry ice/ liquid nitrogen. Aliquots were stored at -80°C.

2.5.3 Purification of plasmid DNA from *E.coli*

Purification of plasmid DNA from *E.coli* was conducted from 5 mL of overnight culture using the QIAprep Spin Miniprep Kit (Qiagen) following manufacturers instructions.

2.6.0 Protein expression and purification

2.6.1 Transformation of plasmid DNA

An aliquot of 50 µl of competent *E.coli* cells were defrosted on ice before the addition of 100 ng of plasmid DNA of each protein and incubation on ice for 20 minutes. The reaction was stopped when the cells were heat shock in a 42°C water bath for 30 seconds and incubated on ice for a further 5 minutes. 450 µl of SOC media was added to the competent cells and incubated at 37°C for 30 minutes at a 250 rpm speed. The cell suspensions were streaked onto LB-agar plates inoculated with an antibiotic appropriate to the strain and plasmid (e.g. ampicillin 100 µg/ml) at 20 µl and 100 µl dilution. Plates were incubated overnight at 37^{o}C to allow colonies to grow.

2.6.2 Clathrin purification

Clathrin purification protocol was adapted from Rothnie *et al.* 2011 (Rothnie *et al.* 2011). Clathrin triskelia were purified from clathrin-coated vesicles extracted from eight frozen (liquid N_2) pig brains (approximately 600g) by differential centrifugation and gel filtration. The first step involves homogenizing the brains in a blender with HKM buffer with a protease inhibitor tablet. Following a low-speed spin at 12 000 × *g* for 30 min at 4°C, the supernatant of this is then ultracentrifuged at 140 000 × g, 45 min, 4 °C, to pellet lipid membrane components. This step was repeated to form 'double' pellet depending on the volume of supernatant in each prep.

The 'double' pellets were re-suspended in approximately 50 ml of buffer 1 and homogenized (>20 strokes). In order to isolate CCV need to remain in

the supernatant, hence the homogenate was then mixed with 6.25% Ficoll/6.25% sucrose buffer and spun at 44 000 × *g* for 20 min at 4 °C, leaving in the supernatant. A further ultracentrifugation step at 140 000 × g for 1 hour at 4 °C pelleted the CCV and allowed removal of the Ficoll/sucrose. The clathrin-coated vesicles were re-suspended in a small volume of HKM buffer and homogenized and spun in a microfuge to remove small cytoskeletal contaminants. The protein coats were stripped off of the lipids by mixing the sample with an equal volume of 2× 1M Tris buffer (1 M Tris, 1 mM EDTA, 2mM DTT, 0.02% sodium azide) and incubating for 1 hour at 4 °C, followed by centrifugation to remove most of the lipids at 135 000 × *g* for 20 min at 4 °C.

Clathrin was then purified by loading the supernatant after the last spin on a Sephacryl 500 HR column (GE) attached to an ÄKTA FPLC system (GE Healthcare). This column allows the separation of clathrin from remaining lipids in the sample and the various adaptor proteins present in coated vesicles. The fractions were analysed by SDS PAGE gel electrophoresis and the fractions containing the purest clathrin were pooled together and concentrated by adding an equal volume of saturated ammonium sulphate, which precipitated the protein and helped to remove contaminants before overnight storage in 4^{o}C.

The precipitated protein was isolated by centrifugation at 48,000 x g and re-suspended in a low volume of 1 M Tris buffer before dialysis into depolymerisation buffer for a minimum of 2 hours. Clathrin that failed to depolymerise was removed by centrifugation at 130,000 x *g*. The supernatant was the loaded onto a Superdex 200 HR column to clean it up and elute pure clathrin. The fractions containing pure clathrin were pooled and again precipitated with ammonium sulphate before overnight storage. Precipitated protein was then re- suspended as previously and dialysed into depolymerisation buffer for a minimum of 2 hours. The dialysis buffer was then switched to polymerisation buffer (pH 6.4) and left to dialyse over night with at least one buffer change. Polymerised clathrin was isolated after

centrifugation at 135,000 x g and re-suspension in polymerisation buffer.

2.6.3 SDS poly acrylamide gel electrophoresis

Gels were cast using a 12 % resolving gel and a 4 % stacking gel for use in a Mini-PROTEAN® system (Bio-Rad). Samples were diluted 1:1 with gel loading dye (x2) and incubated at 37^{o}C for 10 minutes before loading onto the gel. Gels were run at 160 V (~50 mA) for 1 hour or until the dye front reached the bottom of the gel. Gels were stained using Instant Blue Quant LAS 4000 from GE. Protein purity was analysed by running SDS PAGE after purification and for V2R expression. SDS PAGE was used to analyse all the ultracentrifugation/GST pull-down experiments.

2.6.4 Western blot analysis

Appropriate samples were sonicated to lyse the cells in the pellet and break down genomic DNA. After resolving by SDS-PAGE as described protein was transferred to a methanol activated PVDF membrane using a Mini Trans-Blot® system (Bio-Rad) or a semi-dry system (Sigma, UK). Transfer was conducted in NuPAGE buffer for a period of 90 minutes at 160 mA or 2 hours for 200 mA for semi-dry transfer. After transfer the membrane was blocked using a 5 % w/v milk powder TBS-tween solution overnight at 4°C. The membrane was washed thoroughly with TBS-Tween before 1 hour incubation with anti-His antibody (Cell Signaling) in 5% w/v milk (1:1000 dilution). The membrane was then rinsed with 3 successive 15 minute PBS-tween washes before incubation with secondary IgG mouse antibody (Cell Signalling) in 5 % w/v milk powder PBS-tween (dilution of 1:2000) for 1 hour. The membrane was then rinsed with 3 successive 15 minute PBS-tween washes before imaging. Finally, the membrane was washed with ECL reagents as per manufacturers instructions. Image Quant LAS 4000 (GE) was used to image the membrane.

2.6.5 GST-fused protein expression and purification

2.6.6 GST β-Arrestin $1L_{1-418}$ WT and Mutants

Expression: Single colonies from overnight LB/AMP plates were picked to produce 10ml overnight cultures (6x) with 100 µg/ml of ampicillin of the GST β-arrestin 1L WT or mutants. Those overnight cultures were then used to infect 6 x 400ml LB media (total of 2.4 liters). The cultures were incubated at 37^{o}C, 240 rpm and 1mM IPTG was added to each culture after the OD_{600} had reached 0.7-0.9. Post-induction, the cultures were incubated at 160 rpm at 16^{o}C, overnight. The cells were harvested at 4,000 x *g* for 10 min before re-suspending the cell pellets with PBS and storage at -80^{o}C.

Purification: Glutathione (GSH) affinity chromatography and Superdex 75 size exclusion chromatography column were used to purify the protein, using an ÄKTA FPLC system. The purification protocol was adapted and changed from (Nobles *et al.,* 2007). The plasmid constructs were transformed as described in section 2.6.1. The 5 ml expressed pellet was then re-suspended in CB1 buffer, pH 8.0 with protease inhibitor tables and lysed by sonication 5 x 15 sec. Cell debris was removed by centrifugation at 44,000 x *g* for 20 minutes and the supernatant loaded onto a GSTrap FF column. The GST β-arrestin 1L was eluted after running the 10mM GSH elution buffer, pH 7.2. Excess GSH was removed by dialysis against CB1 buffer and addition of Prescission Cleaving Enzyme (Sigma) (2 Unit/100 µg protein) for cleavage of the GST tag for all the β- arrestin 1L mutants, where necessary. The sample was dialysed at 4^{o}C overnight. After cleaving, the sample was loaded on the GSTrap FF column (GE) again to separate the cleaved protein from the un-cleaved. The same procedure was carried out as above with he GST elution buffer. The fractions containing the cleaved protein were concentrated to approximately 1-2 ml and loaded on a Superdex 75 size exclusion column (GE) for further purification. The eluted fractions were concentrated by centrifugation to 1ml. The sample was snap-frozen and stored at -80^{o}C. The protein was quantified as per section 2.8.0.

2.6.7 GST- auxilin$_{401-910}$ WT

Transfection of *GST*- auxilin$_{401-910}$ was carried out as in section 2.6.1. The expression was carried out as per GST- β-arrestin 1L$_{1-418}$ with the exception of 25^{o}C overnight incubation of the induced cultures. The GST tag of the GST- auxilin$_{401-910}$ was removed using digestion with thrombin (Sigma) for 3 hours at a ratio of 1 unit/10 µg protein. The cleaved auxilin and GST tag were separated by GST affinity chromatography in Buffer A, where the GST tag was eluted in GSH elution Buffer A. The cleaved auxilin was concentrated by centrifugation, snap-frozen and stored at -80^{o}C. The protein was quantified as described in section 2.8.0.

2.6.8 GST- β2HA$_{695-983}$ WT

GST-β2 adaptin$_{695-983}$ was transformed and expressed as per the GST- β-arrestin 1L$_{1-418}$ above with the exception of 25^{o}C overnight incubation of the induced cultures. PreScission Cleaving Buffer enzyme was used to cleave the GST tag. The purification was only by GST affinity chromatography as per the *GST- auxilin$_{401-910}$*. The protein was quantified as per section 2.8.0

2.6.9 GST- N-*terminal* domain (TD)$_{1-363}$ WT

The clathrin TD$_{1-363}$ WT were transformed as described in section 2.6.1. A total of 800ml LB media, 10ml overnight cultures, 100 µg/ml of ampicillin was used to grown up to an OD$_{600}$ of 0.7-0.8 while incubating at 37^{o}C, 240rpm. The cultures were induced with 0.1 mM IPTG and grew overnight at 25°C, 160rpm. The 5ml expressed pellet was then re-suspended in CB1 buffer, pH 8.0 with protease inhibitor table and lysed by sonication 5 x 15 sec. Cell debris was removed by centrifugation at 44,000 x g for 20 minutes and the supernatant loaded onto a GSTrap FF column. After loading on the column, the GST-TD$_{1-363}$ was purified as per the *GST- auxilin$_{401-910}$* with the addition of 10 mM GSH. The GST tag was retained for use in pull downs via the affinity tag.

2.6.10 GST-tag purification

A pGEX6P3 (containing GST-tag) was expressed as per GST- beta arrestin 1L and purified using a GST affinity chromatography. The pure GST tag was eluted after the addition of the 10mM GSH Buffer CB1. This GST-tag was used as a control in binding assays and SPR experiments in the next chapters.

2.7.0 His_6 -fused protein expression and purification

2.7.1 His_6 –epsin1$_{1-575}$

The His_6 –epsin1$_{1-575}$ WT and mutants were transformed as described in section 2.6.1. The epsin1 was expressed in 2 x YT media of 2 liters in total at 37^{o}C for 4 hours with 1mM IPTG induction. The harvested cell pellets were re-suspended in buffer B with a protease inhibitor tablet spun at 50,000 x g for 30 minutes to remove lipid contaminants. The supernatant was loaded on a c0mplete His-trap column (Roche) and allowed binding to the column. A washing step was carried out before elution in 20 mM imidazole washing buffer and the His-tagged protein was eluted using 200 mM imidazole elution buffer. The fractions that contain the epsin 1 were dialysed overnight against base buffer to remove the imidazole and then concentrated and loaded on a superdex 200 size exclusion column. The fractions eluted from the Superdex 200 column, pure protein were pooled and concentrated by (centrifugation), snap-frozen and stored at -80°C. The protein was quantified as per section 2.8.0.

2.7.2 His_6 -Hip1RCC$_{346-655}$

The His_6 -Hip1RCC$_{346-655}$ was transformed as described in 2.7.1 and plated on Kanamycin and Ampicilin LB plates. The Hip1CC expression was carried out in LB media of 2.4 litres in total with 1 mM IPTG induction for 4 hours at 22^{o}C. Cell pellets (5ml) were re-suspended in buffer B with a protease inhibitor tablet spun at 50,000 x g to remove lipid contaminants. The

supernatant was loaded on a c0mplete His-trap column (Roche) and allowed binding to the column. A washing step was carried out before elution in 20 mM imidazole washing buffer and the His-tagged protein was eluted using 200 mM imidazole elution buffer. Those fractions containing the His-Hip1RCC were run on SDS-PAGE gel to confirm the purity of the protein before dialyzing overnight in base buffer (to remove 200mM imidazole) and concentrate to be stored for later use.

2.8.0 Protein quantification

The extinction coefficient of each protein (obtained from ProtParam (ExPaSy)) calculated from their amino acid sequence, was used along with the A280 readings from the NanoDrop ND-1000 Spectrophotometer (DE USA), to quantify GST and His – tagged proteins. Clathrin concentration was assayed by titration in 1M Tris-HCl buffer to disassemble cages into triskelia before assaying absorbance at 280 nm using a Cary 100 UV-Vis Spectrophotometer.

2.9.0 Analytical Techniques

2.9.1 Clathrin cage assembled with His_6-epsin1 WT

Clatrhin cages were disassembled at concentrations of 12 µM though dilution in 1 M Tris buffer and dialysis into DEPOL buffer pH 8.0 for a minimum of 4 hours with a buffer change (dialysis buffer volume ratio of 1:200). Disassembled triskelia were then assembled against POL buffer pH 6.4 with the addition of epsin 1 WT at a 30 µM concentration at a final volume of 100 µL, incubated at 4^{o}C overnight. Active β-arrestin 1L (30 µM) was then added to the clathrin cage:epsin complex to then visualize the complex in negative stain electron microscopy.

2.9.2 GST-pulldown binding assays

Glutathione Sepharose 4B beads (Sigma) (50 µl) were added to mini bio-spin® chromatography columns (Biorad) along with the different concentration of the GST- fused protein, for example GST- clathrin N-terminal domain at a constant concentration (e.g. 3 µM) and incubate for 10 minutes at 4^{o}C. This allows the immobilizion of the GST-fused protein on the GSH beads. The samples were then incubated at 4^{o}C for 1 hour after adding the appropriate HKM buffer pH 7.2 volumes and the non-GST tagged protein at appropriate concentration (different ratios), to allow binding of the 2 proteins before elution. The spin columns were washed 3 x with a buffer containing 1x Triton100% and centrifuged in a microfuge at 4^{o}C at 13,000 rpm for 30 seconds. The flow-through after the first wash was saved (supernatant) and subsequently discarded after each wash. This step was repeated 1 x more but this time using the normal HKM buffer pH 7.2 without Triton100%. The protein complex is eluted by the addition of 50 µl of 1x SDS loading dye and allowing the samples to denature before spinning to collect the proteins. The supernatant (unbound) and pellet (bound) samples (1 µg of protein) were analysed by SDS- PAGE in order to visualize the binding or lack of binding of the two-protein complex.

2.9.3 Ultracentrifugation binding assays

The purified 3-2 µM clathrin cages were either dialyzed overnight (where appropriate) in a suitable buffer with the adaptor (β-arrestin 1L) or just added to the β-arrestin 1L directly with incubation for 1 hour only. In the case of no dialysis, the sample containing 2 µM clathrin and increasing concentrations of β-arrestin 1L were incubated for 1 hour at 4^{o}C. The samples were spun using an Beckman benchtop ultracentrifuge (rotor TLA 120.0) for 30 minutes at 55,000 rpm. The supernatant (unbound) was then collected and the pellets (bound) were re-suspended with SDS loading buffer in a volume that will give a 5 folds more concentrated sample. SDS-PAGE gel electrophoresis was used to visualize the samples.

2.9.4 Surface Plasmon Resonance

Quantitative binding studies were carried out using the antibody indirect capturing method (IAC) on a BIAcore 2000 SPR instrument. In general, monoclonal anti-GST antibody (Sigma-Aldrich, USA) pH scouting was carried out using 3.0-5.5 pH range of 10mM sodium acetate to identify the ideal pH for capturing on the chip surface. The anti- GST mAb was then immobilized on a CM5 chip using an amine coupling procedure at 5 µl/min for 12 injections in 10 mM sodium acetate at pH 5.5 (about 16,000-18,000 response units (RU) for the 2 injection experiments and <400 RU for kinetic models) using a programmed procedure on BIAcore 2000 instrument (GE Healthcare, USA).

The anti-GST immobilized chips were then coupled with ~ 800-1000 RUs (with a 1:10 dilution of the anti-GST antibody) of purified pGEX4T2 clathrin-TD WT in buffer (10mM HEPES, 150 mM NaCl, 1mM TCEP, 0.05% Tween 20 pH 7.4) for competition experiments and ~ 20-50 RU for kinetic assays. Initially, binding experiments were performed using the indirect antibody capturing method to investigate the interactions the GST-clathrin TD WT with purified adaptor proteins (WT and mutant forms).

The GST- clathrin TD (ligand) were bound on already coupled (with anti-GST antibody) chips at 20 µl/min flow rate and 40 µl/min for kinetic runs with ~ 200 seconds on injection time, following an equilibration time of 1000 seconds. The adaptor protein (analyte) was then injected for ~ 200 seconds (3 minutes) following an ~ 500 seconds (8 minutes) of dissociation time, at room temperature (20-25 ^{o}C). The chip was regenerated (double injection) with 10 mM glycine HCl pH 3.0-2.0, with a flow rate 30 µl/min, for 30 sec. Where possible, each binding experiment was carried out with a series of three repeat trials on different flow cells, in a random order, with approximately the same anti- GST antibody immobilization (response units).

The SPR technique was further used as 2 – injection experiments, where different adaptors were injected one after the other to determine any competition or cooperate binding. After binding the anti-GST antibody on the chip as above and the GST- clathrin TD binding on the antibody with ~ 800-1000 RU, the first adaptor was passed over in the first injection ~ 200 seconds (3 minutes). A small equilibration time was followed with buffer, and the second injection followed with a different adaptor protein for ~ 200 seconds (3 minutes). Finally, the chip was regenerated as above. The order of the experiments was varied because we observed deterioration in the binding capacity for the GST-fused protein by the anti-GST on the chip in each run, even after successful regeneration. Chapter 5 contains more details on how SPR works and the optimization stages.

2.10.0 General analysis and plotting software

ÄKTA purifier FPLC system (GE healthcare) was operated by the UNICORN® 7.0 software. All graphs were generated using Microsoft Excel (2011) and GraphPad Prism 6.0. Manipulation of protein structural data and images was conducted using USCF Chimera (version 1.11). The visualization of negative stain micrograph was conducted using Image J (Fiji). SPR data analysis of kinetic models was carried out using BIAevaluation software version 4.1 of BIACORE. Word processing was conducted using Microsoft Word (2011). Figures were prepared using Microsoft PowerPoint (2011).

2.11.0 Negative stain Electron microscopy

Copper Formvar/carbon grids (300 mesh) glow-discharged (EMtech K100x unit) at 10mA for 30 seconds before the 5 µL of sample of clathrin only or clathrin with epsin and/or active beta-arrestin 1L was added at 0.5-1 µM concentration. The sample was incubated on the grid for 1 minute and the remaining sample was blotted from the grids using filter paper. The grids were then negatively-stained with the addition of 5 µl of uranium acetate

(2%) and air-dried for 30 seconds and excess uranium acetate was blotted away, prior to imaging. The JEOL 2011 with Gatan Ultrascan 4000 CCD were used to image and collect the data. Images of cages were taken at a range of x 20,000-30,000 magnification unless otherwise stated.

Chapter 3:

Protein Expression and Purification

3.0.0 Introduction

This chapter includes the results from purification methods of clathrin and adaptor proteins by column chromatography and the purity for the proteins were analysed by SDS-PAGE. Adaptor proteins were expressed in *E.coli* and purified via affinity tags while clathrin was purified from porcine brains. These purified proteins were used in binding assays, SPR and microscopy experiments detailed in the future chapters.

3.1.0 Clathrin purification

3.1.1 Formation of clathrin coated vesicles (CCVs)

The clathrin purification procedure was adapted from Rothnie *et al.,* 2011 (Rothnie *et al.,* 2011). Clathrin triskelia were purified from clathrin-coated vesicles extracted from eight frozen (liquid N_2) pig brains by differential centrifugation and gel filtration. The first step involves homogenizing the 600g of pig brains in a blender with HKM buffer (25 mM Hepes pH 7.0, 125 mM pottasium acetate, 5 mM magnesium acetate, 0.02% sodium azide and a protease inhibitor tablet). Following a low-speed spin (12 000 × g, 30 min, 4 °C) to further purify and collect the supernatant of this is ultracentrifuged at 140 000 × g, 45 min, 4 °C, to pellet lipid membrane components. This step was repeated to form a ‘double’ pellet if necessary.

The pellets were re-suspended in approximately 50 ml of HKM buffer and homogenized (>20 strokes). The clathrin coated vesicles need to remain in the supernatant, hence the homogenate was then mixed with buffer containing 6.25% Ficoll/6.25% sucrose and spun at 44 000 × g, 20 min, 4 °C. The Ficoll/sucrose is then removed by ultracentrifugation at 140 000 × *g* for 1 hour at 4 °C. The clathrin-coated vesicles were re-suspended in a small volume of HKM buffer and homogenized and spun in a microfuge to remove small cytoskeletal contaminants. The protein coats were stripped off of the lipids by mixing the sample with an equal volume of 2× 1M Tris buffer and incubating for 1 h at 4 °C, followed by centrifugation at 135 000 × *g* for 20 min at 4 °C to remove most of the lipids.

3.1.2 Size exclusion chromatography and dialysis

Following the centrifugation steps, size exclusion chromatography was used to separate clathrin from the remaining adaptor proteins. The supernatant after the previous spin was loaded on a Sephacryl S500 column equilibrated in 1 x 1M Tris buffer. This column allows the separation of clathrin from remaining lipids in the sample and the various adaptor proteins present in coated vesicles. The lipids were eluted at ~ 140 to 225 ml and clathrin was eluted at ~ 230 to 320 ml peak, following a 'adaptor tail' around 320 ml. Clathrin was concentrated by ammonium sulphate precipitation, which also helped to remove contaminants and preserve the protein overnight.

The pure clathrin was dialyzed overnight at 4^{o}C into depolymerization (DEPOL) buffer (20 mM triethanolamine pH 8.0, 1 mM EDTA, 1mM DTT, 0.02% sodium azide), which prevent large cage formation as it disrupts triskelia-triskelia formation before concentrated by ammonium sulphate precipitation. A superdex 200 size exclusion column was used to clean it up and elute the pure clathrin. This step removes low molecular weight contaminants with clathrin eluting as a single broad peak between 90-120 mL (Figure 3.1.2). Cages were formed *in vitro* by dialyzing overnight at 4^{o}C into polymerization (POL) buffer (100 mM MES pH 6.4, 15 mM $MgCl_2$, 0.2

mM EGTA, 0.02% sodium azide). The pure clathrin was harvested by centrifugation at 135 000 × *g* for 20 min at 4 °C to concentrate it and increase its stabilityas clathrin cages have formed and re-suspended in approximately 100-200 µl of POL and stored at 4 °C for long-term storage up to one month.

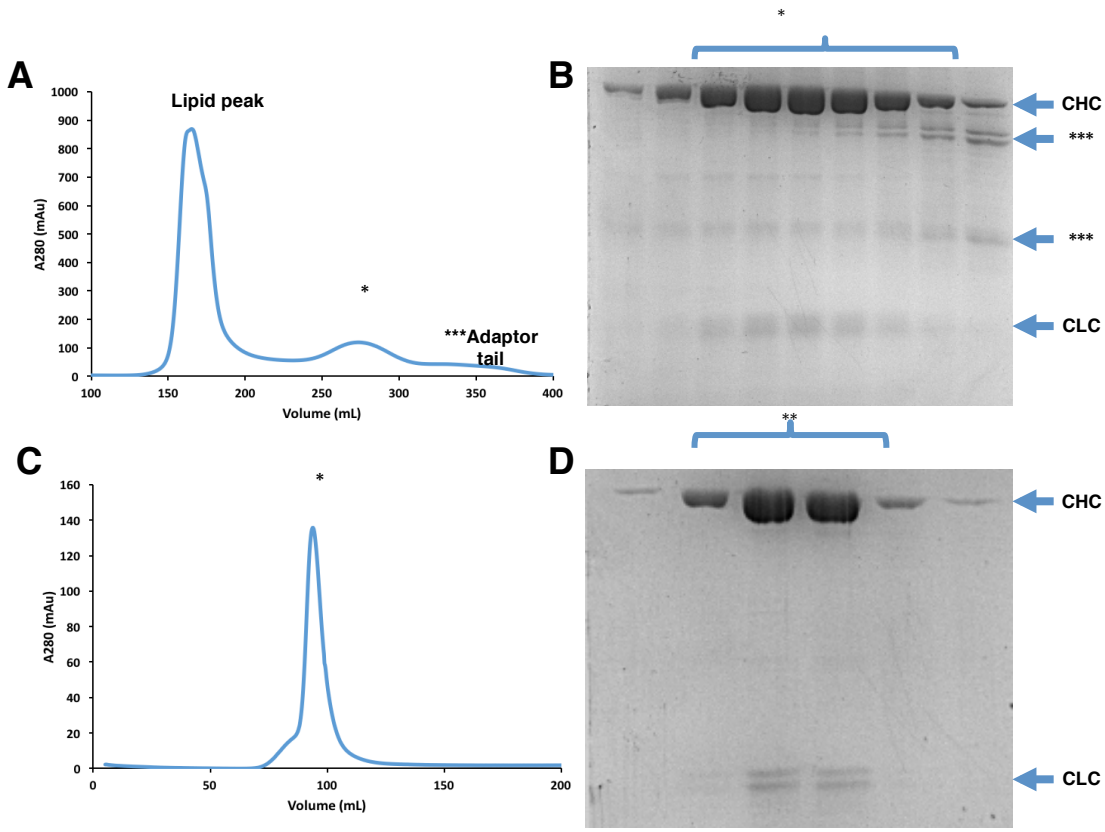

Figure 3.1.2: Clathrin purification by size exclusion chromatography monitored by the A280 absorbance (A, C) and SDS-PAGE gel analysis to confirm the presence and purify of the clathrin at each stage (B, D). (A) *A sephacryl 500 column was used to separate the lipids and the clathrin and adaptors. The lipids eluted between 140-225ml and clathrin elutes at 230-320ml with adaptors eluting 320-400ml. The fractions containing the clathrin (*) are run on SDS-PAGE gel* ***(B)*** *to confirm the presence of clathrin. Clathrin light chains (CLC) are also visible in these fractions. Those fractions were kept in ammonium sulphate overnight before they are loaded on the Superdex 200 column. Fractions also contain contaminants from adaptor proteins (***) **(C)** The clathrin heavy chain (CHC) elutes at 90-120ml as a broad peak (*). **(D)** These fractions were run on SDS-PAGE gel (**), before kept in ammonium sulphate overnight before the final purification stages of dialysing. Clathrin light chains (CLC) are also visible in these fractions.*

3.1.3 Purified clathrin quantification and concentration

To obtain an accurate absorbance measurement (280 nm) the pure clathrin in POL buffer is diluted in 1 M Tris buffer, pH 8.0 in a concentration titration curve manner, which will allow the fast disassembly of the clathrin cages to triskelia, which are easier to measure, reducing interference from light scattering caused by clathrin cage structures. The Beer's Lambert Law was used to determine protein concentration. Both light chains (CLCa and CLCb) were seen by SDS- PAGE analysis, however it is not clear what the relative abundance of each light chain (α and b) are in each clathrin prep. Mass spectrometry analysis could be an option to determine the exact amount ratios of CHC:CLCa:CLCb, even with the evidence that almost all CHCs are saturated with CLC (Girard *et al.,* 2005). However this is considered costly, therefore a 1:1 molar ratio of CHC to CLCb was used. Figure 3.1.3 illustrates an example of such clathrin quantification method using a Cary 100 UV-Vis Spectrophotometer with a yield of 84.4 µM, which is considered an optimal yield.

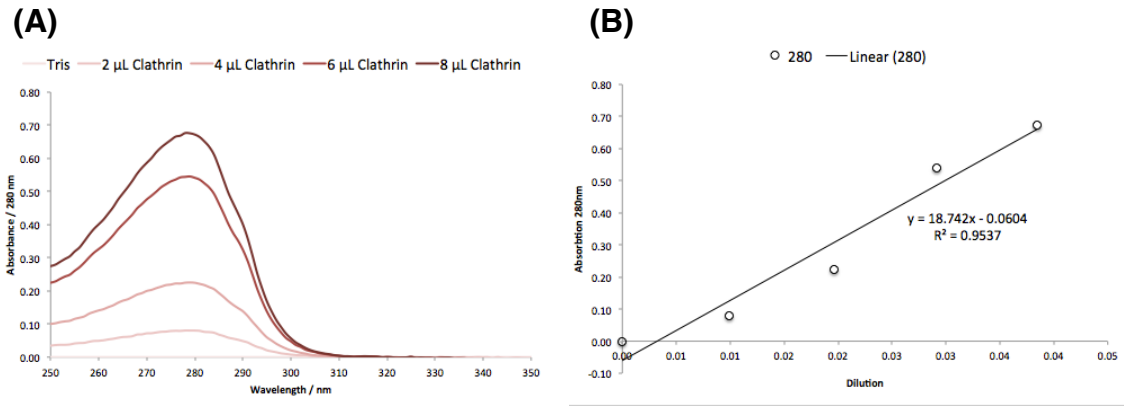

Figure 3.1.3 Quantification of clathrin via titration and absorbance at 280 nm. (A) *Increasing volumes of stock purified clathrin were diluted in 1 M Tris buffer measured at absorbance spectrum of 250 to 350 nm using a Cary 100 UV-Vis spectrophotometer from 2 to 8 µl). (**B**) The peak absorbance at 280 nm was plotted against the dilution factor to generate a standard curve. Beer's Law using the extinction coefficient= 222780 M^{-1} cm^{-1} to measure the pure clathrin concentration for CHC:CLCb, e.g. 84.4 µM in this example.*

3.2.0 Purification of GST-tagged proteins

Some of the adaptor proteins are GST-tagged. These include, GST- β-arrestin $1L_{1-418}$, GST-auxilin$_{401-910}$ and GST β2-adaptin$_{616-937}$(β2-HA), GST-clathrin TD_{1-363}, in pGEX4T-2 or pGEX6P-3 plasmids expressed and purified in *E. coli* cells. All of these proteins were initially purified using GSTrap FF affinity column with subsequent cleavage of the GST-tag using thrombin or Precission Protease Cleaving Enzyme. Size exclusion chromatography was only used for GST- β -Arrestin 1L.

3.2.1 Purification of GST-β-Arrestin $1L_{1-418}$ WT and mutants

BL21 (DE3) competent E. coli cells were transformed with the GST-β-Arrestin $1L_{1-418}$ WT or Mutants plasmids and the protein was expressed as described in Chapter 2. Following pelleting of the cells and lysis the cell debris by 4,000 x *g* for 10 min before re-suspending the cell pellets with PBS and storage at -80^{o}C, purification of GST-β-Arrestin $1L_{1-418}$ was carried out following the method of Nobles *et al.,* 2007. However, the protocol was modified by eliminating the use of a Hi-Trap ion exchange column and all data here is from protein purified without a Hi-Trap column. The reason for this change in protocol was that no significant increase in purity of the protein was observed after His trap purification and the added step also resulted in loss of protein.

The GST-β-Arrestin $1L_{1-418}$ constructs of WT and mutants in pGEX-6P3 plasmid were transformed and expressed as per section 2.3.2. The 5ml expressed pellet was then re-suspended in CB1 buffer, pH 8.0 with protease inhibitor tables and lysed by sonication 5 x 15 sec. Cell debris was removed by centrifugation at 44,000 x *g* for 20 minutes and the supernatant loaded onto a GSTrap FF column. The GST-β-Arrestin $1L_{1-418}$ was eluted after running the 10mM GSH elution buffer, pH 7.2 (Figure 3.2.1). Excess GSH was removed by dialysis against CB1 buffer and addition of Prescission

Cleaving Enzyme (Sigma) (2 Unit/100 µg protein) for cleavage of the GST tag for all the β-arrestin 1L mutants. The sample was dialysed at 4°C overnight. After cleaving, the sample was loaded on the GSTrap FF column (GE) again to separate the cleaved protein from the un-cleaved. The same procedure was carried out as above with the GST elution buffer (Figure 3.2.1). The fractions containing the cleaved protein were concentrated to approximately 1-2ml and loaded on a Superdex 75 size exclusion column (GE) for further purification. The eluted fractions containing GST- β-arrestin 1L eluted at ~ 35-45 ml were concentrated by centrifugation to 1ml and quantified (Figure 3.2.1). The sample was snap-frozen and stored at -80°C.

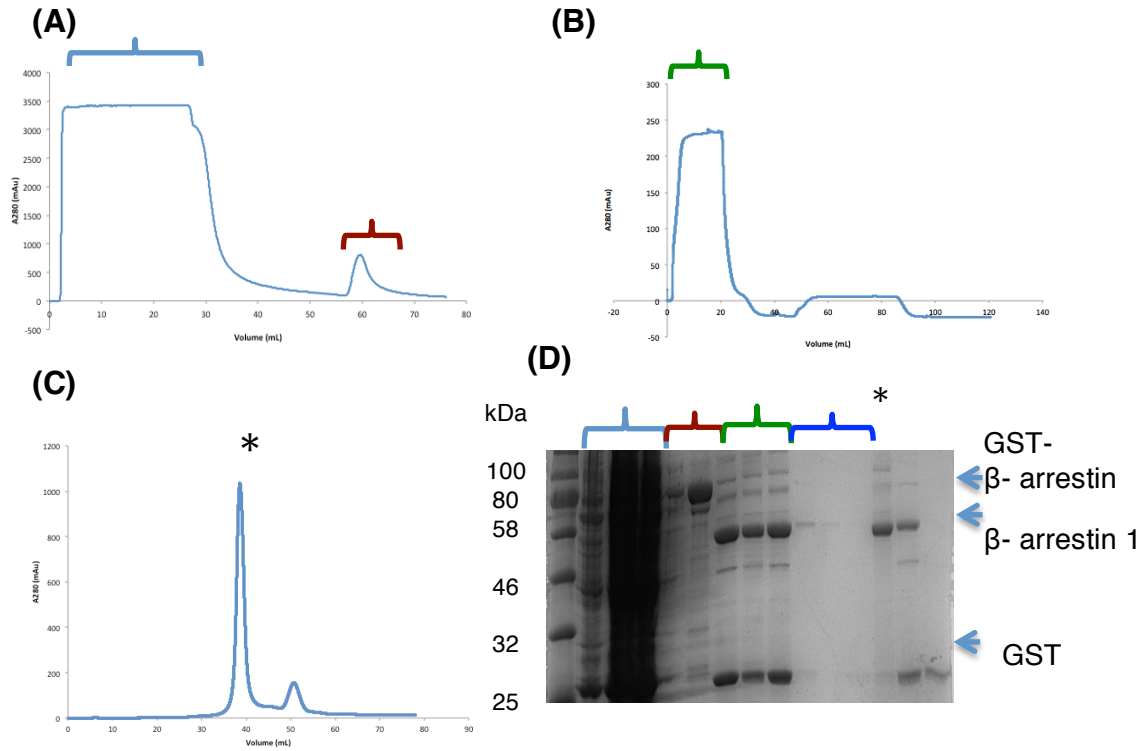

Figure 3.2.1 GST- β—arrestin 1L was purified by affinity and size exclusion chromatography (GST Trap FF and Superdex 75) as monitored by A280 absorbance (A,B,C) and by SDS-PAGE (D). (A) *The supernatant from lysed E. coli cells expressing the protein was loaded onto a GSTrap FF affinity column. The GST- β-arrestin 1L was eluted with GSH buffer (10 mM GSH). Those fractions were dialysed overnight against CB1 buffer with the addition of PreScission Protease Cleaving Enzyme to cleave the GST-tag.* ***(B)*** *The fractions containing cleaved beta-arrestin 1L were pooled together and concentrated before loading on Superdex 75 size exclusion column for further purification.* ***(C)*** *The cleaved beta-arrestin 1L was eluted at approximately 35ml. These fractions were pooled and concentrated for storage.* ***(D)*** *SDS-PAGE confirmed the purified β–arrestin 1L.*

3.2.2 Purification of GST- auxilin$_{401-910}$ WT

The GST- auxilin$_{401-910}$ was transformed and expressed as described in Chapter 2 section (2.7.1 and 2.7.6). The GST tag of the GST- auxilin$_{401-910}$ was removed using digestion with thrombin (Sigma) for 3 hours at 10units per 1 mg of protein per 1 mL, at 4^{o}C dialyzing against buffer A. The cleaved auxilin and GST tag were separated by GST affinity chromatography in Buffer A. The GST tag was eluted after the addition of 10 mM GSH elution buffer A, as shown in Figure 3.2.2. The cleaved auxilin was concentrated by centrifugation, snap-frozen and stored at -80^{o}C. The protein was quantified as described in section 2.9.0.

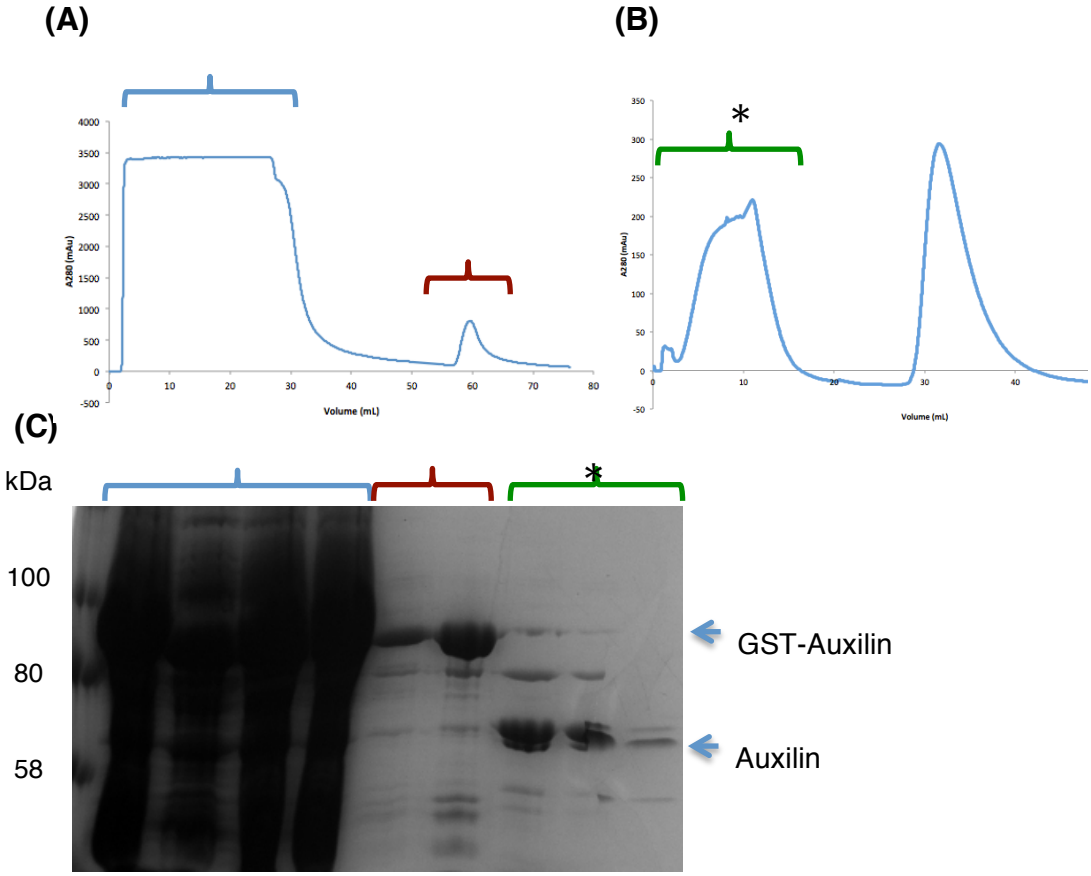

Figure 3.2.2 GST-auxilin by affinity chromatography as monitored by A280 absorbance and the protein purity was determined by SDS-PAGE analysis. (A) *Lysed pellets containing GST-auxilin were loaded on a GSTrap FF affinity column. GST-auxilin was eluted through the addition of 10mM GSH onto the column* ***(B)*** *Thrombin is added to those fractions containing GST-Auxilin to cleave the GST-tag, and fractions were dialysed for 3 hours against buffer A (remove GSH). This sample was loaded back onto a GST Trap FF affinity column and the cleaved auxilin was eluted in the flow through, was collected, concentrated and stored. The left over GST –tag was eluted by 10 mM GSH buffer A. (**C**) SDS-PAGE gel shows the cleaved auxilin after concentrated (*).*

3.2.3 Purification of GST β2-adaptin$_{616-951}$

GST-β2 adaptin$_{695-983}$ was transformed and expressed in the same manner as GST-β-arrestin 1L$_{1-\ 418}$ above with the use of the PreScission Cleaving Buffer enzyme to cleave the GST tag. The purification was carried out by GST affinity chromatography as per the GST- auxilin$_{401-910}$. Figure 3.2.3 show the purification traces and the SDS-PAGE gels confirming the protein purity. The concentrated protein was quantified as per section 2.9.0.

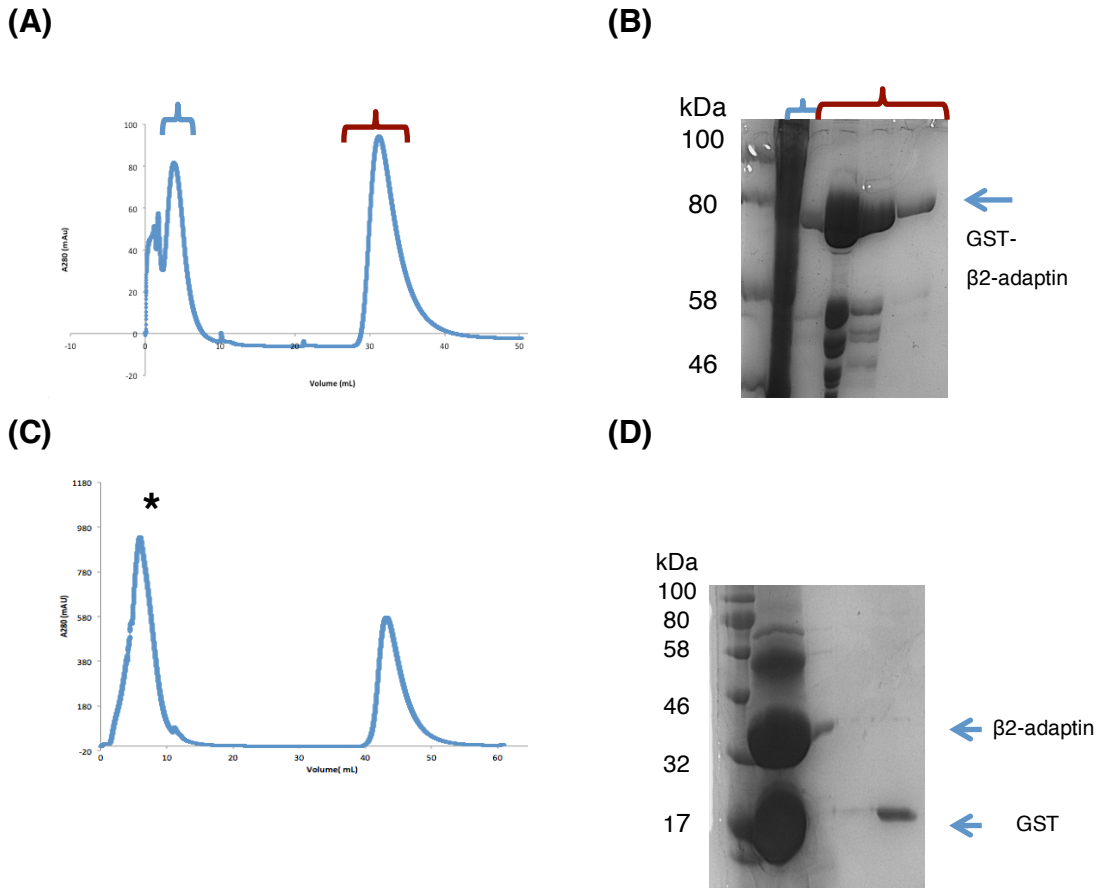

Figure 3.2.3 GST β2-adaptin by affinity chromatography as monitored by A280 absorbance, and SDS-PAGE analysis. The GST-tag was cleaved from the β2-adaptin and determined the protein purity by SDS-PAGE analysis. (A) *GST β2-adaptin collected after a GST-Trap FF affinity column, and pooled together to be concentrated and stored. (**B**) SDS-PAGE determine the presence of the GST β2-adaptin in those fractions. (**C**) GST β2-adaptin sample was dialysed overnight against buffer A to remove GSH and cleave the GST-tag using Precision Cleaving Buffer. This sample was loaded onto a GST Trap FF affinity column and the cleaved β2-adaptin was eluted, concentrated and stored. GSH buffer eluted the left over GST–tag. (**D**) SDS-PAGE determines the cleaved β2-adaptin, which was pooled and concentrated.*

3.2.4 Expression and purification of GST-TD_{1-363} WT

The clathrin TD_{1-363} WT were transformed as described in Chapter 2. The cell debris was removed by centrifugation at 44,000 x *g* for 20 minutes and the supernatant loaded onto a GSTrap FF column. After loading on the column, the GST-TD_{1-363} was purified as per the *GST- auxilin*$_{401-910}$ with the addition of 10 mM GSH (Figure 3.2.4). The GST tag was retained for use in pull downs and SPR via the affinity tag.

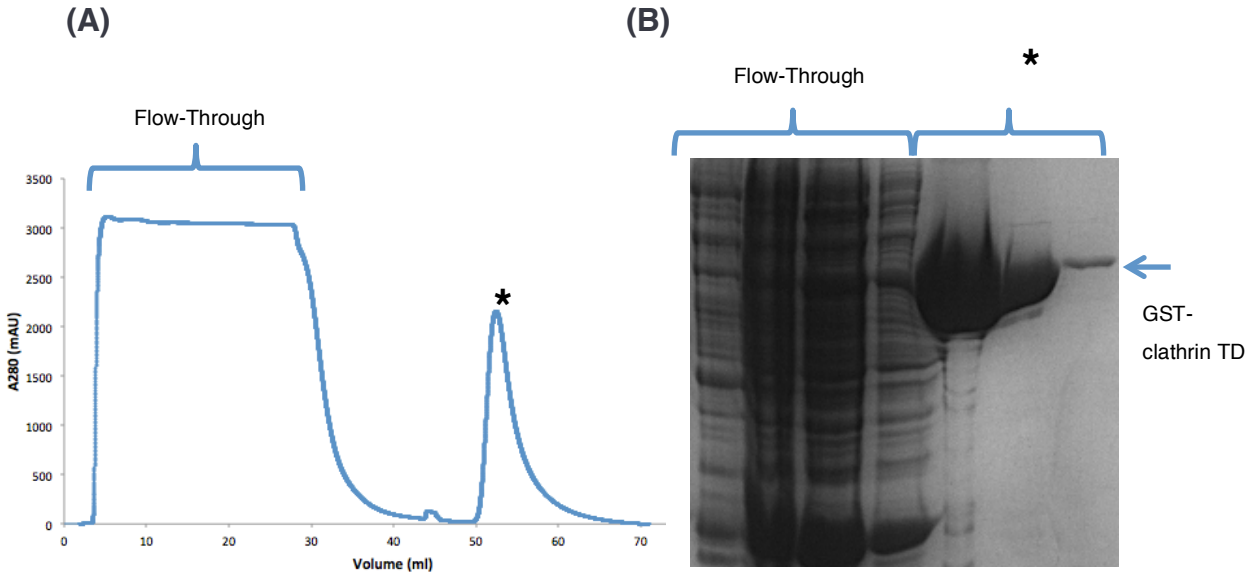

Figure 3.2.4 GST-TD was purified using affinity chromatography as per the absorbance of the A280, and the purity protein was determined by SDS-PAGE gel analysis. (A) *The supernatant of E.coli lysed cells from pellet expressing GST-TD was loaded on the GST Trap FF column. The flow-through was mainly non-binding proteins and the GST-TD was eluted after the addition of the GSH buffer. Those fractions (*) were pooled together, concentrated and stored appropriately. (**B**) SDS-PAGE gel confirming the presence and purify of those eluted fraction containing the GST-TD protein.*

3.2.5 Purification of GST-tag

A GST-tag (pGEX6P3 construct) was expressed as per GST- beta arrestin 1L and purified using a GST affinity chromatography. The pure GST tag was eluted after the addition of the 10mM GSH Buffer CB1 as shown in Figure 3.2.5. This GST-tag was used as a control in GST- pulldowns and SPR experiments in the next chapters.

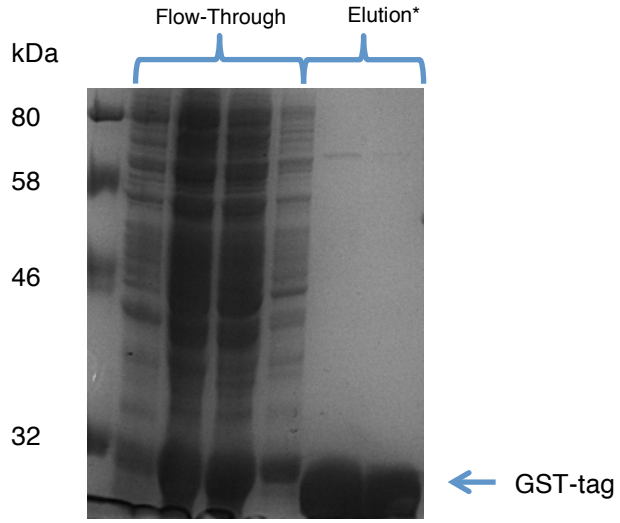

Figure 3.2.5: GST-tag was purified using affinity chromatography as per the absorbance of the A280 and SDS-PAGE gel determined the presence of the GST-tag. *The supernatant of E.coli lysed cells from pellet expressing GST-tag was loaded on the GST Trap FF column. The flow-through was mainly non-binding proteins and the GST-tag was eluted after the addition of the GSH buffer (data not shown). Those fractions (Elution*) were pooled together, concentrated and stored appropriately. The SDS-PAGE gel confirms the presence and purify of those eluted fraction containing the GST-tag.*

3.3.0 Purification of His_6 -tagged proteins

Three different proteins: His_6 $epsin_{1-575}$ (epsin 1) WT and six mutants, His_6 $Hip1RCC_{346-655}$ and $Hip1C_{361-637}$, were expressed in *E. coli* cells. A His-Trap affinity column was used for all the purifications initially. A size exclusion step using superdex 200 was followed to purify degradation products for epsin 1.

3.3.1 His_6 epsin 1_{1-575} WT and mutants

The His_6 –$epsin1_{1-575}$ WT and mutants (257, 480, DKO, ½ DPW, ¼ DPW, ΔDPW) proteins were transformed and expressed as described in section 2.7.5 in Chapter 2. Cell pellets (5ml) were re-suspended in buffer B with a protease inhibitor tablet spun at 50,000 x *g* to remove lipid contaminants. The supernatant was loaded on a c0mplete His-trap column (Roche) and allowed binding to the column. A washing step was carried out before elution in 20 mM imidazole washing buffer and the His-tagged protein was eluted using 250 mM imidazole elution buffer. The fractions that contain the epsin 1 were dialysed overnight against base buffer to remove the imidazole. Those fractions were then concentrated and loaded on a superdex 200 Size exclusion column. The fractions eluted (Figure 3.3.1) from the superdex 200 column, pure protein were pooled and concentrated by (centrifugation), snap-frozen and stored at -80°C. The protein was quantified as per Section 2.8.0. The expression and purification of epsin 1 257,480 and DKO mutants were conducted in the help of Dr. Michael Baker and Dr. Sarah Smith (WT), in some cases. Figure 3.3.1 is the elution profile and the SDS-PAGE gels of the WT epsin, which are representative of the 257, 480, DKO, ½ DPW, ¼ DPW, ΔDPW epsin mutants.

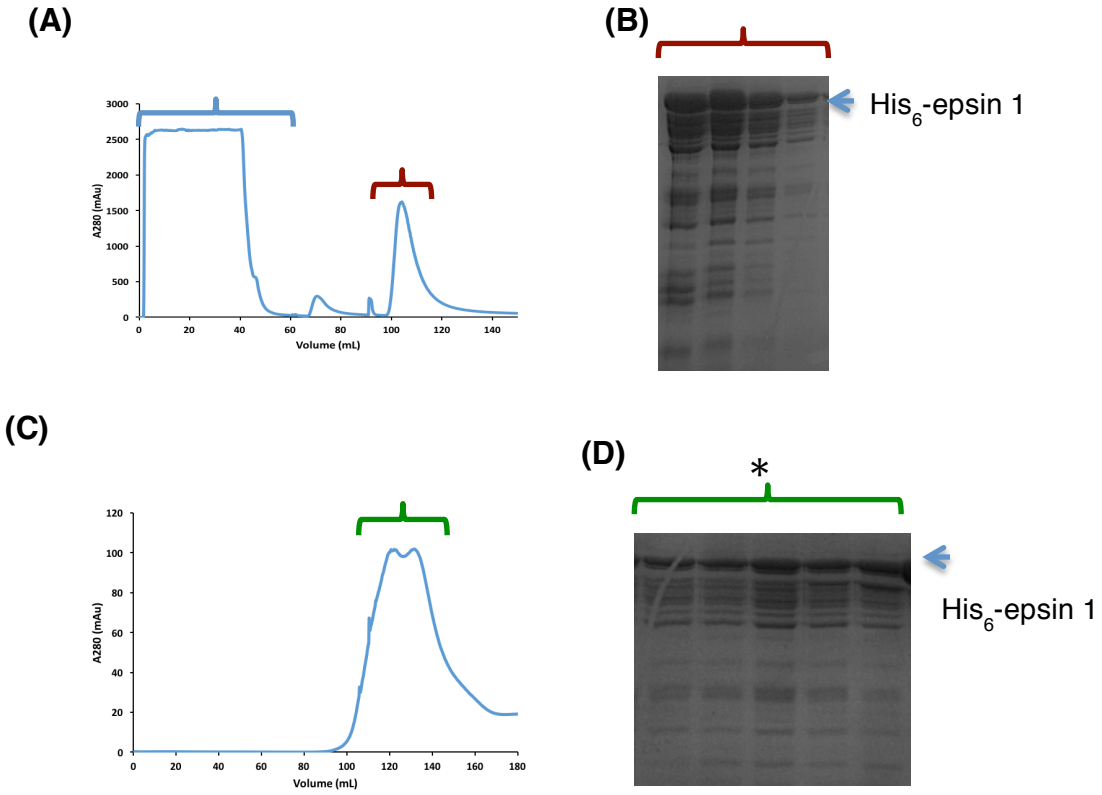

Figure 3.3.1: His_6 epsin 1 WT and mutants were purified by affinity and size exclusion chromatography (c0mplete His-Trap column and Superdex 75) as monitored by A280 absorbance (A,C) and by SDS-PAGE (B,D). (A) *The supernatant from E. coli lysed cells expressing the protein was loaded onto a c0mplete His-Trap affinity column. The flow-through was all the non-binding proteins mostly E.coli proteins. The His-epsin 1 was eluted with 200-250mM imidazole in base buffer. Those fractions of 10 ml each were dialysed overnight against base buffer to remove the imidazole. (**B**) The dialysed fractions presented on this SDS PAGE gel were concentrated before loading on Superdex 200 size exclusion column for further purification. (**C**) The His- epsin 1 protein was eluted at approximately 100-180ml. These fractions were pooled and concentrated for storage. **(D)** SDS-PAGE confirmed the presence of purified His-epsin 1 in those eluted fractions (*) of 10 ml each. These fractions were concentrated down to ~1ml before stored in -80°C.*

3.3.2 His_6 -Hip1RCC$_{346-655}$ and His_6 –Hip1CC$_{361-637}$

The His_6 -Hip1RCC$_{346-655}$ and His_6 -Hip1CC$_{361-637}$ expressions were carried out as described in Chapter 2. The purification was carried out from *E.coli* lysed cell supernatant that was loaded onto the c0mplete His trap column. The proteins were eluted through the addition of 200 mM imidazole (Figure

3.3.2 (A) and (B)). Those fractions containing the protein were run on SDS-PAGE gel before dialyzing overnight in base buffer (to remove 200mM imidazole) and concentrate to be stored for later use. Figure 3.3.2 shows the purification trace and the SDS-PAGE gel for the His_6 -Hip1RCC$_{346-655}$, which representative to the His_6 -Hip1CC$_{361-637}$ purification as well, which was conducted by Dr. Michael Baker.

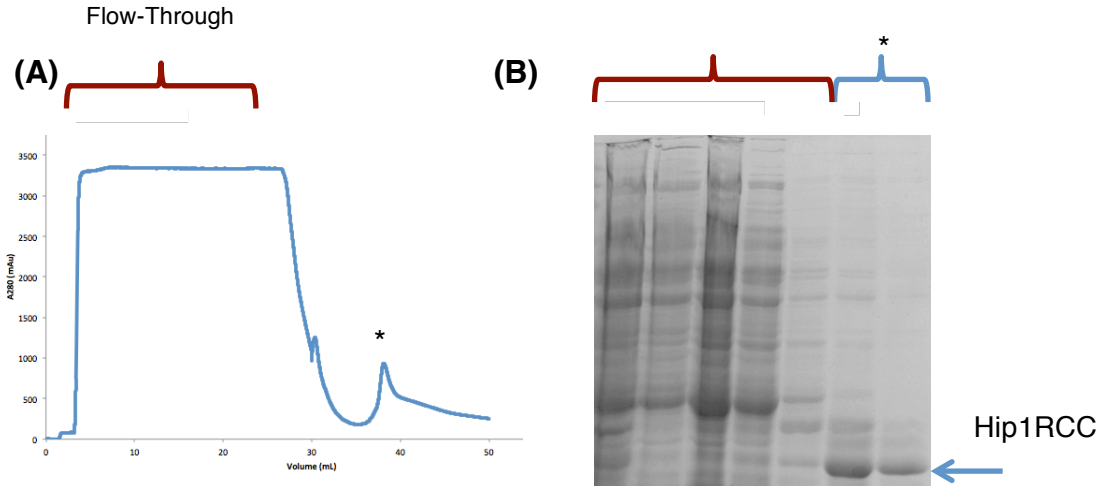

Figure 3.3.2 His_6- Hip1CC was purified by affinity chromatography (c0mplete His-Trap column) as monitored by A280 absorbance (A) and by SDS-PAGE (B). ***(A)*** *The supernatant from E. coli lysed cells expressing the protein was loaded onto a c0mplete His-Trap affinity column. The flow-through was all the non-binding proteins mostly E.coli proteins. The His- Hip1CC was eluted with 200-250mM imidazole in base buffer. The eluted protein fractions were pooled and concentrated for storage.* ***(B)*** *SDS-PAGE confirmed the presence of purified His-Hip1RCC in those eluted fractions (*).*

3.4.0 Protein quantification

The online tool, ProtParam (http://web.expasy.org/protparam/) was used to analyse the protein sequence of each adaptor protein. The extinction co-efficient listed in the Table 1.6.0 below were then used from there to derive the final concentration of the proteins using the Beer's Lambert Law. All purified adaptor proteins, except clathrin, were conducted using A280 absorbance determined using of a Nanodrop ND-1000 spectrophotometer.

Purified proteins	**Extinction co-efficient (M^{-1} cm^{-1})**
Clathrin (CHC:CLCb)	222780
GST- β-arrestin 1L WT or Mutants	62230
Beta-Arrestin 1L WT or Mutants	19370
Auxilin 1	58440
His_6 -epsin 1	97650
GST-clathrin TD	39420
His_6 -Hip1 (Hip1CC)	10095
His_6 -Hip1R (Hip1RCC)	2980
β2 adaptin (β2HA)	30035

Table 1.5.0: The extinction co-efficient used to calculate the purified proteins stated this chapter*. Extinction co-efficient were calculated from the protein sequence using the ProtParam online tool (http://web.expasy.org/protparam/).*

3.5.0 Conclusion

In this chapter I have documented each adaptor and clathrin successful protein expression and purification. The Table 1.7.0 lists the approximate purified concentrations (mg/ml) of these purified proteins (WT and mutants), used for all the experimental work in the future chapters of my thesis.

Proteins	Concentration (mg/ml)	Variants and Mutants
Clathrin (CHC:CLCb)	18 (40-80 uM)	WT
β-arrestin 1L	21.4	WT
β-arrestin 1L	40.7	Active
β-arrestin 1L	11.1	IVF-AAEA
β-arrestin 1L	25.1	WT-AAEA
β-arrestin 1L	4.6	IVF-ΔCB
β-arrestin 1L	18.3	WT-ΔCB
Auxilin 1	5.1	WT
GST- clathrin TD	60.0	WT
His_6 –epsin 1	3.3	WT
His_6 –epsin 1	2.7	257
His_6 –epsin 1	2.2	480
His_6 –epsin 1	3.0	DKO
His_6 –Epsin 1	14.2	½ DPW
His_6 –Epsin 1	7.7	¼ DPW
His_6 –Epsin 1	0.8	ΔDPW
His_6 -Hip1CC	0.7	WT
His_6 -Hip1RCC	2.8	WT
β2 adaptin (β2 HA)	34	WT

Table 1.6.0: All the purified WT and Mutant adaptor proteins used in this thesis along with their approximate concentrations (mg/ml) of the purified proteins.

Chapter 4: Optimisation of binding interactions between clathrin and adaptors

4.0.0 Overview

The aim of this chapter was to investigate the interaction between whole clathrin cages and clathrin N-terminal domain (TD) with the two adaptor proteins epsin 1 and β-arrestin 1L. In this chapter, I discuss experiments comparing different buffer compositions for optimal binding between β-arrestin 1 WT/mutants and whole clathrin cages using ultracentrifugation assays, and clathrin TD using GST- pulldown binding assays. I also explore the buffer/pH conditions for clathrin cages assembled with epsin 1 and β-arrestin 1L individually and in combination using binding assays and negative stain electron microscopy (EM).

4.1.0 Investigating clathrin cages: β-arrestin 1 interaction

4.1.1 Optimisation of clathrin cages: active β-arrestin 1L complex

The active form of β-arrestin 1L was used, as this mutant is hypothesized to bind strongly to clathrin due to its two accessible clathrin box motifs (Kang *et al.,* 2009). This mutant was used to investigate different buffer compositions and buffer pH for ideal β-arrestin 1L-clathrin cage complex formation using ultracentrifugation binding assays. It is important to note that, in previous work in this thesis, the purified active form of β-arrestin 1L demonstrated aggregation in solution and during overnight dialysis (data not shown) in different buffers other than its purification buffer.

A constant concentration of clathrin cages (2.5 μM) was incubated with a varying concentration of β-arrestin 1L from 10-40 μM, in HKM buffer (25 mM Hepes, 125 mM Potassium acetate, 5 mM Magnesium acetate, pH 7.2). The samples were incubated for 1 hour and centrifuged. The pellets, including the bound β-arrestin 1L:clathrin complex, were re-suspended in the HKM buffer and SDS-PAGE was used to analyse the bound and unbound samples. From the results in Figure 4.1.1 (A) and (B), we can observe that β-arrestin 1L is unstable at lower pH since lowering the pH (7.2) from its purification buffer pH (8.0) causes aggregation, causing the protein to pellet even when incubated alone. At pH 8.0 as clathrin is equally present in the pellet (Figure 4.1.1 (B), lanes 1) and in the supernatant (Figure 4.1.1 (B), lanes 2), compared to the equivalent lanes in Figure 4.1.1 (A). This is because at high pH the cages disassemble to clathrin triskelia (clathrin cage assembly at pH 6.4). Additionally, the active β-arrestin 1L appears to bind more favourably to the cages, possibly holding them together and hence we do not observe any clathrin in the supernatant (S) fractions in Figure 4.1.1 (A).

Overall, it was a challenging task to find the ideal conditions where both clathrin and β-arrestin 1L are stable due to contrasting favourable buffer and pH conditions. However, HKM buffer at pH 7.2 was the most appropriate buffer for both proteins. Lastly, these SDS-PAGE results revealed that the approximate saturation molar ratio between β-arrestin 1L and cages was 1:12, as observed in the Figure 4.1.1 (A) and (B), lanes 11 and 12), which formed the basis for the microscopy and SPR experiments carried out in this thesis.

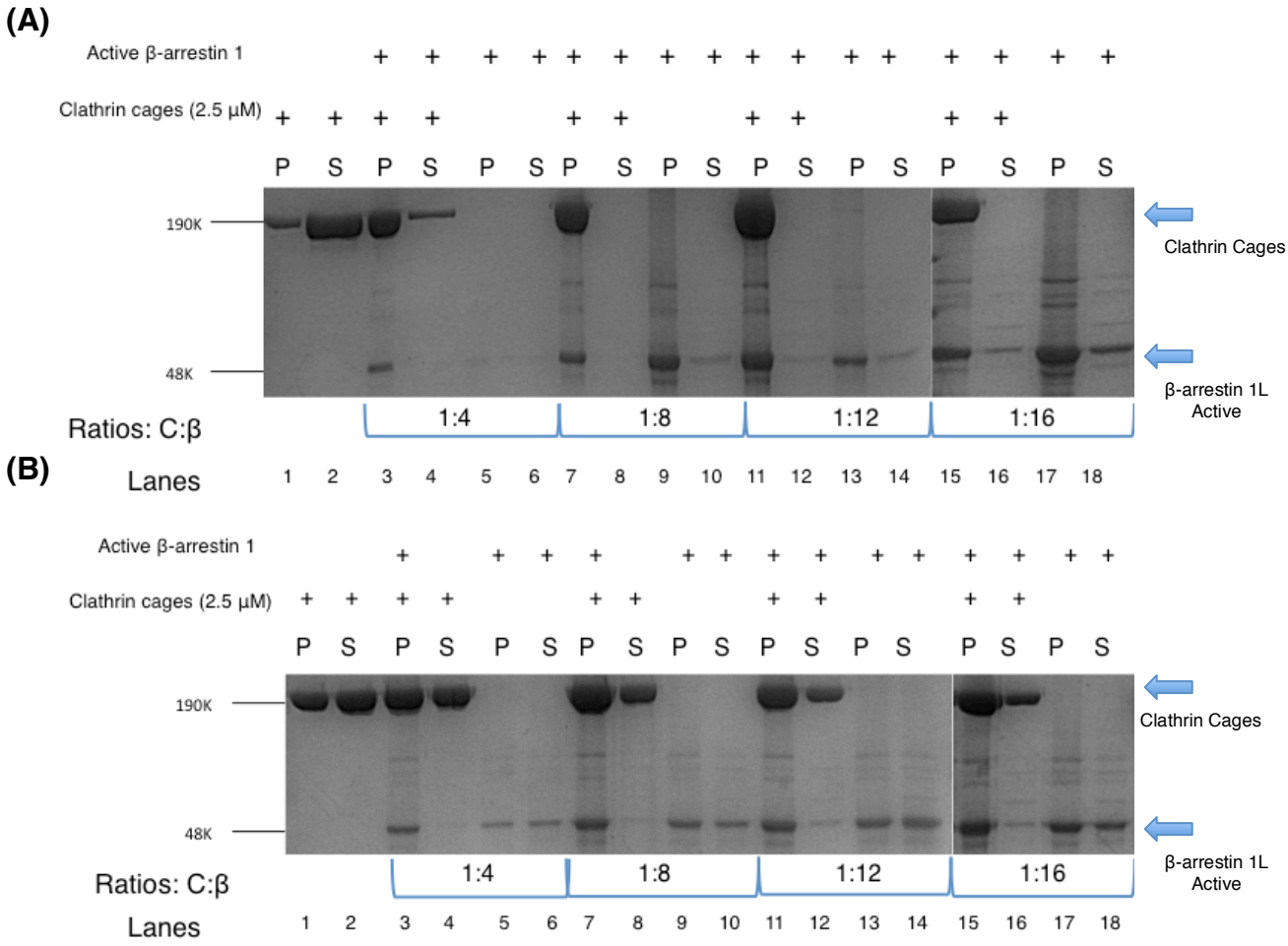

Figure 4.1.1: Ultracentrifugation binding assays were carried out showing saturation between β-arrestin 1L and clathrin cages in two different buffers*. Increasing concentration of β-arrestin 1L (10-40 μM) with constant clathrin cage concentration of 2.5 μM.* ***(A)*** *Binding assays were carried out in HKM buffer, pH 7.2. Clathrin cages have been shown to be more stable in this buffer due to its equal presence in supernatant (S) and pellet (P) fraction when alone. The optimal saturation between β-arrestin 1L and cages was 1:12 ratio.* ***(B)*** *Binding assays were carried out in β-arrestin 1L purification buffer, pH 8.0, which revealed the instability of cages due to its presence in pellet (P) fraction. The optimal saturation between β-arrestin 1L and cages was 1:12 ratio.*

4.2.0 Mutagenesis studies of β-arrestin 1L

The optimal buffer conditions for β-arrestin 1L:clathrin cages complex formation was HKM buffer, pH 7.2, as observed in the previous section. Using ultracentrifugation binding assays, I investigated interactions between β-arrestin 1L WT/mutants with clathrin cages (described in Chapter 2), using the optimized conditions in the previous section.

4.2.1 Investigating clathrin cages: β-arrestin 1L interaction

Ultracentrifugation assays were carried out between purified WT/mutants β-arrestin 1L proteins and clathrin cages in HKM buffer, pH 7.2. For each protein variant used, a constant concentration of clathrin cages (2.5 μM) was incubated with a constant concentration of β-arrestin 1L (30 μM) for a molar ratio of 1:12, which was the minimum concentration possible to reach binding saturation between the two proteins, as observed in the results from the previous section.

The results of such experiments demonstrated that the active form of β-arrestin 1L was shown to bind to clathrin completely as shown in lane 3 of Figure 4.2.1 (A), and the WT β-arrestin 1L binds with proportionally half as much, as seen in Figure 4.2.1 (B), lane 5. These results confirm the observations of Kang *et al.,* 2009, that the active β-arrestin 1L binds the strongest due to its two accessible clathrin box motifs on the opposite side in β-arrestin 1L structure, whereas the WT β-arrestin 1L binds less due to having only one accessible clathrin box motif.

The WT-ΔLIELD mutant showed a certain level of binding with clathrin cages, compared to the rest of the mutants, which showed no obvious binding to clathrin cages when compared with their control experiments in the absence of clathrin cages. The IVF-AAEA mutant was excluded from these experiments due degradation of the protein and which gave inconsistent results. It is important to note that all of the control experiments reveal β-arrestin 1L pelleting even in the HKM buffer, pH 7.2 (Figure 4.3.1 (A) and (B)). Interestingly, the presence of clathrin cages in the pellet in the presence of β-arrestin 1L WT or mutants compared to the control where no β-arrestin 1L is present (lane 1 and 2), could suggest that either β-arrestin 1L is causing clathrin to aggregate or it is holding clathrin cages together. These experiments were carried multiple times, but due to the consistent pelleting of β-arrestin 1L in the absence of clathrin, it was not possible to judge whether

arrestin was binding to clathrin or pelleting due to aggregation. Since the SDS-PAGE analysis has a limited dynamic range and gives largely qualitative results, a more quantitative technique, surface plasmon resonance (SPR) was later used to explore these interactions.

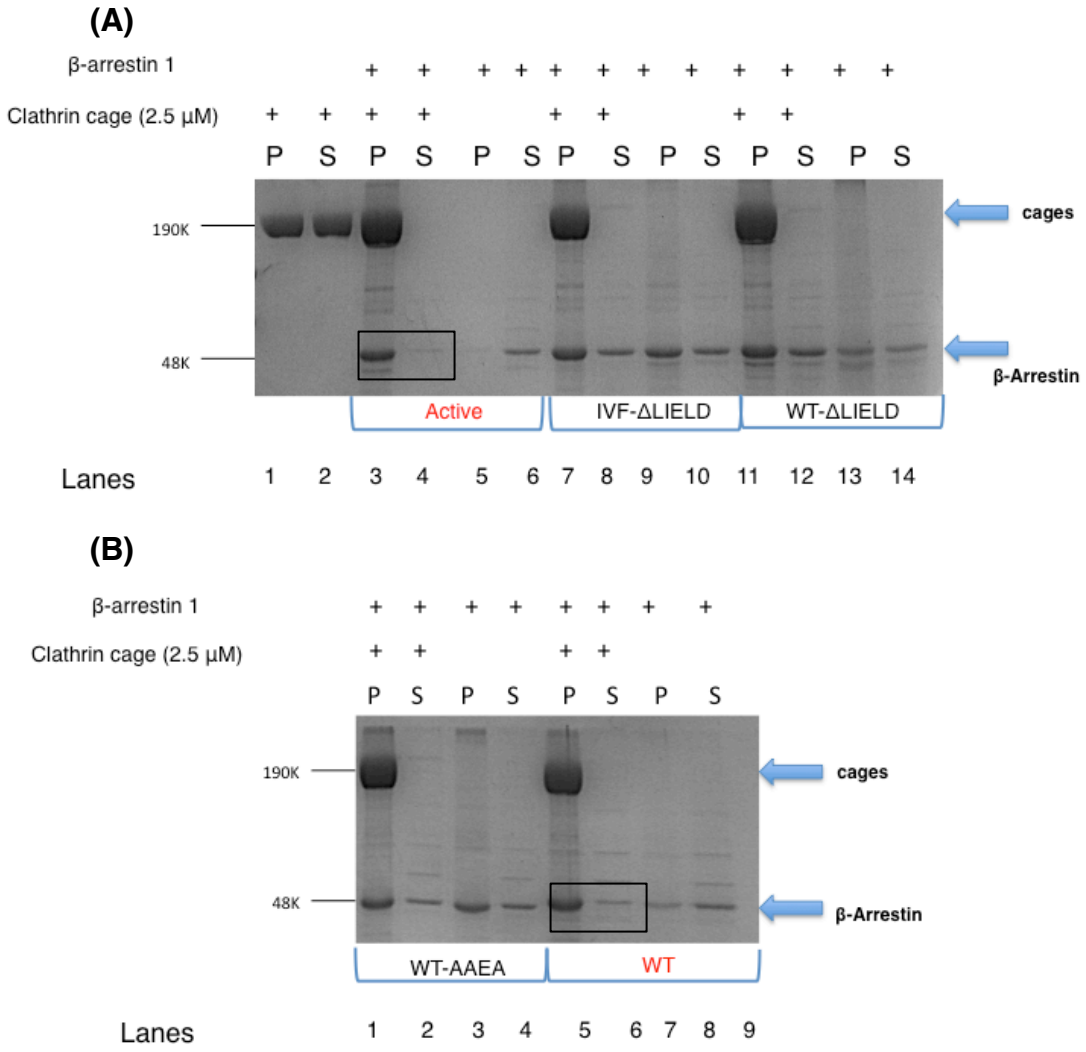

Figure 4.2.1: SDS-PAGE analysis from ultracentrifugation binding assays investigating β-arrestin 1L WT and mutants interaction with clathrin cages in HKM buffer, pH 7.2. *β-arrestin 1L is at 30 μM concentration and clathrin cages 2.5 μM concentration at a 1:12 molar ratio.* ***(A)*** *The active form of β-arrestin 1L was shown to bind to clathrin completely as shown in lane 3. There is no obvious binding between IVF-ΔLIELD mutant and clathrin cages except in the case of WT-ΔLIELD mutant, which a slight binding is observed.* ***(B)*** *WT β-arrestin 1L binds less to clathrin cages as seen in lane 5, compared to the active β-arrestin 1L in* ***(A).*** *Due to aggregation and pelleting of the β-arrestin 1L alone, such SDS-PAGE analysis revealed limited conclusive results. The IVF-AAEA mutant was excluded from these experiments.*

4.2.2 Visualization of clathrin cages: active β-arrestin 1L complex

Ultracentrifugation assays were carried out with clathrin cages (3 μM) bound to active β-arrestin 1L (30 μM) in polymerisation (POL) buffer pH 6.4 or HKM buffer pH 7.2. The results demonstrate active β-arrestin 1L present in the pellet with clathrin cages in both buffer conditions. However, active β-arrestin 1L aggregates and pellets when incubated in POL 6.4 buffer compared to HKM 7.2, as expected (Figure 4.2.2 (A)). Therefore, cages bound to active β-arrestin 1L complex in HKM pH 7.2 was considered the most appropriate sample to visualize the complex using microscopy.

Imaging was used to visualize the clathrin cages: active β-arrestin 1L complex. Negative stain transmission electron microscopy (TEM) microscope was used with 2% uranyl acetate as the negative stain and JEOL 2011 TEM. The samples were diluted in HKM buffer at pH 7.2, to a final concentration of 0.5 μM clathrin cages. The heterogeneous nature of clathrin cage structures was observed in Figure 4.2.2 (B) (black circles), with smaller cage (e.g. mini coat) and larger structures (e.g. barrel), which were also observed Figure 4.2.2 (C) as well after the addition of active β-arrestin 1L to the clathrin cages. The cage distribution is not altered by active β-arrestin 1L.

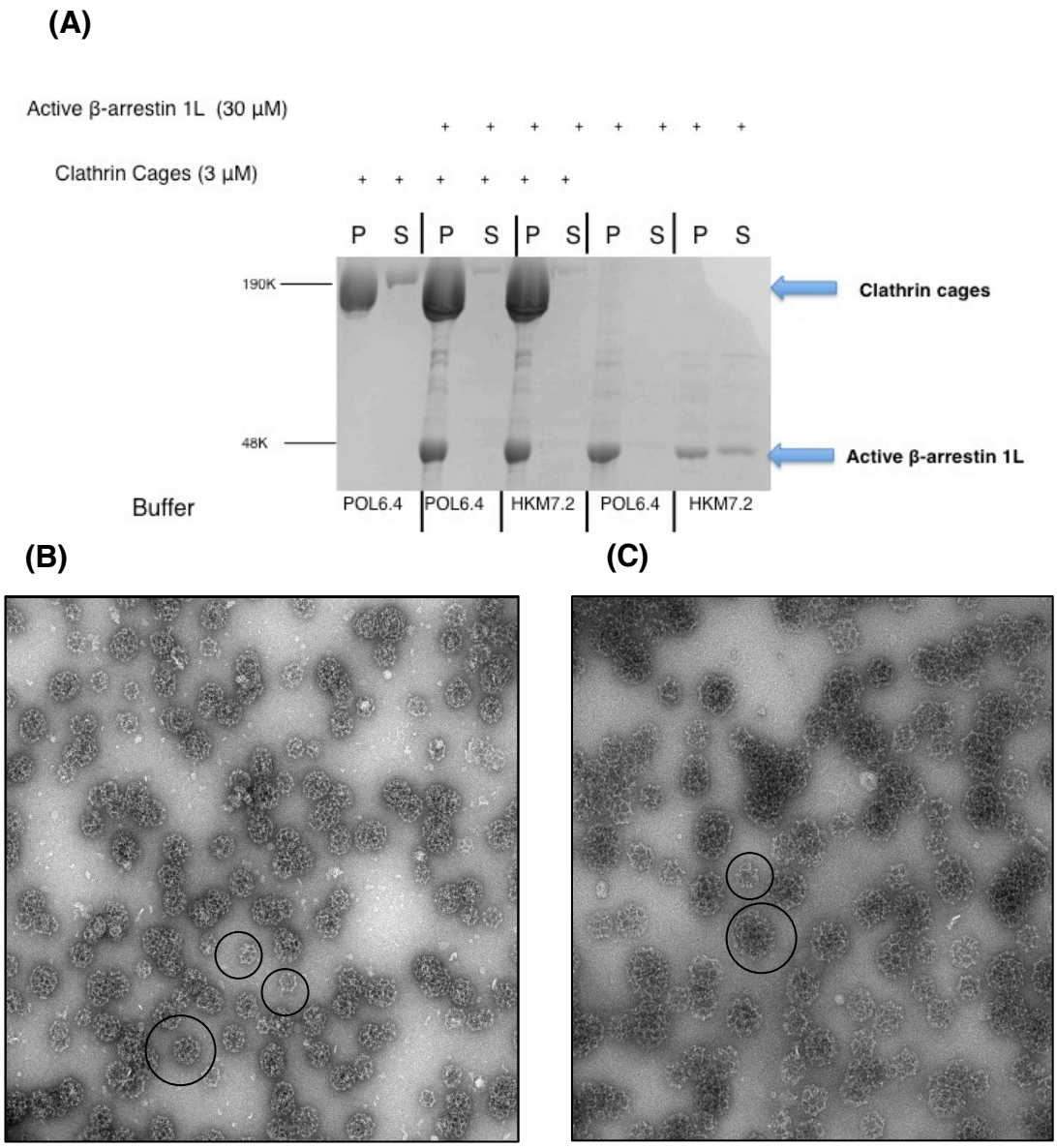

Figure 4.2.2: Analysis of clathrin cages: active β-arrestin 1L complex by SDS-PAGE from ultracentrifugation binding assays and negative stain electron microscopy*. SDS-PAGE analysis of ultracentrifugation binding assays of clathrin cages bound to active β-arrestin 1L in two different buffers (POL 6.4 and HKM 7.2) The ideal buffer for the cages: active β-arrestin 1L complex is the HKM 7.2 as demonstrated in the pellet (P) fraction (black square). (B) 2 % uranyl acetate was used as negative stain to visualise clathrin cages alone (B) and cages: active β-arrestin 1L complex (C) at a final concentration of 0.5 μM using HKM pH 7.2. The images are at 12000X magnification.*

4.3.0 Investigating β-arrestin 1L and clathrin TD interaction

Because of the uncertain results in the previous section for binding between purified WT and the five mutant β-arrestin 1L proteins and clathrin cages; an alternative approach to monitor binding was used. In this approach, binding to only the clathrin N-terminal domain (TD) was monitored using GST-pulldown binding assays between purified WT and mutant β-arrestin 1L proteins and GST-clathrin TD in HKM buffer, pH 7.2. These experiments were also used as the basis for the future SPR experiments in Chapter 6. A constant concentration of clathrin TD (2 μM) was incubated with beads prior the addition of a constant concentration of β-arrestin 1L (30 μM) WT and mutants at a molar ratio of 1:15, which was hypothesised to guarantee saturation between the two proteins, as the clathrin TD are significantly smaller particles with fewer binding sites than clathrin cages.

The results of these experiments demonstrated that the active form of β-arrestin 1L binds more strongly to clathrin TD as shown in lane 5 of Figure 4.3.0 (A), compared to the WT β-arrestin 1L in Figure 4.3.0 (B), lane 11. These confirm the above results with clathrin cages (section 4.2.1) with active β-arrestin 1L binding more strongly to clathrin, whereas the WT β-arrestin 1L binds significantly more weakly. The rest of the β-arrestin 1L mutants showed no specific binding to clathrin TD, as no β-arrestin 1L was observed in the pellet/bound samples on the SDS-PAGE (Figure 4.3.0(A) and (B)), compared to the β-arrestin 1L control experiments in absence of clathrin TD. The IVF-AAEA mutant has previously been shown to be prone to degradation, therefore the results in Figure 4.3.0 (B), lanes 1-4 could not be conclusive.

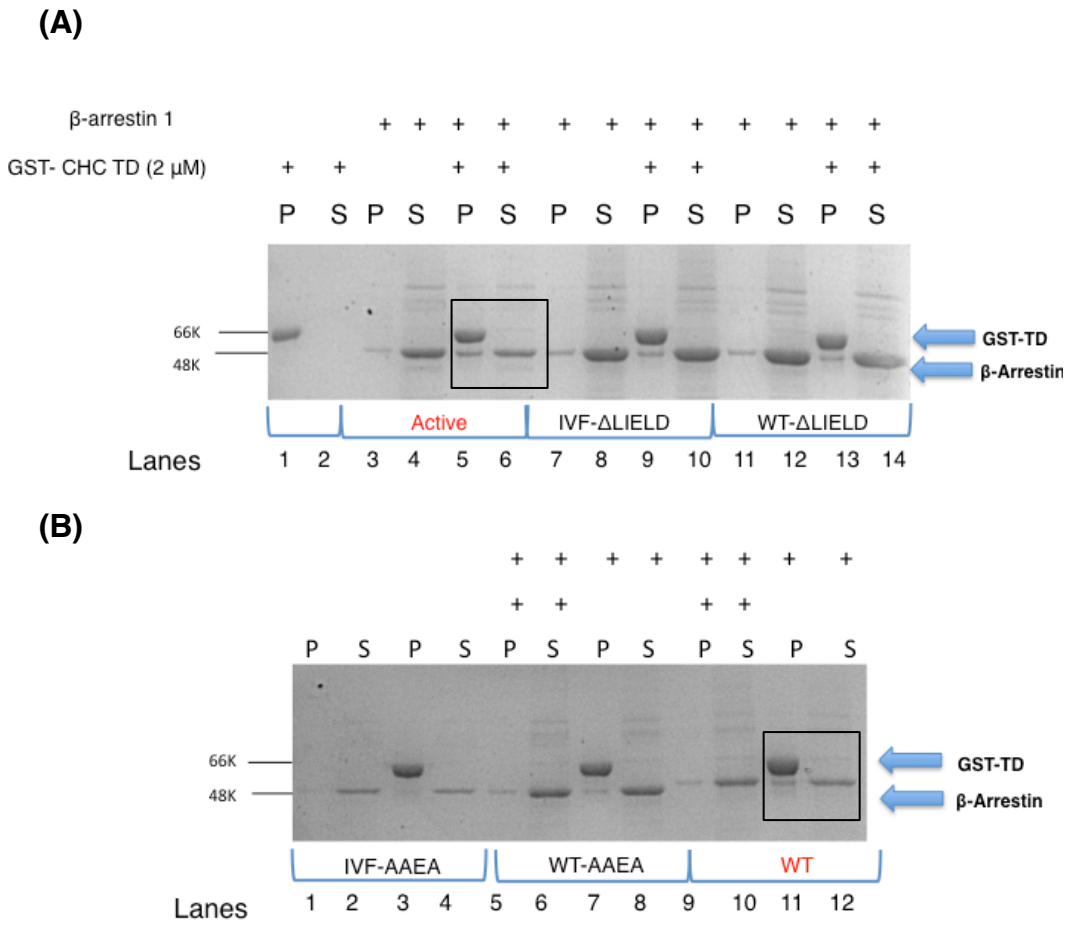

Figure 4.3.0: SDS-PAGE analysis from GST-pulldown binding assays investigating β-arrestin 1L WT and mutants interaction with clathrin TD in HKM buffer, pH 7.2. *β-arrestin 1L is at 30 μM concentration and clathrin cages 2 μM concentration at a 1:15 molar ratio.* ***(A)*** *The active form of β-arrestin 1L was shown to bind to clathrin TD completely as shown in lane 5. There is no obvious binding between IVF-ΔLIELD and WT-ΔLIELD mutants and clathrin TD is observed.* ***(B)*** *WT β-arrestin 1L binds less to clathrin TD as seen in lane 11, compared to the active β-arrestin 1L in* ***(A).*** *The IVF-AAEA and WT-AAEA mutants do not demonstrate any obvious binding with clathrin TD, as they are not present in the pellet fraction. The protein amount loaded on the gels was equal to 1 μg/ml for comparable reasons between all samples.*

4.4.0 Epsin 1 WT binding to clathrin TD

Epsin 1 WT adaptor protein is one of the key adaptor proteins in this thesis, therefore I confirmed its interactions with clathrin TD, which was used in ultracentrifugation binding assays, imaging and SPR experiments. The results demonstrate an increase in epsin 1 WT binding to clathrin TD with

increasing TD concentration, from 2 µM to 3 µM and a constant epsin 1 WT concentration of 10 µM (Figure 4.4.0, lanes 7 and 9).

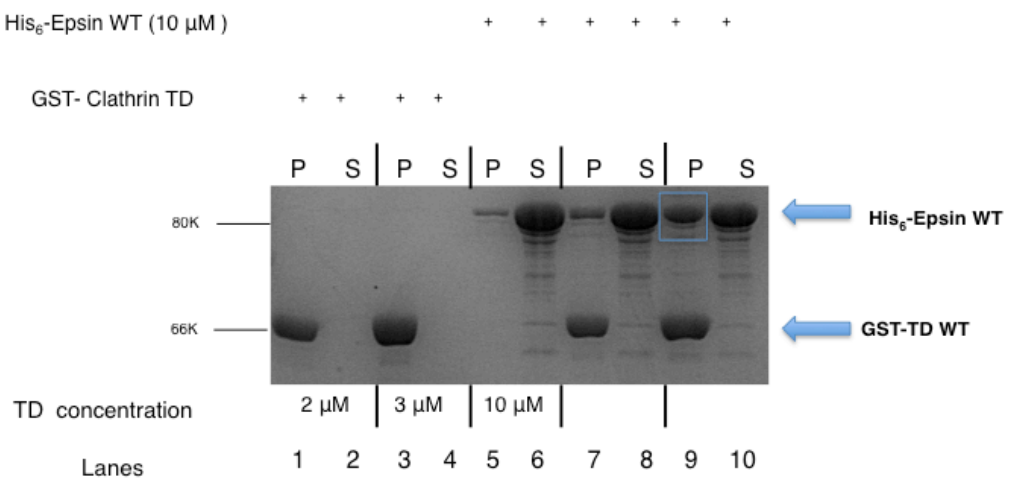

Figure 4.4.0: SDS-PAGE analysis from GST-pulldown binding assays investigating epsin 1 WT interaction with clathrin TD in HKM buffer, pH 7.2. *A constant concentration of epsin 1 WT is at 10 µM was incubated with increasing concentration of clathrin TD of 2 µM to 3 µM concentration. The successful binding of epsin 1 with increasing concentration of clathrin TD was demonstrated in lane 7 and lane 9, where the presence of epsin in lane 9 with 3 µM clathrin TD was stronger than in lane 7 with 2 µM clathrin TD. increasing concentration of clathrin TD.*

4.5.0 Clathrin cage: epsin 1 and β-arrestin 1L (C:E:β) complex formation

4.5.1 Optimization for C:E:β complex formation

Epsin 1, is an important clathrin assembly adaptor protein which has two clathrin box motifs (Drake *et al.,* 2000; Kalthoff *et al.,* 2002), like β-arrestin 1L. Prior to using SPR to investigate the binding interaction of clathrin with these two adaptor proteins in combination, I aimed to explore this interaction using whole clathrin cages assembled with epsin 1 and β-arrestin 1L.

GST-pulldown assays described in Chapter 2, were carried out to investigate whether epsin 1 WT and GST-active β-arrestin 1L interact with each other in the presence of GST beads. SDS-PAGE gels from such experiments illustrate no obvious interaction between these two proteins (Figure 4.5.1 (A)), at a 1:1 and 1:3 molar ratio. However, we cannot rule out the possibility

of transient interactions or interactions that may only occur in the presence of clathrin. Ultracentrifugation binding assays were then carried out, where clathrin cages were dialysed overnight with WT epsin 1 at 1:10 molar ratio of clathrin cages: epsin 1, in different buffer compositions and pHs. Active β-arrestin 1L was then added to the cages:epsin1 complex, at a concentration of 30 μM. The cages:epsin1:β-arrestin 1L complex was incubated for 1 hour prior centrifugation to separate bound and unbound (excess adaptors) in the samples. SDS-PAGE analysis was used to demonstrate the content of bound and unbound samples. Taking into account the challenging buffer composition and pH conditions between clathrin cages and β-arrestin 1L; the buffers used in the experiments were the polymerisation buffer (POL) at pH 6.4 (POL6.4) (ideal for clathrin cage formation) and HKM buffer at pH 6.4 (HKM6.4) and 7.2 (HKM7.2). HKM7.2 is a neutral buffer, which should provide optimum conditions for both clathrin cages and β-arrestin 1L.

Initially, control experiments were carried out in order to confirm the appropriate buffer for all three proteins separately. The results revealed that clathrin cages were most stable in their polymerisation buffer at pH 6.4 (POL 6.4) (Figure 4.5.1 (B), lane 1-2), and were less stable in POL 7.2 and HKM 7.2 (Figure 4.5.1 (B), lane 3-4 and 5-6). β-arrestin 1L is most stable in HKM7.2 (Figure 4.5.1 (B), lane 9-10), where an equal amount of β-arrestin 1L is observed both in the pellet and supernatant in the absence of clathrin. Finally, epsin 1 WT was most stable in POL6.4 and HKM7.2, but not in HKM6.4 (Figure 4.5.1 (C)). Overall, as seen in Figure 4.5.1 (C), lane 9, buffer HKM7.2 provided the best buffer for clathrin cages: epsin 1WT: active β-arrestin 1L complex formation at a 1:10:10 molar ratio.

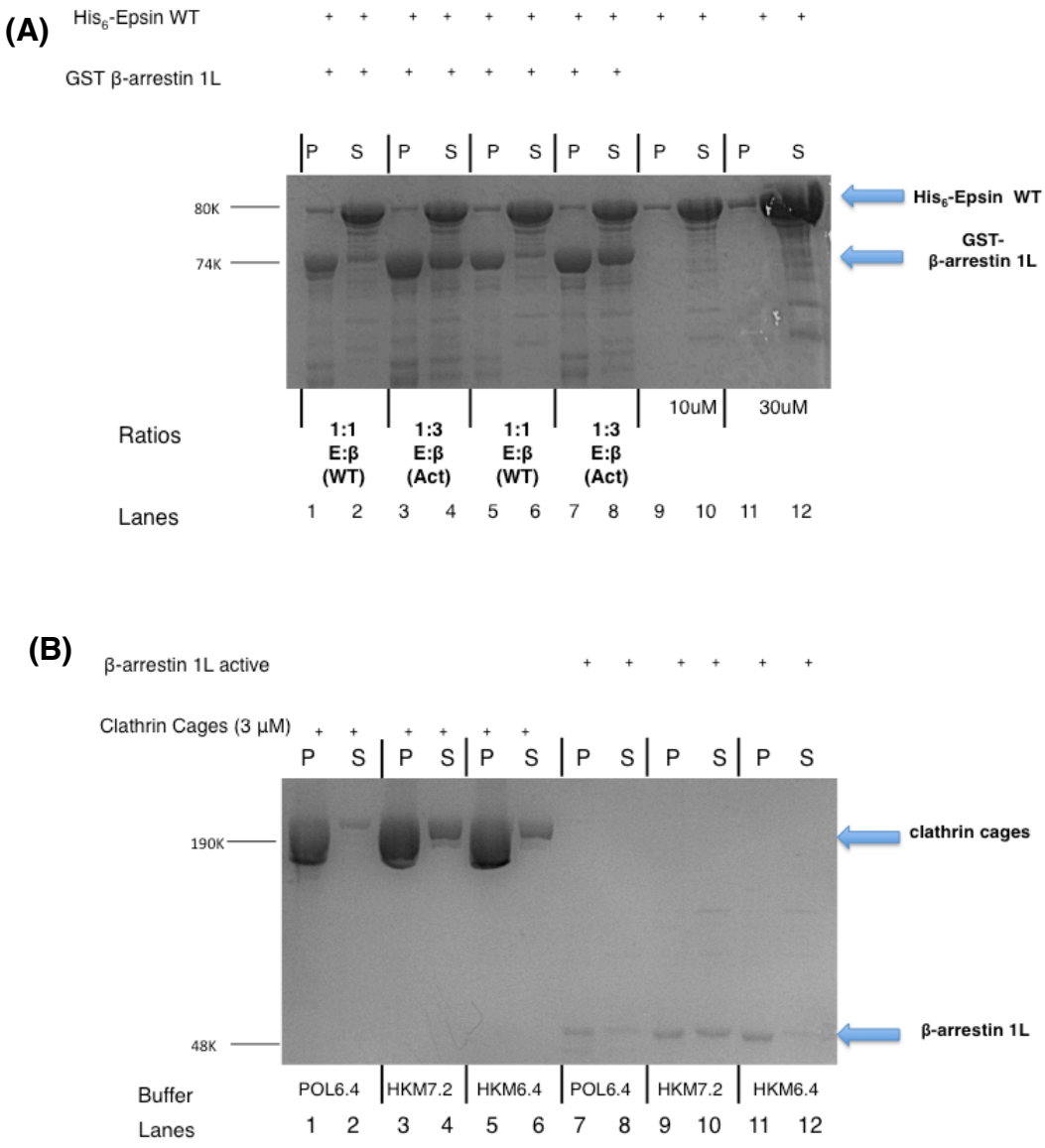
(A)
His6-Epsin WT
GST β-arrestin 1L
P S P S P S P S P S P S
80K
74K
His6-Epsin WT
GST-
β-arrestin 1L
Ratios
1:1
E:β
(WT)
1:3
E:β
(Act)
1:1
E:β
(WT)
1:3
E:β
(Act)
10uM
30uM
Lanes
1 2 3 4 5 6 7 8 9 10 11 12
(B)
β-arrestin 1L active
Clathrin Cages (3 μM)
P S P S P S P S P S P S
190K
48K
clathrin cages
β-arrestin 1L
Buffer
POL6.4
HKM7.2
HKM6.4
POL6.4
HKM7.2
HKM6.4
Lanes
1 2 3 4 5 6 7 8 9 10 11 12

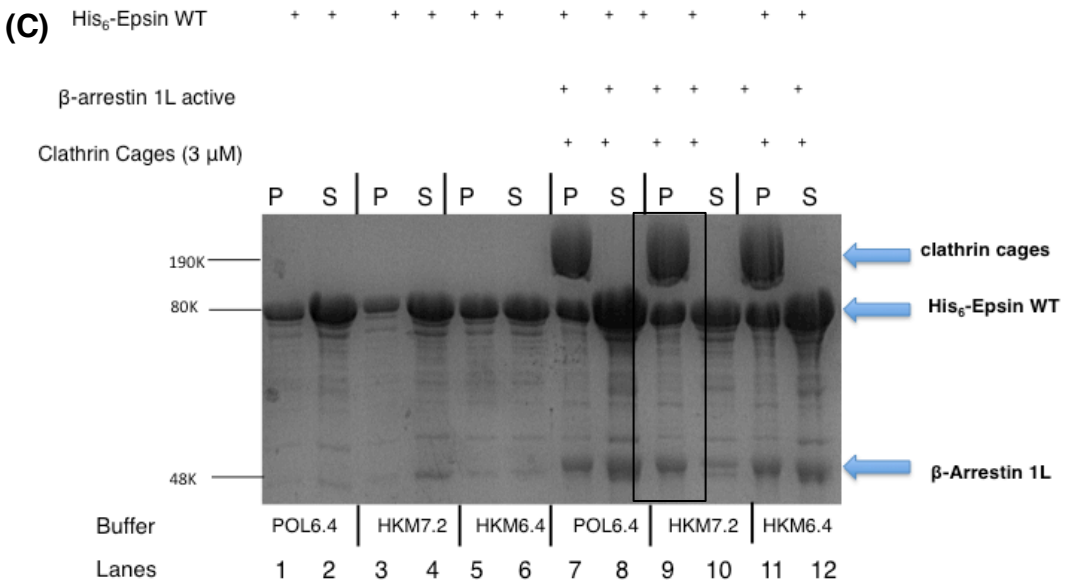

Figure 4.5.1: Analysis of binding interaction between epsin 1 WT and active β-arrestin 1L and between clathrin cages (3 μM), epsin 1 WT (30 μM) and active β-arrestin 1L (30 μM) interaction. (A) *The GST -pulldown binding assays revealed no obvious interaction between epsin 1 and GST- active β-arrestin 1L in the 1:1 and 1:3 ratios of epsin1: β-arrestin 1L. Ultracentrifugation binding assays were carried out to determine the ideal buffer and pH conditions. The buffers used were POL 6.4, HKM 6.4, HKM 7.2. The most stable clathrin cages were observed in POL 6.4 buffer as observed in lane 1-2* ***(B)*** *and active β-arrestin 1L was mostly stable in HKM 7.2 as observed in lane 9-10* ***(B).*** *The ideal buffer condition for the clathrin cages: epsin 1: active β-arrestin 1L complex formation was in buffer HKM, 7.2 which demonstrates the complete binding of active β-arrestin 1L and most of the epsin 1 in the pellet (P) fraction in lane 9* ***(C)*** *(black square).*

4.5.2 Imaging of C:E:β complex in different buffer conditions

The C:E:β complex formation was successfully repeated and revealed complete binding of epsin 1 WT and active β-arrestin 1L in the presence of clathrin cages in HKM 7.2 buffer (Figure 4.5.2 (A), lane 5). This sample was further analysed using negative stain transmission electron microscopy (EM). The images obtained were compared with images obtained for cages with epsin 1WT and active β-arrestin 1L (C:E:β) formed in the other buffer conditions (POL 6.4 and HKM 6.4). It is important to note that epsin 1 has been suggested to form uniform cage size distribution *in vitro* (Kalthoff *et al.,* 2002). The EM images obtained in this investigation showed the presence of numerous uniform sized clathrin cages in all POL6.4, C:E:β and HKM7.2,

C:E:β buffer conditions (Figure 4.5.2 (E) and (G)) with the exception of HKM6.4, C:E:β in Figure 4.5.2 (F) which does not show uniformity in the cage sizes. This confirms the action of epsin 1 as an adaptor protein that promotes uniform sized clathrin cages assembly, especially in POL6.4 as observed in Figure 4.5.2 (C), compared to clathrin cages in the absence of epsin 1 (Figure 4.5.2 (B)). However, active β-arrestin 1L has been demonstrated in previous sections using SDS-PAGE analysis, not to be stable in POL6.4; but only in HKM7.2 (Figure 4.5.2 (D)). Overall, the most homogeneous cage structures of the cages: epsin1: active β-arrestin 1L complex were in HKM7.2 buffer (Figure 4.5.2 (G)). Adaptor proteins are smaller than clathrin cages and any visible electron density at the edges of clathrin cages in the EM images could not be interpreted as being adaptor proteins without refinement of the images and further cryogenic investigation. Hence, the only confirmation of adaptor presence is via the SDS-PAGE gel analysis. Nevertheless, the result of this section provides a novel foundation for future cryogenic EM imaging of clathrin cage bound to two adaptor protein combinations, which has not been investigated before.

(A)

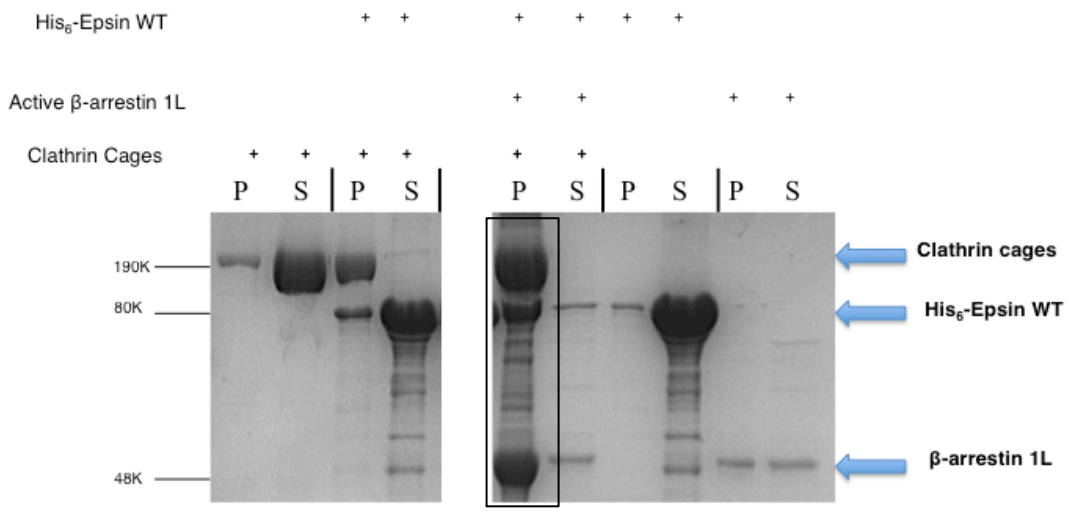

(B)

POL 6.4, **C only**

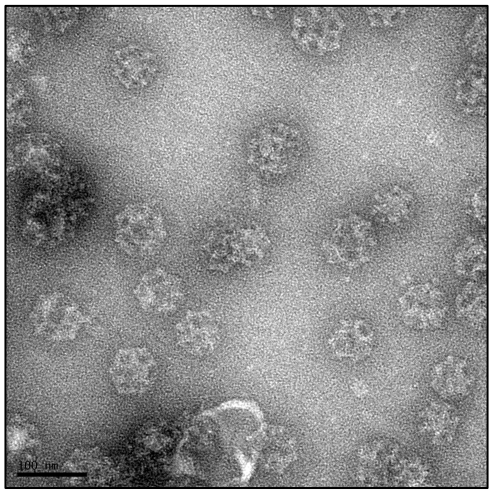

(C)

POL 6.4, **C:E**

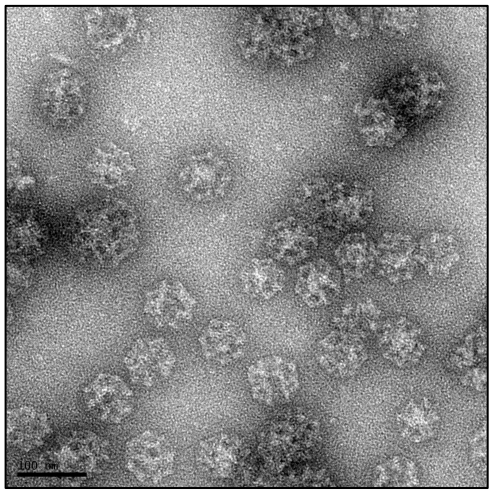

(D)

HKM 7.2, **C:β**

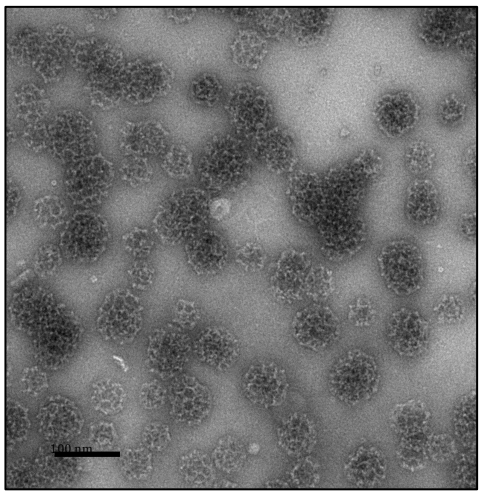

(E)

POL 6.4, **C:E:β**

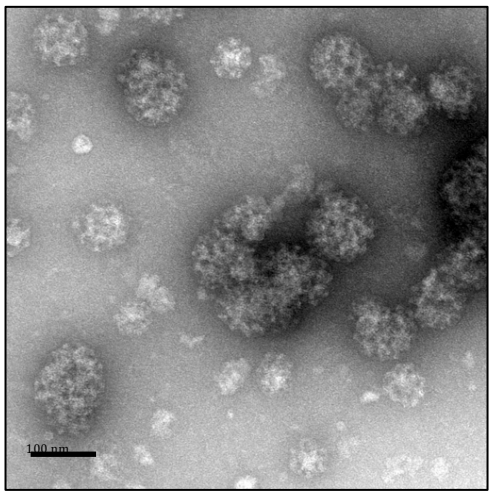

(F) **(G)**

HKM 6.4, **C:E:β** HKM 7.2, **C:E:β**

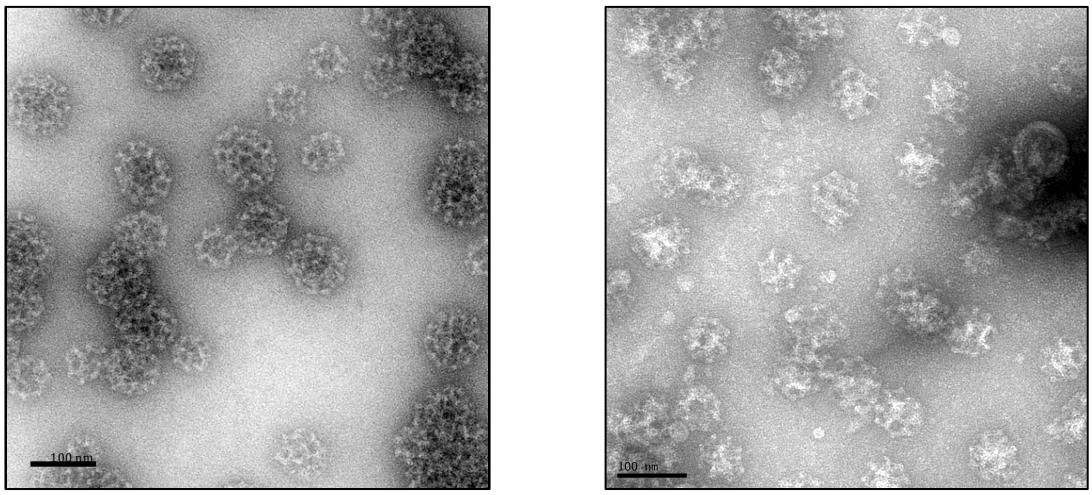

Figure 4.5.2: Analysis of the interaction between clathrin cages assembled with epsin 1 WT and the addition of the active β-arrestin 1L to the cage:epsin 1 complex. (A) *SDS-PAGE analysis from ultracentrifugation assays of the complete binding of epsin 1 WT and active β-arrestin 1L in the presence of clathrin cages in HKM 7.2 buffer was observed in the black square on the gel image. Negative stain transmission electron microscopy (EM) was used to obtain images of cages: epsin 1: active β-arrestin 1L (C:E:β) complex formed in different buffers. The complex formed in buffer POL6.4* ***(E)*** *and HKM 7.2* ***(G)*** *contain numerous uniform sized clathrin cages with the exception of HKM6.4* ***(F).*** *These are compared to control samples imaged containing clathrin only in POL 6.4* ***(A),*** *cages:epsin 1 in POL 6.4* ***(B)*** *and cages:active β-arrestin 1L in HKM 7.2* ***(C).*** *Images were obtained at 30000x magnification, with the exception of Figure* ***(D),*** *which was obtained at a 12000x magnification.*

4.6.0 Discussion

Overall, clathrin cages are mostly stable in their polymerisation buffer (POL6.4), whereas active β-arrestin 1L is mostly stable in its purification buffer (CB1 buffer pH 8.0). However, the results above demonstrate that HKM buffer, pH 7.2 could be used for the formation of stable clathrin cages: β-arrestin 1L complexes. The ultracentrifugation/SDS-PAGE binding assays reveal a strong interaction of active β-arrestin 1L to clathrin cages or clathrin TD compared to WT β-arrestin 1L. These confirm the results from Kang *et*

al., 2009 which demonstrated a ~ 2-fold difference in binding affinity between active and WT β-arrestin 1L using SPR and clathrin TD.

The SDS-PAGE analysis in the previous section, reveals no obvious interaction of clathrin with the rest of the β-arrestin 1L mutants (IVF-AAEA, WT-AAEA, IVF-ΔLIELD or WT-ΔLIELD). This demonstrates that the conserved clathrin box is the major box for clathrin TD interaction and that the second clathrin box has a low binding affinity to clathrin. However, it is possible that these two clathrin box motifs may work synergistically, because when the conserved box (LIELD) is either deleted or mutated in WT or active β-arrestin 1L, there is no interaction with clathrin in the results above. Although, this could be an *in vitro* only phenomenon because *in vivo*, Kang *et al.,* 2009 stated that the second clathrin box ([LI][LI]GXL) is actually a low affinity site for clathrin but could effectively localize receptors to CCPs *in vivo* even in the absence of the conserved clathrin box motifs (Kang *et al.,* 2009).

Lastly, I demonstrate that buffer HKM at pH 7.2 was the most appropriate buffer and pH for clathrin cages: epsin 1: active β-arrestin 1L complex formation. As epsin 1 has been suggested to form uniform cage size distribution *in vitro* like AP180 (Kalthoff *et al.,* 2002), I showed that epsin 1 is able to form uniform size cage distribution in POL 6.4 but also in the HKM 7.2 buffer.

4.7.0 Future work

Due to the competition between epsin 1 and active β-arrestin 1L observed in later stage in this PhD project, further optimisation of the binding assays of cages: epsin1: active β-arrestin 1L, should be considered in the future. It would be interesting to identify the location of certain adaptor proteins in a clathrin cage, but as adaptor proteins are small in size (range from ~ 30kDa to 100 kDa molecular weight), they would not be visible under normal EM conditions. Single particle cryo-EM approach could be investigated to obtain high resolution 3D model of a complex of clathrin cages with two adaptor

proteins as carried out previously by Young *et al.,* 2013 (Young *et al.* 2013) with auxilin and Hsc70. Such a technique is considered challenging and would require a great amount of optimisation. Another approach to detect adaptor protein location could be to use the method of “metalo-tagging” or nanogold-labelling (Ni-NTA Nanogold) (Dubendorff *et al.,* 2010; Morphew *et al.,* 2015; Clarke and Royle, 2017).

Chapter 5:
Investigating clathrin N-terminal domain-adaptor protein interactions using surface plasmon resonance

5.0.0 Overview

This chapter documents the main principles and procedures of the surface plasmon resonance/antibody indirect method (SPR/IAC). The initial aim was to optimise this system before investigating clathrin:adaptor interactions, between β-arrestin 1L and epsin 1 with clathrin N-terminal domain (TD). The rationale behind this chapter was to gain further insight in how how the β-arrestin 1L two clathrin box motifs promote clathrin TD interaction. The biggest aim was to gain quantitative insight into how epsin 1, one of the main clathrin assembly proteins, interacts with clathrin N-terminal domain (TD) (residues 1-363) via multiple clathrin-binding sites. Obtaining quantitative insight into these different clathrin binding sites on epsin 1 could reveal different binding affinities, which inform our understanding of how, when, and where epsin 1 is incorporated into the assembling lattice.

5.1.0 Principles of the surface plasmon resonance (SPR)

Surface plasmon resonance enables real time binding detection and quantification of interactions in microfluidic environments between macromolecules and small molecules without the need for labels.

SPR phenomenon occurs when polarized (incident) light hits a metal thin film (e.g. gold) under total internal conditions that has a boundary with different reflection index. This occurs at specific angle of incidence (larger than the critical angle), which causes total internal reflection. Under total internal reflection, an evanescent light is produced when the photons resonate with the free oscillating electrons (plasmons) in the gold layer on the surface. Changes to the surface from an increased mass of molecules attached or bound to the surface would result to be absorbed and detected by the machine. This detection would result in a dip in the intensity at a certain SPR angle (Figure 5.1.0). Any SPR angle change is proportional to the concentration of the molecules on the surface. This shift is detected on a sensorgram and measured in response units (RU) (Biacore – Sensor Surface Handbook – BR-1005-71 AB (GE Healthcare)).

The sensorgram plot shows the response units (RU) on the y-axis with time in seconds on the x-axis. From the plots we extract information on the rate of association and dissociation, which could result in kinetic rate constants. Additionally, it provides binding affinity constants for quantitative applications (Guiducci, 2011).

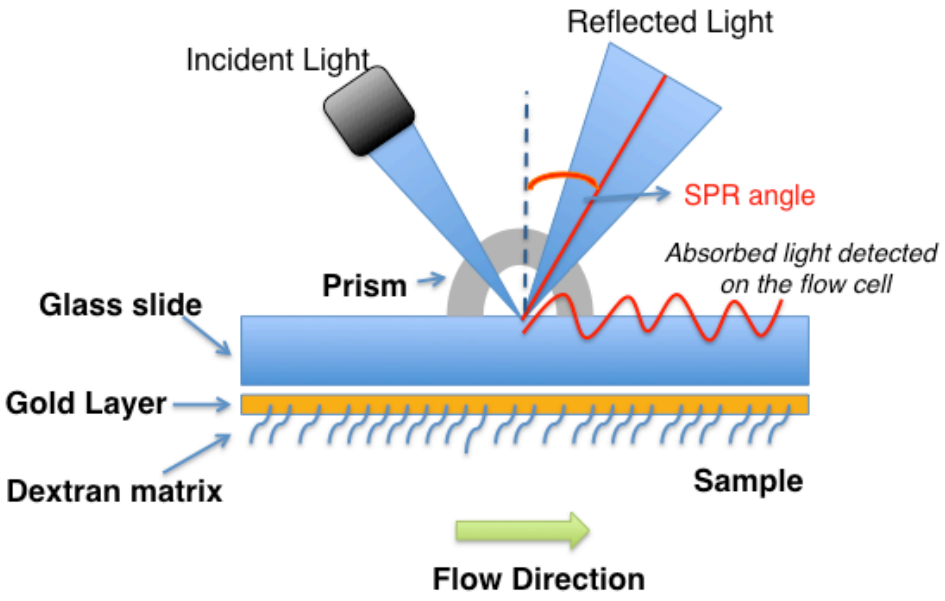

Figure 5.1.0: Schematic of how SPR works. *SPR principles involve plasmons being excited on the gold-layered sensor chip from shining if the incident light under total reflection conditions. The reflected light causes a drop in the SPR angle, which shifts when the mass on the surface of the chip changes as ligand-analyte interact.*

5.2.0 SPR detects binding interactions

In general, one molecule (ligand) is immobilized on the surface of a gold-layered sensor chip (e.g. CM-series) and another molecule (analyte) in solution is injected in a continuous manner over the surface with the immobilized ligand. If there is an interaction between the ligand and the analyte; an increase in the mass on the SPR interface is detected through a shift in the SPR angle due to the resulting change in refractive index. This response is observed via the sensorgram plot (Figure 5.2.0) (Biacore – Sensor Surface Handbook – BR-1005-71 AB (GE Healthcare)).

The increase in the response units on the sensorgram can be fitted to allow the association rate constant (k_{ass}/k_{on}) of the complex formed when the analyte binds to the ligand to be determined. The ligand-analyte complex is separated once buffer is injected over the flow cell, this decreases the mass on the surface and alters the SPR angle. This allows the dissociation rate constant (k_{diss}/k_{off}) to be determined in a similar manner. Once the binding kinetics of the ligand-analyte complex have been determined from both the k_{on} and k_{off} rate constants, which give the equilibrium dissociation constant (K_D) can be calculated using the equation below for the situation A + B = (equilibrium equals sign) AB (Biacore – Sensor Surface Handbook – BR-1005-71 AB (GE Healthcare)):

$$\mathrm{K}_D = \frac{k_{off}}{k_{on}} = \frac{[A].[B]}{[AB]}$$

The flow cells are then regenerated with harsh conditions such as low pH, which will break the binding interactions of the ligand-analyte, but will not interfere with the immobilized ligand on the chip. Hence, the sensor chip can be used for the next analyte injection (Biacore – Sensor Surface Handbook – BR-1005-71 AB (GE Healthcare)).

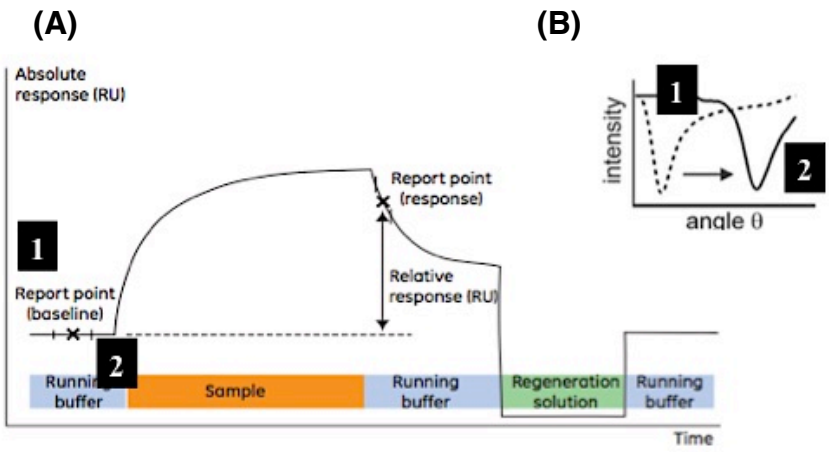

Figure 5.2.0: SPR sensorgram with identified various components of a typical experiment progression. (A) *Initially at the baseline (number 1) a flat line with zero response is observed, once the ligand and analyte interact the response increases (curve) at number 2 step.* ***(B)*** *Same components and numberings demonstrate the SPR angle shift due to the ligand-analyte interaction. Imaged adapted from the Sensor Surface Handbook- BR-1005-71 AB (GE Healthcare).*

5.3.0 Ligand immobilization

There are a variety of methods to bind the ligand to the dextran matrix, such as direct coupling, high affinity tag capture and hydrophobic absorption method (Lang *et al.,* 2005). The most common method is the direct coupling via thiol-disulphide exchange, aldehyde groups and free amino group, via amine coupling, thiol coupling and aldehyde chemistry method (Lang *et al.,* 2005). The direct coupling method does not guarantee its orientation in a uniform manner thus rendering some of the ligand binding sites inaccessible due to the chemical conjugation (Lang *et al.,* 2005). However, the indirect coupling method require affinity tagged-proteins to be used, which is thought to guarantee a better orientation of the ligand due to the position of the tag at the end of the protein sequence (Biacore – Sensor Surface Handbook – BR-1005-71 AB (GE Healthcare; Lang *et al.,* 2005).

In this thesis, CM-series sensor chips were used. More specifically, CM5 chips were used as they have a standard dextran surface. The ligand is immobilized on the experimental flow cell (per sensor chip), which are covered with 150 nm inert, thin and uniform layer of gold, which has covalent

attachment of carboxymethylated (CM) dextran matrix layer of the chip. A reference (blank) flow cell with no ligand immobilization is used to detect any analyte non-specific binding to the matrix itself and subtract from the experimental flow cell.

Also a high affinity tag capturing method was used, called indirect capturing method (IAC) (Figure 5.3.0). In this method, for example a GST- tagged protein e.g. GST-clathrin N-terminal domain (GST- clathrin TD) was used; therefore, a monoclonal anti-GST antibody was immobilized first on the chip dextran matrix surface, which would capture the GST- clathrin TD once passed over the chip. Additionally, a series of experiments were performed for comparison where the GST- clathrin TD was directly immobilized on the chip surface.

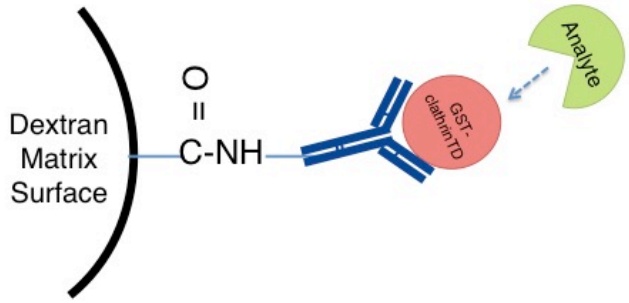

Figure 5.3.0: A schematic of the 'high affinity tag capturing' method*. The affinity tagged- ligand (GST-clathrin TD) of interest is indirectly coupled to the SPR chip surface via a secondary molecule such as an antibody.*

5.3.1 Ligand coupling (scouting) conditions

The dextran matrix is negatively charged above the pH 3.5 and would attract positively charged ligands via electrostatic forces. Hence, the buffer pH of the ligand needs to be between 3.5 and the isoelectric point (pI) for efficient ligand immobilization (Figure 5.3.1). In order to determine the appropriate conditions, pH scouting method is typically performed before immobilization. A range of buffer conditions above 3.5 and below the pI of the ligand need to be scouted. Hence, a 10mM sodium acetate as the buffer with a range of pHs of 3.5, 4.0, 4.5, 5.0 and 5.5 was used (Guiducci, 2011).

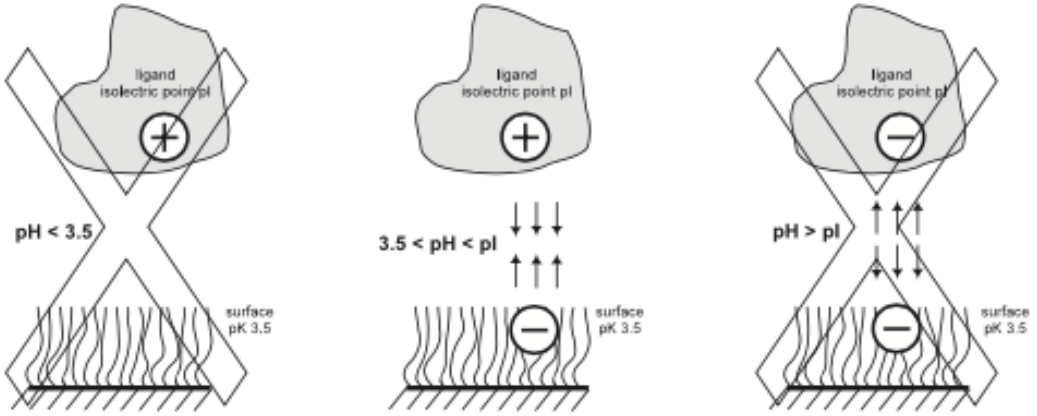

Figure 5.3.1: Electrostatic attraction between the ligand (antibody) on the chip and carboxymethylated (CM) dextran surface is necessary for efficient coupling. *If the buffer pH is lower than 3.5 or when the buffer pH is larger than the pI of the protein, the ligand immobilization fails. Image adapted from Sensor Surface Handbook- BR-1005-71 AB (GE Healthcare).*

5.3.2 Ligand immobilization via amine coupling method

After determining the best pH for ligand immobilization, the ligand needs to be captured on the dextran surface using chemical immobilization reagents/kit. Figure 5.3.2 gives a simple illustration of the amine coupling immobilization method that was the only capturing method used in this thesis During the experiment itself, 0.4M EDC (1-ethyl-3-(3-dimethylaminopropyl) carbodiimide) is mixed with 0.1M NHS (N-hydroxysuccinimide) in a 1:1 ratio. The purpose is to activate the OH moieties of the carboxylic acid groups into a better leaving group by the conversion into a reactive succinimide ester. EDC and the NHS would stabilize the ester groups. Then the monoclonal anti- GST antibody in 10mM sodium acetate pH 5.5 will be conjugated on those ester groups and couple on the surface. Ethanolamine-HCL will then deactivate any remaining activated ester groups (Biacore – Sensor Surface Handbook – BR-1005-71 AB (GE Healthcare)); Fischer, 2010; Guiducci, 2011).

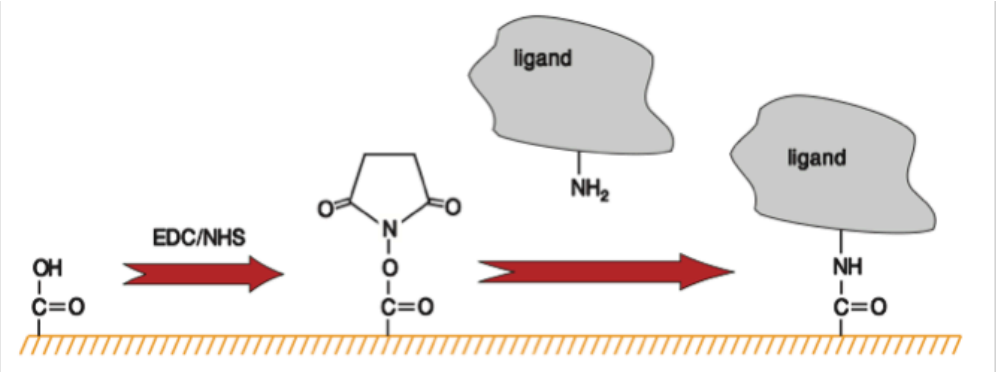

Figure 5.3.2: An overview of the amine coupling method to immobilize the ligand on an activated chip surface. *The diagram illustrates the EDC/NHS chemistry for activating the dextran surface. The ligand is then flown over the chip to couple to the surface on a primary amine groups. Image was taken from the Sensor Surface Handbook- BR-1005-71 AB (GE Healthcare).*

5.6.0 Optimisation of the SPR/IAC method

5.4.1 pH scouting for ligand immobilization

Initially, a Biacore pH scouting routine program was performed to determine the optimal pH for the coupling of the ligand onto the SPR chip dextran, as described section 5.3.0. In this thesis, the monoclonal anti-GST antibody was used to couple on the SPR chip and the GST-tagged ligand e.g. GST-clathrin TD to bound on the antibody, and GST-clathrin TD was also immobilized on the SPR chip directly. A range of pHs were used (3.5-5.5) in 10 mM sodium acetate. For GST-clathrin TD as seen by the Figure 5.4.1 (B), the only pH where any attraction to the surface was measured was 5.5, while of the anti-GST antibody attraction was measured both at 5.5 and 5.0 Figure 5.4.1. (A), but as customary in those cases we select the highest pH, which provides sufficient response units.

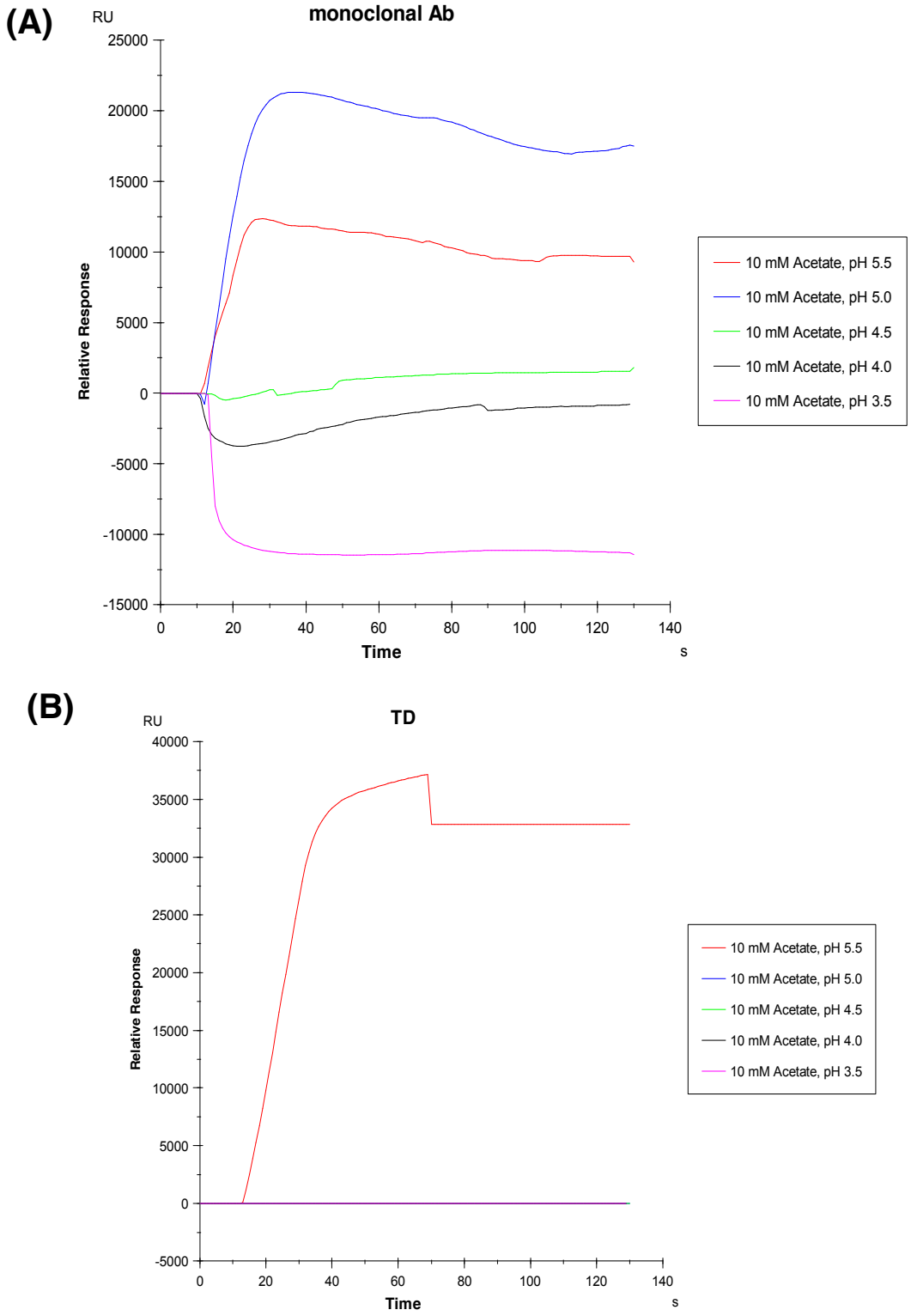

Figure 5.4.1: pH scouting for the immobilization of anti-GST antibody (A) or GST clathrin-TD (B). (A) pH 3.5 (pink curve), 4.0 (black curve) resulted in a negative relative response units and pH 4.5 (green curve) resulted in zero relative response units and were not used in the ligand immobilisation procedure. *The best pH was 5.5 (red curve) and 5.0 (blue curve) for anti-GST-antibody wirh relative response of ~ 20,000 RU and ~ 15,000 RU respectively (B) The only pH for GST-clathrin TD was 5.5 (red curve) with the highest relative response of ~ 35,000.RU. The remaining buffers with lower pH did not give any response.*

5.4.2 Regeneration scouting

Another procedure which required optimization was the regeneration, which takes place after the ligand and analyte complex interact and need to be removed before the next interaction could be carried out on the same flow cell. Multiple regeneration tests were carried out part of the initial optimization stages, with regeneration solutions such as 3M $MgCl_2$, 50mM NaOH and 10 mM Glycine HCl pH 2.0-3.0 (data not shown). It is important to note that the regeneration reagent do not interfere with the anti-GST antibody coupled on the chip or the ligand that has been covalently attached on the chip. The best regeneration condition used for all the SPR experiments in this thesis was 10 mM glycine, pH 2.2 with two injections of 30 seconds each, which was also recommended by the GST capturing kit -Instructions 22-0522-19 AG (GE Healthcare), and which was adequate to bring the response units approximately back to baseline (Figure 5.4.2).

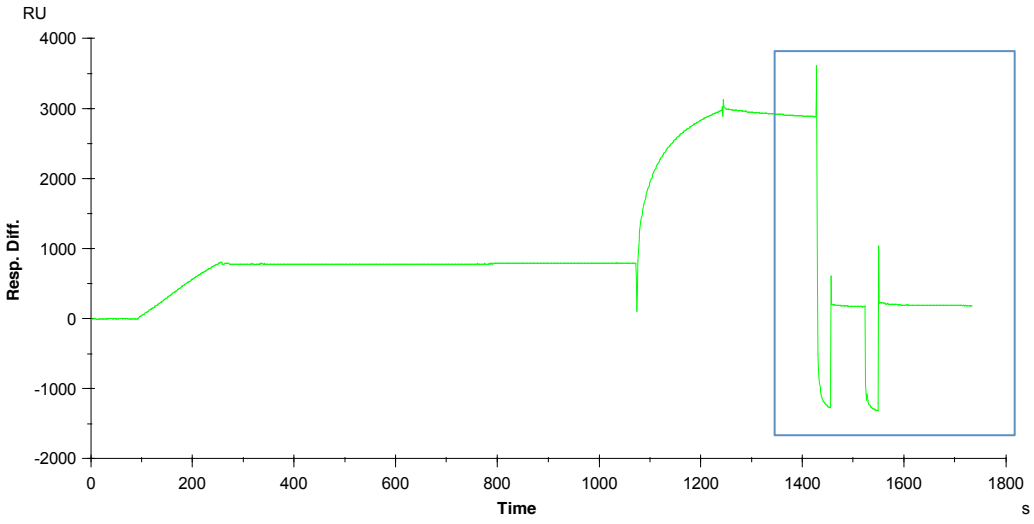

Figure 5.4.2: Two injections of 30 seconds each of 10 mM glycine-HCl pH 2.0-2.2 was used. *The regeneration stages are shown in the blue box and demonstrate how the response returns to baseline after the regeneration conditions, ready for the next experiments.*

5.4.3 Immobilization of anti-GST antibody and GST-clathrin TD

After determining the optimal pH for ligand immobilization, the ligand was covalently immobilized on the chip surface via the free amine groups formed from the amine coupling method detailed in section 5.3.2. The sensorgram plot of the immobilized anti-GST antibody is shown in Figure 5.4.3 (A) and GST-clathrin TD is shown in Figure 5.4.3 (B). The anti-GST antibody was immobilized between ~ 10,000-15,000 RU on the experimental flow cell experiment with a final concentration of 0.5 µM of anti-GST antibody in 10mM sodium acetate at pH 5.5. The GST-clathrin immobilization was achieved at ~ 35,000 RU, with 10 µM concentration of GST-clathrin TD in 10mM sodium acetate at pH 5.5.

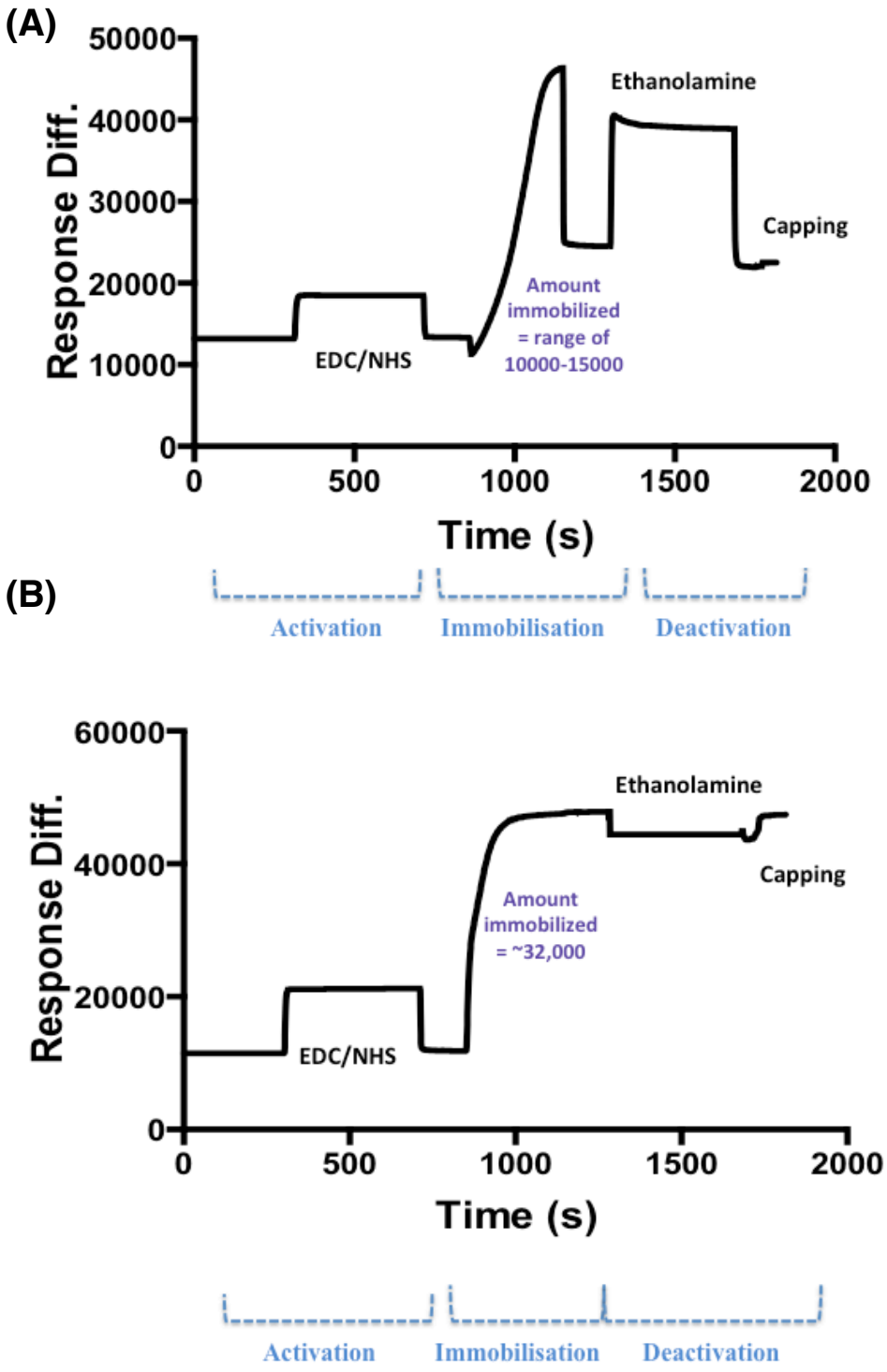

Figure 5.4.3: Sensorgrams demonstrating successful ligand immobilisation. *Activation of the dextran matrix is carried out by EDC/NHS to form free amine groups. Immobilization of the anti-GST antibody (**A**) and GST-clathrin TD (**B**) was then determined at ~ 10,000-15,000 RU for the anti-GST (**A**) and ~ 32,000 RU for the GST-clathrin TD (**B**). Ethanolamine was then used to deactivate and cap the remainder of unbound free amine groups and cap the flow cell.*

5.4.4 Direct capturing method results

The GST-clathrin TD was successfully immobilized on the chip with ~ 35,000 RU using the amine coupling method, as stated above. In order to determine whether the direct capturing method of the GST-clathrin TD was suitable to use for the SPR experiments; active β-arrestin 1L (analyte) was injected onto a flow-cell with immobilised GST- clathrin TD. The SDS-PAGE results from Chapter 4 and previous SPR experiments from Kang *et al.,* 2009 have previously demonstrated that active β-arrestin 1L binds strongly to the GST-clathrin TD via tis two clathrin box motifs on C- and N- terminal domains exhibiting a high response (Kang *et al.,* 2009). Hence, it was the most ideal adaptor protein to test the functionality of the direct capturing method. The results in Figure 5.4.4 showed no increase in response units (RU=0, t=100) when active β-arrestin 1L was flowed over the SPR chip bound directly to GST-clathrin TD. In the direct ligand coupling method proteins are randomly orientated and coupled on the chip (Lang *et al.,* 2005), therefore we can hypothesize that this could be the case with the GST-clathrin TD. Thus, there is a possibly that this method is hindering certain TD binding sites (especially blade 1 and 2 and 4 and 5 where active β-arrestin 1L binds). This is most likely to prevent the active β-arrestin 1L from binding to the TD, resulting in lack of increase in response, as seen in Figure 5.4.4.

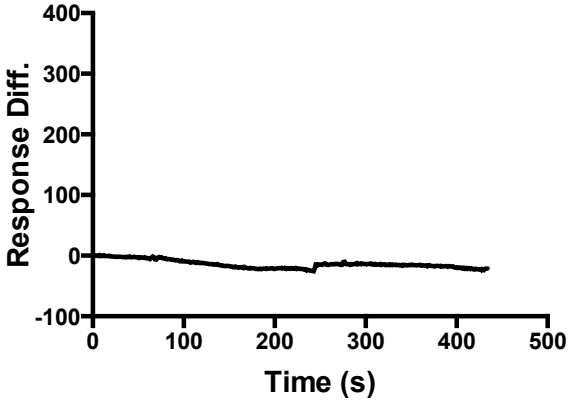

Figure 5.4.4: Sensorgram demonstrating unsuccessful analyte (adaptor protein) binding to ligand (GST-TD) under the direct capturing method. *Once the GST-TD was successfully bound to the SPR chip via the amine coupling method, the active β-arrestin 1L (analyte) was flown over the flow cell for 200 seconds to allow interaction between ligand and analyte. The results revealed no increase in the response units (R=0, t=0), which led to the hypothesis that the GST-TD is orientated randomly in the direct capturing method, potentially obscuring its adaptor protein binding sites and thus preventing active β-arrestin 1L from binding.*

5.4.5 Indirect Antibody Capture (IAC) method

Due to the unsuccessful binding results of the GST-clathrin TD and active β-arrestin 1L via the direct capturing method; the indirect antibody capturing (IAC) method was the next option, which to explore.

To test this method the anti-GST antibody was coupled to the dextran matrix surface of the SPR chip, following optimization as stated in sections 5.4.3, previously in this chapter. Secondly, the ligand, in this case 1 μM GST-clathrin TD was injected over the anti-GST antibody for 100 seconds. Successful binding of the GST-clathrin TD was indicated by the increase in response units (~ 1000 RU) detected (Figure 5.4.5 (A)(i)). A test analyte, purified GST, which is expected to bind, was injected over the cell for 200 seconds, and an increase in the response units detected is shown in Figure 5.4.5 A)(ii). BSA was used as a non-binding control analyte, which should not interact with the anti-GST antibody. No binding was observed when the BSA was injected onto the SPR chip (RU=0) Figure 5.4.5 (A)(iii), as expected. After the injection of the analyte SPR buffer 1 was injected for ~ 500 seconds to allow the dissociation of the complex before regeneration (Figure 5.4.5 (A)(iv)).

The advantage of using an antibody-capture method of an affinity-tagged protein is that it is more likely to orientate the protein (ligand) in a certain favored direction to expose its analyte binding sites (Lang *et al.,* 2005). For the system tested this would mean a more appropriate orientation of the GST- clathrin TD (ligand) with the GST affinity tag being on N-terminal domain attached on chip allowing the ligand to be free in solution at a specific orientation. This would most likely expose its four adaptor binding sites to the adaptor proteins (analyte). A fresh ligand is captured in every new experiment, which is an advantage of the IAC method over the direct capturing method (Lang *et al.,* 2005). A third advantage of the IAC method is that it does not require covalent modifications or interactions of the actual

ligand, in this case GST-clathrin TD, and thus it will not affect the ligand's activity (Lang *et al.,* 2005).

The major disadvantage of the IAC method via antibody capturing, is that the antibody binding capacity decreases after each run and this is detected by a systematic decrease in the clathrin TD binding in majority of the SPR experiments of this thesis. Therefore, each flow cell was only used for up to 6-7 experiments, which significantly increases the cost of this method. This could be because of the harsh regeneration conditions (10 mM glycine-HCl pH 2.0-2.2) applied at the end of each experiment, which removes the ligand-analyte complex, but does not detach the anti-GST antibody bound onto the chip. This decrease was also observed by Snopok *et al.,* 2006 (Snopok *et al.,* 2006), therefore it was considered a systematic issue of this method, which was taken into consideration in the experiments.

The main stages of the IAC method for the clathrin:adaptor system are illustrated in a diagram Figure 5.4.5 (B); based on Karlsson *et al.,* 1994, as the active β-arrestin 1L did not bind to the directly coupled GST-clathrin TD, as described in section 5.4.4, in previous section of this chapter. For the subsequent SPR/IAC clathrin TD:adaptor experiments, GST- clathrin TD at 1 µM concentration in SPR buffer 1 is defined as the ligand and the relevant adaptor protein used at 10 µM total concentration (ratio 1:10) in SPR Buffer 1 is defined as the analyte. This ratio was also used in the GST-pulldown binding assays as well.

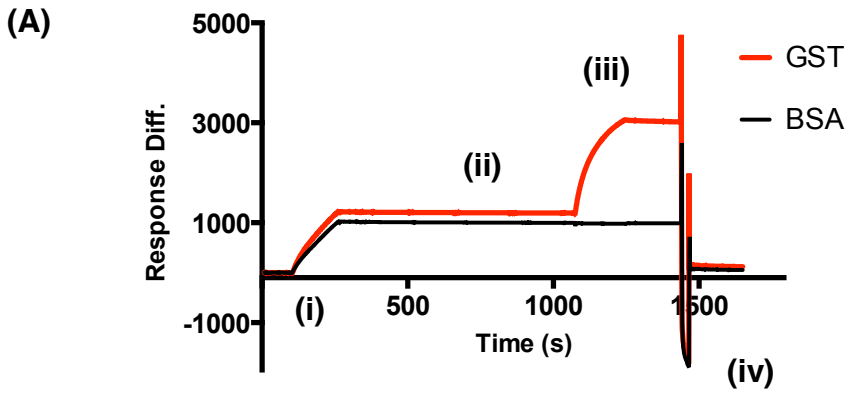

(B)

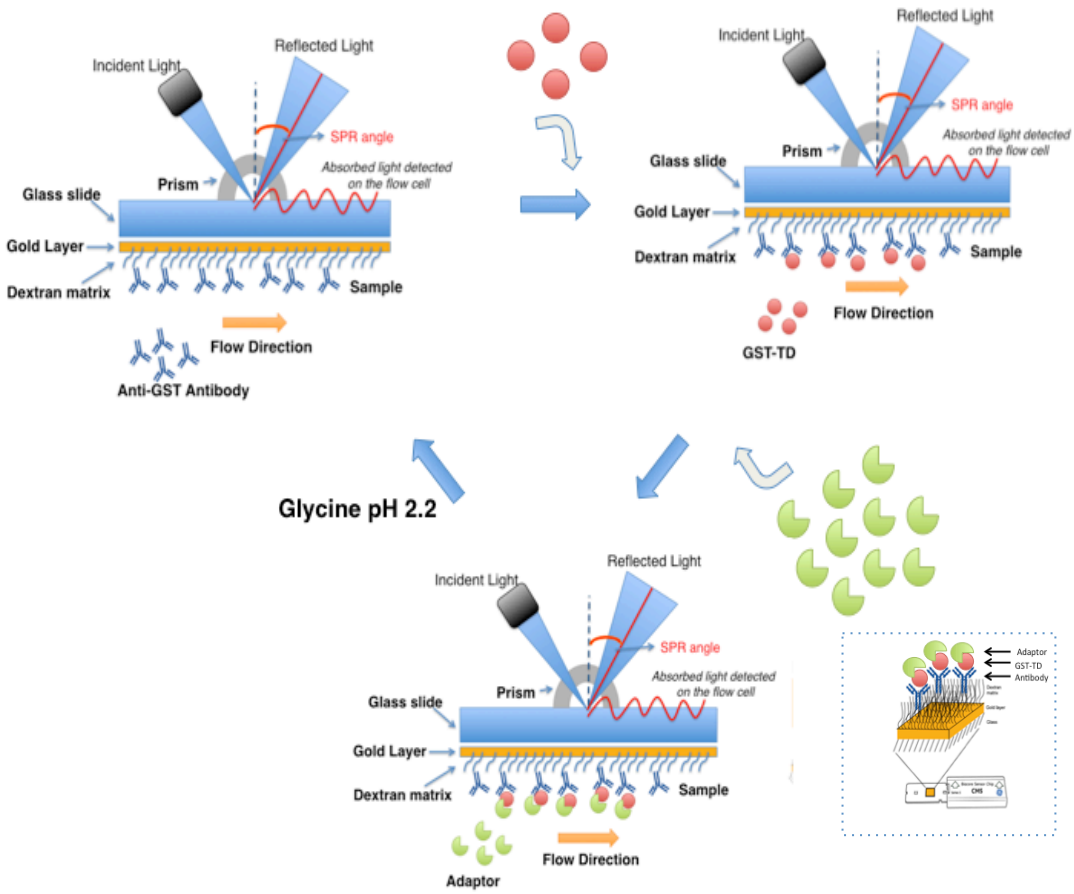

Figure 5.4.5: Control experiments run for the IAC method and illustrating the stages of the method for clathrin:adaptor interactions. ***(A)*** *A sensorgram with results at each stage of sample injection (ligand first and analyte second) The GST-TD is bound with an increase in response units detected on the sensorgram (i), the GST (positive control analyte) binds with an increase in response units (ii). The BSA (negative control analyte) does not bind to GST-TD or antibody hence there is no increase in response units over time (seconds) (iii). After a period of buffer being injected over the flow cell to allow dissociation of the complex of the ligand-analyte, the flow-cell is regenerated (iv) with glycine pH 2.2 in order to be re-used for the next experiment.* ***(B)*** *A simple illustration of the indirect antibody capturing method. The GST-TD (ligand) is bound on the immobilised anti-GST antibody on the selected flow cell. The analyte (adaptor proteins, GST tag or BSA) are then injected over the flow-cell and bind to the GST-TD or antibody. Regeneration of the flow cell with 10 mM Glycine pH 2.2 is carried out. CM5 sensor chip image taken from Biacore Sensor Surface Handbook- BR-1005-71 AB (GE Healthcare).*

5.7.0 Optimisation for Binding Kinetics

5.5.1 Decreasing non-specific binding of epsin 1

Following establishment of the binding method, the next step was to optimize the detection of adaptor protein binding. In the case of epsin 1 we encountered issues with non-specific binding, which was continuously detected as an increase in response on the reference/blank control flow cell trace on the sensorgram. The non-specific binding could be because of the overall negative charge of the surface and the attraction to the dextran matrix or could be due to the complex nature of the epsin 1 structure (long unstructured flexible region). This is a major disadvantage for kinetic runs and therefore needed to be addressed.

Two potential approaches to disrupt the charge interactions between epsin 1 and the dextran-carboxyl surface of the chip were employed and the results are detailed below:

(a) covering the dextran surface of the reference flow cell with a non-interacting protein such as BSA or a different antibody that does not have affinity to epsin 1, e.g. β2-microglobulin Ab-1 (Mouse mAb). The β2-microglobulin Ab-1 antibody immobilization was utilized as the method of choice with same ratio as the anti-GST antibody immobilization. This forms an inert protein layer on the reference flow cell. This method successfully decreased the non-specific binding of epsin 1 (257 mutant) on the reference flow cell (Figure 5.5.1 (A)), but did not eliminate it completely.

(b) SPR running buffer was used with increased NaCl concentrations from 150 mM to 500 mM, as high ionic strength disrupts non-specific binding. Figure 5.5.1 (B) shows the decrease in the non-specific binding of epsin 1 using the higher salt concentration in the running SPR buffer.

As a result of these investigations, it was decided that for any future epsin 1 SPR experiments, a combination of a 500mM NaCl SPR buffer and antibody β2-microglobulin Ab-1 immobilised on the reference flow cell should be, which successfully decreases non-specific binding (Figure 5.5.1 (C)). It was noted that there would be a certain degree of non-specific binding for all proteins in general. For other adaptor protein SPR experiments the standard SPR buffer (150 mM NaCl) was used.

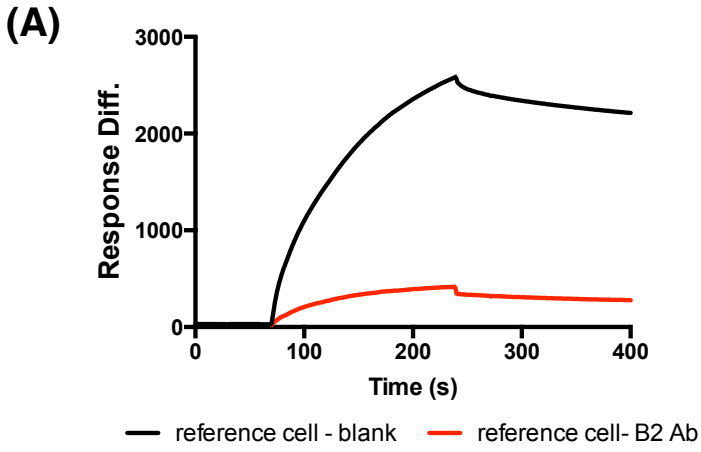

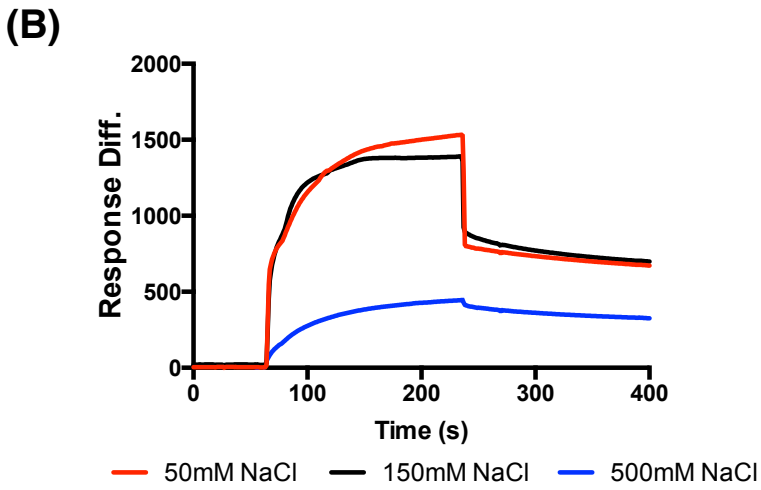

(C)

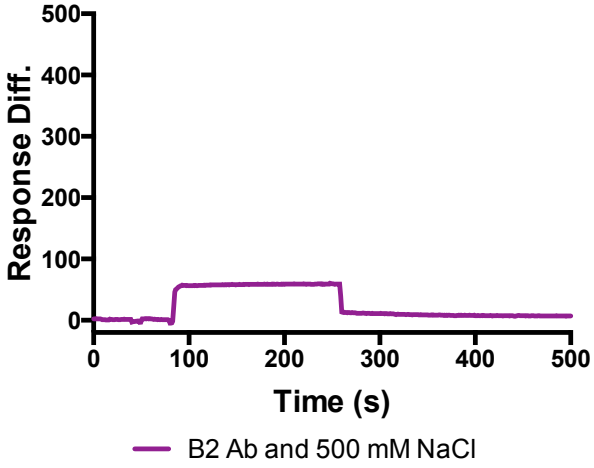

Figure 5.5.1: **Disrupting the charge interactions between epsin 1 and dextran- carboxyl surface of the chip on the reference flow cell.** *These response units are detected on the reference flow cell covered with 0.1 µM GST-TD and 2.5 µM epsin 1. (**A**) A decrease in the non-specific binding of epsin 1 was determined from 2,500RU to 200 RU, when the reference flow cell was immobilized with a β2-microglobulin antibody (**B**) A decrease in the non-specific binding of epsin 1 was determined from 1,500RU to 500 RU, when a high salt (NaCl) concentration of 500 mM was used in the SPR buffer. Decreasing the salt (NaCl) concentration had no difference than the normal 150 mM salt SPR buffer, in the non-specific binding level of epsin 1. (**C**) The non –specific binding is decreased massively (<100 RU) when the flow cell is immobilized with the β2 myoglobin in combination with using 500 mM NaCl in SPR buffer.*

5.5.2 Lowering the ligand (clathrin TD) and analyte (adaptor protein) density

To obtain reliable kinetic binding constants for protein-protein interactions, the response for ligand-analyte complex formation needs to be in the range of 100-300 response units (Van Der Merwe, 2001). In the IAC method, the response obtained upon binding of GST-clathrin TD (ligand) at a final concentration of 1 µM to the SPR chip was ~ 1000 RU, which already exceeds the limit for determining kinetic constants, even without adding the adaptor protein analyte. This was because of the strong binding between the anti-GST antibody of the chip and the GST-affinity tag on the TD at that concentration. Therefore, a great amount of optimization was carried out to decrease the concentration of GST-clathrin TD and the adaptor proteins.

Decreasing the response units of the adaptor proteins, especially for epsin 1 was the most challenging due to its complex interactions between epsin1:clathrin TD. The best result obtained was with the ligand immobilized at 100-200 RU of GST-clathrin TD at 0.1 μM concentration, and 500-600 RU of the adaptor protein (e.g. 257 epsin) at 1.25 μM concentration. This was achieved by decreasing the anti-GST antibody and the β2 myoglobin concentration by half. Overall, 1:10-1:12.5 molar ratios of clathrin:adaptor were kept even when lowering the ligand and analyte concentrations, which was the approximate saturation ratio between clathrin and epsin 1 and β-arrestin 1L, which was previously determined in Chapter 4.

5.6.0 Mass Transport Limitation

5.6.1 Overview of mass transport limitations

In a SPR instrument, the analyte is delivered onto the dextran matrix surface of the SPR chip, by the process of bulk flow and diffusion, prior coming in contact with the ligand. However, mass transport could occur when the binding rate of the analyte to the ligand exceeds the rate at which the analyte is injected to the chip surface (Van Der Merwe, 2001; Lang *et al.,* 2005). Mass transport limitation is detected on a sensorgram as changes in the binding curve shape with different flow rates (μl/min) (Van Der Merwe, 2001).

5.6.2 Decreasing mass transport issues

It is important to consider whether there were any mass transport issues for the epsin 1 WT and mutants, which were key in most SPR/kinetic experiments. Figure 5.6.2 (A) shows how changing the flow rate of the experiments causes the epsin to interact with clathrin TD differently, which has been confirmed by observing the difference in the response curves obtained using different flow rates (10, 20, 30 μl/min). The experiments were run with a longer injection time of 5 minutes (300 seconds) for fitting purposes. These results reveal possible mass transport issues in clathrin:epsin interactions even at 150 RUs. This mass transport observed could be due to: (a) the structure of epsin 1 with the unstructured region

between the two clathrin box motifs, which could promote flexiblility in its binding. (b) the hypothesized multiple interaction of epsin 1 with clathrin TD (c) high ligand density which could increase mass transport issues.

To try to address with mass transport limitation, the following approaches can be used as suggested by Van Der Merwe, 2001: (a) lower the ligand density because high ligand densities on the chip surface would not allow accurate kinetic analysis because of mass transport issues caused (b) increase the flow rate until high enough to compensate for the mass transport limitation and no change is observed of the response curves (> 30 µl/min), as suggested by Lang *et al.,* 2005. (c) mass transport correction is included in certain kinetic fitting models.

The ligand density was optimized in the previous section 5.5.2. Hence, a range of higher flow rates were investigated (40 and 60 µl/min), and a longer injection time of 5 minutes (300 seconds) to allow the epsin to reach saturation levels. Figure 5.6.2 (B) shows no significant difference in the shape in their response curves and response units of epsin 1 binding to the TD, at flow rate 40 µl/min (orange curve) and 60 µl/min (black curve). Overall, taking into account all of the above, the kinetic runs were performed with the lowest 40 µl/min flow rate which would require less protein concentrations. The flow rate of 40 µl/min reduced but did not completely eliminate mass transport issues, which proved challenging to overcome completely. Thus an approach utilizing appropriate kinetic experiments, which take into account the mass transport, was implemented.

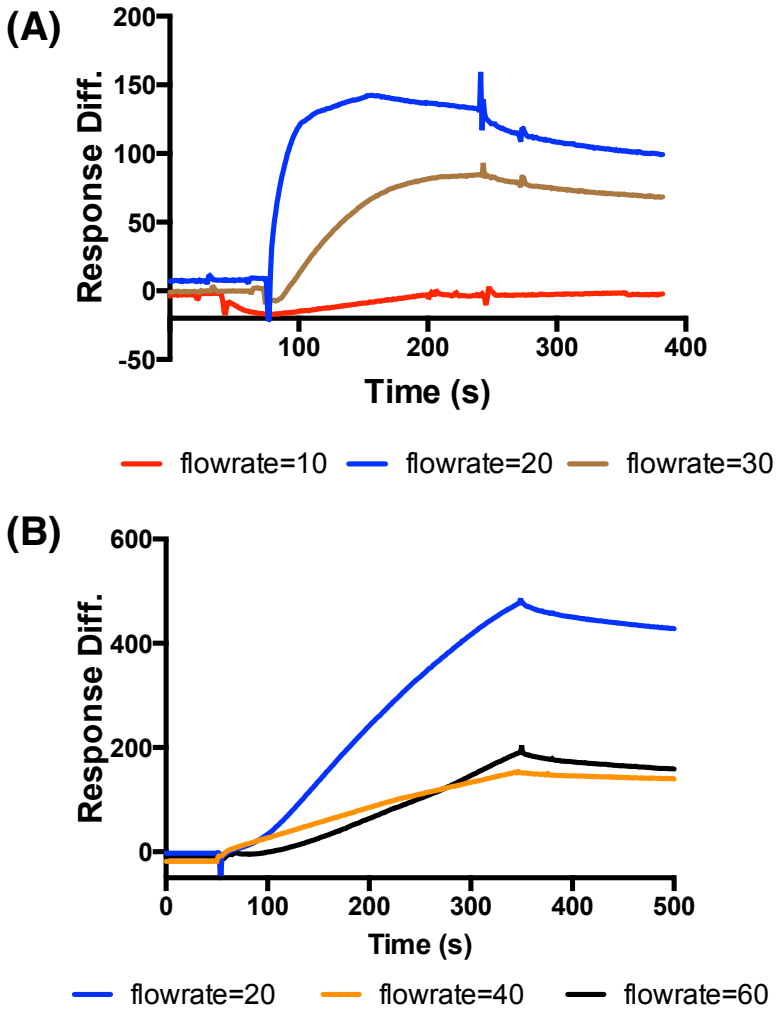

Figure 5.6.2: SPR response curves demonstrating mass transport issues of epsin 1 once injected on an SPR chip with immobilised GST-clathrin-TD. (A) *Epsin 1 -257 mutant (0.625 µM) was used in SPR/IAC experiments which yielded a response of a maximum of ~ 150 RU with a longer injection time of 300 seconds at different flow rates (10, 20, 30 µl/min). These results illustrate the mass transport limitations.* ***(B)*** *Using a higher concentration of epsin 1 – 257 mutant (1.25 µM) and higher flow rates of 20,40,60 µl/min, resulted in eliminating mass transport at higher flow rates of 40 µl/min (orange curve) and 60 µl/min (black curve).*

5.7.0 Quantitative measurements

5.7.1 Kinetics

In order to obtain more quantitative results from the SPR/IAC data, I used the following kinetic models to fit certain SPR experimental data obtained in this project. The fitting software (BIAevaluation version 4.1) is based on the minimization of the least squares, built on the Levenberg-Marquardt algorithm used in minimizing the sum of the squared residuals (S) between the experimental data and the fitted model, as shown below (Biacore – BIAevaluation software Handbook- BR-1002-29 (GE Healthcare))

$$S = \sum_{1}^{n} (r^f - r^x)^2$$

$$S = sum\ of\ the\ squared\ residuals,$$

$$r^f = fitted\ value\ at\ given\ point,$$

$$r^x = experimental\ value\ at\ the\ same\ point$$

The basic principles to obtain binding rate constants and dissociation constants are based on an analyte being injected over a ligand coupled to a chip surface. The ligand-analyte complex formation and separation is recorded on a sensorgram as the 'association phase' (k_{on} /k_{ass}) and the 'dissociation phase' (k_{off}/k_{diss}) respectively. During the 'association phase', A (ligand) + B (analyte) interact to form AB (ligand-analyte) complex, as shown in Eq. [1]. In the 'dissociation phase', the AB complex dissociate back to A + B, as seen in the Eq. [2]. Eq. [3.1] Equilibrium is reached when the rate of formation of product is equal to its rate of dissociation and as a result the concentration of the reactants in the system remains constant. The equilibrium dissociation constant is termed K_D (Eq. [4]) and is derived from rearranging the Eq. [3.2] (equations adapted and modified from Biacore - BIAevaluation software Handbook- BR-1002-29 (GE Healthcare)). The equations below demonstrate how the K_D is obtained:

$$Association\ (A + B \rightarrow AB): \frac{d[AB]}{dt} = k_{ass}.[A].[B] \quad [1]$$

$$Dissociation(AB \rightarrow A + B): -\frac{d[AB]}{dt} = k_{diss}.[AB] \quad [2]$$

Reaction is at equilibrium when the concentrations do not change:

$$\frac{d[AB]}{dt} = k_{ass}. \quad [A].[B] \quad - \quad k_{diss}. \quad [AB] = 0 \quad [3.1]$$

M/S = $M^{-1}s^{-1}$ M M s^{-1} M

Equilibrium is reached when:

$$k_{ass}.[A].[B] = \quad k_{diss}. \quad [AB] \quad [3.2]$$

$$\mathrm{K}_D(M) = \frac{k_{diss}}{k_{ass}} = \frac{[A].[B]}{[AB]} = \frac{s^{-1}}{M^{-1}s^{-1}} \quad [4]$$

5.7.2 Introduction: kinetic models of protein binding

Here, the parameters of each kinetic model chosen are briefly explained and the rationale for deeming that they were appropriate for the clathrin:adaptor system. The data fitting with this models were carried out using the BIAevaluation version 4.1 program (Biacore) which was implemented in the SPR system, and supplementary information from BIAevaluation software Handbook BR-1002-29 (GE Healthcare) was used for guidance to understand the background of each model, as briefly explained below:

I. **1:1 Langmuir,** this is considered the simplest model, where one analyte molecule interacts with one ligand molecule at a 1:1 interaction, as seen in the equation below:

   $A + B \Leftrightarrow AB,\ A(analyte), B(ligand), AB(complex)$

II. **1:1 binding with mass transport**, which is an identical model of the above but takes into account the analyte mass transport issues observed in the experimental data even when the ligand density is low

and the flow rate is increased, which was the situation with the experiments in this thesis for clathrin:adaptor.

III. **Heterogeneous ligand/parallel reactions**, which is used when one analyte e.g. adaptor protein, binds to two independent ligands e.g. two different clathrin TD molecules.

IV. **Bivalent analyte**, which was the most appropriate model for the clathrin:adaptor system. It describes a situation where one analyte e.g. adaptor protein, can bind to one or two sites on the same ligand e.g. TD sites (multivalent binding). This model takes cooperative binding effect into account, but does not show any response of the second site interaction on the sensorgram, because the overall mass on the surface does not change. Thus, this model will provide a single set of rate constants for the first analyte-ligand site interaction and a second set of rate constants for the second analyte-ligand site interaction. The equations which form the basis of this model are presented below adapted from Biacore -BIAevaluation software Handbook- BR-1002-29 (GE Healthcare)).

$$Interaction\ 1: A + B \Leftrightarrow AB; \quad rate\ constants: \frac{ka1}{kd1}$$

$$Interaction\ 2: AB + B \Leftrightarrow AB2; \quad rate\ constants: \frac{ka2}{kd2}$$

A (analyte); B (ligand); AB (analyte-ligand complex)

$$\chi^2 < 10, goodness\ of\ fit\ [\chi^2 = \frac{\sum_1^n (r^f - r^x)^2}{n - p}]$$

$$n = number\ of\ points$$

$$p = number\ of\ fitted\ parametrs$$

5.8.0 Investigating the binding interactions of adaptor proteins with clathrin TD using SPR

5.8.1 Investigating β-arrestin 1L and clathrin TD interactions

5.8.2 Introduction of β-arrestin 1

β-arrestin 1 is a multifunctional protein involved in the "turning-off" (desensitization) and uncoupling of GPCRs from G-proteins causing loss of responsiveness of the receptor to ongoing stimulus. Its main role in CME is to recruit clathrin and other vital adaptors, such as β2-adaptin (AP2), via its conformational change to become an active (longer isoform (L)), and release its C-terminal domain flexible loop, to the plasma membrane to facilitate receptor internalization (Lefkowitz *et al.* 2006; Kang *et al.,* 2009; Gurevich, 2014; Lemmon and Traub, 2012). β-arrestin 1L/arrestin 2L (longer isoform) contains a LIELD (LØXØ[DE] single letter amino acid code where Ø represents a hydrophobic residue) clathrin box motif (357-383 amino acids), which is a conserved clathrin binding motif found in many adaptor proteins. An eight-amino acid β -arrestin 1L splice loop with a clathrin box motif ([LI][LI]GXL) that has also been proposed to bind to clathrin TD at blades 4 and 5 (Laporte *et al*., 2000; Lefkowitz *et al.,* 2006; Burtey *et al.,* 2007; Kang *et al.* 2009; Gurevich, 2014; Lemmon and Traub, 2012). Moreover, it has been confirmed that β-arrestin 1L with the LIELD clathrin box motif deleted still binds to clathrin TD upon agonist treatment (Laporte *et al*., 2000; Kang *et al.,* 2009; Gurevich, 2014).

5.8.3 Aims and objectives

The well-studied β-arrestin 1L was the first adaptor protein to be investigated for clathrin:adaptor interactions using the optimized SPR/IAC method. Experiments were conducted with the following aims in mind:

1. To investigate further, and confirm the suggested functionality of the structure of β-arrestin 1L and whether the second ([LI][LI]GXL) clathrin box motifs acts antagonistically or synergistically with the conserved clathrin box motif (LIELD).

2. To decide if β-arrestin 1L is suitable to be used for adaptor competition experiments, detailed in Chapter 6. The active form of β-arrestin 1L has two clathrin box motif in the opposite direction to its structure and has been hypothesized to have a linking effect with multiple TDs, which is similar to other adaptor protein's functionality e.g. epsin 1. Hence, I aimed to investigate how the action of the second clathrin box motif, which has been shown to bind to the ArrestinBox site on the TD, would interact with clathrin TD in the presence of other adaptor proteins.
3. To confirm that the optimised SPR/IAC method functioned with GST-clathrin TD (ligand) and adaptor proteins (analyte) system before using it for future investigations in clathrin:adaptor competition studies.

5.8.4 Mutagenesis studies of β-arrestin 1L

Mutagenesis is carried out on the conserved clathrin box motif (LIELD), as described in the Table 1.7.0 below. The conserved clathrin box is located on the C-terminal domain flexible loop as illustrated in Chapter 1, section 1.8.1. The mutant abbreviations used in this thesis are as follows: active (IVF), IVF-AAEA, WT-AAEA, IVF-ΔLIELD and WT-ΔLIELD), which were designed in line with Keyel *et al.,* 2008. Each SPR experiment was performed in triplicate and the order of analyte injection was randomised. This was conducted to minimize any systematic error caused by the decreased binding capacity of anti-GST antibody after each regeneration, which was discussed previously.

Number	Mutant Name (abbreviation)	Original motif -> alanine substitution and/or deletions
1	Active	^{386}IVF->AAF
2	IVF-AAEA	^{386}IVF + ^{376}clathrin box (**LIEL**D->AAEA)
3	WT-AAEA	WT + ^{376}clathrin box (**LIEL**D ->AAEA)
4	IVF-ΔLIELD	^{386}IVF + ^{376}clathrin box (**LIEL**D) deleted
5	WT-ΔLIELD	WT + ^{376}clathrin box (**LIEL**D) deleted

Table 1.7.0: Details of the β-arrestin 1L mutants. *The main mutations are activation and release of the conserved clathrin box (LIELD) by mutation the IVF motif to AAF at the beginning of the unstructured loop containing the clathrin box or deleting this clathrin box. Mutations were not performed on the second clathrin box (LIEFD ([LI][LI]GXL)) on the N-terminal domain.*

5.8.5 The LIELD clathrin box motifs the major box

The highest response obtained from the SPR results was determined by the active form of β-arrestin 1L mutant, as shown in the blue curve in Figure 5.8.5 (A), with the WT response greatly reduced (red curve) (Figure 5.8.5 (A)). The rest of the β-arrestin 1L mutants show a complete loss of response when the conserved clathrin box motif is deleted (ΔLIELD). However, in the case of the active mutant with an alanine substitution in the conserved box (IVF-AAEA), a slight increase in response is observed compared to the active mutant response is observed (Figure 5.8.5 (A)). These results represent three independent repeats where the mean of these repeats are plotted on a bar chart for each WT and mutant. This plot demonstrates that the active form has the highest binding response units of 1351 ± 198.6 RU with the WT next with 179 ± 19.96 RU, which is below the half. The rest of the mutants do not show any binding at all except the IVF-AAEA, which resulted in a 29.54 ± 14.81 RU binding only.

These results are similar to the results by Kang *et al.,* 2009 and the overall conclusion suggested that the conserved clathrin box (LΦXΦ[DE]), is the major binding site on the β-arrestin 1 for TD, as the IVF- ΔLIELD and WT-ΔLIELD failed to bind. The WT β-arrestin 1 is assumed to have a more

flexible and mobile unstructured loop where the conserved clathrin box is located, and hence this could suggest the binding of the WT observed in SPR results of this section. However, based on the above results, I appears that the two clathrin box motif act cooperatively, as the highest binding was detected with the active form of β-arrestin 1L with the two boxes open and accessible. Once, the conserved clathrin box motif is deleted, this causes a massive decrease in the binding of clathrin TD. Thus, these results suggest that the second clathrin box motifs is not as efficient for clathrin TD binding independently as the conserved clathrin box motif.

The shape of the curve is indicative of the nature of the interaction The shape of the active β-arrestin 1L response curve could indicate a two binding phases of β-arrestin 1L to clathrin TD, therefore a more complex binding interaction, which has been suggested by Kang *et al.,* 2009 as well as a 2:1 β-arrestin 1L to clathrin (Kang *et al.,* 2009). However, the WT (red curve) could be fitted as a single exponential function due to the smooth curvature of the curve. Additionally, both WT and active forms resulted in a very low dissociation rate form the GST- clathrin TD, as seen on the sensorgram (Figure 5.8.5 (A)). This could suggest strong binding between the β-arrestin 1L and the GST-clathrin TD, as well as the presence of multiple interactions, which could be the cause of this observed stronger interactions due to the cooperative mechanism of the two clathrin box motifs.

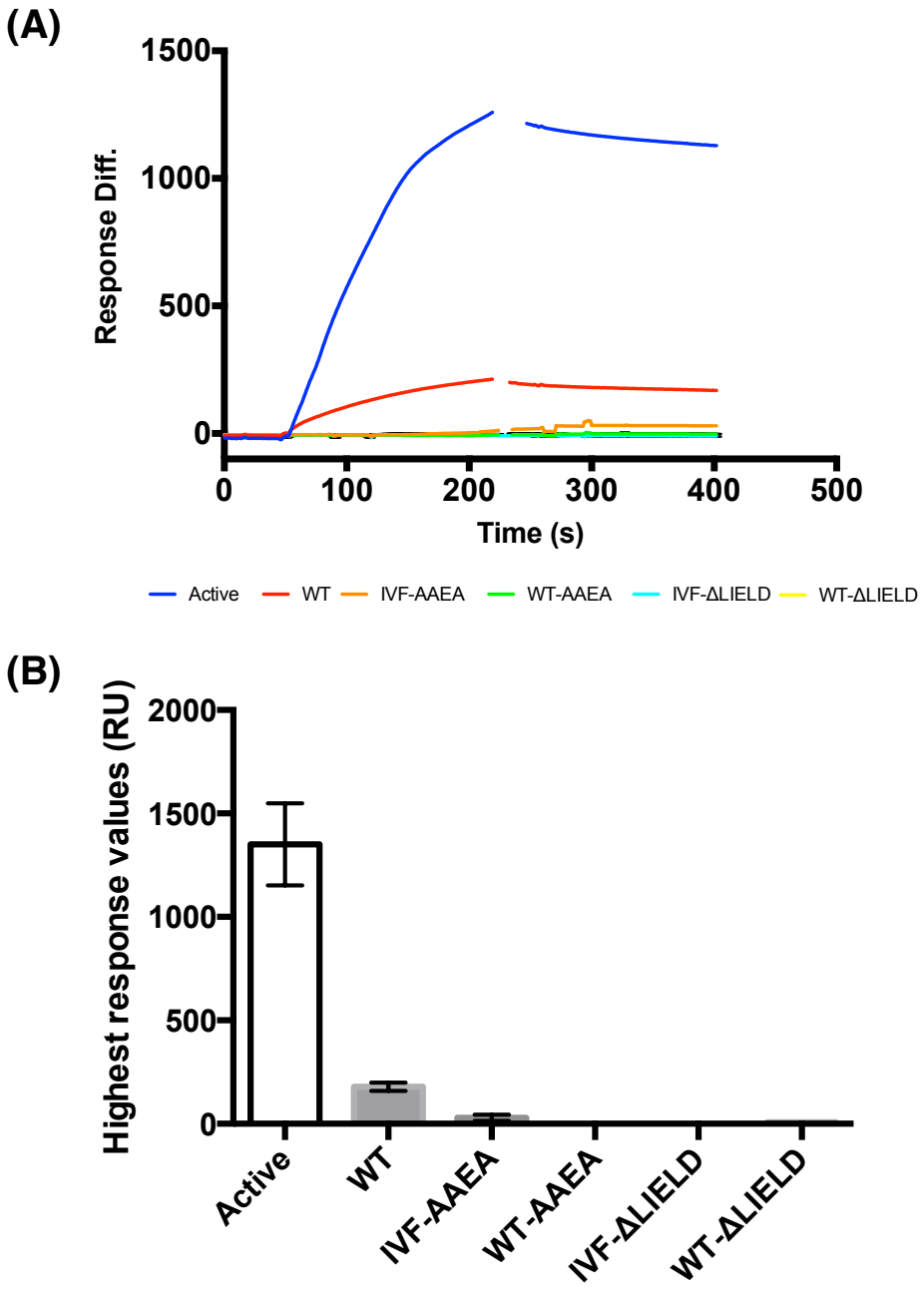

Figure 5.8.5: Binding of β-arrestin 1L WT (10 μM) and mutants to GST-TD (1-363) (1 μM). (A) *Binding of purified β-arrestin 1L WT and 5 mutants to GST-TD. The Active beta-arrestin 1L binds the strongest, whereas the WT shows reduced binding. The IVF-AAEA mutant ha binding higher than all the rest of the mutants (WT-AAEA, IVF- ΔLIELD and WT- ΔLIELD), but shows significantly lower binding than Active or WT. These results are taken from 3 consecutive repeats on monoclonal anti-GST immobilised CM5 chips.* ***(B)*** *The results from (A) are plotted on a bar chart representing the mean from the highest response value of three independent repeats (n=3) and the standard deviation. The Active form has the highest binding response of 1351.0 RU with the WT next with 179.0 RU. The rest of the mutants do not show any binding at all except the IVF-AAEA, which resulted in a 29.54 RU binding only.*

5.8.6 Discussion

The SPR/IAC data obtained for the WT and mutant β-arrestin 1L were similar to the results of Kang *et al.,* 2009. Overall, the second clathrin box ([LI][LI]GXL) on the β-arrestin 1L is open and accessible for binding to the clathrin TD. A cooperative effect could be hypothesized between the two clathrin box motifs from this data, which contradicts the fact that CCPs *in vivo* can localize even in the absence of the conserved clathrin box motifs (Kang *et al.,* 2009). However, SPR results from Kang *et al.,* 2009 revealed a ~2-fold difference in binding affinity between active and WT β-arrestin 1L. The strongest binding was between the clathrin TD and active β-arrestin 1L with a K_D of 0.98 ± 0.01 μM, whereas the K_D of the WT β-arrestin 1L bound to clathrin TD was 2.1 ± 0.4 μM (Kang *et al.,* 2009). These binding affinities confirm the SPR results in this section, stating how the active β-arrestin 1 has the strongest binding capacity to clathrin compared to the WT (inactive β-arrestin 1 form). Further discussion is detailed in Chapter 7.

5.8.7 Conclusion

In conclusion, I confirmed that the optimized SPR/IAC method works successfully for investigating the binding of the GST-clathrin TD and β-arrestin 1L as adaptor protein, and could later be used to determine binding of other adaptor proteins to the clathrin TD. β-arrestin 1L has two clathrin box motifs accessible, which interact strongly with clathrin TD resulting to the highest response and binding affinity (K_D). I confirmed that the active β-arrestin 1L is an ideal adaptor protein to use in the adaptor competition studies described in Chapter 7, as it has two clathrin box motifs and has been hypothesized to have a 'linking effect' of multiple TDs similar to other adaptor proteins such as epsin 1.

5.9.0 Investigating epsin 1 and clathrin TD interactions

5.9.1 Introduction to epsin 1

Epsin 1 is an endocytic adaptor protein, which has been shown to have a fundamental role in clathrin assembly during clathrin- mediated endocytosis (CME), by membrane remodelling to facilitate lattice curvature but also by promoting clathrin assembly influencing the size of clathrin-coated pits and vesicle formation (Drake *et al.,* 2000; Kalthoff *et al.,* 2002; Ford *et al.,* 2002; Holkar *et al.* 2015). However, the exact mechanism by which epsin 1 interacts and facilitates efficient clathrin assembly is still unclear.

The epsin 1 structure consists of two clathrin box motifs (LMDLA (starting residue 257) and LVDLD (starting residue 480)) at the central region, which have been shown to bind to clathrin TD of the clathrin heavy chain (CHC) (Drake *et al.* 2000). The unstructured region is in between the two clathrin box motifs and consists of eight DPW repeated motifs along the long flexible region, which have also been shown to bind to clathrin independently (Drake *et al.,* 2000; Kalthoff *et al.,* 2002; Brett *et al.,* 2002). These DPW motifs also bind to the α-ear and β2 –ear subunit of AP2, which could promote a cooperative effect between epsin 1 and AP2 in clathrin assembly (Drake *et al.* 2002; Brett *et al.,* 2002; Dafforn and Smith, 2004; Edeling *et al.,* 2006a). Interestingly, epsin 1 is hypothesized to bind to three clathrin TD sites via its two clathrin box motifs and the DPW motifs in the unstructured region. The hypothesized TD sites are: 1(CBM), 2 (W box) and 3 (Arrestin box) (Drake *et al.* 2000; Kalthoff *et al.,* 2002). The yeast homolog of epsin (Ent2) has been shown to bind to the CBox (site 1) and W-box (site 2) of the TD sites (Collette *et al.,* 2009). However, it is still yet to be confirmed whether epsin 1 binds to the RoyleBox (site 4), which has been recently characterized (Muenzner *et al.,* 2017).

Epsin has been hypothesised to promote smaller uniform cage structures *in vitro* (Kalthoff *et al.,* 2002). This has been previously seen with another adaptor called AP180, which has a similar unstructured flexible structure with

DLL motif that interact with clathrin (Ahle and Ungewickell, 1986; Greene *et al*. 2000; Morgan *et al*., 1999; Engvist-Goldstein *et al*., 2001;Kalthoff *et al.,* 2002). Negative stain electron microscopy was used to demonstrate the uniform sized cage distribution that epsin 1 promotes (Figure 5.9.1). Despite our existing knowledge of epsin 1 structure and functionality, questions remain to be answered as to how this unique and complex structure of epsin 1, with its multiple 'clathrin binding' components, interacts with clathrin TDs and promotes efficient clathrin assembly and the alteration in size cage distribution.

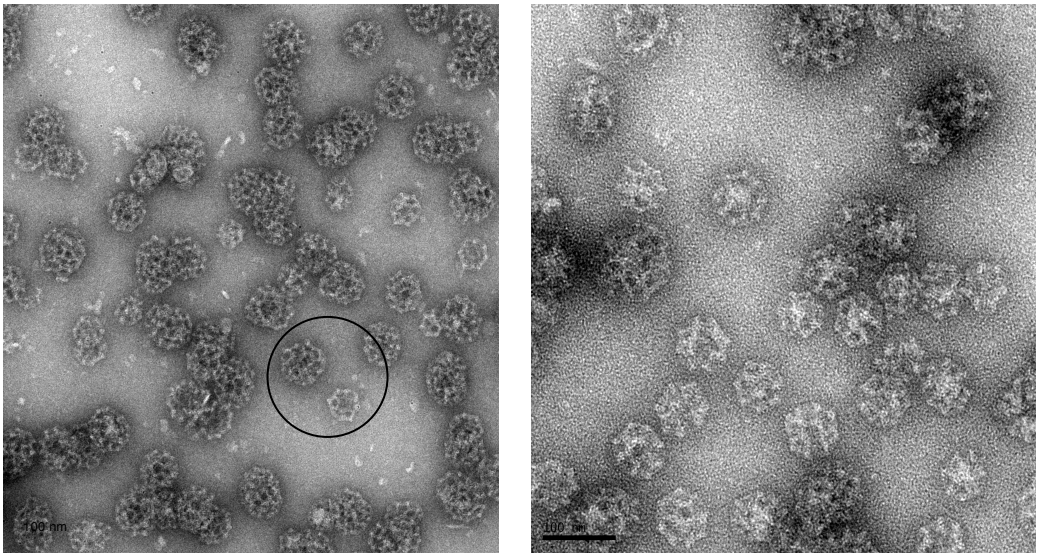

Figure 5.9.1: Images by negative stain EM demonstrating the uniform cage size distribution formed from epsin WT and clathrin cages in vitro. *Clathrin cages were assembled (3 µM) alone (A) and with the presence of epsin 1 WT (30 µM) and imaged using negative stain (2% uranyl acetate) EM at a final concentration of 1uM from the assembled clathrin. Images (**A**) demonstrate the heterogeneity of clathrin cages structures as seen inside the black box. However, in the presence of epsin 1 WT, uniform sized clathrin cages are observed in image (**B**) compared to **(A).** Figure **(A)** is at 25000X magnification and Figure **(B)** is at 30000X magnification using a JEOL 2011 microscope with Gatan Ultrascan 4000 CCD.*

5.9.2 Mutagenesis studies of epsin 1 clathrin box motifs

To investigate this we used mutagenesis studies, where we used full length WT epsin 1 (residues 1-575) and three epsin 1 mutants (257, 480 and DKO) proteins produced from the original WT construct. The mutants were designed in line with Drake *et al.,* 2000 and Holkar *et al.,* 2015. These mutants have alanine substitution at the clathrin binding motifs at the starting residue 257 or 480 or both (DKO), are described in Figure 5.9.2.

Dr. Michael Baker from the Smith group at the University of Warwick first investigated these mutants using ultracentrifugation binding assays/SDS-PAGE analysis and demonstrated that all three mutants of epsin (257, 480 and DKO) still bind to clathrin cages, even when the clathrin box motifs were mutated. He concluded that in all three mutants there was a reduction in clathrin binding of the epsin mutants compared to with WT epsin, with the DKO mutant showing the greatest reduction. He also confirmed the loss of epsin 1 binding to clathrin by carrying out GST-pulldown binding assays of GST-clathrin TD with WT and DKO epsin 1 only. Therefore, he concluded that the deletion of the two clathrin box motifs significantly affects its ability to bind to clathrin TD (Baker, 2016).

As SDS-PAGE analysis is a qualitative technique with a limited dynamic range, I aimed to extend these studies using a quantitative technique, such as the optimized SPR/IAC method, to investigate the binding difference between the WT and the three epsin 1 clathrin box motif mutants for clathrin TD binding.

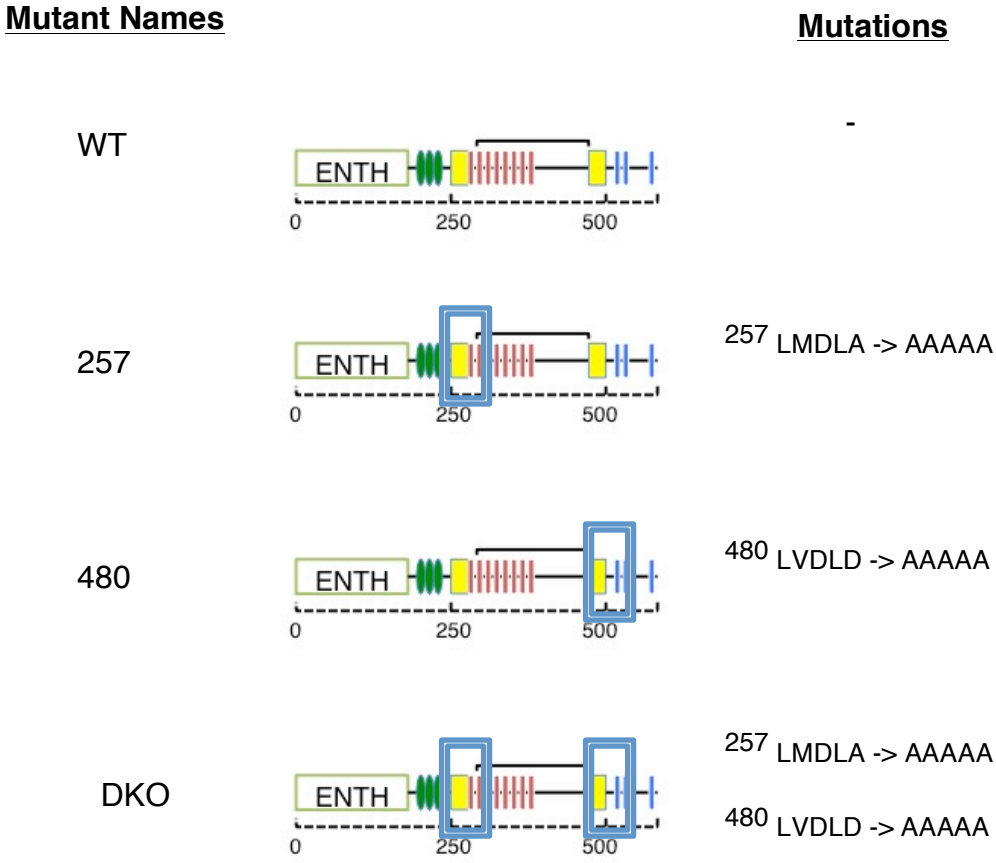

Figure 5.9.2: Diagram illustrating the 'clathrin binding box' motif mutants (257, 480 and DKO) on a linear representation of the epsin 1 structure. The mutants were designed in line with Drake *et al.,* 2000 and Holkar *et al.,* 2015. *The WT form of the epsin 1 structure is represented at the top of the diagram. The 257 mutant has one of the 'clathrin binding boxes' starting at residue 257 mutated to alanines (LMDLA-> AAAAA). The 480 mutant has one of the 'clathrin binding boxes' starting at residue 480 mutated to alanines (LVDLD-> AAAAA). The DKO mutant has both 'clathrin binding boxes' mutated to alanines (LMDLA->AAAAA and LVDLD-> AAAAA).*

5.9.3 Epsin 1 clathrin box motifs have an equivalent clathrin TD binding capacity as its unstructured/DPW region

The SPR/IAC result obtained demonstrated a substantial reduction in binding – half the response of the WT epsin 1 (highest binding response) from the epsin clathrin box mutants. This reduction was equal in all the three mutants (257, 480 and DKO) (Figure 5.9.3 (A)), with no significant difference between them in their ability to bind clathrin TD. These results are representative of three independent repeats (n=3) for each WT and mutant with the mean of

the highest response unit of each sample and standard deviation plotted. The WT epsin 1 has the highest response units of 1171 ± 287.5 RU and the 257, 480 and DKO having significantly lower responses of 586.7 ± 147.2 RU, 578.10 ± 94.43 RU and 550 ± 69.37 RU respectively (Figure 5.9.3 (B)). Overall, these results are consistent with the hypothesis of Drake *et al.* 2000, where reduction of clathrin binding was observed when one clathrin box motif- 257 is deleted and that the unstructured region/DPW between the two clathrin box motifs was suggested to bind to clathrin non-specifically/independently (Drake *et al.,* 2000).

On the other hand, these results are partially consistent with ultracentrifugation assays conducted by Dr. Michael Baker with clathrin cages as described above, with the exception that the SPR data with clathrin TD indicates an equivalent reduction in binding between all three mutants, whereas a greater reduction for the DKO mutant for clathrin TD binding was observed from GST- pulldown assays, as conducted by Dr. Michael Baker (Baker, 2016). It is important to note that pulldown assays were carried out with whole clathrin cages, whereas SPR experiments were carried out using clathrin TD (residue 1-363). An overall reduction in binding is observed between the WT and the three epsin 1 mutants both in cases when clathrin cages (binding pulldown assays) or clathrin TD (SPR data) used.

The two epsin clathrin box motifs function were hypothesized to function cooperatively (Drake *et al.,* 2000; Drake and Traub, 2001), and promote clathrin assembly, a result which was confirmed with evidence from Holkar *et al.* 2015 (Holkar *et al.,* 2015). However, the SPR data in this section indicate a similar binding affinity of the clathrin TD for each of the two clathrin box motifs and the unstructured region/DPW motifs suggesting that they bind in a cooperative manner to clathrin. This was shown from the SPR data, which revealed no significant difference in response between the three mutants (257, 480, DKO). This has not been previously suggested or observed and therefore adds an important insight into how the epsin 1 structure effects the interaction with clathrin.

Preliminary investigations from Dr. Michael Baker confirmed that mutating the epsin 1 clathrin box motifs (257 and 480 mutants) still had a subtle effect on altering the cage size distribution from an average radius of ~ 45 nm to ~ 35 nm, in a manner similar to WT epsin as determined by DLS and EM (Baker, 2016). Even though there are different biodynamic interactions between clathrin cages and clathrin TD, the DLS/EM results could relate to the clathrin-TD SPR data obtained in this section, suggesting that even when the reduction in clathrin TD binding between the epsin 1 clathrin box mutants is equal there is more complex behavior of epsin 1:clathrin interaction is likely much more complex.

A strong epsin-clathrin interaction is suggested due to the slow dissociation of the complex observed in WT and three epsin 1 mutants, with the response curve not reaching the baseline. This could possibility demonstrate the strong and cooperative behavior characteristic of multiple site interaction of epsin 1's two clathrin box motifs and the unstructured/DPW motif region binding to clathrin TD- a much longer dissociation time will be required to disrupt many existing interactions.

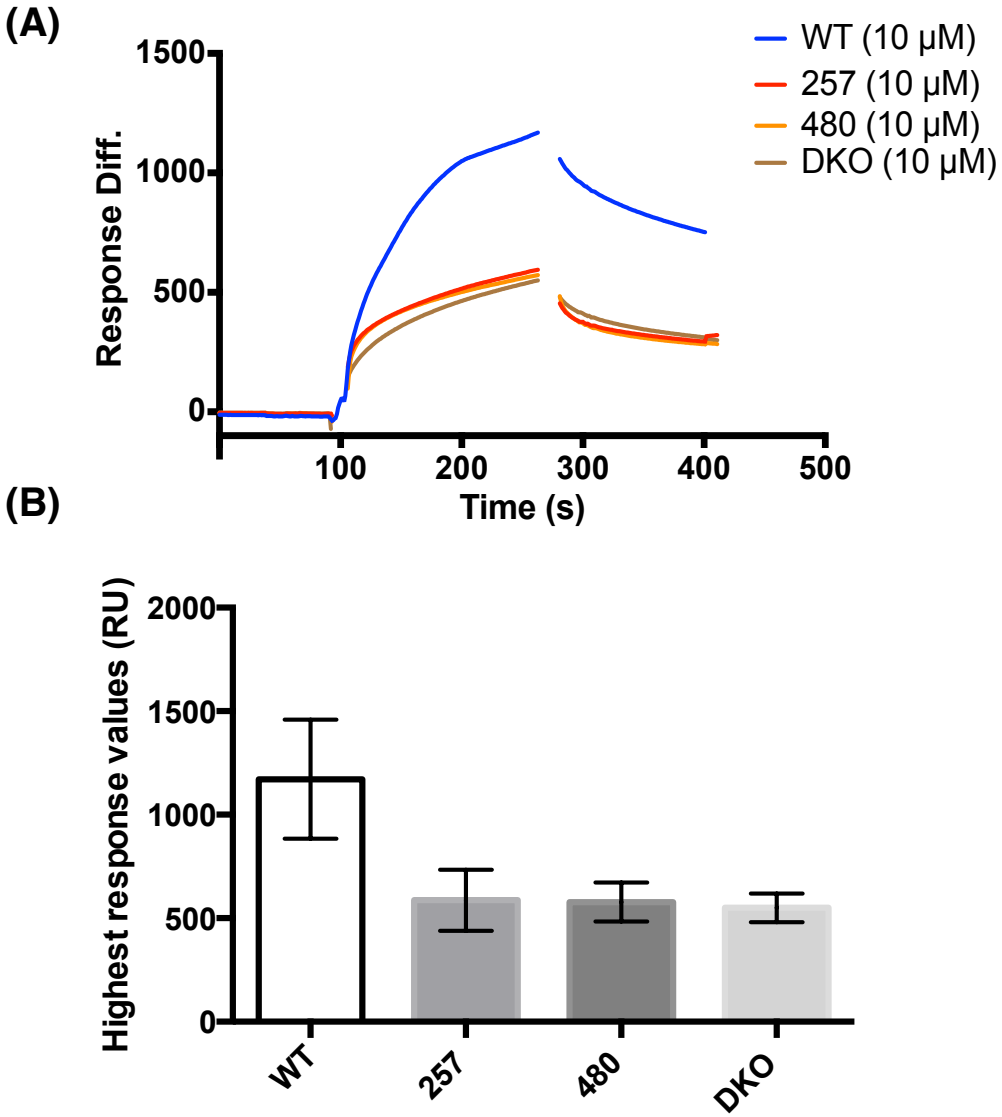

Figure 5.9.3: Binding of epsin 1 full-length (residues 1-575) WT and 'clathrin binding box' mutants (10 µM) to GST-TD (1-363) (1 µM), to investigate epsin:clathrin interactions. (A) *Binding of purified epsin 1 of WT and 3 mutants (257, 480 and DKO) to GST-TD. WT binds the strongest, with an unusual binding curve, which is hypothesized not to be a 1:1 stoichiometric binding with TD. Whereas all the 3 mutants have a very similar binding capacity to the GST-TD with a hypothesised 1:1 stoichiometric ratio, due to the shape of the binding curve. Each experiment was carried out in a series of three repeats in randomised order. Overall, no saturation was observed in the SPR experiments, even in 1:10 molar ratio of clathrin to epsin 1, which was the recommended ratio with excess epsin 1 concentration* ***(B)*** *The results from (A) are plotted on a bar chart representing the mean from the highest response value of three independent repeats (n=3) and the standard deviation. The WT epsin 1 has the highest response of 1171.0 and the 257, 480 and DKO having significantly equal lower responses of 586.7, 578.10 and 550.00 respectively.*

5.9.4 Mutagenesis studies of epsin 1 unstructured/DPW region

Using the SPR/IAC technique, the observation that mutating single clathrin box motifs or both in epsin 1 resulted in a substantial reduction in its ability to bind to clathrin TD was confirmed. In addition, I demonstrated how the clathrin box motifs and the unstructured/DPW region could possibly have an equal contribution to epsin 1 binding to clathrin TD. Thus, both epsin 1 structure components could be equivalently strong in their affinity to bind clathrin TD. A number of interesting questions arose from the above initial observations as to how the two clathrin box motifs and the unstructured/DPW motif function could promote clathrin assembly. Hence, after investigating the two clathrin box motifs; epsin's unstructured/DPW motif region via mutagenesis studies and SPR/IAC technique was aimed to be investigated.

In order to investigate this unstructured/DPW region of epsin 1, we designed and obtained mutants in which the unstructured/DPW region was deleted or shortened, hence reducing the distance between the two 'clathrin box motifs. The mutants are illustrated in Figure 5.9.4 and are abbreviated as follows: ½ DPW, ¼ DPW and ΔDPW. Briefly, in the ½ DPW, 93 amino acids were cut (approx. half of the region) from the original 216 amino acid sequence of the unstructured region. No DPW motifs of the region were deleted in this mutant. In the ¼ DPW mutant, 153 amino acids were deleted (approx. quarter of the region), with four DPW motifs deleted. In the ΔDPW, 209 amino acids were deleted together with all eight DPW motifs in this region. Thus the whole unstructured/DPW region has been completely deleted in this mutant.

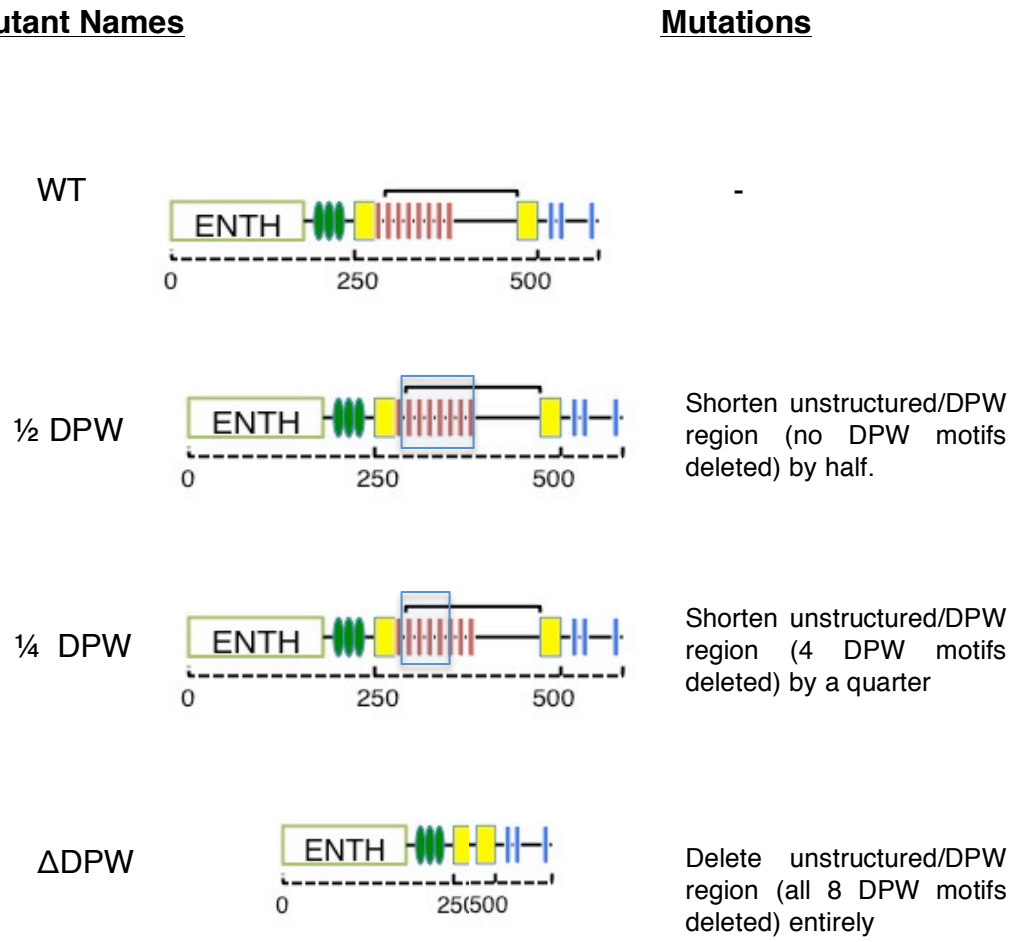

Figure 5.9.4: Diagram illustrating the unstructured/DPW region mutants (½ DPW, ¼ DPW, ΔDPW). *The ½ DPW mutant has a shorter unstructured/DPW region by half (93 amino acids shorter) retaining all eight DPW motifs. The ¼ DPW mutant has shortened by a quarter (60 amino acids shorter, deleting four of the eight DPW motifs. The ΔDPW mutant has deleted the entire unstructured/DPW region and all the eight DPW motifs.*

5.9.5 Shortening the unstructured/DPW region massively reduces its binding for clathrin TD

The primary observation of the SPR data demonstrated that the ½ DPW mutant and the ¼ DPW mutant cause a substantial reduction in clathrin TD binding, compared to the WT epsin binding response, as seen in Figure 5.9.5. This reduction in response was approximately equivalent to the reduction in response of the clathrin box motifs (257, 480 and DKO) epsin 1 mutants (Figure 5.9.3). The fact that the decreased response is very similar

between the two types of epsin mutants could add further insight to the hypothesis that the unstructured/DPW region has an equivalent importance and equal binding capacity as the two clathrin box motifs. A major observation from the SPR data is how the distance of the unstructured/DPW motif and the DPW motifs separately contribute equally to epsin 1 binding to the clathrin TD. This was demonstrated when the binding response of the ¼ DPW mutant was slightly less (~ 200 response units) than ½ DPW mutant (Figure 5.9.5 (B)), demonstrating that when the distance is shortened further and when four DPW motifs have been deleted, this further decreases the ability of the epsin 1 to bind to clathrin TD. Based on these results, I propose that both the distance and the presence of DPW motifs in that unstructured/DPW region are equally important for the manner in which the epsin 1 binds to clathrin TD, until otherwise proven.

It is important to note that the overall maximum response unit of ½ DPW is 766.7 ± 244.9 RU which is the highest in all the epsin 1 mutants used with ¼ DPW at 550.0 ± 233.3 RU which is similar to the response units of 257, 480 and DKO epsin mutants as shown in Figure 5.9.5 (B). This supports the idea that the presence of the two clathrin box motifs, as in the case of ½ DPW, provides a strong binding interaction with clathrin TD, however shortening the unstructured/DPW region has clearly played a major role in reducing epsin's ability to link multiple clathrin TDs. Shortening the unstructured/DPW region distance even further (¼ DPW mutant) demonstrates how this mutant has equal response units with mutating the clathrin box motifs individually (257 and 480) or both together (DKO).

The lowest response (174.7 ± 44.47 RU) observed in these SPR results, was the ΔDPW epsin mutant (Figure 5.9.5) where the complete unstructured/DPW region and the eight DPW motifs have been deleted. There are several possible explanations for this observation. An initial observation could be that in the ΔDPW epsin mutant the two clathrin box motifs are in a very close proximity lacking the flexibility offered from the

unstructured/DPW region. This could affect the way the two clathrin box motifs bind to clathrin TD. If these two clathrin box motifs bind to different clathrin TD sites on multiple TDs from the cooperative behaviour with the unstructured/DPW region (Morgan *et al.,* 1999; Greene *et al.,* 2000; Drake *et al.,* 2000; Drake and Traub, 2001; Kalthoff *et al.,* 2002; Dafforn and Smith, 2004), shortening the distance between the two clathrin boxes, could prevent epsin 1's multiple TD linking interaction effect. This effect would result in a large reduction in the affinity of epsin 1 binding to clathrin TD, compared to the other mutants, as seen in the SPR data for ΔDPW mutant (Figure 5.9.5 (B)). Alternatively, if epsin 1 normally binds to multiple TD sites (CBox, ArrestinBox and W-box) on a single clathrin TD; this would not be possible with a ΔDPW epsin 1 mutant, as the shortening of the unstructured/DPW motif region would not allow long-distance interactions and the two clathrin box motifs could bind on multiple TD sites on a single ~ 5 nm sized TD. Nevertheless, taking into account the above results, I conclude by proposing that both the distance of the unstructured region, and the DPW motifs of the region are equally important for efficient interaction of epsin 1 to clathrin TD.

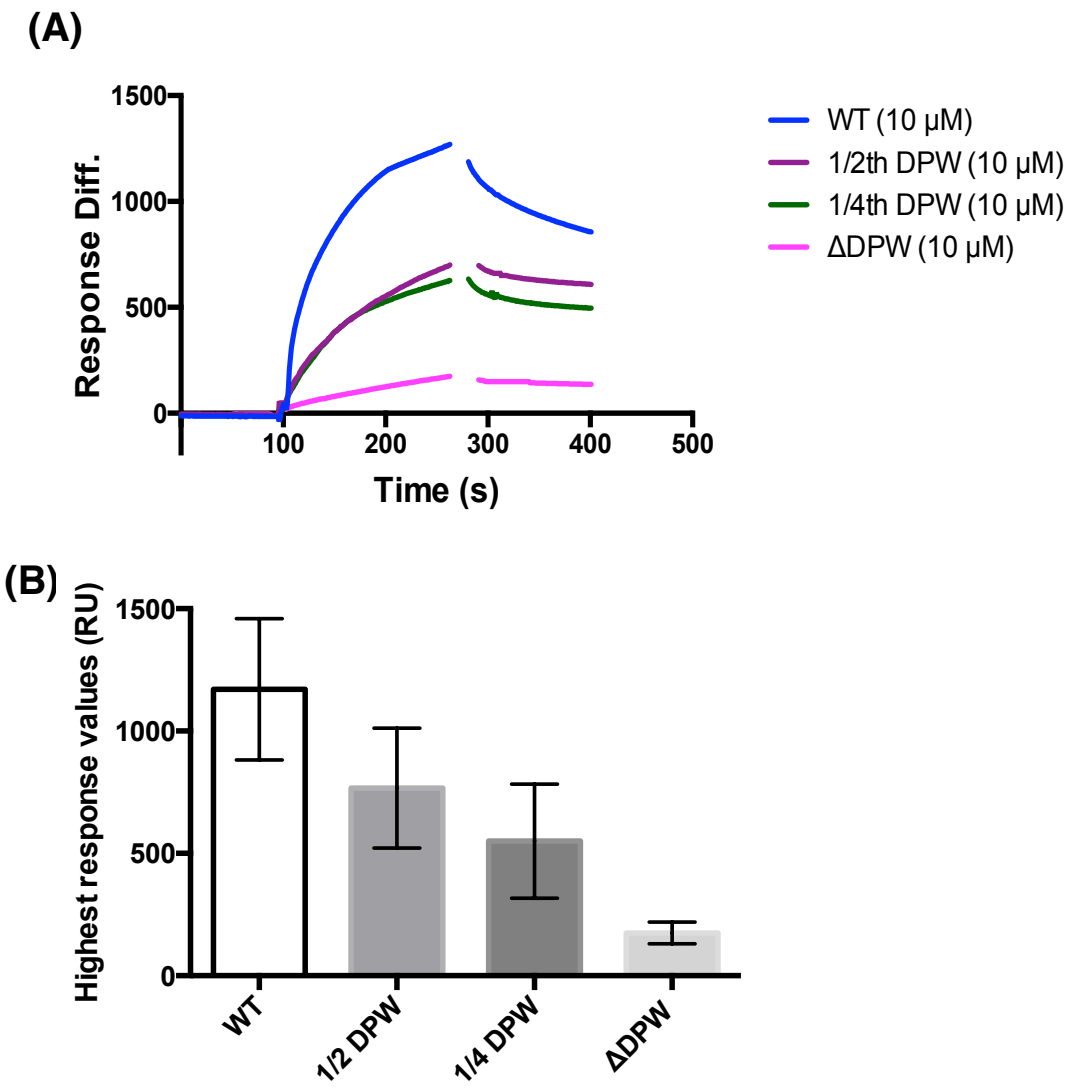

Figure 5.9.5: Binding of epsin 1 full-length (residues 1-575) WT and 'unstructured/DPW' mutants (10 µM) to GST-TD (1-363) (1 µM), to investigate epsin:clathrin interactions. *(**A**) Binding of purified epsin 1 of WT and three mutants (½ DPW, ¼ DPW and ΔDPW) to GST- clathrin TD immobilized on the SPR chip via IAC method. WT binds the strongest, with an unusual binding curve, which is hypothesized not to be a 1:1 stoichiometric binding with TD. Whereas all the three mutants have a very similar binding capacity to the GST- clathrin TD with a hypothesised 1:1 stoichiometric ratio, due to the shape of the binding curve. Each experiment was carried out in a series of three repeats in randomised order. Overall, no saturation was observed in the SPR experiments, even in 1:10 molar ratio of clathrin to epsin 1, which was the recommended ratio with excess epsin 1 concentration (**B**) The results from (A) are plotted on a bar chart representing the mean from the highest response value of three independent repeats (n=3) and the standard deviation. The WT has the highest response units followed by the ½ DPW which has a response unit of 766.7 and the ¼ DPW has a response unit of 550.0 RU. The ΔDPW has the lowest response units of 174.7 RU.*

5.9.6 Differences in TD binding modes between epsin 1 mutants

Epsin's structure displays a level of complexity, which is hypothesized to be due to multiple factors as found in the published literature and the results in this chapter. The SPR response curves obtained have different shapes between the WT epsin 1 and the six epsin 1 mutants. Interestingly, the clathrin box motif mutants have a significant difference in the SPR response curves compared to the shortened/deleted unstructured/DPW region mutant SPR response curves.

Initially, the shape of the WT epsin 1 curve in Figure 5.9.6 (blue curve) was observed to contain a change in the slope of the curve, which could suggest a two-phase binding interaction that would not be a 1:1 stoichiometry. This is consistent with the fact that there are two components in the epsin 1 structure (WT form) that bind to clathrin TD, which are the two clathrin box motifs and the unstructured/DPW motif region. Thus, a 'two level' interaction could explain such a change in the slope of the curve.

However, based on the observed SPR response curves, not all the epsin 1 mutants demonstrate the two-phase binding as WT epsin 1. The clathrin box mutants (257, 480, DKO) and 'unstructured/DPW motif mutants (½ DPW, ¼ DPW and ΔDPW), were observed to have similar curve shapes between each set of mutants, which could suggest a 1:1 stoichiometry of clathrin TD to epsin (Figure 5.9.6). Although, if we compare the curve shape of all the clathrin binding box mutants (257, 480 and DKO) with those of the unstructured/DPW motif region (½ DPW, ¼ DPW and ΔDPW) mutants; we can observe a subtle difference. A sharp increase in response at the start of the curve of the clathrin box mutants is observed, which is not seen in the unstructured/DPW region mutants (Figure 5.9.6). This could be because the clathrin box mutants could be associating with clathrin TD quicker and with a stronger interaction mode than the unstructured/DPW motif mutants. These differences in curve shape could give further insight into the different manner in which epsin 1 binds to the clathrin TD and the hierarchy in the binding of

the different clathrin binding components of epsin 1, and aid into future questions as to how the 'multiple TD linking' behaviour of epsin 1 changes depending on the mutating/deleting of different components of its structure.

These observations are semi-quantitative, they could not be conclusive as further quantitative analysis is required which would result in obtaining binding and dissociation rate constants for the WT and all epsin 1 mutants, in order to verify such hypothesis.

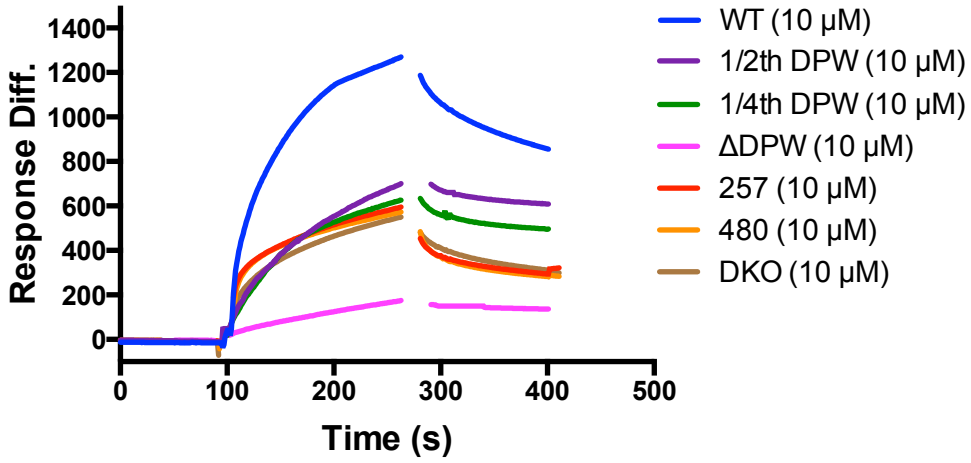

Figure 5.9.6: A SPR sensorgram plot illustrating the difference in response curve results between epsin 1 'clathrin binding box' mutants and 'unstructured /DPW region' mutants. *SPR/IAC experiments were carried out for WT and mutant epsin 1 for clathrin TD. We can clearly observe difference between the 257,480, DKO mutants compared to the ½, ¼, ΔDPW mutants. This could demonstrate the difference in the mode of interaction when different components of epsin 1 structure have been mutated or deleted. The WT epsin 1 response curve demonstrates how epsin could bind to clathrin TD in a multivalent manner linking different multiple TD together.*

5.9.7 Interpreting complex interactions of disordered proteins using SPR kinetic analysis

A binding affinity of ~ 156 μM ± 6.00 has been determined previously in the Smith's group between 257 epsin 1 clathrin box peptide and clathrin TD using fluorescence anisotropy (Sarah Batson, unpublished data). This is considered a very weak binding, which could be due to the use of peptides. In this thesis, full-length epsin 1 WT and mutants (257, 480, DKO) were used for kinetic analysis. The outcome of binding rate and dissociation rate

constants will be based on the data collected from SPR/IAC experiments. Careful optimization was carried out as discussed earlier in this chapter for epsin 1 WT and mutants, prior any kinetic experiments and analysis. The final parameters for the kinetic experimental runs for epsin 1 include six analyte concentrations ranging from 5 μM to 0.3125 μM, which would result to lower response units, ideal for kinetic model fitting analysis.

Problems with the SPR instrument failure due to age of the instrument resulted into spikes in unfortunate positions in the resulting experimental data of the WT and mutant epsin 1, and time did not permit additional experiments. The only experimental data set with no anomalies/spikes was for the 480 epsin 1 mutant data, which was the only one fitted. The kinetic models fitted were 1:1 Langmuir, 1:1 binding with mass transport, heterogeneous ligand/ parallel reaction, bivalent analyte, which were discussed earlier as well. No binding rate and dissociation constants have yet been determined for the 480 epsin 1 mutant, binding to clathrin TD, thus this preliminary new data shown below and kinetic fits/rate constants provide a basic initial insight into the role of 480 epsin clathrin box.

The kinetic analysis of the 480 epsin 1 mutant, illustrated the complexity of the epsin's structure and the complex epsin:clathrin interactions. Initially, the simplest model, the 1:1 Langmuir model was fitted. The results demonstrated a χ^2 of 71 (best χ^2 <10) and a K_D of 3.4 μM (Figure 5.9.7i (A), Table 1.8.0). Additionally, due to the mass transport limitation detailed previously in this chapter, the 1:1 binding with the mass transport model was the next to be explored. Even though the results revealed a better χ^2 of 58.9 than the 1:1 Langmuir χ^2, the K_D (3.1 μM) was not significantly better (Figure 5.9.7i (B), Table 1.8.0).

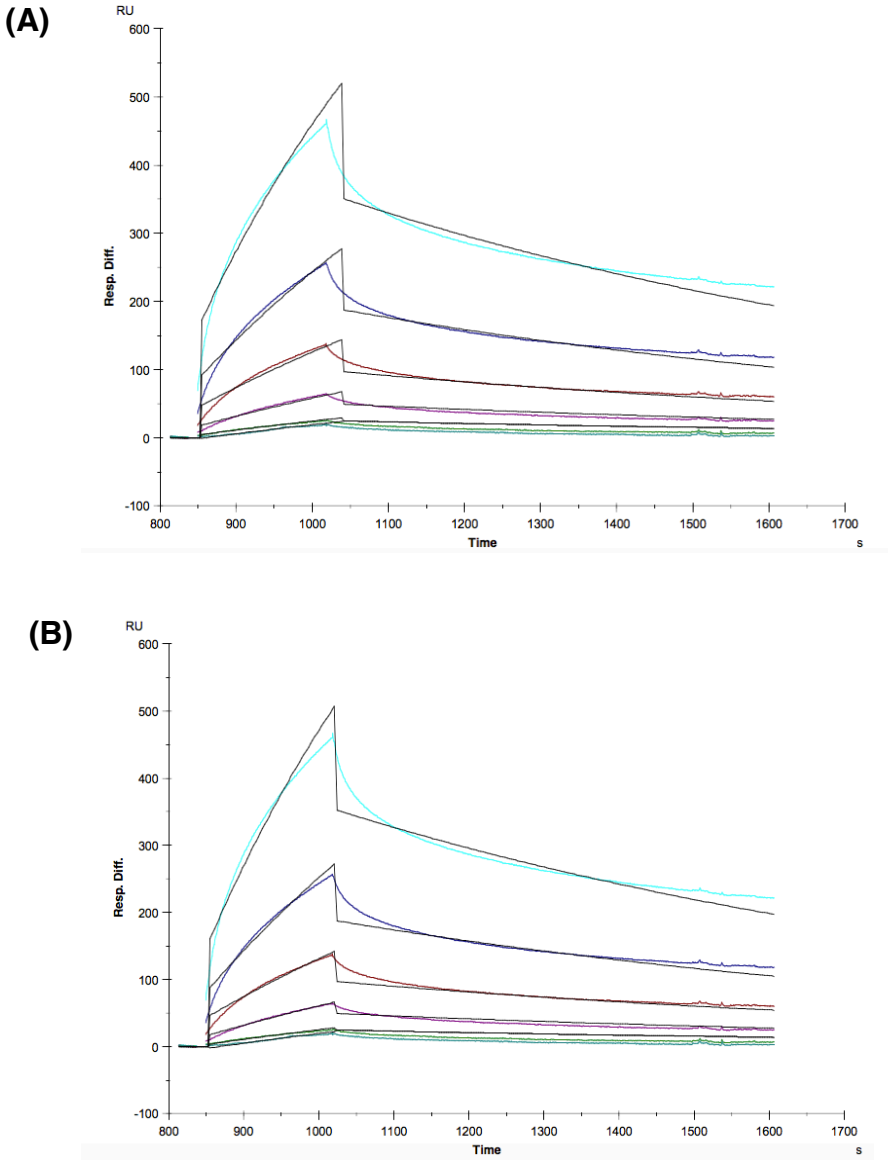

Figure 5.9.7i: Fitting of the experimental data of 480 epsin 1 mutant 1:1 simple kinetic models at a concentration range of 5 µM to 0.3125 µM *(**A**) the initial model was the 1:1 Langmuir model, which is considered the simplest model (**B**) The same 1:1 Langmuir model was fitted which took account the mass transport issue, which remained not an ideal model for the experimental data. These models are found in the BIAevaluation program version 4.1 of BIAcore system of the SPR instrument (Biacore 2000), and all the data fitting and rate constants obtained was carried in the BIAevaluation program implemented in the SPR system.*

These results indicate that 480epsin:clathrin is not a 1:1 stoichiometry interaction. The heterogeneous ligand/parallel reaction model used resulted to a χ^2 of 51.2, which is better than any of the 1:1 models above; and a K_D of 0.009623 μM (Figure 5.9.7ii (A), Table 1.8.0), which is not considered a better K_D value. The best-suited model was the bivalent analyte model where we observed the lowest χ^2 of 48.9 and K_D of 21.4 μM (Figure 5.9.7ii (B), Table 1.8.0). However, the improvement of the χ^2 value from a 1:1 to two-step model analysis, the χ^2 values are very high hence the fitting of the experimental data with the model is very poor. Assuming that mass transport is not a limiting factor here, we could hypothesize that the heterogeneous curve shape of the experimental data could result from an inherent property of 480epsin:clathrin. The challenge in fitting the experimental data has suggested that the 480epsin:clathrin interaction could be a multivalent interaction and not a 1:1 stoichiometric complex. This could add further information to the previous hypothesis in this thesis that such an epsin 1 mutant could have a multivalent interaction with multiple clathrin TDs. This could be due to the interaction of the 257 clathrin box motif and the unstructured/DPW motif with the clathrin TD. This supports the proposed hypothesis that clathrin box motifs and the unstructured/DPW motif region are more likely to have a cooperative effect in binding to the clathrin TD. However, further optimization is required in analysis of these results, but due to the complexity and time constraints, this was not possible. The experiment-to-model fits were not a perfectly convincing fits thus a more complicated fitting model, which takes into account the 'multiple site linking' behavior of epsin 1 needs to be fitted to this experimental data. The development of a new kinetic model is a complex task, which is currently continuing in collaboration with Dr. Veselina Uzunova.

(A)

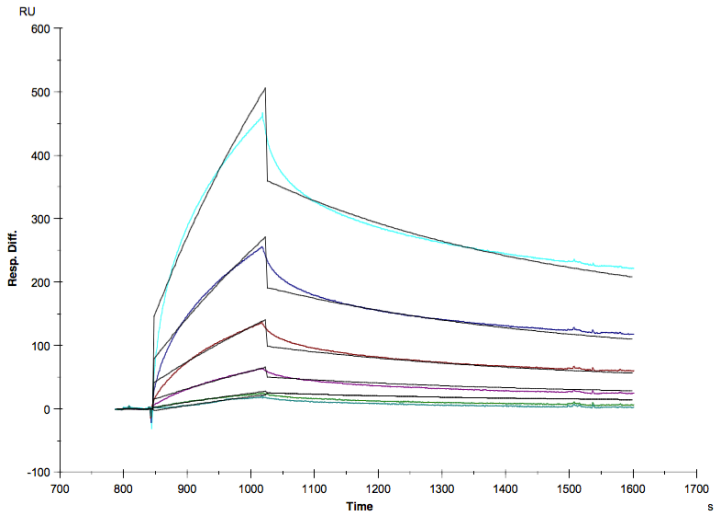

(B)

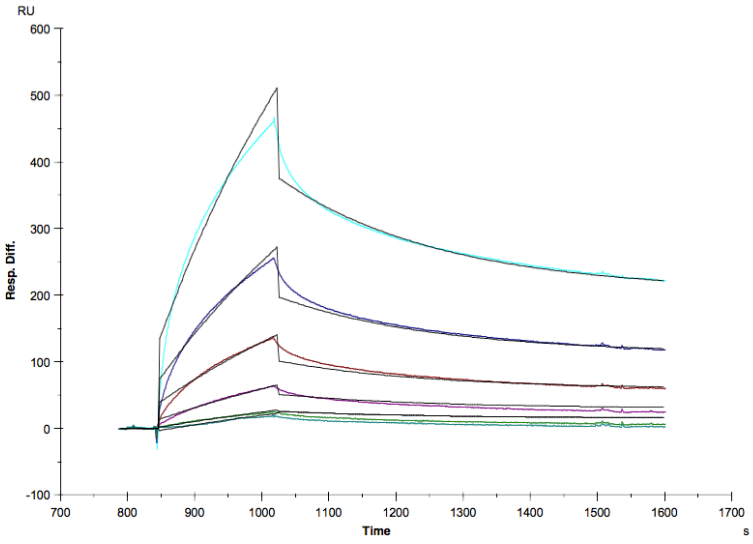

Figure 5.9.7ii: Fitting of the experimental data of 480 epsin 1 mutant two-step kinetic models at a concentration range of 5 μM to 0.3125 μM (A) *The heterogenous ligand/parallel reaction model was used where it involved the analyte interacting with two ligands at the same time* ***(A).*** *The bivalent analyte model was also used which involved the analyte interacting with two sites on the same ligand* ***(B).*** *The fitting of the experimental data (coloured curved) and the model (black curves) releaved very high* χ^2 *values. However, the fits were better than in the 1:1 models and therefore epsin could be suggested to have a multivalent binding interaction manner with clathrin TD. This demonstrates the complexity of epsin structure as a whole constructs were used to carry out these kinetic analysis. These models are found in the BIAevaluation program version 4.1 of BIAcore system of the SPR instrument (Biacore 2000), and all the data fitting and rate constants obtained was carried in the BIAevaluation program implemented in the SPR system.*

Protein (Epsin)	Model type	k_a (1/Ms)	k_d (1/s)	$k_{D=(}\ k_{d/}\ k_{a)}$ (M)	k_D (µM)	χ^2
480	1:1 Langmuir	308	$1.05x\ 10^{-3}$	$3.41x10^{-6}$	3.4	71
480	1:1 binding with mass transport	318	$9.97x\ 10^{-4}$	$3.14x10^{-6}$	3.1	58.2
480	Heterogenous ligand/parallel reactions	214	$2.06x10^{-6}$	$9.63x10^{-9}$	0.009 623	51.2
480	Bivalent analyte	107	$2.3x10^{-3}$	$2.14x10^{-5}$	21.4	48.9

Table: 1.8.0: Illustrating the results from kinetic analysis of the 480 epsin 1 mutant data fitted in four different models *The binding rate constants (k_a), the dissociation rate constants (k_d), the equilibrium constant (K_D) and the χ^2 of each model-experimental fitting of the 480 epsin 1 mutant data using a concetrstion series of 5 µM – 0.3125 µM. The models are found in the BIAevaluation program of BIAcore system of the SPR instrument, and all the data fitting and rate constants obtained was carried in the BIAevaluation program.*

5.9.8 Further optimization for kinetic analysis

The majority of the preliminary work to optimize the SPR/IAC method for kinetic analysis for the clathrin-adaptor system has been already carried out in this thesis. The preliminary kinetic analysis provided essential information which confirms that epsin:clathrin complex is not a 1:1 binding interaction. Further kinetic optimisations were suggested by Prof. Richard Napier (University of Warwick) and Dr. Petr Kuzmic (BioKit Ltd., USA) through personal communication. These are listed below and could be addressed in the future:

I. attach His_6 -epsin 1 on the chip (sensor NTA chip), as the bigger protein of 78 kDa, and flow over the GST-TD (66 kDa) and compare

these findings to the ones already obtained with GST- clathrin TD bound on the CM5 sensor chip via anti-GST antibody capturing. This will eliminate the use of an antibody capturing which is an additional complicating factor for the analysis and mass transport.

II. Lower the response units obtained from the ligand-analyte interaction to ~ 100-200 RU. This is ideal as mass transport could still be observed in response units of even 500-600 RU (Lang *et al.,* 2005). However, keeping low RU in all experiments has previously been challenging in this thesis due to the complex epsin 1 structure and its complications with non-specific binding and mass transport.

III. Vary the concentration range and ratios of clathrin:epsin in order to reach an appropriate saturation level and targeted low response units.

IV. A more complicated model needs to be derived which takes into consideration the 'linking behavior' of epsin for multiple clathrin TD(s) binding.

V. Future kinetic experimental runs could be carried out using a more sensitive and advanced SPR instrument e.g. Biacore T200. The sensitivity of such an instrument could ideally minimize the mass transport issues and provide more accuracy in the data obtained. Hence, result to more accurate binding affinities obtained from kinetic analysis.

5.10.0 Biological application of epsin's structure in CME: how the epsin 1 structure facilitates clathrin TD binding for efficient clathrin assembly

5.10.1 Scenarios based on epsin clathrin box mutants

Taking into account the above SPR data of WT epsin1 and mutants (257, 480, DKO), I propose the below three possible scenarios on how epsin 1 could be interacting with clathrin TD to facilitate an efficient clathrin assembly and promote uniform smaller sized cage distribution. These scenarios are

based on the results obtained in this thesis as well as previous published information.

(1) The two clathrin box motifs have been proposed to work cooperatively to assemble clathrin (Drake *et al.,* 2000; Drake and Traub, 2001; Holkar *et al.,* 2015). However, based on the results in this Chapter, I propose that the unstructured/DPW motif region of epsin 1 could equally have a cooperative effect with the two clathrin box motifs, as well as the two clathrin box motifs between them, to promote efficient clathrin assembly. This scenario could be very plausible, as the unstructured/DPW motif region has been observed to have equivalent binding capacity as the two clathrin box motifs. This hypothesis is based on the SPR data in this chapter, where the highest response in the SPR data was observed from the WT epsin 1, whereas by mutating the two clathrin box motifs respectively (257 and 480) or together (DKO), the binding response was greatly reduced in all three mutants. Interestingly, the reduction was equivalent in all three mutants, even when both clathrin box motifs have been mutated (DKO).

(2) Epsin 1 has previously been hypothesized to have a linking effect between multiple clathrin TDs (Morgan *et al.,* 1999; Greene *et al.,* 2000), Drake *et al.,* 2000; Drake and Traub, 2001; Kalthoff *et al.,* 2002; Dafforn and Smith, 2004; Holkar *et al.,* 2015), but was yet to be proven. Quantitative data from SPR/IAC method, suggested that epsin 1 could be interacting with multiple adjacent clathrin TD. This could be due to the flexibility of the unstructured/DPW region (Dafforn and Smith, 2004), where the two clathrin box motifs are hypothesized to be separated by a distance shorter than 155 nm (Kalthoff *et al.,* 2002). Therefore, it has been hypothesized that a single epsin 1 molecule could simultaneously engage with two different sites on two different clathrin TD, which are in close proximity, instead of only a single TD. This states that epsin 1 could be promoting linking of multiple clathrin TD. This effect could potentially stabilize clathrin cages via the extra interactions between linked triskelia and offer a more compact cage structure. Hence,

facilitating uniform and smaller cage distribution, as suggested by Kalthoff *et al.,* 2002 (Kalthoff *et al.,* 2002).

(3) the two clathrin box motifs on a single epsin 1 molecule could be binding and interacting with two different sites (TD has four distinct sites) on a single TD or on multiple TDs. More interestingly, one of the clathrin box motif in epsin 1 at residue 257 (LMDLA) has been proposed to be similar to the W-box motif of amphiphysin (WLDWP) and hence may interact with the clathrin TD at the same site e.g. site 2, W-box site (Drake and Traub, 2001; Miele *et al*., 2004). The yeast homolog of epsin (Ent2) has been shown to bind to CBox and the W-box of the TD sites (Collette *et al.,* 2009). Thus, I propose that epsin 1 might be interacting with sites 1 (C-box site), site 2 (W-box) and site 3 (Arrestin site) on the clathrin TD. In order for epsin 1 to perform such an interaction, the long and flexible unstructured/DPW motif region would be promoting the flexibility of the two clathrin box motifs to interact on the same clathrin TD. This permits the unstructured/DPW motif region to contact with the same TD or interacting with other adaptor proteins e.g. AP2 promoting efficient clathrin assembly (Drake *et al.,* 2002; Brett *et al.,* 2002; Dafforn and Smith, 2004; Edeling *et al.,* 2006a).

5.10.2 Scenarios based on unstructured/DPW region mutants

According to Drake *et al.,* 2000, the region between the two clathrin box motifs in the epsin 1 structure binds to clathrin independently, which I hypothesize has an equally strong contribution to epsin 1 binding to clathrin, similar to the two clathrin box motifs (Drake *et al.,* 2000). Investigating this unstructured region further resulted in very interesting outcomes on how epsin 1 interacts with clathrin TD. Considering those outcomes, I propose below three possible scenarios to how epsin 1 interacts with clathrin TD:

(1) I demonstrated using SPR/IAC method, that disrupting this region either by shortening this region by half (~ 78 nm) or by quarter (~ 38 nm) causes a

massive reduction to epsin 1's ability to bind to clathrin TD. This reduction is equivalent to that of the clathrin box mutants (257, 480, DKO). Hence, I suggest that the unstructured/DPW motif region binds to clathrin with equal binding capacity as the two clathrin box motifs. This could validate the observation proposed in scenario (1), section 5.10.1.

(2) the distance and the DPW motifs in the unstructured/DPW region are equally important in affecting how epsin 1 binds to the clathrin TD via long-distance interactions. This was confirmed with the SPR data that revealed the response of the ½ DPW mutant and ¼ DPW mutant to bind to clathrin TD decreased compared to the WT epsin 1. The ~ 200 RU difference observed between the ½ DPW mutant and ¼ DPW mutant, with the ¼ DPW mutant being lower, could suggest that both the distance and DPW motifs are important without clearly prioritizing one over the other. Additionally, the unstructured/DPW region is hypothesized to be long enough and even if it has been shortened by half or by quarter, it most likely still promote long-distance interactions between multiple clathrin TDs but in a lesser extend. Replacing the unstructured/DPW region with a fake linker sequence that does not bind to epsin 1 could clarify further as to whether distance of the DPW motifs is the most important component in this region for epsin 1:clathrin interaction. However, additional motifs could be present in the unstructured/DPW region, which could aid to this long-distance interaction effect of epsin 1. However, this might not be the case *in vivo*, and thus shortening (half or quarter) the distance of the region could prevent epsin 1 multiple TDs linking effect. Another option could be that the ½ DPW and ¼ DPW mutants could be binding to the same clathrin TD but on a different site, or one clathrin box motif would bind to single clathrin TD and the other clathrin box motif would be free in solution.

(3) I propose that deleting the unstructured/DPW motif region (ΔDPW epsin 1 mutant) and bring the two clathrin box motifs in very close proximity, would prevent the flexibility of epsin's structure preventing the linking multiple TDs

effect. This should result in a massive reduction in the affinity of epsin 1 binding to clathrin TD, which was observed in the SPR results. I suggest that the ΔDPW epsin 1 mutant would only bind to single TD, with the interaction of one of the clathrin box motifs, and the second clathrin box motif would be left free in solution. This is because the two clathrin box motifs would be in too close proximity with each other, which would prevent interaction of the clathrin box motifs with different TDs, but only with another site on the same TD, if possible. This also confirms the hypothesis that epsin 1 links multiple clathrin TDs.

5.11.0 Future work

Epsin 1 is considered one of the main clathrin assembly adaptor proteins, as it is highly expressed in the brain and has been implicated in synaptic development and plasticity (Vanlandingham *et al*., 2013). Therefore, understanding the mode in which it interacts with clathrin is crucial due to its role in the CME. In light with the above findings, a variety of scenarios have been proposed as to which components of epsin 1 structure interacts with clathrin and which parts of these components are important and could be hypothesized to promote a more efficient clathrin assembly. Certain results in this chapter open up questions for future avenues to verify certain conclusion.

5.11.1 Exploring further the 'unstructured/DPW' region

The experiments carried out using SRP/IAC method with clathrin box mutants and the unstructured/DPW motif region mutants have yielded interesting observations. I proposed that the unstructured/DPW motif region has equivalent strong binding capacity to clathrin TD as the two clathrin boxes promoting a linking effect with multiple TDs, and the distance and the DPW motifs of this region are essential clathrin binding components. More interestingly, I propose that the distance of this unstructured/DPW motif region could be considered the major factor for this hypothesized linking effect of epsin. In order to confirm this hypothesis, I suggest to obtain an

epsin 1 mutant where the unstructured/DPW region has been replaced with a fake linker sequence that does not bind to clathrin, therefore keeping the distance between the two clathrin box motifs in epsin's structure. This will allow us to determine whether the distance between this two clathrin box motifs is the main factor for the TD bridging effect or whether DPW motifs, or any other motifs in that region do actually play a major role as well. Although, if this linking effect is a mechanical effect of epsin 1 linking multiple clathrin together in a cage; atomic-force microscopy (AFM) could be carried out to determine the force required for epsin's mechanical effect, as previously used by Sousa *et al.,* 2016 (Sousa *et al,* 2016).

Through private communication with Stephen Royle, University of Warwick and with some of his group members; I obtained further information about epsin-clathrin interactions *in vivo*. They suggest that the distance between the two clathrin box motifs appears to be vital for artificial initiation of endocytosis in cells either. Their artificial constructs containing three epsin clathrin box motifs in close proximity did not efficiently promote endocytosis (private communication). More interestingly, one of their artificial constructs with the unstructured/DPW region of epsin 1 replaced with a different linker sequence which would not bind to clathrin, allowing the distance between the two clathrin box motifs to remain unchanged. This construct showed no endocytosis in cells, as well (private communication). These findings add further support to the hypothesis that both the DPW motifs of this unstructured/DPW region are a vital component for the linking effect of epsin 1, but also that both the two clathrin box motifs and the distance between them (the unstructured/DPW region) are required for effective binding and functionality of epsin 1 via long-distance interactions.

5.11.2 Using clathrin TD mutants to investigate epsin:clathrin interactions

Additionally, we hypothesize that epsin 1 binds to three different sites on the TD, like AP180 (Zhuo *et al.,* 2015). In order to investigate and confirm this hypothesis, SPR/IAC method could be used with a series of TD mutants in which the four binding sites on TD have been selectively impaired. This would allow us to determine whether epsin clathrin box motifs and the unstructured/DPW region are preferentially favoured to bind to one TD over another, or whether they could bind to multiple different clathrin TD sites at the same time. This would provide a substantial new insight into the hypothesised scenarios in section 5.10.1.

The clathrin TD mutants were designed in line with Muenzner *et al.,* 2017 (Muezner *et al.,* 2017). These mutants were then tested for expression and purification conditions. Smaller scale expression confirmed the successful expression of the constructs, detailed in Chapter 10, but when scaling up the expression the proteins became unstable and were prone to degradation. Unfortunately, due to time constraints, the expression issues could not be further addressed and these mutants were not used in this thesis.

5.11.3 Using epsin 1 peptides of clathrin box motifs with SPR/IAC method for understanding further epsin-clathrin interaction

Full-length epsin protein (residues 1-575) have been used in the SPR/IAC experiments which allow analyzing the protein as a whole, which has allowed to investigate all its clathrin components together. However, due to the complex nature of epsin structure as observed by the kinetic analysis in this chapter, and the mass transport limitations observed when using a full length protein construct; peptides could be a good replacement, as we can isolate the different clathrin components of epsin 1 and investigate them individually. Therefore, individual epsin clathrin box motif peptides and peptides produced

from sections of the unstructured/DPW region could be analyzed using the SPR/IAC method to determine binding and dissociation rate constants for clathrin TD binding. Such an investigation could result in discovering other motifs in the unstructured region, which have not been proven to interact with clathrin. Certain peptides are already available for use, designed and synthesised by Alta Bioscience, UK with the clathrin box residues are in bold: (1) peptide 1: 257 clathrin box motif: ESS**LMDLA**DVF (2) peptide 2: 480 clathrin box motif: NAA**LVDLD**SLV. Such experimental information could validate greatly certain hypothesis regarding the cooperative manner of these two clathrin box motifs and obtain appropriate binding affinity constants.

5.11.4 Investigation of other adaptor proteins with similar structure to epsin 1

Other long unstructured adaptor proteins such as AP180 could act in a similar manner to epsin 1, by linking multiple TDs together and allow effective clathrin assembly and promoting small uniform cage distribution (Kalthoff *et al.,* 2002). In this thesis, AP180 construct was used, which lacks the ANTH domain and consists only with the unstructured D[IL][LF] motifs has been shown by circular dichroism to be fully unstructured. Thus, it may promote non-specific binding in a similar manner to epsin 1. It is important to state that preliminary optimization has been carried out in this thesis for AP180 binding with the SPR/IAC method (*data not shown*). The SPR/IAC method showed massive non-specific binding in the reference flow cell as expected. This was minimised to a certain extent by the use of β2-myoglobin antibody coupled on the reference flow cell and using SPR buffer 2 (500 mM NaCl), making it feasible to investigate AP180 with the SPR/IAC method. The goal of such investigations is to obtain further information as to whether or not other adaptor proteins share similar clathrin TD binding properties to epsin 1. Additionally, such adaptor proteins as AP180 could be used in adaptor competition studies (SPR/IAC (2-injection) method) described in Chapter 6.

5.12.0 Conclusion

In conclusion, the results presented in this chapter confirm that disrupting one or both epsin 1 clathrin box motifs had a detrimental effect on binding to clathrin TD. However, binding persisted even when both clathrin box motifs were removed, suggesting a more complex mode of interaction, involving the unstructured/DPW region in between these two clathrin box motifs. After investigating this unstructured/DPW region, I hypothesize that the most effective binding of epsin 1 to clathrin is when the two clathrin box motifs and the unstructured/DPW motif region act synergistically to promote effective clathrin interactions via long-distance linking effect between multiple TDs or via multiple TD site interaction on a single TD. Deleting the unstructured/DPW region causes massive reduction in clathrin TD binding, hence the DPW motifs and the distance between the two clathrin box motifs, have been shown from the data above to play a critical role in the epsin:clathrin interactions. Additional future experiments using epsin peptides and TD mutants could further confirm the suggested mechanism and the exact TD site binding of epsin 1. We obtain additional understanding on how epsin 1 interacts with clathrin TD in the presence of other endocytic adaptor proteins in the adaptor competition studies described in Chapter 6.

Chapter 6:
Clathrin-adaptor competition studies using surface plasmon resonance

6.0.0 Overview

The aim of this chapter was to investigate adaptor competition between certain combinations of adaptors present in different stages of CME. This would provide a vital insight into how adaptor proteins co-exist and act during the different stages of endocytosis. Here, I describe the newly established technique called SPR/IAC (2 –injection), which is a modification of the SPR/IAC method used in Chapter 5. The SPR/IAC (2-injection) method developed in this thesis is novel for investigating competition for clathrin N-terminal (TD) domain binding between structurally and functionally diverse endocytic adaptor proteins, which has not been used before.

In addition to β-arrestin 1L, epsin, which were studied in Chapter 6, the following adaptor proteins (β2-adaptin (part of the AP2 complex), auxilin 1, Hip1CC and Hip1RCC) were selected for this study. Initially, the interaction of the individual proteins with clathrin N-terminal domain (TD) was investigated using the SPR/IAC method before using them in the competition studies. Adaptor protein combinations for the competition studies were chosen according to their biological role in the CME. The SPR results from this chapter provide further insights into:

I. the behaviour of different endocytic adaptor proteins in the presence of other endocytic adaptor proteins and clathrin TD.
II. the mode of interaction between epsin 1 and clathrin TD.

6.1.0 The 2-injection SPR method

6.1.1 Introduction and description

Initially, the SPR/IAC method was successfully optimized and used in Chapter 5, to investigate clathrin:adaptor interactions using one-step detection. This involves clathrin TD being attached on the chip via the IAC method and one adaptor protein injected over that flow cell to form a complex with the immobilized clathrin TD. In this chapter, I used the SPR/IAC method using a two-step detection process, where one adaptor protein is injected to form a complex with clathrin TD immobilized on the chip, prior to the injection of the second adaptor protein onto that complex. This technique is called SPR/IAC (2-injection). This method was developed in order to investigate clathrin adaptor protein competition for clathrin TD binding between combinations of adaptor proteins.

An example sensogram of the outcome when the method is applied is shown on Figure 6.1.1 First, once the GST- clathrin TD is bound to the chip surface via the IAC method as explained in Chapter 5; following that, (i) one adaptor protein is injected over that flow cell to form a complex with clathrin TD (first purple curve) (ii) a small volume of buffer is injected to wash the flow cell and eliminate any excess adaptor protein not bound, but not to cause significant dissociation, (iii) a second injection of a different adaptor protein is then performed which is allowed to interact with the complex (second purple curve). This second interaction step is followed by a longer buffer injection time before regeneration of the flow cell.

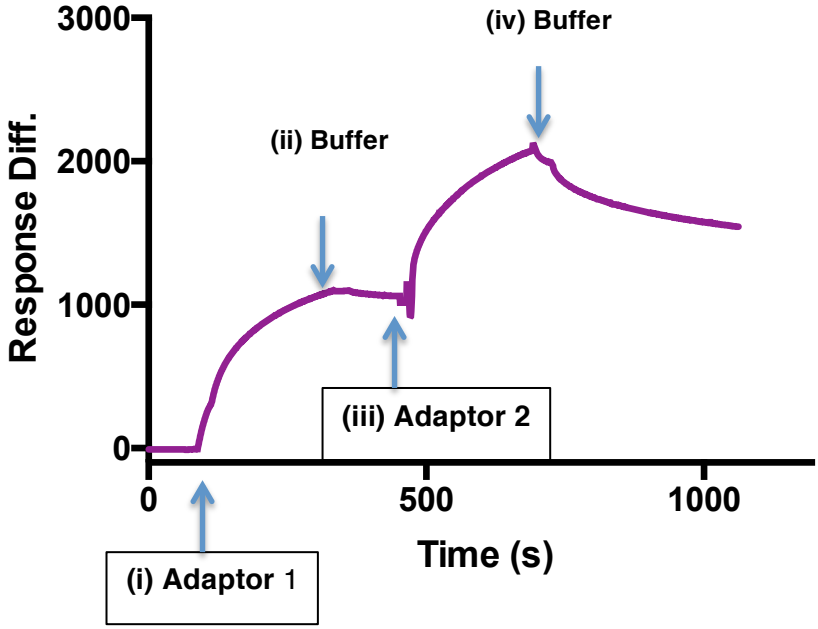

Figure 6.1.1: Illustrating the stages of SPR/IAC (2-injection) method. *(i) the first adaptor protein is injected over the flow cell, (ii) first injection is followed by a small buffer injection period to eliminate any of the excess unbound protein (iii) the same/different adaptor proteins are injected onto the flow cell (iv) a longer washing time is carried out before the normal regeneration step (10 mM Glycine pH 2.0).*

6.1.2 Development of the 'two step' SPR technique

The SPR/IAC (2-injection) method has not been utilized previously for studying protein-protein interactions. The rational behind the development of this technique was to investigate competition between different adaptor proteins for clathrin binding that could normally co-exist *in vivo* situation. Published knowledge on the principles of antibody analysis and competition detection using SPR described below:

Epitope mapping analysis, where an antigen is coupled on the chip and a variety of antibodies are sequentially injected over the antigen to determine more efficient antibody binding. In 2014, Goh *et al.,* used SPR to investigate relative binding of two compounds to a relative antibody in a similar mode to the SPR/IAC (2-injection) system introduced in this chapter. However, their system was based on antibody very well defined binding sites (Goh *et al.,* 2014). This SPR competition assays provided an initial basis for designing

the SPR/IAC (2-injection) experiments to investigate competition between two adaptor proteins for clathrin binding when injected one after the other. Such a method is considered novel for clathrin:adaptor interactions. Based on the successful competition assays published previously, SPR could be used to attempt to address such questions.

'Competitive BIAcore reactions' reported by Karlsson, 1994 (Karlsson, 1994). Interestingly, the following year Karlsson *et al.,* 1995 demonstrated how high molecular weight and a low molecular weight analytes injected at the same time over the chip surface coupled with a ligand, could demonstrate competition between these analytes for the binding sites on the immobilized ligand (Karlsson *et al.,* 1995). This is analogous to radiolabelled and non-radiolabelled ligand competing for the same binding site on a specific receptor (Karlsson *et al.,* 1995; Morelock *et al.,* 1995); Karlsson, 2004). In relation to endocytic adaptor proteins (analyte) in CME have different molecular weight depending on their structure, and such assays would not limit the ability to obtain competition between them due to variations in their molecular mass. However, optimisation needs to be carried out for such a system for each adaptor protein.

6.1.3 Advantages of SPR/IAC (2-injection) method

a) All experiments/controls could be carried out on the same flow cell for efficient comparison. However, this depends mainly on the performance of the chip and the antibody's binding capacity following (harsh) regeneration. For this SPR/IAC system, a full set of 6-7 experiments can be carried out on a single flow cell. Any further experiments result in a decrease in binding, which is noticed with a lower clathrin TD binding to the anti-GST antibody immobilized on the flow cell.
b) Detect accurate competitive binding between purified proteins, instead of peptides, using a small sample size with low protein concentrations, compared to other techniques e.g. Isothermal Titration Calorimetry.

c) Label-free real-time straightforward method without the need of fluorescent tags, radiolabelled tags and isotope tag labeling.

6.2.0 Investigating the molecular binding interactions of other adaptor proteins (β2-adaptin, Hip1CC/ Hip1RCC and auxilin 1) for clathrin TD

6.2.1 Overview

Other endocytic adaptor proteins were used with the optimized SPR/IAC method in order to confirm their binding activity with clathrin TD. These adaptor proteins will be key in the adaptor competition experiments. These adaptor proteins are not full-length and the specific residues of the construct are detailed in the section below.

6.2.2 SPR/IAC analysis: β2-adaptin-clathrin, auxilin 1-clathrin and Hip1RCC-clathrin

AP2 was of interest to investigate in our competition experiments due to its pivotal role in endocytosis and its ability to stimulate clathrin coat assembly. The AP2 clathrin box motif (LLNLD) is located on the long flexible unstructured linker of the large β2-subunit, which is hidden in the core of the AP2 structure when in its closed conformation (Collins *et al.,* 2002). AP2 interacts with the clathrin N-terminal domain TD (Shih *et al*., 1995; Clairmont *et al*., 1997; Owen *et al*., 2000) and with a stoichiometry of 3:1 AP2:clathrin according to peptide assays (Zhuo *et al.,* 2015), which is contrary to the most recent data which suggest a 2:1 stoichiometry of AP2:clathrin (Muenzner *et al.,* 2017). The SPR results confirm the strong binding of the β2-adaptin$_{616-951}$ construct (β2HA- longer hinge region making it more stable) to the clathrin TD (Figure 6.2.2, yellow curve), which is used in the adaptor competition studies.

The Hip1/Hip1R endocytic adaptor protein on the other hand, has been found to preferentially bind to clathrin light chains (CLC) (Chen and Brodsky, 2005).

The coiled-coil (CC) domain of both proteins promotes dimerization of the protein and interaction with clathrin light chain (CLC), which in turn aids the formation of clathrin cages *in vitro* (Ybe *et al.,* 2007; Niu and Ybe, 2007; Ybe *et al.,* 2009). This allows the recruitment of Hip1/Hip1R to the membrane where it binds releasing the interactions with the CLC and allows it to interact with actin and promoting assembly (Hyun *et al*., 2004; Ybe *et al.,* 2009; Gottfried *et al.,* 2010). Hip1 consists of a clathrin box motif (LMDMD), which binds to clathrin N-terminal domain, and FXDXF and DPF motifs (X denotes any amino acid) bind to the AP2 complex (α-adaptin) (Mishra *et al.,* 2001; Legendre-Guillemin *et al.,* 2002; Chen and Brodsky, 2005; Hyun *et al.,* 2004; Ybe *et al.,* 2009). More interestingly, Hip1CC was demonstrated to interact with CHC via a proposed motif of VDLE, which has suggested by Waelter *et al.,* 2001 (Waelter *et al.,* 2001), in contrast to Hip1RCC (Chen and Brodsky, 2005), which is included in the construct used for the SPR/IAC experiments. The SPR data (Figure 6.2.2) demonstrate that the Hip1RCC does not bind to the clathrin TD, which was observed via the zero response units on the sensorgram. However, with $Hip1CC_{361-637}$ construct we observe an increase of ~ 200 RU, which demonstrates a weak interaction with clathrin TD. The reason for this increase in response could be due the interaction of Hip1 CC with clathrin TD via the proposed motif of VDLE, which has suggested by Waelter *et al.,* 2001 that binds to clathrin heavy chain. The Hip1 CC was preferentially used in the competition assays, due to its binding capacity for clathrin TD.

One of the major clathrin disassembly adaptor proteins is auxilin 1. Auxilin 1 contains a clathrin box 'LLGLE' motif (residues 496-500), which interacts in peptide form with the clathrin TD (Smith *et al.,* 2004). More specifically, DPF motifs bind to both the CHC and the ear domain of α-adaptin in AP2 and DLL motifs bind to clathrin (Scheele *et al.,* 2001; Fotin *et al.,* 2004). The SPR data revealed strong binding between the $auxilin_{401-910}$ construct and the clathrin TD, as seen in Figure 6.2.2.

Overall, the β2-adaptin shows the highest response units of 840.30 ± 136.8 RUs, followed by auxilin 1 with 589.8 ± 55.64 and Hip1CC with 168.0 ± 29.46 RUs. Hip1RCC does not bind to clathrin and thus the response units are zero (RU=0).

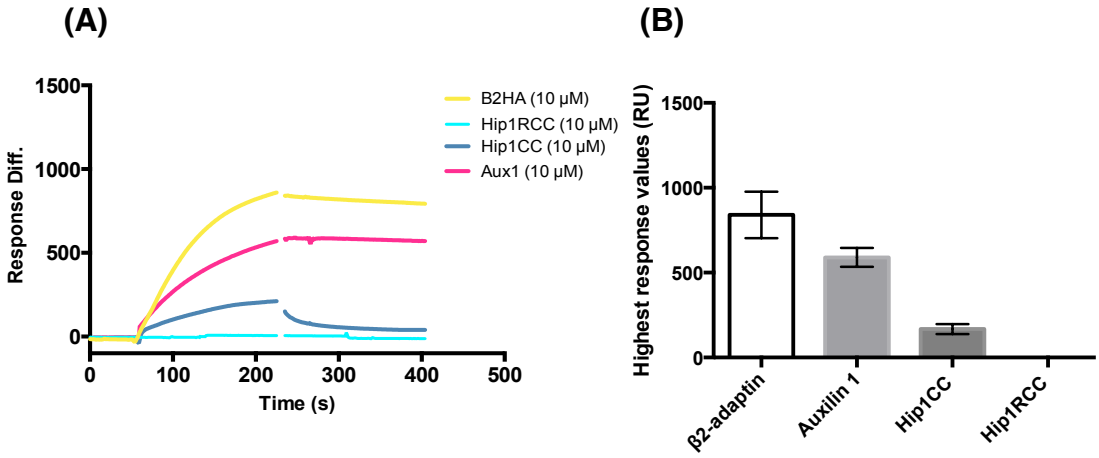

Figure 6.2.2: Binding of β2-adaptin, Hip1R/Hp1 CC and auxilin 1 to GST-clathrin TD (1 μM). (A) *The strongest binding to clathrin TD is by of β2-adaptin ~ 1000 RU, with the auxilin 1 following at ~ 700 RU. The Hip1RCC does not bind to TD due to the zero RUs and Hip1CC binds with ~ 200 RU to clathrin TD.* ***(B)*** *The mean highest response units from three independent experiments (n=3) is plotted on a bar chart illustrating the difference in binding between the three adaptor proteins, which have different binding capacity. The β2-adaptin shows the highest response units of 840.30 RUs, followed by auxilin 1 with 589.8 and Hip1CC with 168.0 RUs. Hip1RCC does not bind to clathrin and thus the response units are zero (RU=0).*

6.2.3 Conclusion

This section confirms the binding capacity of the β2-adaptin, auxilin 1, Hip1CC and Hip1RCC to the clathrin TD. Using the SPR results above, I demonstrated that the β2-adaptin is the adaptor protein that shows the strongest response in the SPR/IAC experiments, as expected. The second in turn is the auxilin 1 with Hip1CC following next with a lower binding response and concluding that the Hip1RCC does not bind to clathrin TD, as expected. This confirms that the SPR/IAC can discriminate between non-specific and functional binding. These adaptor proteins are key for the competition studies detailed later in this chapter.

6.3.0 Adaptor competition for clathrin TD binding

6.3.1 Introduction

Approximately 25 different adaptor proteins are recruited in an ordered sequence to the plasma membrane during CME, requiring numerous potential clathrin-adaptor interactions (Merrrifield and Kaksonen, 2014; Traub 2011). This raises the question of whether certain adaptor proteins compete for binding to clathrin or whether some adaptor proteins can bind to clathrin simultaneously, during the different stages of the CME. It has been hypothesized that certain adaptor proteins with high binding affinity for clathrin could possibly prevent low binding affinity adaptor proteins from interacting with clathrin, through competition for the same site (Lindner and Ungewickell, 1992). More specifically, the majority of adaptor proteins bind to clathrin TD via their single or multiple clathrin box motifs. The TD has four distinct adaptor protein binding sites (CBox, ArrestinBox, W-Box, RoyleBox). Different adaptor protein peptide ligands have been shown to bind to one or more of these sites simultaneously (Muenzner *et al.,* 2017). In theory, the affinity and number of clathrin binding sites could allow one adaptor protein to displace another from the clathrin TD sites, influencing the progress of CCV formation (Zhuo *et al.,* 2015). It is critical to understand this mechanism of engagement, which will aid in the understanding of how CME is successfully regulated *in vivo*. Thus, our hypothesis is that the engagement of certain adaptor proteins with clathrin TD sites is managed through competition and simultaneous binding. In order to address this hypothesis in this chapter, I aimed to investigate combinations of the five adaptor proteins (Figure 6.3.1) choosen in my project based on the:

I. Roles in endocytosis (e.g. assembly, disassembly etc.)
II. Structural diversity
III. Analogous ‘clathrin binding motifs’
IV. Equivalent number of clathrin box motifs or components in the structure

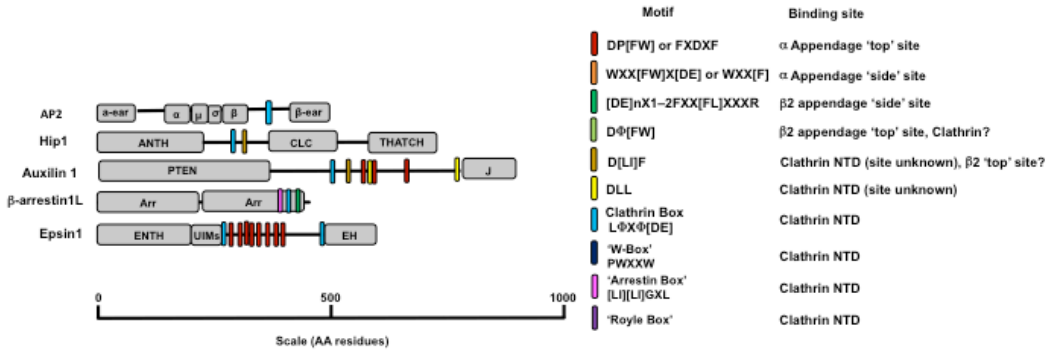

Figure 6.3.1: A diagram illustrating five different adaptor proteins (AP2, Hip1, Auxilin 1, β-arrestin 1L Epsin 1) with diverse structure and function in relation to their structure importance in binding to clathrin and other adapotors, such as AP2. *Motifs are listed in the on the right along with their binding location on AP2 or clathrin. The other domains detailed in the figure are as follows: THATCH,* talin-HIP1/ R/Sla2p actin-tethering C-terminal homology*ANTH, AP180 N-Terminal Homology Domain, Arr, Arrestin Domain; EH, Epsin Hand; ENTH, Epsin N-Terminal Homology Domain; J, J-domain; UIM, Ubiquitin Interacting Motif. Image adapted from Smith et al., 2017.*

These adaptor combinations were investigated for their binding to clathrin TD using GST pull-down binding assays and SDS-PAGE analysis with either cages or clathrin TD as an initial observation for obvious competition. Certain GST-pulldown binding assays were repeated in this thesis and demonstrated a reproducible competition or no competition pattern between different adaptor protein combinations in the presence of clathrin. However, the repeats did not result in consistent band intensities. The limited dynamic range of SDS-PAGE analysis led us to the use of a more quantitative method, such as the SPR/IAC (2-injection) method, detailed in the previous section. The concentration ratio used for all the SPR/IAC (2-injection) experiments was 1:10 molar ratio of 1 μM of GST-clathrin TD to 10 μM of each adaptor protein, which was used for most SDS-PAGE pulldown binding assays as the saturation level of adaptor to clathrin.

6.4.0 β2-adaptin and β-arrestin 1

6.4.1 Introduction: structural and functional differences

AP2 is considered the major clathrin assembly initiation adaptor protein, which interacts with the clathrin N-terminal domain TD via its clathrin box

motif (LLNLD) located in the long flexible unstructured β2 hinge (Shih *et al.,* 1995; Clairmont *et al.,* 1997; Owen *et al.,* 2000), which is hidden in the core of the AP2 structure when in its closed conformation (Collins *et al.* 2002). On the other hand, the β-arrestin 1L (longer isoform) structure consists of two independent clathrin box motifs (LIELD and LIEFD) on C- and N- terminal domains, which recruit clathrin to the plasma surface (Kang *et al.* 2009). It is important to note that these two adaptor proteins interact with each other via the IVF motif on the C-terminal domain of β-arrestin 1L and the β2-adaptin subunit of AP2 (Ferguson, 2001; Burtey *et al.,* 2007). Both β2-adaptin and β-arrestin 1L bind to two TD sites (CBox and ArrestinBox) in blades 1 and 2 and blades 4 and 5 in the TD. β2-adaptin (part of AP2 complex) and the active form of β-arrestin 1L were used in the SDS-PAGE binding assays and SPR/IAC (2-injection) experiments, where the IVF motifs on β-arrestin 1L (which interacts with β2-adaptin) had been mutated to AAF motif in order to release the loop exposing the conserved clathrin box. β2-adaptin interacts with this β-arrestin 1L form (active) via the F-residue, as shown in ITC results from Burtey *et al.,* 2007 (Burtney *et al.,* 2007).

6.4.2 Investigating binding between β2-adaptin and β-arrestin 1L to clathrin TD

6.4.3 GST-pulldown (SDS-PAGE) binding assays of β2-adaptin and β-arrestin 1L for clathrin TD

Initially, β2-adaptin and the active form of the β-arrestin 1L were investigated with GST-pulldown binding assays and analysed by SDS-PAGE. The pulldown assays revealed preferential binding of β2-adaptin to clathrin TD when in the presence of an increased concentration of active β-arrestin 1L (Figure 6.4.3 (B), lane 17) compared to WT β-arrestin 1L (Figure 6.4.3 (C), lane 17), and no obvious competition between the two adaptor proteins. This is revealed when the band intensity of the two adaptors in the pellet fraction is higher in the presence of clathrin TD, compared to the control experiments with the adaptors without the presence of clathrin TD. It is important to note that in previous studies, it has been demonstrated how active β-arrestin 1L

and β2-adaptin interact with each other (Burtey *et al.,* 2007), which was not demonstrated in these pulldown results (Figure 6.4.3 (C), lanes 9 and 10). This could be because the mutation of I and V residues to alanine residues in the IVF motif on the active β-arrestin 1L, could have reduced the binding interaction between these adaptors. Nevertheless, I used the SPR/IAC (2-injection) method to investigate the interaction between β2-adaptin and active form of β-arrestin 1L in the presence of to the clathrin TD.

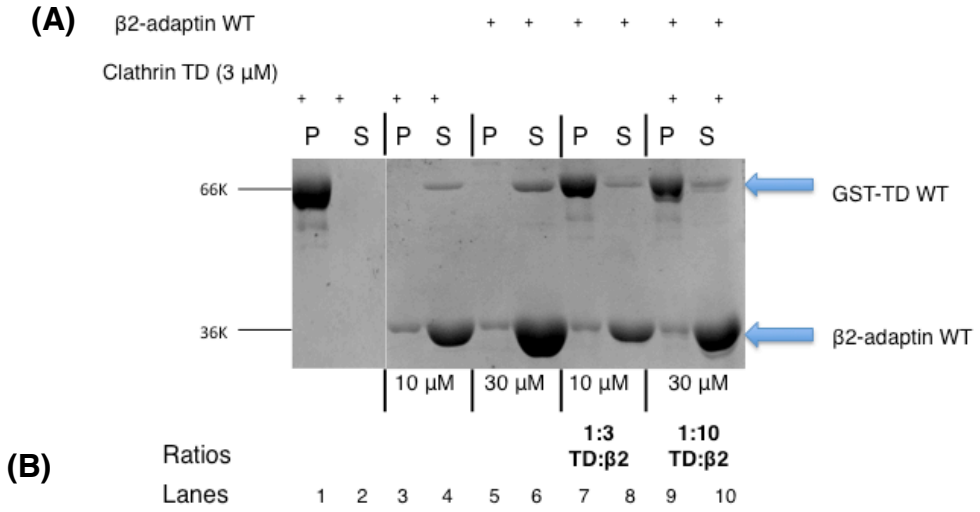

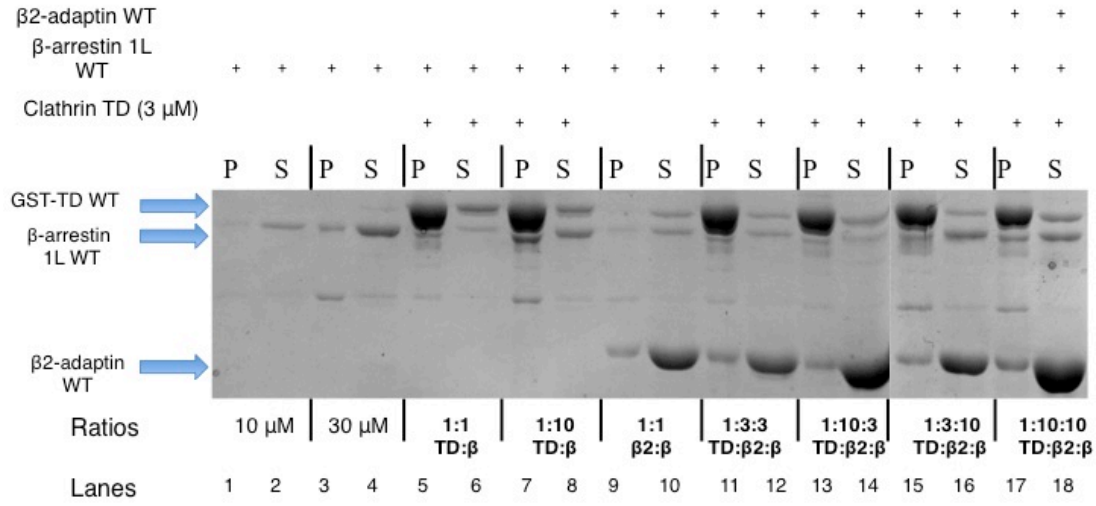

(C)

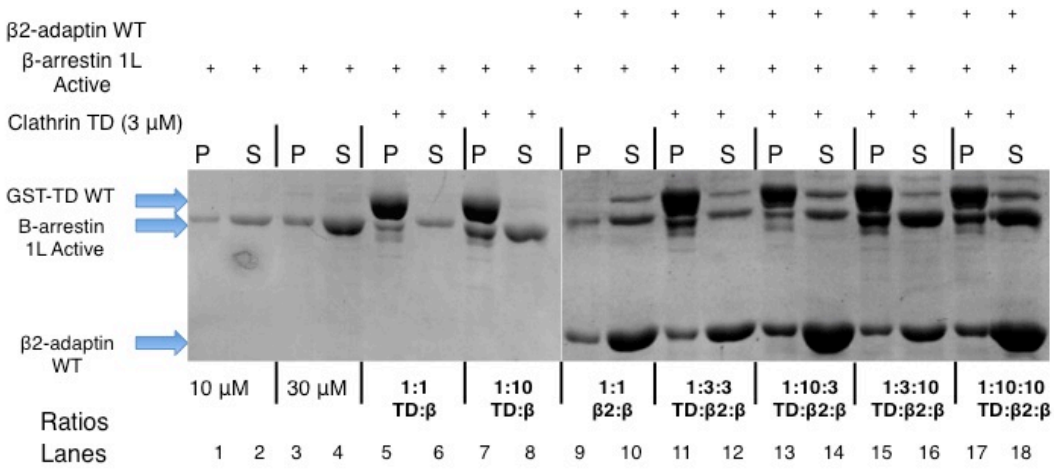

Figure 6.4.3: GST- SDS-PAGE pulldown assays between β2-adaptin (β2) and β-arrestin 1L(β) in the presence of clathrin TD. *Clathrin TD is at a constant concentration of 3μM.* ***(A)*** *Controls are carried out with clathrin TD only and β2-adaptin only as well as active and WT β-arrestin 1L at a 1:3 to 1:10 molar ratio.* ***(B)*** *Control and experimental analysis of WT β-arrestin 1L with an without the clathrin TD, which reveals no obvious competition between the two adaptor proteins* ***(C)*** *Control and experimental analysis of active β-arrestin 1L demonstrating no obvious competition the two adaptor proteins, but increasing the concentrations of active β-arrestin promotes the binding of β2-adaptin to clathrin TD at 1:10:10 molar ratio. These experiments and SDS-PAGE analysis are representative of multiple experiments.*

6.4.4 SPR/IAC (2-injection) method of β2-adaptin and β-arrestin 1L for clathrin TD

A massive increase in response units (~ 1500 RU) was observed once the β2-adaptin (β2HA) was injected over the β-arrestin 1L (ActArr)-clathrin TD complex (Figure 6.4.4 (A), second blue curve). It is possible that a certain proportion of the response seen could be of β2-adaptin binding to clathrin TD and some of the response could relate to β2-adaptin binding to the ActArr, which has already been bound to the clathrin TD. Interestingly, this pattern was not observed when the order of adaptor protein injected was switched around (brown curve in Figure 6.4.4 (A)). A possible explanation could be that β2-adaptin has bound to both of the two TD sites (CBM and ArrestinBox), which can also bind β-arrestin 1L, thereby, blocking those sites. Alternatively, β2-adaptin could be changing its conformation when bound to the clathrin TD and as a result causing sites for β-arrestin 1L

interaction to be hidden (Figure 6.4.4 (A)). These experiments were run in duplicates or triplicates and the difference between the maximum point of curve one (peak 1) and curve two (peak 2) (Δpeak2-peak1) is plotted from each repeats in Figure 6.4.4 (B)).

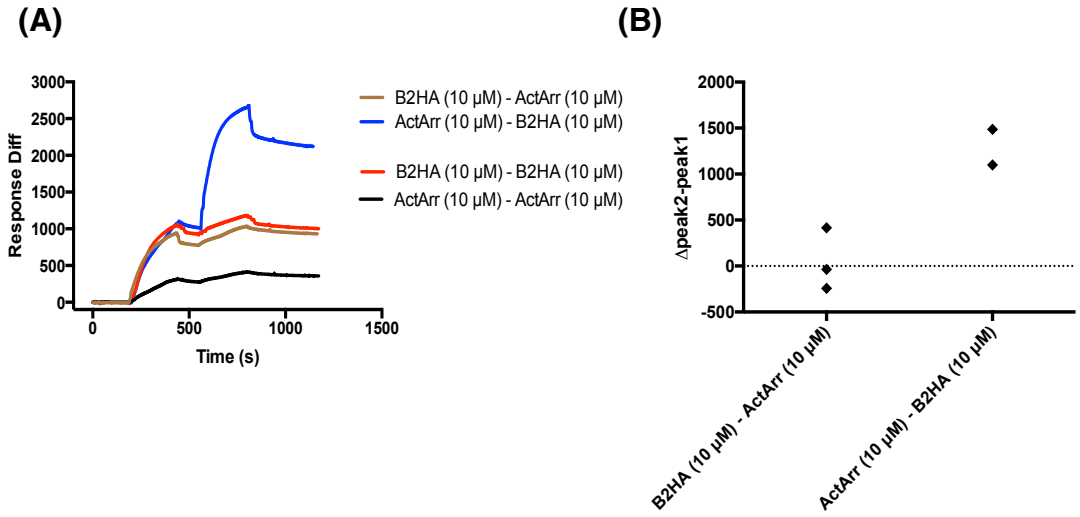

Figure 6.4.4: SPR sensorgrams showing the binding between β2-adaptinHA (26kDa) (10 μM) and active β-arrestin 1L (48kDa) (10 μM) for GST-clathrin TD (1 μM) using SPR/IAC (2-injection) method. *The plot clearly suggests competition between β2-adaptinHA and active beta-arrestin 1L as per the orange coloured curve, when β-arrestin 1L is flowed over the chip first. This was confirmed with a reduced binding of the β-arrestin 1L when injected second over the chip (black curve). These plots are repeats of two or three series of trials averaged together. The ActArr-ActArr demonstrates a low response than expected even when repeated; this could be due to the deterioration of the chip.*

6.4.5 Discussion: β2-adaptin and β-arrestin 1L

In this section, I have investigated possible competition between β2-adaptin and active β-arrestin 1L using two methods. The pulldowns reveal a cooperative interaction effect between the two adaptor proteins for binding to clathrin TD. The SPR results could suggest simultaneous binding of the two adaptor proteins onto clathrin TD. Although, due to the result where β-arrestin 1L does not bind to the β2-adaptin:clathrin TD complex, we could suggest that no other TD sites are free and available for β-arrestin 1L to bind and that it is most likely unable to compete off the β2-adaptin bound to the clathrin TD due to β2-adaptin having a stronger binding affinity for those TD

sites than the active β-arrestin 1L. Overall, I partially confirm existing results that state that AP2 (β2-adaptin subunit) and β-arrestin 1L work cooperatively in binding to clathrin TD (Burtey *et al.,* 2007). In an *in vivo* scenario, cooperative binding will allow β-arrestin 1L to bind and recruit AP2 and clathrin to the surface allowing the AP2 complex to bind to clathrin TD at the same time and initiate clathrin assembly. Further discussions of these findings are described in Chapter 7. In conclusion, this initial analysis confirmed that the newly developed SPR/IAC (2-injection) method works for the clathrin:adaptor system to obtain reliable results.

6.5.0 Epsin 1 and β-arrestin 1L

6.5.1 Introduction: structural and functional differences

Epsin 1 is recruited at the clathrin assembly initiation stage of CME as a key clathrin assembly protein, whereas β-arrestin 1 is also recruited during the CME initiation stage but is not involved in the clathrin assembly process. Structurally, epsin 1 contains two clathrin box motifs (LMDLA and LVDLD), which interact with clathrin, and eight DPW motifs located between the two clathrin box motifs which have been suggested that bind to clathrin non-specifically (Drake *et al.,* 2000), which have a role in the clathrin assembly and are hypothesized to link multiple clathrin triskelia (bridging effect) during assembly, thus forming uniform cage sizes (Drake *et al.,* 2000; Kalthoff *et al.,* 2002). Interestingly, β-arrestin 1L's structure consists of two independent clathrin box motifs (LIELD and LEFD) on opposite sites (each C- and N-domains), just like epsin 1 (Kang *et al.,* 2009). The LIELD motif has been found in other adaptor proteins such as AP2, AP180, amphiphysin, and epsin (Owen *et al.,* 2004), therefore β-arrestin 1L could promote competition with other adaptor proteins for clathrin TD. These two independent clathrin box motifs have been hypothesized to bridge between two clathrin molecules in a lattice (Kang *et al.,* 2009), but not yet proven. This linking effect has been hypothesized because the two clathrin box motifs are ~ 68 Å apart, and the clathrin triskelion within the lattice has a distance of ~ 64 Å between adjacent

clathrin terminal domains, as suggested by Kang *et al.,* 2009 (Kang *et al.,* 2009). This multiple clathrin linking manner has been hypothesized for epsin 1 as well, but not yet proven. These two adaptor proteins have structural similarities regarding their clathrin components, however, the difference in their role in CME and binding manner could suggest competition for clathrin binding between them.

6.5.2 Competition between epsin 1 and β-arrestin 1

6.5.3 Preliminary SDS-PAGE binding assay data reveal competition between epsin 1 and β-arrestin 1L for clathrin TD

Epsin 1 and β-arrestin 1L were ideal candidates for studying adaptor competition studies due to their different roles in CME and their structural and functional diversity. Importantly, epsin 1 and active β-arrestin 1L do not have a common site for interaction with each other. This was confirmed by GST-pulldown SDS-PAGE binding assays using GST- β-arrestin 1L active form with epsin 1 WT without the presence of clathrin TD. The results illustrated in Figure 6.5.3 (A), lanes 1,3,5,7 show that epsin 1 does not pellet even in increasing active or WT/active β-arrestin 1L concentration, at molar ratio of 1:1 or 1:3 of epsin1: β-arrestin 1L.

Interestingly, the SDS-PAGE analysis of the GST-pulldown binding assays reveal reduction in band intensity of epsin in the pellet (Figure 6.5.3 (C), lanes 3 and 5) in the presence of constant concentration of β-arrestin 1L at 10 μM. The band intensity is compared with pellets from the control experiments of epsin with clathrin TD alone (Figure 6.5.3 (B), lanes 1 and 3) at the same 1:3 and 1:10 molar ratios. Interestingly, increasing the concentration of β-arrestin 1L approximately 3 folds, the epsin band in the pellet remains reduced as observed in Figure 6.5.3 (C), lanes 7 and 9), compared to the control experiments Figure 6.5.3 (B), lanes 1 and 3). Overall, these results revealed competition between epsin 1 and β-arrestin 1L for clathrin TD. These primary observations were the basis of further

investigation between these two adaptor proteins using the SPR/IAC (2-injection) method in order to confirm this competition in a more quantitative way.

(A)

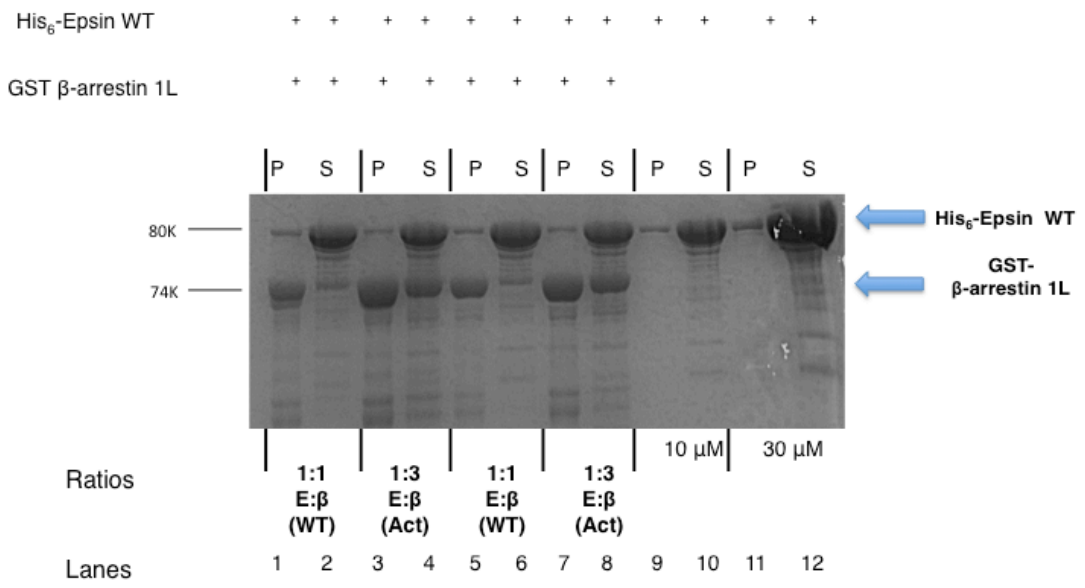

(B)

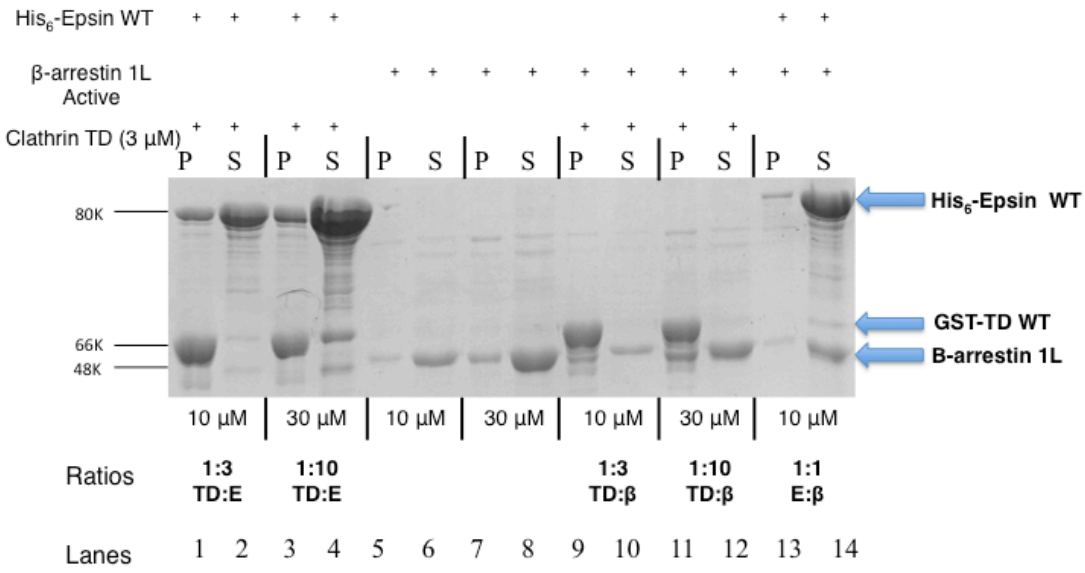

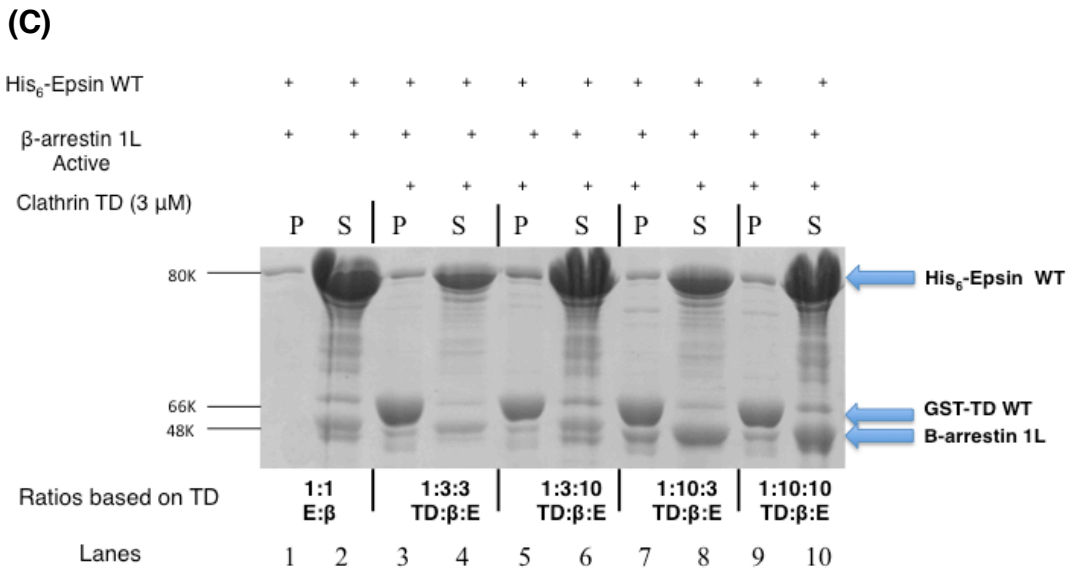

Figure 6.5.3: GST- SDS-PAGE pulldown assays which reveal competition between β-arrestin 1L (β) and epsin 1 WT (E) for clathrin TD. *Clathrin TD is at a constant concentration of 3μM.* ***(A)*** *Controls are carried out with clathrin TD only and epsin 1 WT only as well as active GST- β-arrestin 1L with different epsin 1 WT concentrations without the presence of clathrin TD. The results revealed no interaction between epsin and GST- β-arrestin 1L.* ***(B)*** *Representing control experiments of epsin with clathrin TD at 1:1 and 1:3 molar ration and β-arrestin 1L control experiments without the presence of clathrin TD (lanes 9-14).* ***(C)*** *and* ***(D)*** *SDS PAGE gels demonstrating competition between epsin 1 and active β-arrestin 1L for clathrin TD, at 1:10:3 TD:E:β molar ratio ratio (lanes 7 and 8) and even at high concentrations of β-arrestin at 1:10:10 TD:E:β molar ratio (lanes 9 and 10) using active β-arrestin 1L. These experiments and SDS-PAGE analysis are representative of multiple experiments.*

6.5.4 Competition between epsin 1 (WT and mutants) and β-arrestin 1L for clathrin TD binding confirmed by SPR

The SPR/IAC (2-injection) results revealed a high response of ~ 1000 RU (blue first curve, Figure 6.5.4 (A) when active β-arrestin 1L (ActArr) was injected first on the flow cell, forming a complex with the clathrin TD coupled on the chip. Once epsin 1 WT was injected over the ActArr-clathrin TD complex, a large increase in response of ~1000 RU was observed (second blue curve, Figure 6.5.4 (A)). Interestingly, by switching the order of the injection of adaptor proteins, with epsin 1 WT injected first (forming epsin 1-clathrin TD complex) and ActArr injected second on the clathrin:epsin 1

complex, we observed no increase in response (second brown curve, Figure 6.5.4 (A)). These experiments were run in duplicates and triplicates and the difference between the maximum point of curve 1 (peak 1) and curve two (peak 2) (Δpeak2-peak1) is plotted from each repeats in Figure 6.5.4 (E), column 1-2). A concentration titration for both adaptor proteins was not conducted due to time constraints.

A number of questions arose after these initial observations with wild type (WT) epsin 1. Would mutations in the epsin 1 structure cause resistance to the competition observed between epsin 1 and β-arrestin 1L? To address this question, I aimed to investigate whether this competition pattern was also observed with epsin 1 clathrin box motif mutants (used in chapter 5) and the ActArr. These mutants were 257 (mutating clathrin box 1), 480 (mutating clathrin box 2) and the DKO (mutation of both clathrin box motifs). This study would provide more insight into whether the synergistic action of both epsin clathrin box motifs is required in order to promote competition with another endocytic adaptor protein for clathrin TD binding, and whether epsin's unstructured/DPW region would still be sufficient to promote this competition. These experiments were run in duplicates or triplicates and the difference between the maximum point of curve 1 (peak 1) and curve two (peak 2) (Δpeak2-peak1) is plotted from each repeats in Figure 6.5.4 (E), column 1-2).

The results from SPR/IAC (2-injection) experiment are in Figure 6.5.4 (B), (C),(D) where the colour scheme and injection order is as described above. To our surprise, the SPR results revealed the same competition pattern as observed with the wild type (WT) form of epsin 1, with the difference of lower response units, which are expected for these epsin mutants. As observed in previous SPR/IAC results in Chapter 6; the responses of the 257, 480, DKO mutants are half of that of the epsin 1 WT, thus the mutant response units ranged between 400-600 RUs. The slight difference in response units between control runs (orange and black curves) and experimental runs (blue

and brown curves) is considered due to the deterioration of the SPR chip and the antibody binding capacity, as explained in previous chapters.

The 480 mutant showed half the response units (~ 400 RU) (Figure 6.5.4 (C)) than the 257 mutants (~ 800 RU) (Figure 6.5.4 (B)). This difference could suggest that one clathrin box motif has an increased ability to compete off ActArr from its already occupied sites on TD, or it has a greater capacity to bind to other sites on the TD, however this cannot be conclusive. On the other hand, the DKO mutant which is expected to have a lower response than either of the other mutants, as both clathrin box motifs have been mutated, resulted to an increase of ~1300 RUs when injected on the ActArr-clathrin TD complex (Figure 6.5.4 (D)). As this was of surprise to us, we are unsure as to why we observe such a higher response for the DKO mutant. Based on previous data in this thesis (Chapter 5), the unstructured/DPW region has equal binding capacity to TD compared to the two clathrin box motifs on epsin. We could therefore expect the response units to be somehow similar to those observed by the 257 and 480 epsin mutants, of around 400-800 RUs. However, the DKO/ActArr experiments were run once, so additional repeats are required before we can be certain of these results. Overall, I demonstrate that cooperative effect between the two clathrin box motif on β-arrestin 1L are not strong enough to outcompete the strong interaction epsin 1 makes with clathrin TD, due to the 'three clathrin component' structure of epsin 1. This could also confirm that the second clathrin box of β-arrestin 1L has a weak affinity for clathrin, which was suggested by Kang *et al.,* 2009 (Kang *et al.,* 2009).

The shape of the curves for epsin 1 and the three epsin mutants was observed to differ since there was a clear change in the slope of the epsin mutant curves in comparison to the smooth curvature observed in the epsin WT curves. This could be due to issues with the BIAcore 2000 SPR instrument during data collection, as this was observed in other experiments as well. However, if this is not due to instrumental failure, it could be a result

of the inherent structure of epsin 1, where mutating important clathrin binding components in epsin 1 structure could affect the manner in which it binds to clathrin TD. In order to confirm this hypothesis, these experiments should be repeated on a more sensitive SPR instrument e.g. Biacore T200.

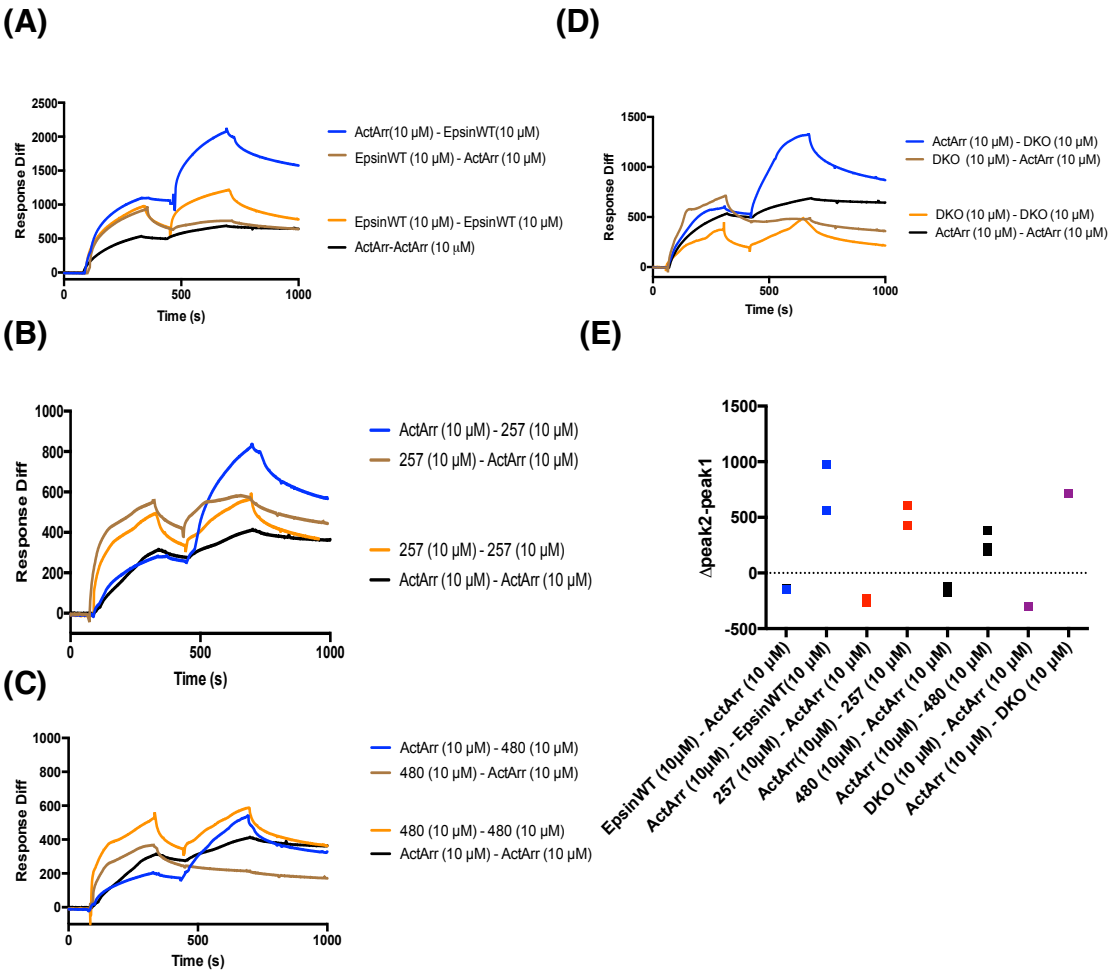

Figure 6.5.4: Competitive binding between epsin 1 WT and clathrin box mutants (10 μM) and active β-arrestin 1L (10 μM) for GST-clathrin TD (1 μM) using SPR/IAC (2-injection) method. *The overall pattern is similar between the WT epsin 1* ***(A)*** *and the mutants* ***(B), (C), (D).*** *When the epsin 1 WT or mutant is injected on the clathrin:ActArr complex, the epsin binds to the complex as shown by the increase in the second blue curve in* ***(B),(C),(D).*** *However, when switching the order around, the ActArr does not bind on the clathrin:epsin 1 complex as seen in the second brown curve of* ***(B), (C), (D).*** *The active β-arrestin 1L control (black) curve has lower response units than the experimental (blue) curve. This might be due to the deteriorating performance of the SPR chip. ActArr; active β-arrestin 1L. Control and experiments are run on the same flow cell, but due to the deterioration of the SPR chip after 6 experiments, the each epsin mutant experiment was run on a different flow cell in a randomised order to prevent any significant systematic error in the binding responses.* ***(E)*** *The Δpeak2-peak1 of triplicate runs of 2-injection experiments plotted for all the epsin 1 WT and mutant combinations with the ActArr.*

6.5.5 SDS-PAGE binding assay data revealed competition between WT β-arrestin 1 and epsin 1 WT and mutants

As we were unclear whether these two clathrin box motifs could be working antagonistically, I also carried out identical GST-pulldown assays and SPR/IAC (2-injection) experiments with the WT (inactive) form of β-arrestin 1L. The WT form has only the second clathrin box on the N-terminal end available for binding to clathrin, whereas the conserved clathrin box in the unstructured loop is hidden.

Interestingly, the SDS-PAGE analysis of the GST-pulldown binding assays reveal reduction in band intensity of epsin in the pellet (Figure 6.5.5 (B), lanes 13 and 15) in the presence of constant concentration of β-arrestin 1L at 10 μM. The band intensity is compared with pellets from the control experiments of epsin with clathrin TD alone (Figure 6.5.5 (A), lanes 1 and 3) at the same 1:3 and 1:10 molar ratios. Interestingly, increasing the concentration of β-arrestin 1L approximately 3 folds, the epsin band in the pellet remains reduced as observed in Figure 6.5.5 (B), lanes 17 and 19), compared to the control experiments Figure 6.5.5 (A), lanes 1 and 3). Overall, these results revealed competition between epsin 1 and β-arrestin 1L for clathrin TD. These primary observations were the basis of further investigation between these two adaptor proteins using the SPR/IAC (2-injection) method in order to confirm this competition in a more quantitative way. Overall, there was no significant difference between the band intensity of epsin in the pellet in the presence of either WT β-arrestin 1 (Figure 6.5.5 (B), lanes 19 and 20) and active β-arrestin 1L (Figure 6.5.3 (B), lanes 9 and 10 in previous section) with clathrin TD, as observed in the GST-pulldown assays. Thus, in both cases we observe equal competition between β-arrestin 1 active and WT form and epsin 1 for clathrin TD. However, due to the SDS-PAGE assay's limited accuracy, this competition was investigated with the SPR/IAC (2-injection) technique as well.

(A)

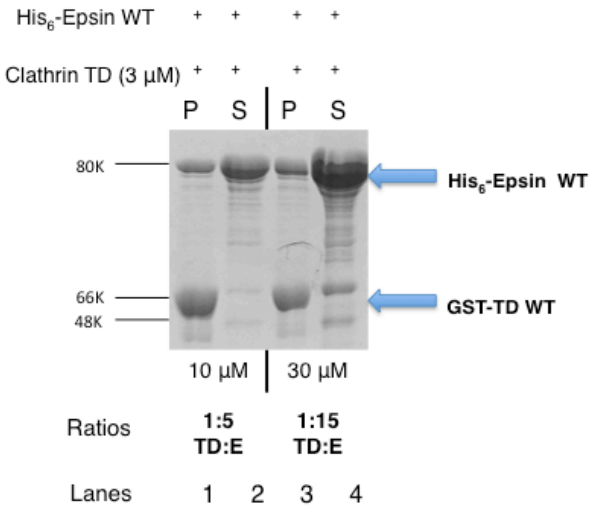

(B)

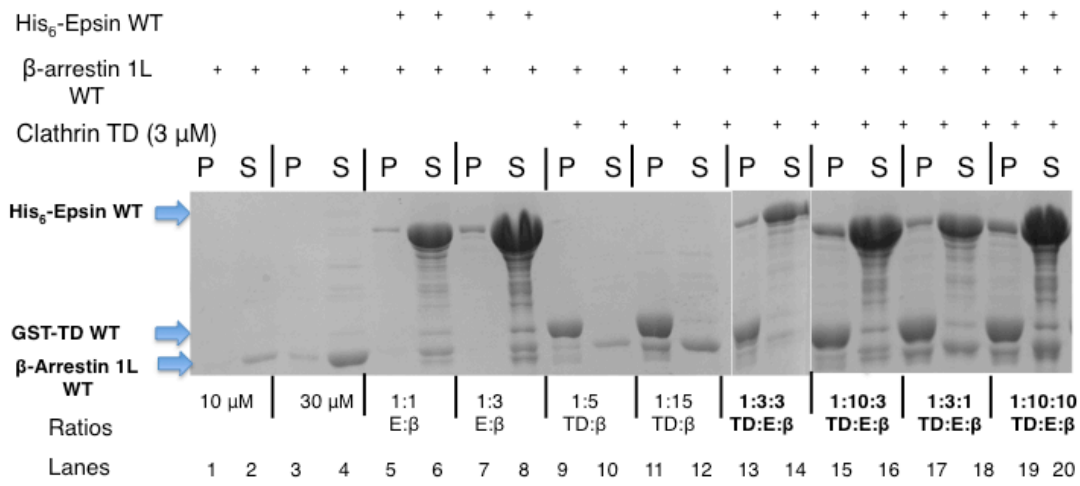

Figure 6.5.5: SDS-PAGE analysis of GST- pulldown assays demonstrate competition between WT β-arrestin 1L (β) and epsin 1 WT (E) for clathrin TD. *GST- clathrin TD (3 µM) was incubated with GST-affinity beads in the presence of WT β-arrestin 1L and epsin 1 WT in increasing molar ratios. The pellet (P) and supernatant (S) fractions were analysed by SDS-PAGE. (A) epsin WT binds to clathrin TD in both 1:5 or 1:15 molar ratio. (B) SDS PAGE gels demonstrating competition between epsin 1 and WT β-arrestin 1L for clathrin TD, even at high concentrations of WT β-arrestin at 1:10:10 C:E:β molar ratio. These experiments and SDS-PAGE analysis are representative of multiple experiments.*

6.5.6 Competition between WT β-arrestin 1 and epsin 1 WT and mutants confirmed by SPR

The SPR/IAC (2- injection) results are shown in Figure 6.5.6 (A) and (B) demonstrate how the competition pattern observed between epsin 1 WT and active β-arrestin 1L, was also observed with WT β-arrestin form. No increase in response from the WT β-arrestin was observed when epsin 1 WT was injected first and formed a complex with clathrin TD. This is also observed in Figure 6.5.6 (C) where no significant difference is observed between the pairs of WT or active form of β-arrestin for the difference between the maximum point of curve 1 (peak 1) and curve two (peak 2) (Δpeak2-peak1) plotted for each repeated experiment.

One interpretation of these results could be that the second clathrin box of β-arrestin 1 does not have a sufficiently strong binding affinity to displace epsin 1 in the epsin:clathrin complex, hence no increase in the response units (RU) was observed in the SPR results below. Another interpretation could be due to epsin 1's length (long unstructured region) and binding manner (occupy larger space on TD); once epsin 1 is bound to clathrin TD, it may block some of the available sites that β-arrestin could occupy, and β-arrestin 1L is not able to displace epsin 1 from its occupied TD site since neither the WT nor the active β-arrestin can interact with clathrin TD in the presence of epsin 1.

All in all, as adaptor proteins have weak electrostatic interactions with fast on and off rate, it is important to note that epsin 1 due to its strong binding affinity and complex binding manner to clathrin, it would occupy majority of the clathrin TD sites and leave rarely unoccupied for β-arrestin 1L to bind, and would not allow β-arrestin 1L to outcompete for epsin 1's occupied TD sites, due to its possible weaker affinity and binding manner to clathrin TD.

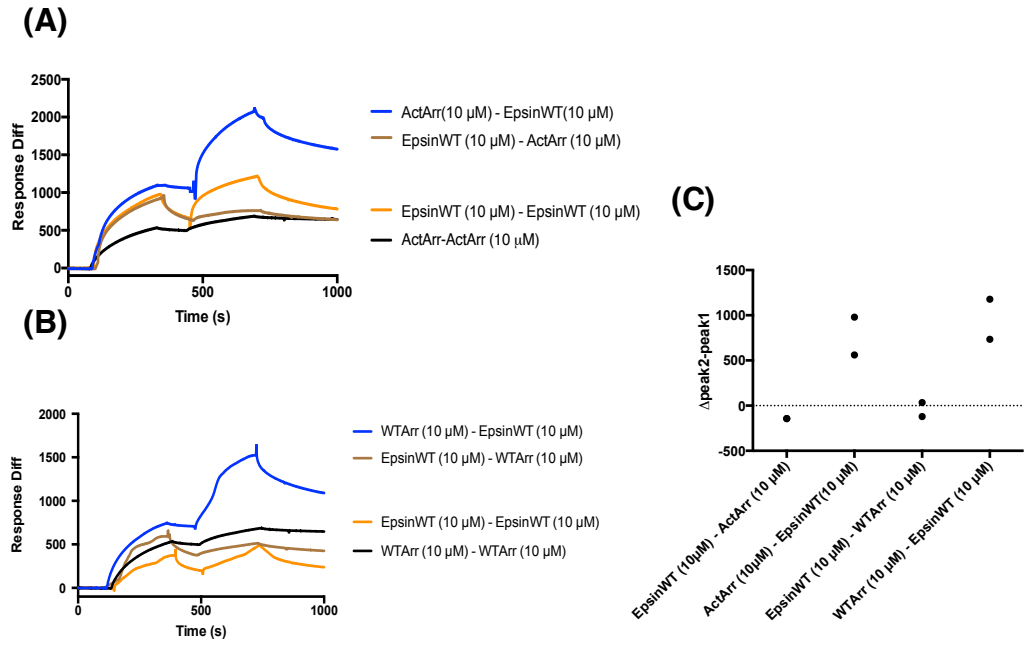

Figure 6.5.6: Competitive binding between epsin 1 WT (10 μM) and WT β-arrestin 1L (48kDa) (10 μM) for GST-clathrin TD (1 μM) using SPR/IAC (2-injection) method. *The overall pattern is similar with the Figure 6.5.4 and 6.5.5. When the epsin 1 WT is injected on the clathrin:WTArr complex, the epsin 1 binds to the complex as shown by the increase in the second blue curve in* ***(A)*** *and* ***(B).*** *However, when switching the order around, the WTArr does not bind on the clathrin:epsin 1 complex as seen in the second brown curve of* ***(A)*** *and* ***(B).*** *The active β-arrestin 1L control (black) curve has lower response units than the experimental (blue) curve. This might be due to the deteriorating performance of the SPR chip. WTArr; active β-arrestin 1L. Control and experiments are run on the same flow cell, but due to the deterioration of the SPR chip after 6 experiments, the each epsin mutant experiment was run on a different flow cell in a randomised order to prevent any significant systematic error in the binding responses.* ***(E)*** *The Δpeak2-peak1 of single or dublicate runs of 2-injection experiments plotted for all the epsin 1 WT combinations with the WTArr and ActArr (taken from Figure 6.5.4 for comparison reasons).*

6.5.7 Epsin mutants (257,480, DKO) and WT β-arrestin 1L

WT β-arrestin 1L (WTArr) binding was also investigated in the presence of the clathrin box motif epsin mutants, in order to confirm whether the competition pattern observed with the WT epsin 1 is not altered due to the mutations of important components in epsin 1's structure. To address this question, SPR/IAC (2-injection) experiments were carried out, where the colour scheme and injection order is as described above. An overall competition between the epsin mutants (257,480, DKO) and WT β-arrestin

1L was observed (Figure 6.5.7 (A),(B),(C)). There is a strong interaction of the epsin mutants 257 and 480 epsin with clathrin TD even when injected over a β-arrestin 1L:clathrin TD complex, which resulted in an increased difference (Δpeak2-peak1) of ~ 900 RU for 257 and 480, and ~ 800 RU for DKO as seen in the single point plots in Figure 6.5.7 (D). This confirms that epsin 1's structure remains complex even when mutating important clathrin binding component of its structure and despite these mutations it still seems to be able to occupy or occlude clathrin TD sites, and prevent WT β-arrestin 1L binding.

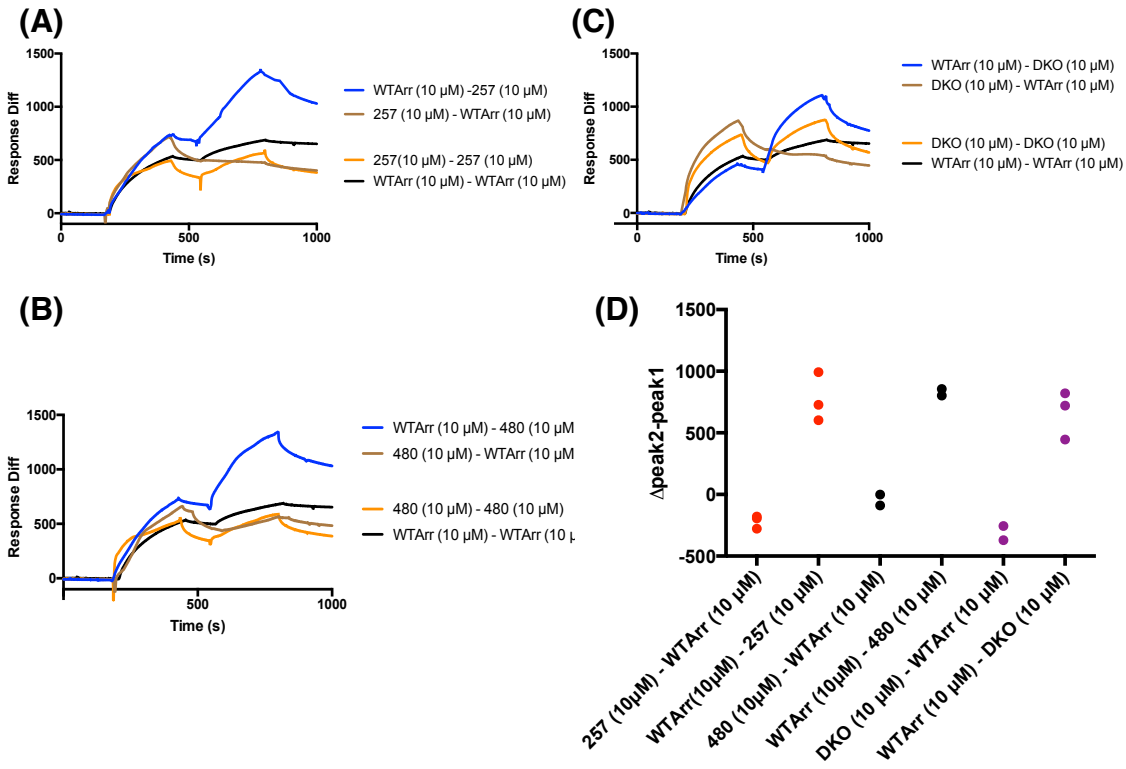

Figure 6.5.7: Competitive binding between epsin 1 clathrin box mutatns (10 μM) and WT β-arrestin 1L (10 μM) for GST-clathrin TD (1 μM) using SPR/IAC (2-injection) method. *The overall pattern is similar with the Figure 7.5.4. When the epsin 1 mutant is injected on the clathrin:WTArr complex, the epsin 1 binds to the complex as shown by the increase in the second blue curve in* ***(B),(C),(D).*** *However, when switching the order around, the WTArr does not bind on the clathrin:epsin 1 complex as seen in the second brown curve of* ***(B), (C), (D).*** *The active β-arrestin 1L control (black) curve has lower response units than the experimental (blue) curve. This might be due to the deteriorating performance of the SPR chip. WTArr; active β-arrestin 1L. Control and experiments are run on the same flow cell, but due to the deterioration of the SPR chip after 6 experiments, the each epsin mutant experiment was run on a different flow cell in a randomised order to prevent any significant systematic error in the binding responses.* ***(E)*** *The Δpeak2-peak1 of dublicate or triplicate runs of 2-injection experiments plotted for all the epsin 1 mutant combination with the WTArr.*

6.5.8 Discussion: epsin 1 and β -arrestin 1L

From the SDS-PAGE binding assay analysis I have shown how epsin and β-arrestin 1L do not interact, however we are uncertain whether there is an interaction between these two adaptors in the present of clathrin. In this section, I demonstrate competition between epsin 1 WT and active form of β-arrestin 1L (ActArr). This is based on the SPR data observations that ActArr does not bind to the clathrinTD:epsin1 complex, whilst epsin 1 can bind to the clathrin TD:ActArr complex. This competition pattern was observed with the WT β-arrestin form and the epsin clathrin box motif mutants as well. This could be a result of: (a) once epsin 1 binds to clathrin TD at certain single or multiple TD sites, ActArr might not have sufficient binding affinity to displace epsin 1 from its originally bound site on TD (b) epsin 1 length (long unstructured region) and binding manner (occupy larger space on TD) is different from β-arrestin 1L, such that when epsin 1 forms a complex with the clathrin TD it could be blocking other available TD sites that β-arrestin could bind to. Therefore, considering the results above, we could hypothesize that in either of these scenarios, epsin 1's structure could be blocking the binding of other endocytic adaptor proteins during clathrin assembly initiation such as β-arrestin 1L.

On the other hand, β-arrestin 1L would only be recruited when a GPCR is required desensitization and recycling (Gurevich, 2014), thus β-arrestin 1L is not an adaptor protein that would be continually present at the surface, but is only likely to be recruited "on demand". Thus, in a situation where β-arrestin is required, a 'burst' of high concentration would be accumulating at the surface. This could possibly promote binding to the unoccupied TD sites. In addition it could be that β-arrestin 1 is only required for initial clathrin recruitment and that epsin 1 displaces it during the growth of the vesicle. Therefore, if by increasing the β-arrestin 1 active or WT form concentration (doubling the concentration), would we see the same competition pattern? This suggests future investigation of a concentration titration of both epsin 1

WT and mutants and β-arrestin with the SPR/IAC (2-injection) method, which was not possible to be carried out for this thesis due to time restraints.

All in all, I demonstrate how using this novel SPR/IAC (2- injection) technique I was able to obtain interesting *in vitro* insights into how two adaptor proteins behave when mixed simultaneously, in the presence of clathrin TD. Additionally, I further demonstrate insights into the binding of epsin 1 and how it could interfere with the functionality of other adaptor proteins during the initial clathrin assembly stages of CME. However, such results need to be confirmed with *in vivo* experiments for more conclusive outcome. Further discussion and future work is described in Chapter 7.

6.6.0 Epsin 1 and auxilin 1

6.6.1 Introduction: structural and functional differences between epsin 1 and auxilin 1 for clathrin binding

Epsin 1 and auxilin 1 have 'opposing' roles in CME. Epsin 1 is involved in clathrin assembly in the initiation stage and auxilin 1 is involved in clathrin disassembly. Structurally, epsin 1 structure consists of two clathrin box motifs on each C- and N- domains (LMDLA and LVDLD), and the unstructured/DPW region which is hypothesized to interact with clathrin independently and aid in clathrin assembly into a uniform cage size distribution (Drake *et al.,* 2000; Kalthoff *et al.,* 2002). On the other hand, auxilin 1 has several DLL and DPF motifs in its structure, which have been suggested to bind to clathrin (Scheele *et al.,* 2001; Fotin *et al.,* 2004), but more specifically, auxilin contains a clathrin box motif 'LLGLE', which binds to the clathrin TD (Smith *et al.,* 2004). Auxilin 1 promotes interaction of Hsc70 with assembled clathrin after the CCV has been formed.

These adaptor proteins are an ideal combination to investigate competition for clathrin TD due to their different roles in CME. They have been hypothesized to bind to three similar TD sites (CBox site 1, W-box site 2 and

Arrestin Box site 3), although this has yet to be confirmed (Scheele *et al.,* 2001; Drake *et al.,* 2000; Kalthoff *et al*., 2002). However, the epsin yeast homolog (Ent2) has been shown to bind to the CBox as well as W-box on the TD sites (Collette *et al.,* 2009), and DLL motifs are hypothesized to bind to the CBox and ArrestinBox, due to their similarity to these sites. Additionally, the F residue of the DPF motifs of auxiln 1 is hypothesized to bind to the W-box of the clathrin TD, as it is a largely hydrophobic. The adaptor proteins used for the GST-pulldowns and SPR/IAC (2-injection) competition studies were the epsin 1 WT form and the auxilin 1 WT form of the clathrin box motif. The concentration ratio used was 1 in 10 molar ratio with 1 μM of GST clathrin TD to 10 μM of each adaptor protein.

6.6.2 Preliminary SDS-PAGE binding assay data reveal competition between epsin 1 and auxilin 1

Ultracentrifugation binding assays were carried out initially by Dr. Michael Baker to demonstrate whether there was any obvious competition between these two adaptor proteins for clathrin binding. The binding assay results show no strong interaction between these two adaptor proteins when mixed together (Figure 6.6.2 (B)). Although, we cannot rule out the possibility of transient interactions or interactions that may only occur in the presence of clathrin. Interestingly, no obvious competition was observed at a 1:1 ratio of the two adaptor (epsin1:auxilin1) in the gels, but by increasing the auxilin 1 concentration 5 folds (1:5), we observed a decrease in bound epsin 1 (Figure 6.6.2 (A), lane 12). This demonstrated competition between the two adaptor proteins with increased auxilin 1 concentration in the presence of clathrin cages. As SDS-PAGE analysis has a limited dynamic range, I aimed to use a more quantitative technique to investigate this competition using clathrin TD.

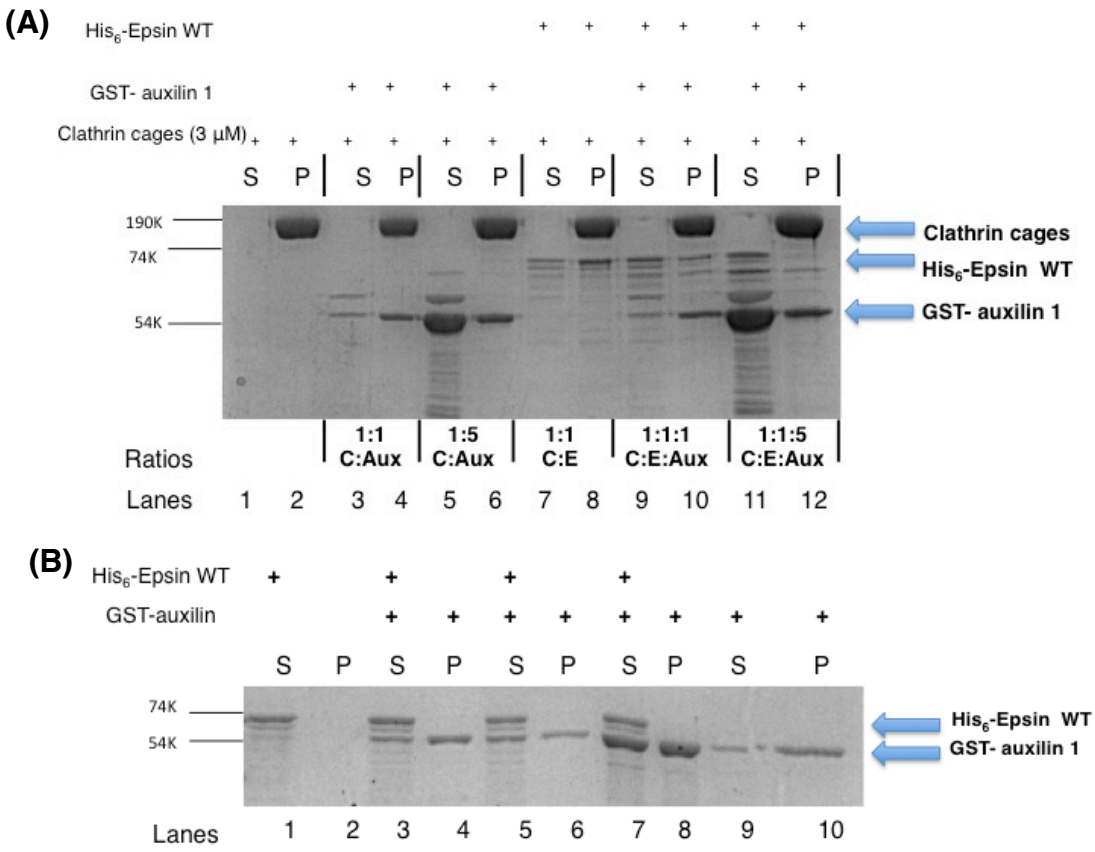

Figure 6.6.2: Ultracentrifugation and GST- SDS-PAGE pulldown assays were carried out showing competition between auxilin 1 and epsin 1 WT for clathrin TD. *Clathrin cages (3 uM) were incubated with increasing molar ratios of auxilin (Aux) with or without the presence of epsin (E). The pellet (P) and supernatant (S) fractions were analysed by SDS-PAGE. (**A**) Both auxilin (C:Aux 1:1 and 1:5) and epsin (CE) bind to clathrin. When increasing the concentration of auxilin in the presence of epsin we can see a decrease in the epsin band present in the pellet fraction in the 1:1:1 C:E:Aux ratio and the complete shift of epsin to the supernatant at the high concentration of auxilin (CE:Aux 1:1:15). (**B**) GST-pulldown assays were used to analyse GST-auxilin in the presence or absence of epsin and supernatant and pellet fractions were analysed by SDS-PAGE. GST-auxilin is pulled down in the presence of beads where as epsin is not. When epsin and auxilin are mixed epsin remains in the supernatant and GST-auxilin is present both in the supernatant and pellet. These experiments and SDS-PAGE were conducted by Dr. Michael Baker (Baker Michael, 2016).*

6.6.3 Competition between epsin 1 WT and auxilin 1

6.6.4 A 1:1 ratio of epsin 1WT:auxlin 1

SPR/IAC (2-injection) was used to confirm such competition using the same colour scheme and injection order are as described in the above sections. Interestingly, the SPR results show competition between epsin 1 and auxilin 1 for clathrin TD binding at a 1:1 molar ratio of epsin:auxilin. This was demonstrated in the SPR results when an increase in response of ~ 700RU was detected in the SPR sensorgram when auxilin 1 was injected first (first blue curve) (Figure 6.6.4). This corresponds to the clathrinTD:auxilin1 complex formation. When the epsin 1 is injected onto the clathrinTD:auxilin1 complex as a second adaptor injection, we observe an equivalent increase of response (second blue curve) of ~ 1000 RU, which could suggest that all epsin was able to bind to the TD sites (Figure 6.6.4).

From this strong response of epsin 1 WT, we could hypothesize that epsin 1 WT could be binding to available TD sites, which are un-occupied from auxilin 1. However, this does not rule out the possibility that epsin 1 WT could be displacing and competing for the same TD sites that auxilin 1 was already bound when injected first. This is because epsin 1 has been shown to have greater binding capacity for clathrin TD in Chapter 6 due to its complex structure. On the other hand, by switching the order of the adaptor protein injection, with epsin 1 WT injected first and auxilin 1 injected second; we do not see the same pattern. We observe that auxilin 1 does not bind to the epsin 1:clathrin TD complex (second brown curve), as there is no significant increase in response on the sensorgram (Figure 6.6.4). This could be a result caused by the inability of auxilin 1 to displace epsin 1 from the occupied TD sites due to the possibility of low binding affinity to those sites, which are common with epsin 1. Due to SPR instrumental failure, these experiments were carried out as single runs and repetitions are necessary in order to validate these observations.

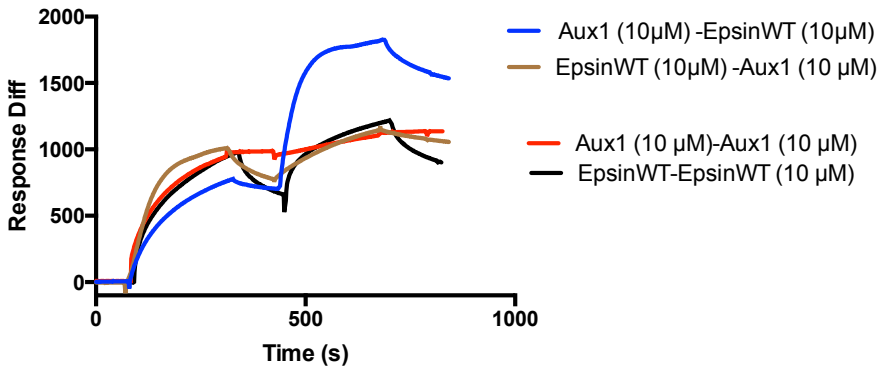

Figure 6.6.4: Competition between epsin 1 WT and auxilin 1WT using SPR/IAC (2-injection) method. *When the epsin 1 mutant is injected on the clathrin:auxilin1 complex, the epsin 1 binds to the complex as shown by the increase in the second blue curve However, when switching the order around, the auxilin 1 does not bind on the clathrin:epsin 1 complex as seen in the second brown curve. Due to SPR instrumental failure, these experiments were carried out as single runs and repetitions are necessary in order to validate these observations.*

6.6.5 A 1:2 ratio of epsin 1 WT:auxilin 1

The initial competition observed posed multiple questions as to how certain endocytic adaptor proteins perform assembly and disassembly efficiently *in vivo.* Therefore, I aimed to investigate this further by doubling the concentration of each adaptor protein sequentially. This phenomenon would mirror *in vivo* situation where each specific adaptor protein would have a 'burst' of high concentration to initiate its role in the different stages of CME.

Thus, the concentration of auxilin 1 was doubled to 20 μM and the epsin 1 WT concentration was kept constant at 10 μM as in the previous experiments, resulting to a 1:2 molar ratio of epsin1:auxilin1. The SPR/IAC (2-injection) experiments were run as detailed above and the results are demonstrated in Figure 6.6.5 as dotted response curved following the previous colour scheme, and the straight lined response curves are from previous section 6.6.4 at a 1:1 molar ratio of epsin 1: auxilin 1. These results are merged together for comparison reasons between 1:1 and 1:2 epsin 1:auxilin 1 molar ratios. When injecting auxilin 1 (20 μM) first (first dotted blue curve) to form the auxilin:clathrin TD complex and then injecting the epsin 1 WT (10 μM) (second dotted blue curve) a binding of epsin 1 WT to

the complex at a response of ~ 1000 RU is observed (Figure 6.6.5). This binding of epsin 1 WT suggest two scenarios: (a) epsin 1 WT is able to bind to other clathrin TD sites even in the presence of higher auxilin 1 concentration, (b) epsin 1 WT could completely displace auxilin 1 from its occupied clathrin TD binding site(s). More interestingly, we observed that the competition between epsin 1 and auxilin 1 is altered when the concentration of auxilin 1 is doubled. This is confirmed when epsin 1 WT (10 μM) was injected first in our experiment (first dotted brown curve) to form the epsin 1:clathrin TD complex, and then auxilin 1 (20 μM) was injected over the complex. Auxilin 1 bound to the complex with an increase response of ~1300 RU (brown dotted line), which was not observed when the auxilin 1 concentration was at 10 μM (brown smooth line). However, the ~ 1300 RU increase observed which is not equal to the ~2300 RU observed when auxilin 1 is bound alone to clathrin-TD. This could be because of epsin 1 blocking some of the clathrin TD sites where auxilin 1 binds, due to its larger length (large unstructured region) and binding manner (occupy larger space on TD). Also epsin 1's affinity to clathrin TD might be stronger for certain clathrin TD sites than auxilin 1's. Though, by increasing the concentration of the auxilin 1, the number of auxilin 1 molecules injected onto the immobilized clathrin TD surface increases compared to the injected epsin 1 samples. This could provide more possibility for auxilin 1 to enter un-occupied TD sites or outcompete epsin 1 for its occupied TD sites, which are common between the two adaptor proteins (CBox, W-box, ArrestinBox TD sites). However, we are uncertain whether this concentration of auxilin 1 is actually saturating all TD binding sites on the chips surface. The Δpeak2-peak1 of the runs of 2-injection experiments plotted for all the epsin 1 and auxilin 1 for the 1:1 molar ratio and the 1:2 molar ratio (Figure 6.6.5 (B)).

Overall, there could still be competition between epsin 1 WT and auxlin 1 even at higher auxilin 1 concentrations, as epsin 1 WT could be initially bound to different TD site(s) which are common with auxilin 1, but due to auxilin 1's hypothesized lower binding affinity for some of those common TD

site, it could be hypothesized that auxilin 1 would not be able to compete and displace all of the epsin 1 form those TD sites. Due to SPR instrument deterioration I was not able to carry out the experiments where epsin 1 concentration is increased (double) and auxilin 1 concentration is kept constant. I hypothesize that the results from these experiments would not alter the competitive effect observed between epsin 1 and auxilin 1.

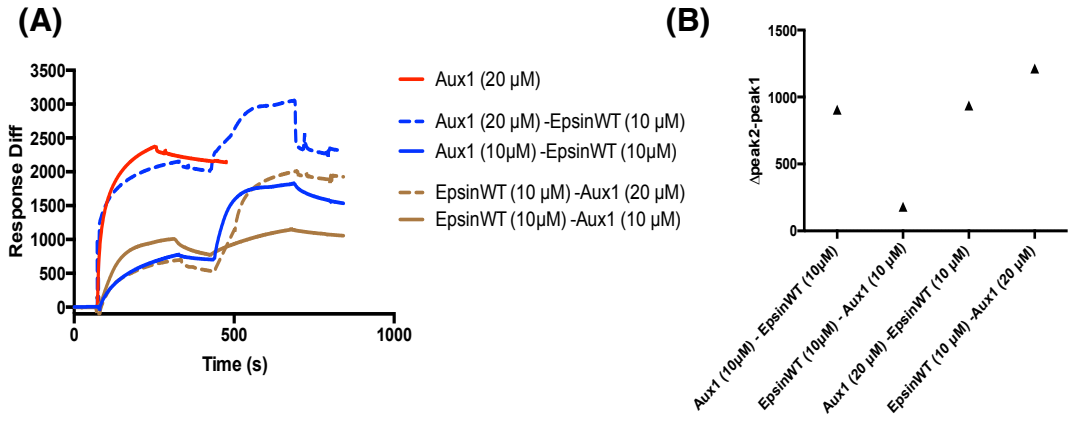

Figure 6.6.5: The competitive binding between epsin 1 and auxilin 1 for GST-clathrin TD at 1:1 molar ratio and 2:1 molar ratio. (A) *The sensorgram plot from the SPR/IAC (2-injection) method demonstrated that when the epsin 1 mutant is injected on the clathrin:auxiln 1 complex, the epsin 1 binds to the complex as shown by the increase in the second blue curve. However, when switching the order around, the auxilin 1 does not bind on the clathrin:epsin 1 complex as seen in the second brown curve. Increasing the auxilin 1 concentration to 20 μM and keeping epsin 1 concentration constant still promotes competition and an increase in response is observed when auxilin 1 was bound on the clathrin:epsin 1 complex. However, this competition is caused by auxilin either binding to unoccupied TD or outcompeting epsin 1 from its already bound TD sites. Due to SPR instrumental failure, these experiments were carried out as single runs and repetitions are necessary in order to validate these observations.* ***(E)*** *The Δpeak2-peak1 of the runs of 2-injection experiments plotted for all the epsin 1 and auxilin 1 for the 1:1 molar ratio and the 1:2 molar ratio.*

6.6.6 Discussion: epsin 1 and auxilin 1

Competition between epsin 1 WT and auxilin 1 WT was investigated based on previous results from pulldown/SDS-PAGE assays that have revealed competition between these two adaptor proteins for clathrin TD. In order to address these results further with a more quantitative technique, the newly developed SPR/IAC (2-injection) technique was employed.

The initial SPR results obtained in this section demonstrate clear competition between epsin 1 and auxilin 1 at a 1:1 molar ratio of epsin1:auxilin1. Increasing the concentration of auxilin, we noticed that competition was altered with auxilin 1 being able to bind on the epsin1:clathrinTD complex. In addition, other binding motifs such as the DLL and DPF/W motifs are shared between auxilin 1 and adaptors such as epsin 1 (Drake *et al.,* 2000; Scheele *et al,* 2001; Kalthoff *et al.,* 2002), which could contribute to the competition observed. It has been hypothesised that auxilin 1 may actively compete with adaptor binding to clathrin to displace adaptors from binding to clathrin (Scheele *et al.,* 2001; Smith *et al.,* 2004). Taking into consideration these observations, along with the structural nature of epsin 1 (two clathrin box motifs and unstructured/DPW region), and auxilin 1, the following interpretations of these results is proposed:

(a) based on the previous hypothesis in this thesis on how epsin interacts with clathrin, I suggest that epsin 1 WT once injected first onto the SPR chip surface could possibly bind to one or multiple hypothesized TD sites on a single TD e.g. CBox, ArrestinBox and W-box, which are suggested to be common to auxilin 1 as well (Drake *et al.,* 2000; Scheele *et al.,* 2001; Collette *et al.,* 2009), with a stronger binding affinity than auxilin 1 and occupying a larger space on the TD. Thus, if epsin 1 WT occupies majority of the TD sites on a single TD, this would limit the chance for auxilin 1 to bind when injected on the clathrinTD:epsin1 complex. Auxilin 1 might not be able to compete off the epsin 1 from its occupied TD sites. However, in the case where auxilin 1 is injected first and forms the clathrinTD:auxilin1 complex, epsin 1 once injected could either outcompeting the site(s) where auxlin 1 was bound to TD or bind to other multiple available TD sites which have not be bound to auxilin 1. Interestingly, pulldown assays from Scheele *et al.,* 2001 show that AP180, a similar assembly protein as epsin 1, is blocked from interacting with TD when auxilin is added in excess, even at lower concentration (Scheele *et al.,* 2001).

(b) epsin 1's length and binding manner and the large unstructured structure of epsin 1, could occupy a larger space on the TD, potentially hindering other available clathrin TD sites that auxilin 1 could potentially bind. Therefore, auxilin 1 would not be able to bind to clathrin TD, once injected in the epsin1:clathrin TD complex. However, in a situation where the auxilin 1 concentration is increased, it either to interacts with other available TD sites or outcompete epsin 1 for these binding sites. This causes an alteration in the competition intitially observed between these two adaptors and it is still detected as an increase in band intensity or response units in pulldowns and SPR results.

These *in vitro* observations and hypotheses provide more insight into how assembly adaptor proteins act in the presence of other disassembly endocytic adaptor proteins. Most interestingly, once again we can elucidate that epsin 1's complex structure prevents other endocytic adaptor binding to clathrin. However, these observations are *in vitro*, and could be the basis for *in vivo* future work to confirm such interactions.

6.7.0 Biological relevance of the competition between epsin 1 and auxilin 1

Epsin 1 is a vital clathrin assembly protein for initiation of CME, whereas auxilin 1 is a clathrin disassembly protein, which is used at the conclusion of clathrin-mediated endocytosis. However, as epsin 1 is one of the first adaptor proteins to arrive at the site of initiation, compared to auxilin 1, and interact with clathrin TD before auxilin 1 in an *in vivo* situation. The precise location of epsin 1 during cage disassembly is still not known (Chen *et al.,* 1998; Rappoport *et al.,* 2006; Edeling *et al.,* 2006a; Hawryluk *et al.,* 2006; Henne *et al.,* 2010). However, it has been suggested that at least some epsin 1 is present in CCP at the point of clathrin disassembly (Rapport et al., 2006; Hawryluk *et al.,* 2006; Edeling *et al.,* 2006a). Although, epsin 1 is suggested to be present in 90% of endocytic events in various cell lines (Taylor *et al.,* 2011), this could vary within cell lines, especially at a mature CCV where

epsin 1's concentration could be low and could make way for other adaptor proteins e.g. auxilin 1 to bind to clathrin. Epsin 1 has a concentration dependent inhibitory effect on clathrin cage disassembly of CCVs (Baker, 2016) and thus would play a role in making clathrin cages more resistant to disassembly *in vivo*. *In vivo* auxilin 1 and Hsc70 play a role in remodelling the clathrin lattice (Popova and Petrenko, 2013) and the presence of epsin 1 could therefore play a role in stabilising structures due to its 'linking effect' of clathrin. Thus, this could play a role in forming lattices and in driving a CCP towards maturation.

Additionally, Massol *et al.,* 2006 states that small and variable amounts of auxilin are recruited transiently with a 'burst' of higher concentration seen after the dynamin recruitment peak and interaction with lipid head groups. Thus, the timing of auxilin 1 recruitment determines the onset of uncoating (Massol *et al.,* 2006). Based on this knowledge, I suggest that the competition between epsin 1 and auxilin 1 for clathrin TD observed in the SPR results above is expected and hence comparable to the epsin inhibitory effect observed with the clathrin cages. Thus, I hypothesize that the concentration of auxilin 1 in the presence of epsin 1 affects the extent of disassembly *in vivo*. We clearly also observe this in the SPR results in this chapter where, at a higher concentration of auxilin 1, competition is still observed where auxilin 1 is able to bind to the epsin:clathrin TD complex either in the unoccupied TD sites or outcompeting epsin 1 in its already bound TD sites. It would be interesting to use mutants with impaired TD sites in order to attempt to obtain confirmation as to whether epsin 1 and auxlin 1 have common TD sites as hypothesised. Nevertheless, from this investigation we obtained novel information on the mechanism of epsin 1:clathrin TD interactions as well as how this could affect the way other adaptor proteins bind to clathrin TD e.g. auxilin 1.

6.8.0 Competition between β2-adaptin and auxilin 1

6.8.1 Introduction: structural and functional differences between β2-adaptin and auxilin 1

AP2 and auxilin 1 are considered an ideal combination to investigate competition for clathrin TD as they have very 'opposing' roles in the CME. An AP2 peptide has been shown to bind to the CBox site 1, W-box site 2 and Arrestin Box site 3 on the TD (Zhuo *et al.,* 2015), which are hypothesized to be common sites for auxilin 1 with clathrin TD (Drake *et al.,* 2000; Scheele *et al.,* 2001; Kalthoff *et al.,* 2002).

6.8.2 SDS-PAGE binding assay data reveal no competition between β2-adaptin and auxilin 1

Ultracentrifugation SDS-PAGE assays were previously conducted by Dr. Michael Baker with these two structurally diverse adaptor proteins to determine competition for clathrin TD binding (Baker, 2016). Based on previous literature, there is no specific interaction between these two adaptor proteins *in vitro and* that β2-adaptin and auxilin 1 has previously been shown to bind to clathrin at the same time (Boecking *et al*., 2011). No obvious competition was observed between these two adaptors for clathrin TD (Figure 6.8.2) at a 1:1 molar ratio of β2-adaptin:auxilin1 and a 1:5 of clathrin cages:adaptor. In the contrast, Smith *et al.,* 2004 demonstrate a level of competition for clathrin TD binding between β2-adaptin and auxilin with clathrin box peptides of both adaptor proteins in peptide competition assays. To address this opposing results, the SPR/IAC (2-injection) technique was used to investigate whether there is competition between β2-adaptin and auxilin 1 at a 1:1 and 2:1 molar ratio β2-adaptin:auxilin1 in the presence of clathrin TD.

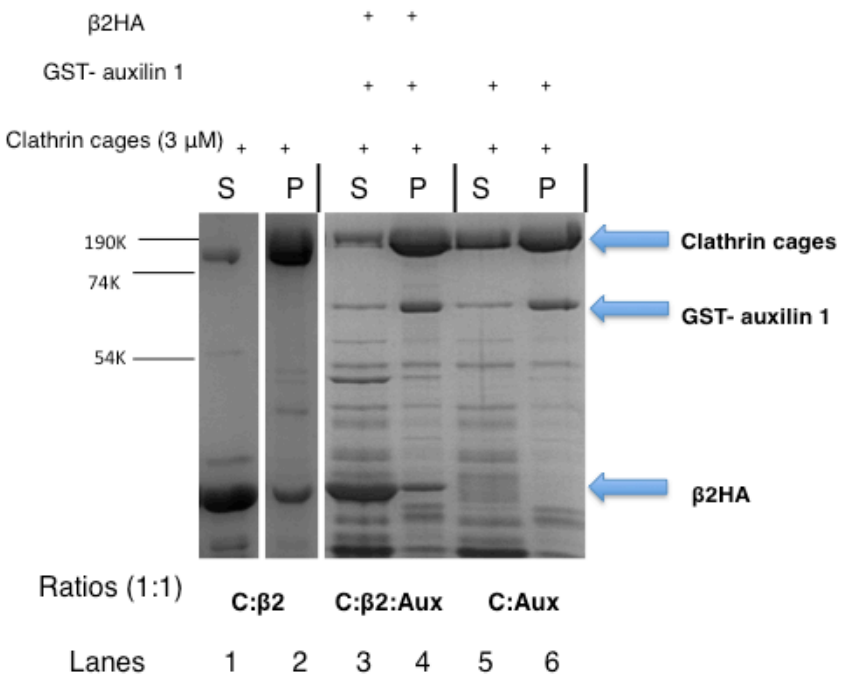

Figure 6.8.2: Ultracentrifugation analysis was conducted for β2HA and GST-auxilin 1 binding to clathrin cages*. Both β2HA and GST-auxilin 1 bind to clathrin cages (3 μM), as 1:5 molar ratio of clathrin cages:β2 show β2 present in the pellet (P) suggesting binding. Similarly, the GST-auxilin 1 pellets with clathrin cages at a 1:5 molar ratio. Both GST-aux and β2 HA can bind to clathrin cages when mixed together (C: β2:Aux) as both bands can be seen in the pellet(P) with clathrin. These experiments and SDS-PAGE analysis was conducted by Dr. Michael Baker (Baker Michael, 2016).*

6.8.3 SPR data reveal no significant competition between β2-adaptin and auxilin 1

To add further insight into the opposing views regarding β2-adaptin and auxilin 1 competition for clathrin TD, the newly established SPR/IAC (2-injection) method was used, where the colour scheme and injection order as well as the clathrin TD: adaptor (1:10) ratio are as described above. In Figure 6.8.3 (A) of the SPR results, we observe that when the β2-adaptin was injected (second blue curve) after formation of auxilin1:clathrin complex (first blue curve), we observe an increase in response to ~ 380 RU. When the adaptor protein order was switched around, with auxilin 1 injected (second brown curve) on β2-adaptin:clathrin complex (first brown curve), we observe an increase in response of ~ 750 RU. The Δpeak2-peak1 of the runs of 2-injection experiments plotted (Figure 6.8.3 (C)). This is a relatively small

difference, suggesting that these two adaptor proteins could favorably bind to clathrin TD simultaneously but with slight difference in their binding affinity. Based on these *in vitro* results, I suggest that β2-adaptin and auxilin 1 could bind to clathrin TD at the same time, and disassembly would not be inhibited at such ratios of adaptor proteins *in vivo*. This might be due to similar binding capacity of this two adaptor proteins to clathrin TD as seen in section 6.2.2.

When the β2-adaptin concentration was doubled it caused a complete inhibition of the auxilin 1 to the binding to clathrin TD. This is seen in the SPR data in Figure 6.8.3 (B), where injecting auxilin 1 (second brown dotted curve) on the β2-adaptin-clathrin complex (first brown dotted curve), no increase in response is observed. However, the sharp decrease during the buffer wash, after the first injection in the brown dotted curve, is considered unusual and possibly to the instrument failure. Thus, repetition is required to confirm the observed results. SPR experiments were run once with higher auxilin concentration keeping the β2-adaptin concentration the same. However, due to SPR instrument failure, the results were not presented, and all the experiments in Figure 6.8.3 were run only once.

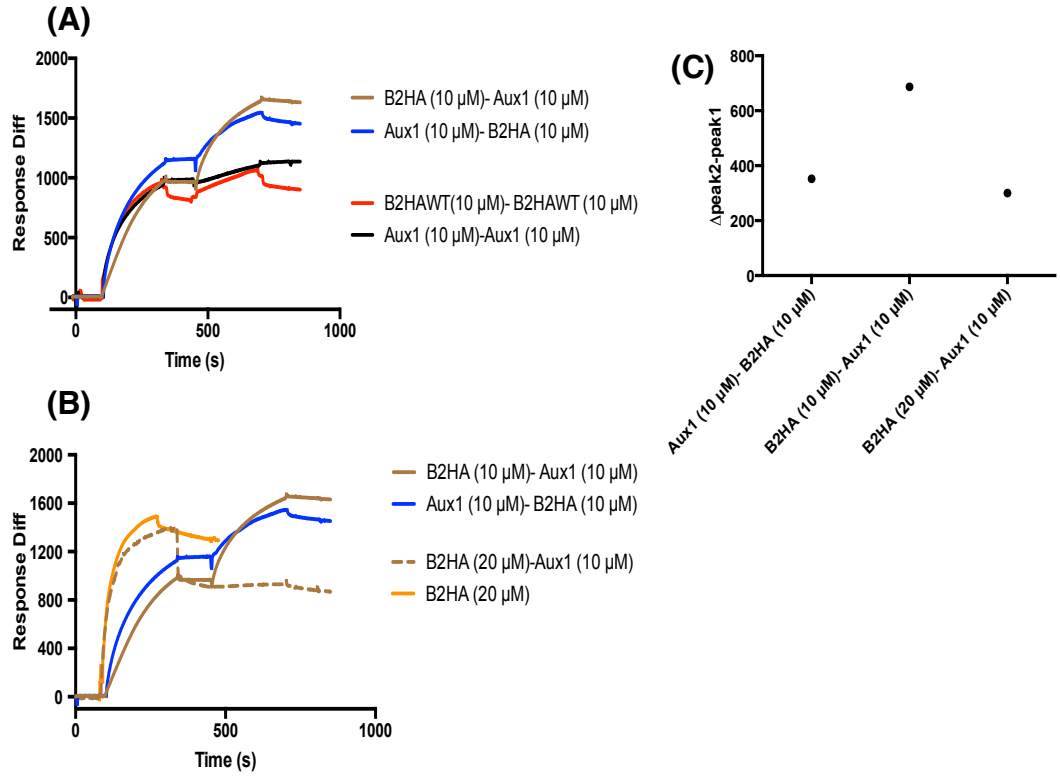

Figure 6.8.3: The competitive binding between β2-adaptin and auxilin 1 for GST-clathrin TD at 1:1 molar ratio, which is more obvious when the β2-adaptin concentration is increased. (A) *The sensorgram plot from the SPR/IAC (2-injection) method demonstrated that when β2-adaptin is added to the clathrin:auxilin1 complex, the β2-adaptin binds to the complex as shown by the increase in the second blue curve with ~ 380 RU difference between peak 1 and peak 2. When switching the order around, the auxilin 1 binds on the clathrin:β2-adaptin complex as seen in the second brown curve, but with ~ 750 RU difference between peak 1 and peak 2.* ***(B)*** *Increasing the β2-adaptin concentration to 20 μM and keeping auxilin 1 concentration constant enhances this competition as no increase in response curve was observed when auxilin 1 was injected on the clathrin: β2-adaptin complex (brown dotted line). Due to SPR instrumental failure, these experiments were carried out as single runs and repetitions are necessary in order to validate these observations.* ***(C)*** *The Δpeak2-peak1 of the runs of 2-injection experiments plotted for all the epsin 1 and auxilin 1 for the 1:1 molar ratio and the 1:2 molar ratio.*

6.8.4 Discussion: β2-adaptin and auxilin 1

In this section, I demonstrate how β2-adaptin and auxilin 1 would not compete for clathrin TD binding at a 1:1 molar ratio of adaptor proteins. However, competition is more obvious when increasing the concentration of one of the adaptor proteins as seen in the SPR data above. For example, doubling the concentration of β2-adaptin (β2HA) inhibited the binding of the

auxilin 1 to the clathrin: β2HA complex, and more specifically to clathrin TD. This causes displacement of certain adaptor proteins with others for certain TD sites. For example, β2-adaptin has been suggested to bind to three of TD binding sites (Cbox, ArrestinBox and W-box), as AP2 clathrin box motif peptide has demonstrate that has a 3:1 stoichiometric binding ratio of AP2 to clathrin TD with a low affinity (Zhuo *et al.,* 2015). Auxilin 1 has also been hypothesized to bind to the same three TD sites, CBox, ArrestinBox and W-box (Scheele *et al.,* 2001). Thus, in an *in vivo* situation we can hypothesize that during the 'burst' of β2-adaptin concentration at clathrin assembly initiation stage, β2-adaptin could bind to majority of the TD sites available with possibly a stronger binding affinity than auxilin 1. Thus, due to this hierarchy auxilin 1 could not displace β2-adaptin and inhibit the assembly process.

Focusing on the clathrin disassembly process, Massol *et al.,* 2006 state that small and variable amounts of auxilin are recruited transiently but that a much larger burst of association occurs after the peak of dynamin signal at scission (Massol *et al.,* 2006; Taylor *et al.,* 2011) and interaction with lipid head groups. Thus, the timing of auxilin 1 recruitment determines the onset of uncoating (Marssol *et al.,* 2006). It is interesting to note that the clathrin:AP2 ratio changes during flat-to-curved transition of the clathrin lattice *in vivo,* with a clathrin content of ~ 70%, which indicates completion of coat assembly (Bucher *et al.,* 2017). Thus the concentration of AP2 varies at various stage of CCV assembly. Therefore, during the disassembly stage *in vivo*, AP2 could be in low concentrations and thus the auxilin 1 'burst' in concentration could initiate the disassembly process without any competition for clathrin binding between the two adaptor proteins. Future experiments should be performed where the concentration of auxilin 1 is doubled whilst the concentration of β2HA is kept constant, in order to observe whether this competition can be eliminated in the presence of higher auxilin 1 concentration, as in a disassembly environment.

In the 1:1 adaptor molar ratio in the SPR results, we observed that in both situations where auxilin 1 was injected second or when β2-adaptin was injected second, we still observed a significant binding of the second adaptor to clathrin TD. Therefore, according to the SPR results I suggest that neither assembly nor disassembly processes would be completely terminated in an *in vivo* environment at 1:1 molar ratio. This could be because a redundant auxilin 1 binding site on the clathrin TD would ensure that auxilin 1 binds even in the presence of potentially competing proteins (Scheele *et al.,* 2001). However, it is still not certain that other factors, such as the binding of other adaptor proteins to a clathrin:β2-adaptin:auxilin 1 complex could be altering auxilin binding due to their highly dynamic interaction which is caused from hierarchical and sequential interaction with clathrin TD.

In 2004, Smith *et al.,* demonstrate a level of competition for clathrin TD binding between β2-adaptin and auxilin using peptide competition assays with clathrin box peptides of both adaptor proteins. Smith *et al.,* used a peptide, which give a weak binding interaction for clathrin TD to be determined (Smith *et al.,* 2004). In the SPR/IAC experiments, protein constructs have been used so we see how these binding sites operate in their original context within the protein. Our observations suggest that the protein binds with stronger affinity to terminal domain than an isolated peptide ligand. Therefore, the competitive effect between these two adaptors for clathrin TD binding observed in the results from Smith *et al.,* 2004 oppose the results from SPR/IAC (2-injection) method and pulldown/SDS-PAGE assays, which reveal no obvious competition between the two adaptors for clathrin TD. However, increasing the ratio of adaptor proteins could result into a more visible competitive effect. In addition, Dr. Michael Baker has demonstrated no significant inhibitory effect on clathrin cage disassembly from the addition of β2-adaptin (in excess) at 1:1 and 1:5 molar ratio of clathrin to β2-adaptin (Baker, 2016). It is important to note that auxilin 1 is able to interact with other clathrin heavy chain regions (Fotin *et al.,* 2004) where β2-adaptin cannot and so we do not see inhibition of disassembly, nor

obvious competition in cage pull down assays.

6.9.0 No competition between Hip1 CC and β-arrestin 1L

7.9.1 Introduction: structural and functional differences between Hip1 CC and β-arrestin 1L

β-arrestin 1L structure consists of two independent clathrin box motifs (LIELD and LEFD) on opposite sites (each C- and N- domains), which could bridge two clathrin molecules in a lattice (Kang *et al.,* 2009). The role of β-arrestin 1L is to bind and recruit clathrin to the plasma surface, for clathrin assembly. Hip 1/Hip1R endocytic adaptor protein on the other hand, has been stated to preferentially bind to CLC (Chen and Brodsky, 2005). The coiled-coil (CC) domain of both proteins promotes dimerization of the protein and interaction with clathrin light chain (CLC), which promotes the formation of clathrin cages in vitro (Ybe *et al.,* 2007; Niu and Ybe, 2007), (Ybe *et al.,* 2009). This allows the recruitment of Hip1/Hip1R to the membrane and release of the interactions with the CLC (Hyun *et al*., 2004; Ybe *et al.,* 2009; Gottfried *et al.,* 2010). More specifically, Hip1 has a potential clathrin box motif (VDLE), which is hypothesized to bind to CHC (Waelter *et al.* 2001). Thus, SDS-PAGE pulldowns and the SPR/IAC (2-injection) method were carried out to demonstrate whether there is competition between two adaptor proteins (the active form of beta-arrestin 1L and Hip1 coil-coil domain), which are required at different stages of the CME, and functionally different

6.9.2 SDS-PAGE binding assay data revealed no competition between Hip1CC and β-arrestin 1L

Initial investigation of competition of these two structurally diverse adaptor proteins, was carried out using GST- pulldown binding assays, which revealed no obvious competition between these two adaptors for clathrin TD with increasing concentration of either adaptor. More specifically, at a 1:1 molar ratio of β-arrestin 1L:Hip1CC, both adaptor proteins bind to clathrin TD (Figure 6.9.2 (B), lane 7 and 9; Figure 6.9.2 (D) lanes 1 and 3) compared to the control experiments with the adaptors alone, without the presence of

clathrin TD (Figure 6.9.2 (A) lanes 3-6, 11-14), with Hip1CC slightly pelleting on its own. At 1:3 molar ratios of β-arrestin 1L:Hip1CC (Figure 7.9.2 (B), lane 11 and 13; Figure 6.9.2 (D) lanes 5 and 7), the same results are observed, with the slight difference Figure 6.9.2 (D), lane 5, where the Hip1CC in the pellet has a less intense band then expected. However, this could be an anomaly in the results. Overall, Hip1 CC and active or WT β-arrestin 1L could bind to clathrin and co-exist. Additionally, we can confirm from the results that there is no specific interaction between these two adaptor proteins *in vitro.*

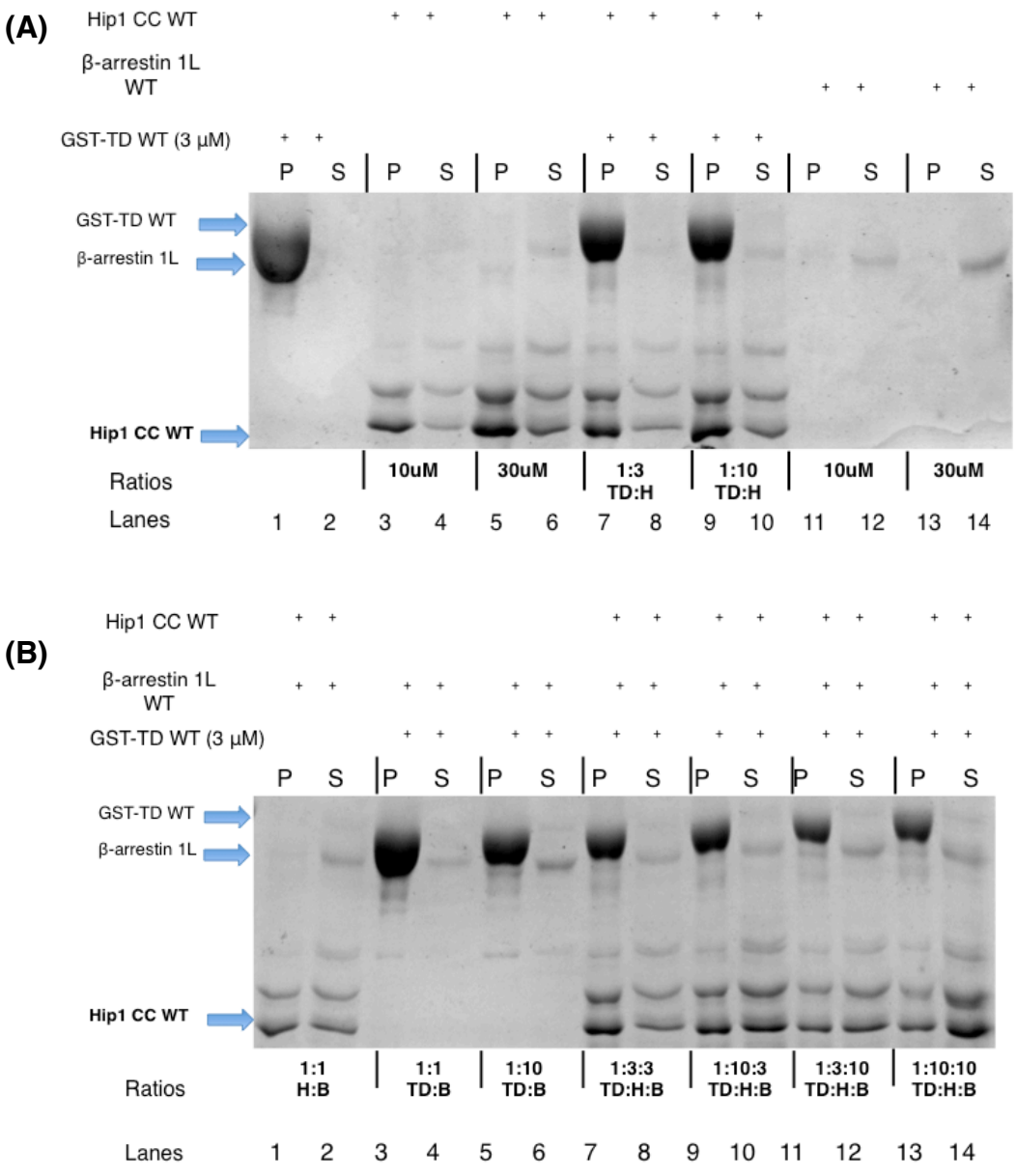

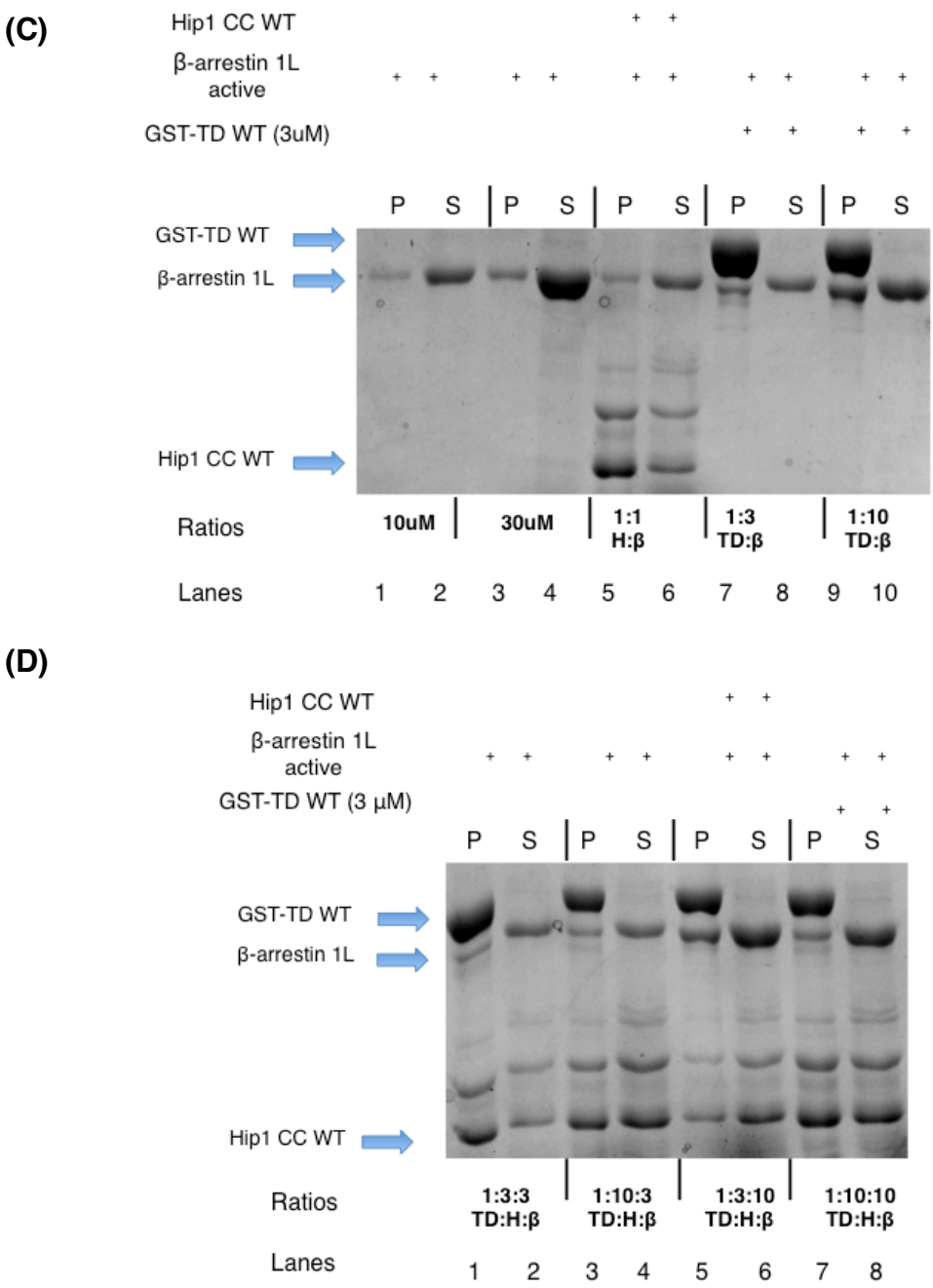

Figure 6.9.2: SDS-PAGE analysis of GST-pulldown assays demonstrating no obvious competition between β-arrestin 1L (β) and Hip 1 (H) for clathrin TD (C). At 1:1 or 1:3 of Hip1:β-arrestin 1L. *GST-clathrin TD (3 µM) was incubated with GST-affinity beads in the presence of active and/or WT β-arrestin 1L in increasing concentrations with His-Hip 1 at 1:1 and 1:3 molar ratios. The pellet (P) and supernatant (S) fractions were analysed by SDS-PAGE.* ***(A)*** *and* ***(C)*** *Controls are carried out with clathrin TD only (lanes 1 and 2) and His-Hip1 only (lanes 3-6) as well as GST- β-arrestin 1L (lanes 11-14), but also Hip1 in combination with clathrin TD at 1:3 and 1:10 ratio (lanes 7-10).* ***(B)*** *These two adaptor proteins have been shown that they do interact with each other (lane1-2).* ***(B) and (D)*** *No obvious significant competition between Hip 1 and active or WT β-arrestin 1L for clathrin TD, even at high concentrations of WT β-arrestin at 1:10:10 C:E:β molar ratio (lanes 13-14). However, due to the pelleting of Hip1 on its own, this competition is not conclusive. These experiments and SDS-PAGE analysis are representative of multiple experiments.*

6.9.3 Hip1 CC and β-arrestin 1L could be competing for clathrin TD binding as revealed from SPR data

In order to confirm the absence of any competition between these two adaptor proteins for clathrin TD binding, we carried out experiments using the newly developed SPR/IAC (2-injection) method using Hip1CC WT and active β-arrestin 1 (ActArr). The SPR results in Figure 6.9.3 revealed interesting observations where Hip1CC binding was negligible once injected on the ActArr-clathrin TD complex (Figure 6.9.3, second blue curve). But ActArr was able to bind to Hip1-clathrin TD complex (Figure 6.9.3, second brown curve). However, we have to note that the binding capacity of ActArr to clathrin TD alone is massively lower in these experiments, which could be the result of chip malfunction; these experiments need to be repeated to confirm such observations.

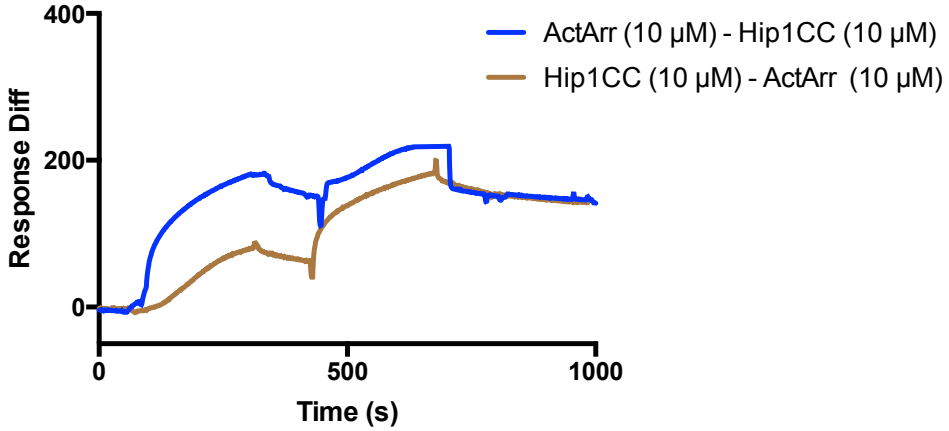

Figure 6.9.3: SPR sensorgram plot demonstrating the binding between Hip1 CC (10 μM) and active β-arrestin 1L (10 μM) to GST- clathrin TD (1 μM). *Once the Hip1CC is injected onto the immobilised clathrin TD, the response units are very low (~ 50 RU), and the ActArr injected second was able to bind even with low reponse units. The response units of the ActArr:clathrin TD are very low (first blue curve) compared to previous experiments in this Chapter, hence the low response units observed when bound to clathrin:Hip1 complex is expected. These results could be due to the deterioration of the SPR chip and would require repetition to confirm the results. Due to SPR instrument failure these were not repeated.*

6.9.4 Discussion: Hip1 and β-arrestin 1L

The observed SPR results between Hip1 CC and active β-arrestin 1L based on the SPR results could not be conclusive due to reasons stated in section 7.9.3. Based on previous knowledge, these adaptor proteins are functionally diverse. More importantly, the Hip1 is hypothesized to be mainly located on the outside of the clathrin cage rather than on the inner layer (Wilbur *et al*. 2008), due to its role in actin recruitment and organisation. Hip1 CC demonstrated a weak interaction with clathrin TD, which could be via the proposed motif of VDLE, suggested by Waelter *et al.,* 2001. Compared to β-arrestin 1L, which most likely localizes on the inside of the clathrin cage (Gurevich V.V., 2014). β-arrestin 1L's main interaction with clathrin is via the TD, whereas for Hip 1 this interaction is primarily via CLC but with TD as well via weak interactions (Waelter *et al.* 2001; Kang *et al.* 2009; Gurevich, 2014). However, the mechanism to disrupt an interaction between Hip1 and clathrin is not yet known.

6.10.0 Conclusion

In conclusion, the newly established SPR/IAC (2-injection) technique was used to investigate competition between structurally and functionally diverse endocytic adaptor proteins (epsin 1, auxilin 1, β-arrestin 1, β2-adaptin, Hip1 CC) for clathrin TD. The results from such investigation provided a vital insight into how certain adaptor proteins co-exist and could bind to clathrin TD together, such as auxilin 1 and β2-adaptin (AP2), however it is yet unclear whether a certain level of competition could inhibit assembly or disassembly processes. Additionally, epsin 1's structure and complex binding behaviour to clathrin, seems to relate to the competition observed between various adaptor proteins, such as β-arrestin 1L and auxilin 1. Overall, varying concentrations of the adaptor proteins as well as obtaining binding rate constants from SPR/IAC (2-injection) method would provide us with a greater understanding on the binding interactions with clathrin between different proteins in the presence of others. More detailed discussion and further work are to be found in Chapters 7.

Chapter 7: Final Discussion

7.0.0 Overview

Although our understanding has grown on the roles of adaptors at different stages of the CME, due to their complex structure, we currently have limited knowledge of their binding interactions with the clathrin TD. In this thesis, I aimed to address the manner in which β-arrestin 1L and epsin 1 bind to clathrin TD using mutagenesis studies, SDS-PAGE binding assays and SPR/IAC method.

Initially, I focused on whether the two clathrin box motifs on β-arrestin 1L structure, act antagonistically or synergistically. The action of the second clathrin box ([LI][LI]GXL)) and its potential to link multiple clathrin TDs could alter the interaction of other adaptor proteins which bind to clathrin TD, at the same time. This could also be the case for epsin 1 which also has two clathrin box motifs and an unstructured/DPW region structure, which were investigated in this thesis that could work cooperatively to link TDs and promote efficient clathrin assembly. This complex mode of binding by epsin 1 could interfere with the action of other adaptor proteins for clathrin TD.

I developed the SPR/IAC (2-injection) method in this thesis, in order to explore and gain further insight into whether certain adaptor proteins, which are structurally and functionally diverse, would compete for binding to clathrin TD or whether they would co-exist and bind simultaneously. This method was used along with mutagenesis studies and SDS-PAGE binding assays. In this chapter I discuss the implications of these interesting results based on the aims as per Chapter 1, section 1.11.0, and how this information relates to the situation *in vivo*. This chapter includes potential avenues for future work that could be explored based on the current results as well as further optimization of the SPR/IAC (2-injection) technique for clathrin:adaptor investigations.

7.1.0 SPR/IAC (2-injection) method: a tool used for investigating competition between adaptor proteins for clathrin TD binding

A 'two step' method was developed where an adaptor protein would bind to clathrin TD forming a complex (as in SPR/IAC), prior to the addition of another adaptor protein to the complex, in order to determine their binding interaction. The results obtained from this technique have yielded information regarding how certain adaptor proteins act in the presence of others for clathrin TD binding. These results open up additional questions, which can be addressed in future assays, described in section 7.6.0. Currently, this method is at the early stages of development and it is considered a semi-quantitative method, which we aim to progress to a fully quantitative analysis method for clathrin:adaptor interactions with certain future optimization steps. This progression will make it possible to obtain direct comparisons of binding affinity constants at a 'two-step' binding level between two adaptor proteins bound to clathrin TD at the same time (3 protein interactions). This type of assessment would be novel for the field of clathrin:adaptor, indicating any competition between adaptor proteins for clathrin in a quantitative way.

7.2.0 The conserved LIELD clathrin box motif in β-arrestin 1L is the major box for clathrin interaction

The SPR/IAC data obtained in this thesis for the purified WT and mutant β-arrestin 1L were mostly comparable to the results of Kang *et al.,* 2009. Overall, the second clathrin box ([LI][LI]GXL) on the β-arrestin 1L is accessible for binding to the clathrin TD, and therefore the active form of β-arrestin 1L with both clathrin box motifs accessible, demonstrated the strongest binding to clathrin TD in the SPR results of this thesis. The WT β-arrestin 1 which has the conserved clathrin box hidden, presents approximately half the binding response to the TD, which suggests that the conserved LIELD clathrin box motif is the major box for clathrin interaction. This is supported by the evidence from by Kang *et al.* 2009, that there is a ~

2-fold difference in binding affinity between active and WT β-arrestin 1L (Kang *et al.,* 2009). The strongest binding was between the clathrin TD and active β-arrestin 1L with a K_D of 0.98 ± 0.01 μM, whereas the K_D of the WT β-arrestin 1L bound to clathrin TD was 2.1 ± 0.4 μM (Kang *et al.* 2009). Evidence from this thesis shows that mutating or deleting the conserved LIELD clathrin box motif acts negatively on how β-arrestin 1L interacts with clathrin TD causing a large decrease in the SPR response. This adds further support to the idea that the conserved clathrin box is the major clathrin interacting box, and that the second clathrin box ([LI][LI]GXL) cannot act as efficiently in isolation. However, we would still be uncertain whether these two clathrin box motifs act synergistically to link multiple clathrin TD, as suggested by Kang *et al.,* 2009, as we have not investigated mutants of the second clathrin box motif. However, evidence from Kang *et al.,* 2009 utilising TIRF microscopy for GPCR trafficking in HEK293 cells shows that β-arrestin 1L still interacts with clathrin and promotes effective localization of β_2AR to CCPs even in the absence of the conserved LIELD clathrin box motif (Kang *et al.,* 2009). It is still unclear whether they bind to the same TD but a different sites (CBox- site 1 or ArrestinBox-site 3), and/or via multiple TD interactions. Hence, in future, the use of clathrin TD mutants with impaired sites could provide substantial information on the suggested linking TD effect of β-arrestin 1L.

As the second clathrin box is suggested to have a low affinity for clathrin and does not function in isolation (Kang *et al.,* 2009), it could be that these clathrin box motifs act cooperatively. Such a cooperative effect is supported by that fact that the two independent clathrin box motifs are ~ 68 Å apart and could be bridging multiple adjacent clathrin molecules in a lattice which are ~ 64 Å in distance (Kang *et al.,* 2009). This 'linking effect' for multiple adjacent TDs has been hypothesized for other adaptor proteins such as epsin 1 (more details in Chapter 6). The conserved clathrin box motif (LIELD) has been found in other adaptor proteins such as AP2, AP180, amphysisin and epsin 1, and the second clathrin box motif of β-arrestin 1L has also been found in

other endocytic adaptor proteins, and binds to the ArrestinBox TD site (Kang *et al.,* 2009; Lemmon and Traub, 2012), suggesting that β-arrestin 1L has the potential to compete for binding with other adaptor proteins.

7.3.0 The complex interaction of epsin 1 and clathrin TD

The clathrin adaptor epsin 1 is crucial for CME but the mechanism by which it interacts with clathrin and regulates clathrin assembly remains unclear. It has been hypothesized that epsin's mode of interaction with clathrin is not simple and is most likely to consist of multiple components of its structure. Mutating any of those components massively decreases epsin's binding to clathrin TD.

The two clathrin box motifs of epsin 1, which interact with clathrin via specific motifs, have been proposed to work cooperatively to assemble clathrin (Drake *et al.,* 2000; Drake and Traub, 2001; Holkar *et al.,* 2015), and mutation of either of these motifs inhibits clathrin assembly on liposomes *in vivo* (Holkar *et al.,* 2015). However, using the epsin clathrin box mutagenesis and SPR results in this thesis, I propose that the unstructured/DPW region, which has been suggested to bind to clathrin non-specifically (Drake *et al.,* 2000), has an equal binding capacity for clathrin TD as the two clathrin box motifs. This effect provides an interesting discussion point as to whether the two clathrin box motifs have a cooperative effect between them, as well as with the unstructured/DPW region in binding to clathrin. Would this hypothesized cooperative effect promote efficient clathrin assembly *in vivo*?
Further investigations using epsin 1 unstructured/DPW region mutants confirmed the value of this region and the DPW motifs in the unstructured/DPW region, in the manner in which epsin 1 interacts with clathrin TD. The two clathrin box motifs are separated by 233 amino acids of a distance shorter than 155 nm (Kalthoff *et al.,* 2002; Dafforn and Smith, 2004). Shortening (by half or quarter) this distance significantly decreased the binding capacity of epsin to bind to clathrin TD. This decrease is approximately equal with the decrease observed with the clathrin box epsin

mutants (257,480 and DKO). Thus, shortening the distance by half (~ 50 nm) or by quarter (~ 78 nm) decreases greatly the extent of the long-distance interactions between epsin 1 and clathrin. Based on previous structural studies on clathrin cages, the approximate distance between CBox site 1 clathrin TD site is approximately ~ 5-10 nm depending on the cage size formation (Kirchhausen, 2000), (Fotin *et al.,* 2004). Hence, shortening or deleting this distance, would prevent the stretching of the epsin molecule to link multiple clathrin TD together. This information also confirms the proposed scenario where the two clathrin box motifs and the unstructured/DPW region have a cooperative effect in binding to clathrin. More interestingly, deleting the whole unstructured/DPW region resulted in an even lower binding capacity for clathrin TD, confirming once again the importance of the distance and DPW motifs, in the unstructured/DPW region.

Alternatively, two different sites on a single TD could be occupied with a single epsin 1 (Morgan *et al.,* 1999; Greene *et al.,* 2000; Drake *et al.,* 2000; Drake and Traub, 2001; Kalthoff *et al.,* 2002; Dafforn and Smith, 2004; Holkar *et al.,* 2015). Epsin 1 has been suggested to interact with three TD sites e.g. site 1 (CBox), site 2 (W-box) and site 3 (ArrestinBox) as the first clathrin box of epsin 1 (LMDLA) has been proposed to be similar to the W-box motif of amphiphysin (WLDWP) which binds to W-box TD site (Drake and Traub, 2011; Scheele *et al.,* 2001; Miele *et al.,* 2004), and the epsin yeast homolog (Ent2) has been shown to bind to CBox and the W-box of the TD sites (Collette *et al.,* 2009). Therefore, the cooperative effect of the two clathrin box motifs and long and flexible unstructured/DPW region could very well promote epsin 1's linking effect on multiple adjacent clathrin TDs or the interaction with multiple sites on the same TD by stretching of this region, which could be prevented once this region is shortened or deleted. Additionally, such a flexible region could reduce mobility of the clathrin TD by wrapping around the TD and stabilizing the conformation, thereby forming a compact environment which permits cooperative assembly with other binding partners, such as AP2 (Drake *et al.* 2002; Brett *et al.* 2002; Dafforn and Smith, 2004; Edeling *et al.,* 2006a).This is consistent with the hypothesis that

clathrin assembly *in vivo* requires the action of both epsin clathrin box motifs, but also facilitating membrane curvature by generating steric hindrance especially via this unstructured/DPW region (Busch *et al.,* 2015). This could be key for determining the hierarchy of molecular interactions in CME budding *in vivo* (Holkar *et al.,* 2015). Overall, these results have opened certain future avenues, which are described in Chapter 6, section 6.7.0.

Epsin 1 has been shown to have an inhibitory effect on clathrin cage disassembly through competition with auxilin 1, where epsin 1 could effectively block the preferred binding sites of auxilin 1 at low concentrations (Baker, 2016). This effect could be explained by epsin's complex binding manner which could block other available TD sites or cause competition for the same occupied TD sites between other endocytic adaptor proteins from different CME stages, at the same time. This is further explored in the following section.

7.4.0 Adaptor competition studies

7.4.1 Overview

The timeframe of complete CCP formation and clathrin uncoating is ~ 90 seconds (Loerke *et al.,* 2009), with a combination of at least 25 different adaptor proteins recruited to the plasma membrane during CME in an ordered sequence and timing, orchestrating clathrin polymerization and disassembly (Traub, 2011; Taylor *et al.,* 2011; Merrrifield and Kaksonen, 2014). This makes CME a complex mechanism to understand. Adaptors could undergo rapid cycles of binding and dissociation from clathrin via weak molecular binding interactions (~ 1 second) causing sequences with weaker clathrin binding affinity to be displaced by others (Shih et al., 1995; Traub, 2011; Zhuo *et al.,* 2015; Muenzner *et al.,* 2017). It has been stated that a single clathrin TD could bind to three peptides, thereby enabling variety of different adaptor proteins to simultaneously interact with single or multiple sites on clathrin TD, (Willox and Royle, 2012; Zhuo *et al.,* 2015; Muenzner *et al.,* 2017). A great deal of knowledge already exists on the individual role and

functionality of adaptor proteins in CME. However, it is still unclear whether certain adaptor proteins, which are structurally and functionally diverse, cooperate or compete for clathrin TD binding, at the different stages of CME. Such information could support certain hypothesis on how adaptor proteins promote successful clathrin coat assembly and disassembly during CME *in vivo.*

7.4.2 Adaptor competition for clathrin TD

At the early stages of CME, AP2 (β2-adaptin subunit) and activated β-arrestin 1L have been demonstrated to work cooperatively in binding to clathrin TD due to their different roles. β-arrestin 1L only recruits clathrin to the plasma surface whilst AP2 initiates clathrin assembly (Owen and Evans, 1998; terHaar *et al.,* 2000; Collins *et al.,* 2002; Burtey *et al.,* 2007). A AP2/ β-arrestin 1L/clathrin interaction targets GPCRs for internalization via efficient localization in CCPs (Laporte *et al.,* 2000; Tian *et al.,* 2014). The SPR results in this thesis, demonstrate that β2-adaptin binds to clathrinTD:β-arrestin 1L complex, but β-arrestin 1L does not bind to the clathrinTD:β2-adaptin complex. One explanation could be that β2-adaptin obscures β-arrestin 1L interacting sites because of the way it is bound to the clathrin TD on the SPR chip. In an *in vivo* situation, this could suggest that β2-adaptin can stop β-arrestin 1L or the GPCR/ β-arrestin 1L complex from entering into the CCPs.

An alternative model suggested by Laporte *et al.,* 2000 was that AP2 would be recruited once β-arrestin 1L binds to the phosphorylated GPCR (Laporte *et al.,* 2000; Kim and Benovic, 2002; Tian *et al.,* 2014). Hence, the β2-adaptin (AP2) would bind to β-arrestin 1L and be recruited to the surface and cooperatively bind with clathrin TD in a sequential manner, as previously stated (Kim and Benovic, 2002; Tian *et al.,* 2014). Such cooperative manner could be suggested from SPR/IAC (2-injection) results where β2-adaptin binds to the clathrin:β-arrestin 1L complex.

Another important adaptor protein, epsin 1, has been previously suggested to promote uniform sized clathrin cages due to its interaction with multiple neighbouring triskelia (Drake *et al.,* 2000; Drake and Traub, 2011; Kalthoff *et al.,* 2002). The observation that epsin 1 and β-arrestin 1L compete at a 1:1 molar ratio in the same manner as epsin 1 and auxilin 1, could further confirm the complex epsin 1 interaction with clathrin via long-distance multiple TD linking interactions through the hypothesized three TD sites (CBox, ArrestinBox and W-box). This is due to the cooperative behavior of its two clathrin box motifs and its long unstructured region, as mutating any of the epsin 1 clathrin box motifs still promotes competition between epsin 1 and WT or active form of β-arrestin 1L. This suggests that epsin 1 most likely occupies more TD sites than any other adaptor proteins studied in this thesis, potentially blocking a greater extent of TD sites and space, which could have been occupied with a different adaptor protein such as β-arrestin 1L or auxilin 1. Additionally, clathrin:epsin 1 interactions could be strong enough to prevent β-arrestin 1L or auxilin 1 to outcompete for its occupied TD sites, due to its presence in 90% of most cell lines in the initiation stage (Taylor *et al.,* 2011) but most importantly due to its multiple clathrin binding components which are in line with the SPR results in Chapter 5.

Considering GPCR internalization via CME, β-arrestin 1L would only be recruited when a GPCR is targeted for internalization via a desensitization and recycling pathway (Gurevich, 2014). β-arrestin 1L is an activator of cell signaling and modulator of endocytic trafficking, hence it is considered to have multiple functions. Therefore, its role in CME is not considered broad, unlike an adaptor protein such as epsin 1. This makes β-arrestin 1L an adaptor protein “on demand”, where it is not continually required and present at the plasma membrane (Gurevich, 2014). In a situation where β-arrestin 1L is required *in vivo*, a ‘burst’ of high concentration would accumulate at the plasma membrane during the initiation process of CME. This could possibly promote binding to the unoccupied TD sites, aiding in the initial clathrin recruitment to the surface and interaction with AP2. Epsin 1 could then

displace it immediately after the clathrin assembly initiation process begins. In addition, it could be that β-arrestin 1L is only helpful in initial clathrin recruitment after its activation by a phosphorylated GPCR, so that epsin 1 displaces it during the growth of the clathrin coated vesicle (CCV). It has been suggested that β-arrestin 1L is present during CCV formation but dissociates before the CCV is pinched off (Koppen and Jakobs, 2004). Such competition suggests that the second clathrin box on β-arrestin 1L would not be sufficient on its own or in combination with the conserved clathrin box on β-arrestin 1L, to outcompete the epsin 1 from its already occupied TD sites. Overall, this could suggest the importance of the hierarchy of the adaptor proteins during CME.

During clathrin disassembly at the later stages of CME, the precise location and fate of epsin 1 is unknown (Chen *et al.,* 1998; Rappoport *et al.,* 2006; Edeling *et al*., 2006a; Hawryluk *et al.,* 2006; Saffarian *et al.,* 2009; Henne *et al.,* 2010) and debatable whether epsin would most likely be present in CCPs at the point of clathrin disassembly, after completion of its clathrin assembly initiation role. While epsin 1 is suggested to be present in 90% of endocytic events in various cell lines (Taylor *et al.,* 2011), this could vary within cell lines, especially at a mature CCV where epsin's concentration could be low and would allow other adaptor proteins e.g. auxilin 1 to outcompete epsin 1 for clathrin binding. Interestingly, epsin 1 has been suggested to have a concentration dependent inhibitory effect on clathrin cage disassembly *in vitro* though competition with auxilin 1 (Baker, 2016). If this was the case *in vivo* as well, it would play a role in making clathrin cages more resistant to clathrin disassembly. This information could elucidate the competition observed between epsin 1 and auxilin 1 at a 1:1 molar ratio in the SPR experiments in Chapter 6. *In vivo*, a 'burst' of auxilin 1 recruitment at the plasma membrane determines the onset of clathrin uncoating (Massol *et al.,* 2006; Taylor *et al.,* 2011). Thus, increasing the concentration of auxilin 1 in the SPR experiments (1:2 molar ration of epsin1:auxilin1), the competition for clathrin binding between the adaptors was altered, as auxilin 1 was able to

bind to either unoccupied TD sites or compete off epsin 1 from its already bound TD sites. The exact TD sites that epsin 1 and auxilin 1 bind are still unclear, but it is hypothesised that they share the same clathrin TD site interactions as well as DLL and DPF/W motifs (Drake *et al.,* 2000; Scheele *et al.,* 2001; Kalthoff *et al.,* 2002). Consequently, if the TD competition between these two adaptors is the case *in vivo* as well, the concentration of auxilin 1 in the presence of epsin 1 is the key factor in the extent of cage disassembly. On the other hand, it is important to consider however that auxilin 1 interacts with the CHC leg domains as well in order to perform its dissasmbly role (Edeling *et al.,* 2006), thus auxilin 1 rearrangement would be different in the different classes of cages eg. hexagonal, pentagonal etc. In this case competition between epsin 1 and auxilin 1 for the TD would not affect auxilin 1 binding to the leg and disassembly could still proceed.

AP2 has been suggested to be present during the clathrin uncoating process (Mettlen *et al.,* 2009; Saffarian *et al.,* 2009; Taylor *et al.,* 2011), which could promote competition between the adaptors for clathrin TD binding and affect the onset of the disassembly process. Smith *et al.,* 2004 demonstrated a level of competition for clathrin TD binding between β2-adaptin and auxilin 1 clathrin box peptides using competition assays *in vitro.* However, based on the SDS-PAGE binding assays and preliminary SPR results in Chapter 6, it is debatable as to whether β2-adaptin and auxilin 1 do actually compete with each other for clathrin TD binding. At a 1:1 molar ratio of β2-adaptin:auxilin 1, a certain level of competition is observed in the SPR/IAC (2-injection) results, which is not as obvious or significant as other adaptor competition profiles such as epsin 1 and β-arrestin 1L. Thus, I suggest that overall β2-adaptin and auxilin 1 would preferentially bind to different TD sites and in an *in vivo* situation neither assembly nor disassembly processes would be completely terminated, as assembled clathrin can be disassembled even when auxilin does not bind to the clathrin TD directly (Ungewickell *et al.,* 1995), as auxilin 1 binds to multiple sites on the clathrin leg (Edeling *et al.,* 2006b; Young *et al.,* 2013).

More obvious competition was observed when increasing the concentration of the β2-adaptin in the preliminary SPR experiment (these results are preliminary and the reasons behind it are stated in Chapter 6). This could be addressed with the recent evidence from Bucher *et al.,* 2017, where the AP2/clathrin ratio changes in a flat-to-curved transition of the clathrin lattice *in vivo.* This transition occurs when the content of clathrin is around 70% indicating the completion of the coat assembly (Bucher et al., 2017). Therefore, β2-adaptin, more specifically AP2, would be present during uncoating but perhaps at a low concentration and thereby a 'burst' of high concentration of auxilin 1 (Massol *et al.,* 2006; Taylor *et al.,* 2011) could be enough to outcompete any TD sites occupied by β2-adaptin. Similarly, auxilin 1 could bind to TD sites, which are not occupied by β2-adaptin. This could be a plausible scenario as β2-adaptin has been suggested to bind to three of TD binding sites (Cbox, ArrestinBox and W-box), where AP2 clathrin box motif peptide has demonstrate a 3:1 stoichiometric binding ratio of AP2 to clathrin TD but with a low affinity (Zhuo *et al.,* 2015). Auxilin 1 has also been hypothesised to bind to the same three TD sites, CBox, ArrestinBox and W-box (Scheele *et al.,* 2001). Overall, to confirm such hypothesis, SPR experiments with auxilin 1 increased concentration to be carried out in the future as well as clathrin TD mutants, which have impaired each TD site separately in order to confirm the favored TD site interaction of auxilin 1. Further evidence demonstrating how these two adaptors can bind to clathrin at the same time was shown when no significant inhibitory effect on clathrin cage disassembly was observed from the addition of β2-adaptin (in excess) (Baker, 2016). β2-adaptin did not inhibit the normal cage disassembly and the action of auxilin 1 as the initiator of the disassembly process. Auxilin 1 is able to interact with other clathrin heavy chain regions (Fotin *et al.,* 2004) where β2-adaptin cannot and so we do not see inhibition of disassembly, nor obvious competition in clathrin cage (Baker, 2016).

Lastly, the SDS-PAGE binding assays and SPR results observed between Hip1CC and β-arrestin 1L suggest no obvious or significant competition

between these two adaptors for clathrin TD. This is confirmed with our current knowledge of their location in the clathrin cage and primary clathrin binding interaction, which is discussed in section 6.9.0. However, SPR experiments require repetition due to the low response units observed due to potential SPR chip deterioration.

In vivo, the AP2/clathrin ratio changes at the end of the initiation stage in CME (flat to curved transition) (Bucher *et al.,* 2017), therefore, a 'burst' of higher concentration of specific adaptor protein according to their primary role in CME, could outcompete other adaptor proteins for clathrin binding which are already occupied on TD. And even though Willox and Royle, 2012, has suggested that a single clathrin binding box motif is sufficient to promote endocytosis *in vivo*; such competition patterns demonstrate the importance of such adaptor proteins binding to multiple specific sites on the TD (Willox and Royle, 2012). Although, it is of course possible that multiple interactions are required for the stabilisation of clathrin:adaptor interactions as shown by Zhuo *et al.,* 2015, where most adaptor proteins cooperatively interact with clathrin *in vivo* to allow dynamic reorganization of clathrin during its assembly and disassembly. The major test is to transfer the mutagenesis and competition between adaptor proteins investigation to an *in vivo* system, which would clarify whether these competitions exist and are important for the CME. Nevertheless, the SPR competition results from this thesis have expanded certain novel aspects of the mechanism and behavior of certain adaptor proteins in the presence of others for clathrin TD binding.

7.5.0 Clathrin cages assembled with epsin 1 and β-arrestin 1L

Optimisation of different buffer conditions has shown that cages containing epsin 1 and active β-arrestin 1L are most stable in HKM pH 7.2 have more uniform cage structures. In future, the location of adaptor proteins in clathrin cages could be identified through a cryo EM model of such a complex. This was further described in Chapter 4. Investigations for epsin 1, active β-arrestin 1L and cages were performed before the development of the adaptor competition studies and SPR/IAC (2-injection) technique (more details in Chapter 6), which reveal competition between epsin 1 and active β-arrestin 1L for clathrin TD binding at 1:1 molar ratio. However, it is important to note that this competition may not exist in the presence of whole clathrin cages as saturation of all binding sites could not be full field.

7.6.0 Future work: optimization of SPR/IAC (2-injection) method

In order to progress the SPR/IAC (2-injection) method to a fully quantitative technique and obtain appropriate binding rate constants (K_D) for a 'two level' interaction, further optimization stages are required which have been suggested through personal communication with Prof. Richard Napier and Prof Petr Kuzmic. Lowering the response units of a protein-protein interaction to 100-300 RU, was the initial suggestion, which will help eliminate mass transport issues and allow more accurate data for kinetic analysis to be obtained. Due to the complex structural behavior of epsin 1, a range of concentrations is necessary in order to obtain the appropriate ratio for lowering the RUs. However, in this thesis I have tested lowering the response to 100-300 RU of epsin-clathrin interactions with little success. This is hypothesized to be due to the complex epsin 1 structure and its complications on non-specific binding and mass transport.

A more sensitive SPR instrument needs to be used, e.g. Biacore T200, to carry out all the adaptor competition experiments. However, a T200 instrument could also offer 'single cycle kinetic' (SCK) method for SPR assays to be carried out for adaptor competition. SCK was introduced from Karlsson and co-workers in 2006, which offers automatic kinetic titration series experimental runs without surface regeneration required between each injection (Karlsson *et al.,* 2006; Palau and Primo, 2013) However, initial optimization would be required to test if this method is appropriate for the complex clathrin:adaptor system. The advantages of this method are: (a) lower the antibody deterioration issue, improving the systematic error observed in the SPR/IAC method (b) less time consuming due to automated set up to run experiments compared to the manual operation used in SPR/IAC (2-injection) method in this thesis. (c) direct quantitative comparison between binding affinities of adaptor protein combinations on the same flow cell, and carrying out a series of concentration ranges and fit an appropriate kinetic model to experimental data, in order to obtain binding constants (K_D). Overall, the results obtained from the SCK method could be comparable to the results obtained from (manual set up) of SPR/IAC (2-injection) method used in this thesis.

7.7.0 Future work: Adaptor protein competition for clathrin binding

7.7.1 Different adaptor protein combinations

Another avenue of exploration would be to investigate different adaptor protein combinations for competition assays. AP180 does not have a specific clathrin box motifs that bind to clathrin TD, but it consists of eight repeated D[IL][LF] motifs throughout its unstructured region that primarily binds to clathrin TD non-specifically with a strong affinity (Drake *et al.* 2000; Kalthoff *et al.,* 2002; Zhuo *et al.,* 2015). Additionally, four sequence repeats of D[IL][LF] motifs have also been found in auxilin 1 (Scheele *et al.,* 2001). AP180 has been shown to compete with auxilin 1 for the same site on the α-

ear domain of the AP2 complex (Scheele *et al.,* 2001). Furthermore, Zhuo *et al.,* 2015 has demonstrated that AP2 and AP180 peptides can simultaneously bind to three TD sites (CBM, W-box and ArrestinBox) (Zhuo *et al.,* 2015). It would be interesting to test whether AP180 has an inhibitory effect on disassembly similar to that of epsin 1. Taking all this into consideration, AP180 could be a possible new adaptor protein to investigate with SPR/IAC (2-injection) method in combination with β-arrestin 1L, epsin 1 and β2-adaptin.

7.7.2 Clathrin TD mutants

The results presented in Chapter 6, have opened a number of avenues of enquiry on the exact TD site interaction of adaptor proteins in the presence of others, especially with the complex adaptor protein epsin 1. Interestingly, both epsin 1 and auxilin 1 have been hypothesized to have common multiple binding sites on the TD, which are site 1 (CBox), site 2 (W-box) and site 3 (ArrestinBox), these are yet to be confirmed. Thus, it would be interesting to use clathrin TD (residues 1-363) mutants with the four TD sites impaired separately and SPR/IAC method in order to add further support on the preferred TD sites of epsin 1 and auxilin 1. The newly established SPR/IAC (2- injection) method could then be used, with the analogous adaptor protein combinations to observe the competition patterns in the presence of immobilized clathrin TD mutants on the SPR chip.

Chapter 8: Appendix

8.0.0 Overview

The results presented in Chapter 6 and 7, have opened a number of avenues of enquiry on the exact TD site interaction of epsin 1 and auxilin 1. They have been hypothesized to have common multiple binding interactions with the TD, via the site 1 (CBox), site 2 (W-box) and site 3 (ArrestinBox). However, these TD site interactions have not yet been confirmed. By using clathrin TD (residues 1-363) mutants with the four TD sites mutated separately and binding interactions tested using the SPR/IAC method, we could add further support on the preferred TD sites of the epsin 1 based on its complex multiple clathrin binding components and auxilin 1.

8.1.0 Mutagenesis of clathrin TD mutants

The TD mutants in pGEX (4T-2) plasmid were designed in line with Muenzner *et al.,* 2017 and detailed in the Table 1.10.0, with mutations at the four TD motifs alone or in combination. Three mutants ((CBox/ArrB), ArrestinBox and Full del) were tested for expression and purification conditions, in this thesis.

Number	***Mutant Name (abbreviation)***	***Details of mutation***
1	CBox and ArrestinBox (CBox/ArrB)	T87A, Q89A and Q192Y
2	ArrestinBox	Q192Y
3	W-box	Q152L, I154Q
4	Royle box	F9W
5	CBox, ArrestinBox, W-box, Royle box (Full del)	F9W, T87A, Q89A, Q152L, I154Q, Q192Y

Table 1.9.0: Details of the clathrin TD mutants and the details on the exact sites being impaired.

8.2.0 Small-scale protein expression of clathrin TD mutants

8.3.0 Increasing IPTG concentration

The three GST-tagged TD mutants ((CBox/ArrB), ArrestinBox and Full del) were initially expressed in a small scale of 20 ml total volume using different conditions, such as increasing final concentrations of IPTG or decreasing the temperature during expression. Initially, the mutants were expressed in varying IPTG concentrations (0.1 mM, 0.2 mM, 0.5 mM and 1 mM) with either a longer incubation time (20 hours) or shorter incubation time (16 hours) post-induction at the same temperature of 22^{o}C at 180 rpm. Soluble and insoluble fractions were taken prior to induction, at 2 hours post induction, 4 hours post-induction and after overnight harvesting of the cultures. These fractions were analysed by western blot using anti-GST antibody (*data not shown*) and showed an equally weak expression yield between all the mutants at the appropriate molecular weight, compared to the well-expressed WT GST-clathrin TD. Largely intense bands at lower molecular weight range (~ 26 kDa) were present which is likely to be the GST-tag, which demonstrates possible degradation of proteins in all the TD mutants. There was no obvious difference in expression between the different IPTG concentrations or between the 2 hour, 4 hour or harvested cells post-induction.

8.4.0 Decreasing the temperature

The following modification to increase the expression yield was to lower the temperature of the expression to provide enough time for stable expression. The temperatures used were 18 ^{o}C and 16 ^{o}C, in combination with two different IPTG final concentrations (0.2 mM and 1 mM), 0.2 % glucose (to potentially reduce leaky expression) added to the cultures and incubated for 20 hours post-induction. The harvested fractions were analysed by western blot and the results of ArrestinBox TD mutant are shown in Figure 8.4.0. The results were almost identical as with the previous section, with a weak

expression yielded of the mutants and no obvious difference in band intensity between the two temperatures. The intense lower band (e.g. GST-tag) was present in these expression trials as well, suggesting the degradation and unstable behaviour of all the TD mutants. There was no obvious difference of expression between the two different IPTG concentrations or between the 2 hour, 4 hour or harvested cells post-induction. These mutants were characterised using circular dichroism by Muenzner *et al.,* 2017, and the most stable mutants were used for this thesis. However, the difference between Muezner's constructs was the presence of a NEMO tag, whereas our constructs were designed with a GST-tag due to the SPR/IAC method. NEMO tags could have provided more stability to these mutants.

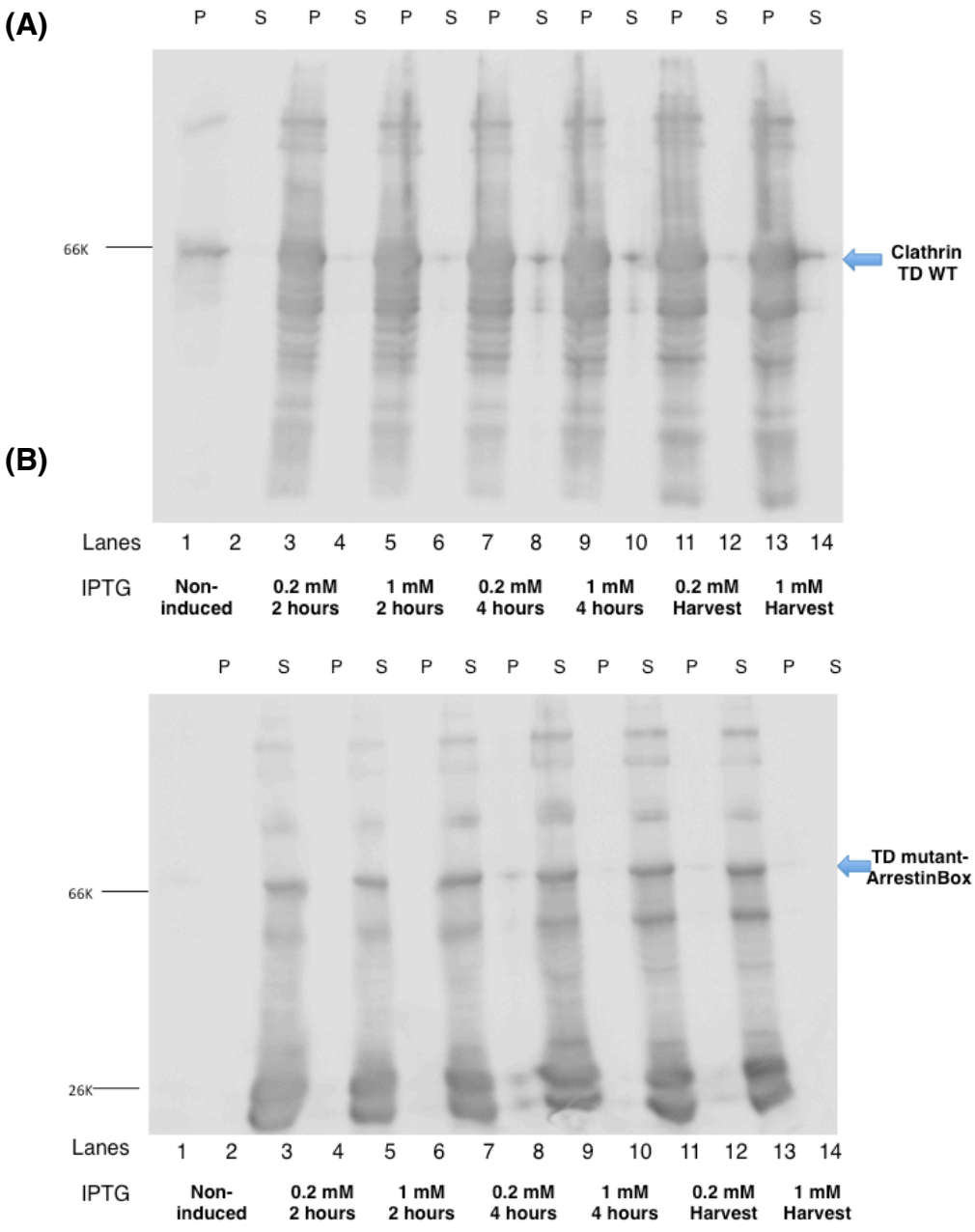
(A)
P S P S P S P S P S P S P S
66K
Clathrin
TD WT
(B)
Lanes 1 2 3 4 5 6 7 8 9 10 11 12 13 14
IPTG Non-induced 0.2 mM 2 hours 1 mM 2 hours 0.2 mM 4 hours 1 mM 4 hours 0.2 mM Harvest 1 mM Harvest
P S P S P S P S P S P S P S
66K
26K
TD mutant-ArrestinBox
Lanes 1 2 3 4 5 6 7 8 9 10 11 12 13 14
IPTG Non-induced 0.2 mM 2 hours 1 mM 2 hours 0.2 mM 4 hours 1 mM 4 hours 0.2 mM Harvest 1 mM Harvest

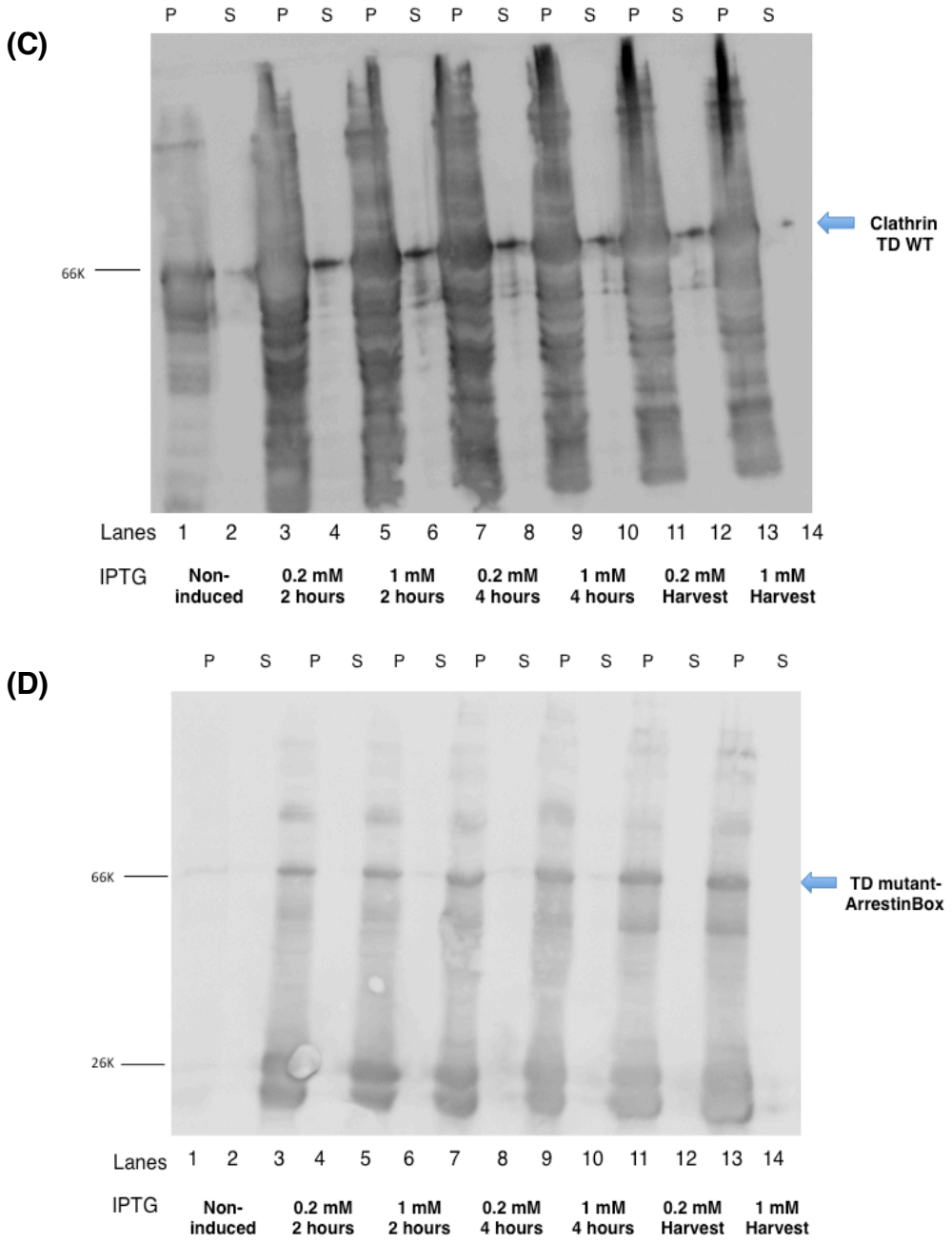

Figure 8.4.0 Western blot analysis of the soluble (S) and insoluble (P) sample from harvested pellets from small-scale expression of ArrestinBox clathrin TD mutant. *GST- clathrin TD WT is expressed in 0.2 mM and 1mM IPTG at 18°C (A) and 16 °C (C), and the harvested samples (soluble and insoluble) fractions demonstrate a good yield of the expressed protein at 66 kDa at 2 hours, 4 hours and after overnight harvest. These act as control experiments. The ArrestinBox TD mutant expressed in 0.2 mM and 1mM IPTG at 18°C (B) and 16°C (C) at 2 hours, 4 hours and overnight harvested cells. The results demonstrate weak expression of the TD mutant at 66 kDa and there is no difference in the expression yielded at the different IPTG concentrations or the two different temperatures. There is an intense band at around 26 kDa, which is suggested to be the GST-tag. This illustrates the unstable behaviour and degradation of the ArrestinBox TD mutant.*

8.5.0 Protein purification of clathrin N-terminal domain (TD) mutants

Despite the results from small-scale expression, I attempted to express the TD mutants in a large scale (4.8 liters) using final concentration of 1 mM IPTG, 0.2 % glucose at 16 ^{o}C for 18-20 hours incubation, 180 rpm. The harvested pellet from this expression was purified as per the WT GST clathrin TD construct, as described in Chapter 2. The affinity chromatography trace is not shown here but the SDS-PAGE analysis of the fractions eluted from the purification of the Full del TD mutant, are shown in Figure 8.5.0. However, purifications have been carried out using large scale expressed pellets from ArrestinBox TD mutant and well as CBox/ArrB TD mutant, which resulted in similar results as the Full del mutant once analysed by SDS-PAGE.

The concentrated sample in Figure 8.5.0, which should include the purified mutant, is not considered pure due to the presence of other unknown proteins (intense bands). A smearing effect is visible in the concentrated sample, which suggests degradation of the protein. A size exclusion chromatography step could have been used in the purification. In addition, mass spectrometry could have been used to determine the nature of those unknown bands. However, most importantly, further optimization is required to establish appropriate expression and purification conditions for these TD mutants, which was not explored in this thesis due to time restraints.

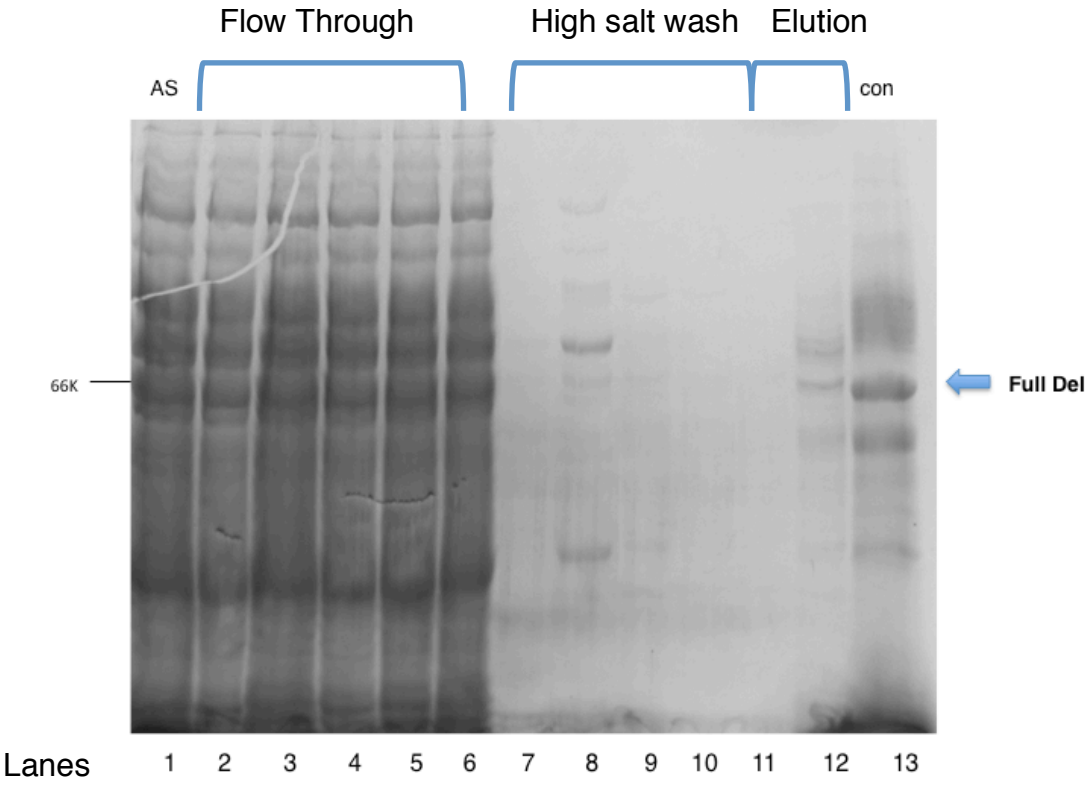

Figure 8.5.0 SDS-PAGE analysis of the fractions eluted at each stage of GST-affinity chromatography to confirm the purity of the Full del clathrin TD mutant. *The harvested expressed pellet from large scale (4.8 litres) by centrifugation and re-suspended in CB1 buffer before loaded on the GST-affinity column. The flow-through of the sample is shown in lanes 1-6 and the elution from a high salt wash (500mM NaCl) (lanes 7-10) does not elute the protein. The TD mutant elutes after the addition of GSH+CB1 Buffer (lanes 11-12) and concentrated down to ~ 1 ml. The concentrated fraction in lane 13, which demonstrate that the sample is not as pure as needed and the smearing effect observed could suggest degradation of the protein.*

Chapter 9: References

AHLE, S. & UNGEWICKELL, E. 1990. Auxilin, a newly identified clathrin-associated protein in coated vesicles from bovine brain. *Journal of Cell Biology,* 111**,** 19-29.

ANDERSON, D., HARRIS, R., POLAYES, D., CICCARONE, V., DONAHUE, R., GERARD, G. & JESSEE, J. 1996. Rapid Generation of Recombinant Baculoviruses and Expression of Foreign Genes Using the Bac-To-Bac® Baculovirus Expression System. 17**,** 53-58.

AVINOAM, O., SCHORB, M., BEESE, C. J., BRIGGS, J. A. G. & KAKSONEN, M. 2015. Endocytic sites mature by continuous bending and remodeling of the clathrin coat. *Science,* 348**,** 1369-1372.

BAKER, M. 2016. *The Assembly and Disassembly of Clathrin Cages.* Doctor of Philosophy, University of Warwick.

BARAK, L. S., OAKLEY, R. H., LAPORTE, S. A. & CARON, M. G. 2001. Constitutive arrestin-mediated desensitization of a human vasopressin receptor mutant associated with nephrogenic diabetes insipidus. *Proc Natl Acad Sci U S A,* 98**,** 93-8.

BEAUTRAIT, A., PARADIS, J. S., ZIMMERMAN, B., GIUBILARO, J., NIKOLAJEV, L., ARMANDO, S., KOBAYASHI, H., YAMANI, L., NAMKUNG, Y., HEYDENREICH, F. M., KHOURY, E., AUDET, M., ROUX, P. P., VEPRINTSEV, D. B., LAPORTE, S. A. & BOUVIER, M. 2017. A new inhibitor of the beta-arrestin/AP2 endocytic complex reveals interplay between GPCR internalization and signalling. *Nat Commun,* 8**,** 15054.

BIRNBAUMER, M. 2000. Vasopressin receptors. *Trends Endocrinol Metab.,* 11**,** 406-410.

BOCKING, T., AGUET, F., RAPOPORT, I., BANZHAF, M., YU, A., ZEEH, J. C. & KIRCHHAUSEN, T. 2014. Key interactions for clathrin coat stability. *Structure,* 22**,** 819-29.

BOECKING, T., AGUET, F., HARRISON, S. C. & KIRCHHAUSEN, T. 2011. Single-molecule analysis of a molecular disassemblase reveals the mechanism of Hsc70-driven clathrin uncoating. *Nature Structural & Molecular Biology,* 18**,** 295-301.

BOETTNER, D. R., FRIESEN, H., ANDREWS, B. & LEMMON, S. K. 2011. Clathrin light chain directs endocytosis by influencing the binding of the yeast Hip1R homologue, Sla2, to F-actin. . *Molecular Biology of the Cell,* 22**,** 3699- 3714.

BRADY, R. J., DAMER, C. K., HEUSER, J. E. & O'HALLORAN, T. J. 2010. Regulation of Hip1r by epsin controls the temporal and spatial coupling of actin filaments to clathrin-coated pits. *J Cell Sci,* 123**,** 3652-61.

BRETT, T. J., LEGENDRE-GUILLEMIN, V., MCPHERSON, P. S. & FREMONT, D. H. 2006. Structural definition of the F-actin-binding THATCH domain from HIP1R. *Nature Structural & Molecular Biology,* 13**,** 121-130.

BRETT, T. J., TRAUB, L. M. & FREMONT, D. H. 2002. Accessory protein recruitment motifs in clathrin-mediated endocytosis. *Structure,* 10**,** 797-809.

BRODSKY, F. M. 2012. Diversity of clathrin function: new tricks for an old protein. *Annu Rev Cell Dev Biol,* 28**,** 309-36.

BRODSKY, F. M., HILL, B. L., ACTON, S. L., NATHKE, I., WONG, D. H., PONNAMBALAM, S. & PARHAM, P. 1991. Clathrin light-chains - arrays of protein motifs that regulate coated-vesicle dynamics. *Trends in Biochemical Sciences,* 16**,** 208-213.

BUCHER, D., FREY, F., SOCHACKI, K. A., KUMMER, S., BERGEEST, J. P., GODINEZ, W. J., KRÄUSSLICH, H. G., ROHR, K., W.TARASKA, J., SCHWARZ, U. S. & BOULANT, S. 2017. Flat-to-curved transition during clathrin-mediated endocytosis correlates with a change in clathrin-adaptor ratio and is regulated by membrane tension. *bioRxiv*.

BURTEY, A., SCHMID, E. M., FORD, M. G., RAPPOPORT, J. Z., SCOTT, M. G., MARULLO, S., SIMON, S. M., MCMAHON, H. T. &

BENMERAH, A. 2007. The conserved isoleucine-valine-phenylalanine motif couples activation state and endocytic functions of beta-arrestins. *Traffic,* 8**,** 914-31.

BUSCH, D. J., HOUSER, J. R., HAYDEN, C. C., SHERMAN, M. B., LAFER, E. M. & STACHOWIAK, J. C. 2015. Intrinsically disordered proteins drive membrane curvature. *Nat Commun,* 6**,** 7875.

BUSS, F., LUZIO, J. P. & KENDRICK-JONES, J. 2001. Myosin VI, a new force in clathrin mediated endocytosis. *FEBS Lett,* 508**,** 295-9.

CAHILL, T. J., 3RD, THOMSEN, A. R., TARRASCH, J. T., PLOUFFE, B., NGUYEN, A. H., YANG, F., HUANG, L. Y., KAHSAI, A. W., BASSONI, D. L., GAVINO, B. J., LAMERDIN, J. E., TRIEST, S., SHUKLA, A. K., BERGER, B., LITTLE, J. T., ANTAR, A., BLANC, A., QU, C. X., CHEN, X., KAWAKAMI, K., INOUE, A., AOKI, J., STEYAERT, J., SUN, J. P., BOUVIER, M., SKINIOTIS, G. & LEFKOWITZ, R. J. 2017. Distinct conformations of GPCR-beta-arrestin complexes mediate desensitization, signaling, and endocytosis. *Proc Natl Acad Sci U S A,* 114**,** 2562-2567.

CHANDRASEKAR, I., GOECKELER, Z. M., TURNEY, S. G., WANG, P., WYSOLMERSKI, R. B., ADELSTEIN, R. S. & BRIDGMAN, P. C. 2014. Nonmuscle myosin II is a critical regulator of clathrin-mediated endocytosis. *Traffic,* 15**,** 418-32.

CHEN, C. Y. & BRODSKY, F. M. 2005. Huntingtin-interacting protein 1 (Hip1) and Hip1-related protein (Hip1R) bind the conserved sequence of clathrin light chains and thereby influence clathrin assembly in vitro and actin distribution in vivo. *J Biol Chem,* 280**,** 6109-17.

CHEN, C. Y., REESE, M. L., HWANG, P. K., OTA, N., AGARD, D. & BRODSKY, F. M. 2002. Clathrin light and heavy chain interface: alpha-helix binding superhelix loops via critical tryptophans. *Embo Journal,* 21**,** 6072-6082.

CHEN, H., FRE, S., SLEPNEV, V. I., CAPUA, M. R., TAKEI, K., BUTLER, M. H., DI FIORE, P. P. & DE CAMILLI, P. 1998. Epsin is an EH-domain-

binding protein implicated in clathrin-mediated endocytosis. *Nature,* 394**,** 793-797.

CLAIRMONT, K. B., BOLL, W., ERICSSON, M. & KIRCHHAUSEN, T. 1997. A role for the hinge/ear domain of the beta chains in the incorporation of AP complexes into clathrin-coated pits and coated vesicles. *Cellular and Molecular Life Sciences,* 53**,** 611-619.

CLARKE, N. I. & ROYLE, S. J. 2017. FerriTag: A Genetically-Encoded Inducible Tag for Correlative Light-Electron Microscopy. *bioRxiv*.

COCUCCI, E., AGUET, F., BOULANT, S. & KIRCHHAUSEN, T. 2012. The first five seconds in the life of a clathrin-coated pit. *Cell,* 150**,** 495-507.

COLLETTE, J. R., CHI, R. J., BOETTNER, D. R., FERNANDEZ-GOLBANO, I. M., PLEMEL, R., MERZ, A. J., GELI, M. I., TRAUB, L. M. & LEMMON, S. K. 2009. Clathrin Functions in the Absence of the Terminal Domain Binding Site for Adaptor-associated Clathrin-Box *Molecular Biology of the Cell,* 20**,** 3401–3413.

COLLINS, B. M., MCCOY, A. J., KENT, H. M., EVANS, P. R. & OWEN, D. J. 2002. Molecular architecture and functional model of the endocytic AP2 complex. *Cell,* 209**,** 523-535.

COOKE, R. M., BROWN, A. J., MARSHALL, F. H. & MASON, J. S. 2015. Structures of G protein-coupled receptors reveal new opportunities for drug discovery. *Drug Discov Today,* 20**,** 1355-64.

CORDELLA, N., LAMPO, T. J., MELOSH, N. & SPAKOWITZ, A. J. 2015. Membrane indentation triggers clathrin lattice reorganization and fluidization. *Soft Matter,* 11**,** 439-48.

DAFFORN, T. R. & SMITH, C. J. 2004. Natively unfolded domains in endocytosis: hooks, lines and linkers. *EMBO Rep,* 5**,** 1046-52.

DANNHAUSER , P. N., PLATEN, M., BOENING, H., UNGEWICKELL, H., SCHAAP, I. A. T. & UNGEWICKELL, E. J. 2015. Effect of Clathrin Light Chains on the Stiffness of Clathrin Lattices and Membrane Budding. *Traffic* 16**,** 519-533.

DANNHAUSER, P. N. & UNGEWICKELL, E. J. 2012. Reconstitution of clathrin-coated bud and vesicle formation with minimal components. *Nat Cell Biol,* 14**,** 634-9.

DE LUCA-FLAHERTY, C., MCKAY, D. B., PARHAM, P. & HILL, B. L. 1990. Uncoating protein (hsc70) binds a conformationally labile domain of clathrin light chain lca to stimulate atp hydrolysis. *Cell,* 62**,** 875-887.

DELL'ANGELICA, E. C., KLUMPERMAN, J., STOORVOGEL, W. & BONIFACINO, J. S. 1998. Association of the AP-3 Adaptor Complex with Clathrin. *Science,* 280**,** 431-434.

DELOM, F. & FESSART, D. 2011. Role of Phosphorylation in the Control of Clathrin-Mediated Internalization of GPCR. *Int J Cell Biol,* 2011**,** 246954.

DOHERTY, G. J. & MCMAHON, H. T. 2009. Mechanisms of Endocytosis. *Annual Review of Biochemistry,* 78**,** 857-902.

DONG, Y. Z., WU, H., RAHMAN, H. N. A., LIU, Y. J., PASULA, S., TESSNEER, K. L., CAI, X. F., LIU, X. L., CHANG, B. J., MCMANUS, J., HAHN, S., DONG, J. L., BROPHY, M. L., YU, L. L., SONG, K., SILASI-MANSAT, R., SAUNDERS, D., NJOKU, C., SONG, H., MEHTA-D'SOUZA, P., TOWNER, R., LUPU, F., MCEVER, R. P., XIA, L. J., BOERBOOM, D., SRINIVASAN, R. S. & CHEN, H. 2015. Motif mimetic of epsin perturbs tumor growth and metastasis. *Journal of Clinical Investigation,* 125**,** 4349-4364.

DORR, J. M., SCHEIDELAAR, S., KOORENGEVEL, M. C., DOMINGUEZ, J. J., SCHAFER, M., VAN WALREE, C. A. & KILLIAN, J. A. 2016. The styrene-maleic acid copolymer: a versatile tool in membrane research. *Eur Biophys J,* 45**,** 3-21.

DRAKE, M. T., DOWNS, M. A. & TRAUB, L. M. 2000. Epsin binds to clathrin by associating directly with the clathrin-terminal domain - Evidence for cooperative binding through two discrete sites. *Journal of Biological Chemistry,* 275**,** 6479-6489.

DRAKE, M. T. & TRAUB, L. M. 2001. Interaction of two structurally distinct sequence types with the clathrin terminal domain beta-propeller. *J Biol Chem,* 276**,** 28700-9.

DRUGMAND, J., SCHNEIDER, Y. & AGATHOS, S. 2012. Insect cells as factories for biomanufacturing. . *Biotechnology Advances,* 30**,** 1140-1157.

DUBENDORFF, J. W., LYMAR, E., FURUYA, F. R. & HAINFELD, J. F. 2010. Gold Labeling of Protein Fusion Tags for EM. *Microsc. Microanal,* 16.

EDELING, M. A., MISHRA, S. K., KEYEL, P. A., STEINHAUSER, A. L., COLLINS, B. M., ROTH, R., HEUSER, J. E., OWEN, D. J. & TRAUB, L. M. 2006a. Molecular switches involving the AP-2 beta2 appendage regulate endocytic cargo selection and clathrin coat assembly. *Dev Cell,* 10**,** 329-42.

EDELING, M. A., SMITH, C. & OWEN, D. N. R. 2006b. Life of a clathrin coat: insights from clathrin and AP structures. *Molecular Cell Biology,* 7**,** 32-44.

ENGQVIST-GOLDSTEIN, A. E., WARREN, R. A., KESSELS, M. M., KEEN, J. H., HEUSER, J. & DRUBIN, D. G. 2001. The actin-binding protein Hip1R associates with clathrin during early stages of endocytosis and promotes clathrin assembly in vitro. *J Cell Biol,* 154**,** 1209-23.

ERDELYI, L. S., MANN, W. A., MORRIS-ROSENDAHL, D. J., GROSS, U., NAGEL, M., VARNAI, P., BALLA, A. & HUNYADY, L. 2015. Mutation in the V2 vasopressin receptor gene, AVPR2, causes nephrogenic syndrome of inappropriate diuresis. *Kidney Int,* 88**,** 1070-8.

FERGUSON, F. 2001. Evolving concepts in G protein-coupled receptor endocytosis: the role in receptor desensitization and signaling. . *Pharmacol Rev.,* 53**,** 1-24.

FERREIRA, F., FOLEY, M., COOKE, A., CUNNINGHAM, M., SMITH, G., WOOLLEY, R., HENDERSON, G., KELLY, E., MUNDELL, S. & SMYTHE, E. 2012. Endocytosis of G protein-coupled receptors is regulated by clathrin light chain phosphorylation. *Curr Biol,* 22**,** 1361-70.

FISCHER, M. J. 2010. Amine coupling through EDC/NHS: a practical approach. *Methods Mol Biol,* 627**,** 55-73.

FORD, M. G. J., MILLS, I. G., PETER, B. J., VALLIS, Y., PRAEFCKE, G. J. K., EVANS, P. R. & MCMAHON, H. T. 2002. Curvature of clathrin-coated pits driven by epsin. *Nature,* 419**,** 361-366

FORD, M. G. J., PEARSE, B. M. F., HIGGINS, M. K., VALLIS, Y., OWEN, D. J., GIBSON, A., HOPKINS, C. R., EVANS, P. R. & MCMAHON, H. T. 2001. Simultaneous binding of PtdIns(4,5)P-2 and clathrin by AP180 in the nucleation of clathrin lattices on membranes. *Science,* 291**,** 1051-1055.

FORTIAN, A., DIONNE, L. K., HONG, S. H., KIM, W., GYGI, S. P., WATKINS, S. C. & SORKIN, A. 2015. Endocytosis of Ubiquitylation-Deficient EGFR Mutants via Clathrin-Coated Pits is Mediated by Ubiquitylation. *Traffic,* 16**,** 1137-1154.

FOTIN, A., CHENG, Y., SLIZ, P., GRIGORIEFF, N., HARRISON, S. C., KIRCHHAUSEN, T. & WALZ, T. 2004. Molecular model for a complete clathrin lattice from electron cryomicroscopy. *Nature,* 432**,** 573-9.

FUJIMOTO, L. M., ROTH, R., HEUSER, J. E. & SCHMID, S. L. 2000. Actin assembly plays a variable, but not obligatory role in receptor-mediated endocytosis in mammalian cells. *Traffic,* 1**,** 161-171.

FUTATSUMORI-SUGAI, M. & TSUMOTO, K. 2010. Signal peptide design for improving recombinant protein secretion in the baculovirus expression vector system. *Biochem Biophys Res Commun,* 391**,** 931-5.

GHOSH, E., KUMARI, P., JAIMAN, D. & SHUKLA, A. K. 2015. Methodological advances: the unsung heroes of the GPCR structural revolution. *Nat Rev Mol Cell Biol,* 16**,** 69-81.

GIRARD, M., ALLAIRE, P. D., MCPHERSON, P. S. & BLONDEAU, F. 2005. Non-stoichiometric relationship between clathrin heavy and light chains revealed by quantitative comparative proteomics of clathrin-coated vesicles from brain and liver. *Mol Cell Proteomics,* 4**,** 1145-54.

GODLEE, C. & KAKSONEN, M. 2013. From uncertain beginnings: Initiation mechanisms of clathrin-mediated endocytosis. *The Journal of Cell Biology,* 203**,** 717-725.

GOH, A. X., BERTIN-MAGHIT, S., PING YEO, S., HO, A. W., DERKS, H., MORTELLARO, A. & WANG, C. I. 2014. A novel human anti-interleukin-1beta neutralizing monoclonal antibody showing in vivo efficacy. *MAbs,* 6**,** 765-73.

GOLDSTEIN, J. L., BROWN, M. S., ANDERSON, R. G. W., RUSSELL, D. W. & SCHNEIDER, W. J. 1985. Receptor-mediated endocytosis - concepts emerging from the ldl receptor system. *Annual Review of Cell Biology,* 1**,** 1-39.

GOODMAN, O., KRUPNICK, J., GUREVICH, V., BENOVIC, J. & KEEN, J. 1997. Arrestin/Clathrin Interaction. *Journal of Biological Chemistry,* 272**,** 15017-15022.

GOTTFRIED, I., EHRLICH, M. & ASHERY, U. 2010. The Sla2p/HIP1/HIP1R family: similar structure, similar function in endocytosis? *Biochem Soc Trans,* 38**,** 187-91.

GREENER, B., LIU, S. H., WILDE, A. & BRODSKY, F. M. 2000. Complete reconstitution of clathrin basket formation with recombinant protein fragments: Adaptor control of clathrin self-assembly. *Traffic,* 1**,** 69-75.

GUIDUCCI, C. 2011. *Surface Plasmon Resonance Based Systems* [Online]. Available: http://lben.epfl.ch/files/content/sites/lben/files/users/179705/Surface Plasmon Resonance Handout.pdf

GUREVICH, V. 2014. *Arrestins - Pharmacology and therapeutic potential,* USA, Springer.

HALEBIAN, M., MORRIS, K. & SMITH, C. 2017. Structure and Assembly of Clathrin Cages. *In:* HARRIS, R. & WRIGHT, J. (eds.) *Subcellular Biochemistry.* Switzerland: Springer.

HAMDAN, F. F., ROCHDI, M. D., BRETON, B., FESSART, D., MICHAUD, D. E., CHAREST, P. G., LAPORTE, S. A. & BOUVIER, M. 2007. Unraveling G protein-coupled receptor endocytosis pathways using

real-time monitoring of agonist-promoted interaction between beta-arrestins and AP-2. *J Biol Chem,* 282**,** 29089-100.

HAN, M., GUREVICH, V., VISHNIVETSKIY, S., SIGLER, P. & SCHUBERT, C. 2001. Crystal Structure of β-Arrestin at 1.9 Å: Possible Mechanism of Receptor Binding and Membrane Translocation. . *Structure,* 9**,** 869-880.

HANNAN, L., NEWMYER, S. & SL, S. 1998. ATP- and cytosol-dependent release of adaptor proteins from clathrin-coated vesicles: a dual role for hsc70. . *Mol Biol Cell 1998,* 9**,** 2217-2229.

HAWRYLUK, M. J., KEYEL, P. A., MISHRA, S. K., WATKINS, S. C., HEUSER, J. E. & TRAUB, L. M. 2006. Epsin 1 is a polyubiquitin-selective clathrin-associated sorting protein. *Traffic,* 7**,** 262-81.

HENNE, W. M., BOUCROT, E., MEINECKE, M., EVERGREN, E., VALLIS, Y., MITTAL, R. & MCMAHON, H. T. 2010. FCHo Proteins Are Nucleators of Clathrin-Mediated Endocytosis. *Science,* 328**,** 1281-1284.

HIRST, J., MILLER, S. E., TAYLOR, M. J., VON MOLLARD, G. F. & ROBINSON, M. S. 2004. EpsinR is an adaptor for the SNARE protein Vti1b. *Molecular Biology of the Cell,* 15**,** 5593-5602.

HOLKAR, S. S., KAMERKAR, S. C. & PUCADYIL, T. J. 2015. Spatial Control of Epsin-induced Clathrin Assembly by Membrane Curvature. *J Biol Chem,* 290**,** 14267-76.

HOLLOPETER, G., LANGE, J. J., ZHANG, Y., VU, T. N., GU, M. Y., AILION, M., LAMBIE, E. J., SLAUGHTER, B. D., UNRUH, J. R., FLORENS, L. & JORGENSEN, E. M. 2014. The Membrane-Associated Proteins FCHo and SGIP Are Allosteric Activators of the AP2 Clathrin Adaptor Complex. *Elife,* 3**,** 65.

HOLSTEIN, S. E. H., UNGEWICKELL, H. & UNGEWICKELL, E. 1996. Mechanism of clathrin basket dissociation: Separate functions of protein domains of the DnaJ homologue auxilin. *Journal of Cell Biology,* 135**,** 925- 937.

HOM, R. A., VORA, M., REGNER, M., SUBACH, O. M., CHO, W., VERKHUSHA, V. V., STAHELIN, R. V. & KUTATELADZE, T. G. 2007. pH-dependent binding of the Epsin ENTH domain and the AP180 ANTH domain to PI(4,5)P2-containing bilayers. *J Mol Biol,* 373**,** 412-23.

HUANG, R., ZHU, G., JING ZHANG, YUXIONG LAI, YU XU, HE, J. & XIE, J. 2017. Betanodavirus-like particles enter host cells via clathrin-mediated endocytosis in a cholesterol-, pH- and cytoskeleton-dependent manner. *Veterinary Research,* 48.

HYUN, T. S., RAO, D. S., SAINT-DIC, D., MICHAEL, L. E., KUMAR, P. D., BRADLEY, S. V., MIZUKAMI, I. F., ORAVECZ-WILSON, K. I. & ROSS, T. S. 2004. HIP1 and HIP1r stabilize receptor tyrosine kinases and bind 3- phosphoinositides via epsin N-terminal homology domains. *Journal of Biological Chemistry,* 279**,** 14294-14306.

JACKSON, L. P., KELLY, B. T., MCCOY, A. J., GAFFRY, T., JAMES, L. C., COLLINS, B. M., HOENING, S., EVANS, P. R. & OWEN, D. J. 2010. A Large-Scale Conformational Change Couples Membrane Recruitment to Cargo Binding in the AP2 Clathrin Adaptor Complex. *Cell,* 141**,** 1220-1229.

JAKOBSSON, J., GAD, H., ANDERSSON, F., LOW, P., SHUPLIAKOV, O. & BRODIN, L. 2008. Role of epsin 1 in synaptic vesicle endocytosis. *Proc Natl Acad Sci U S A,* 105**,** 6445-50.

JAMSHAD, M., CHARLTON, J., LIN, Y. P., ROUTLEDGE, S. J., BAWA, Z., KNOWLES, T. J., OVERDUIN, M., DEKKER, N., DAFFORN, T. R., BILL, R. M., POYNER, D. R. & WHEATLEY, M. 2015. G-protein coupled receptor solubilization and purification for biophysical analysis and functional studies, in the total absence of detergent. *Biosci Rep,* 35.

JAMSHAD, M., LIN, Y. P., KNOWLES, T. J., PARSLOW, R. A., HARRIS, C., WHEATLEY, M., POYNER, D. R., BILL, R. M., THOMAS, O. R., OVERDUIN, M. & DAFFORN, T. R. 2011. Surfactant-free purification

of membrane proteins with intact native membrane environment. *Biochem Soc Trans,* 39**,** 813-8.

KALTHOFF, C., ALVES, J., URBANKE, C., KNORR, R. & UNGEWICKELL, E. J. 2002. Unusual structural organization of the endocytic proteins AP180 and epsin 1. *J Biol Chem,* 277**,** 8209-16.

KANG, D. S., KERN, R. C., PUTHENVEEDU, M. A., VON ZASTROW, M., WILLIAMS, J. C. & BENOVIC, J. L. 2009. Structure of an arrestin2-clathrin complex reveals a novel clathrin binding domain that modulates receptor trafficking. *J Biol Chem,* 284**,** 29860-72.

KANG, Y., ZHOU, X. E., GAO, X., HE, Y., LIU, W., ISHCHENKO, A., BARTY, A., WHITE, T. A., YEFANOV, O., HAN, G. W., XU, Q., DE WAAL, P. W., KE, J., TAN, M. H. E., ZHANG, C., MOELLER, A., WEST, G. M., PASCAL, B. D., VAN EPS, N., CARO, L. N., VISHNIVETSKIY, S. A., LEE, R. J., SUINO-POWELL, K. M., GU, X., PAL, K., MA, J., ZHI, X., BOUTET, S., WILLIAMS, G. J., MESSERSCHMIDT, M., GATI, C., ZATSEPIN, N. A., WANG, D., JAMES, D., BASU, S., ROY-CHOWDHURY, S., CONRAD, C. E., COE, J., LIU, H., LISOVA, S., KUPITZ, C., GROTJOHANN, I., FROMME, R., JIANG, Y., TAN, M., YANG, H., LI, J., WANG, M., ZHENG, Z., LI, D., HOWE, N., ZHAO, Y., STANDFUSS, J., DIEDERICHS, K., DONG, Y., POTTER, C. S., CARRAGHER, B., CAFFREY, M., JIANG, H., CHAPMAN, H. N., SPENCE, J. C. H., FROMME, P., WEIERSTALL, U., ERNST, O. P., KATRITCH, V., GUREVICH, V. V., GRIFFIN, P. R., HUBBELL, W. L., STEVENS, R. C., CHEREZOV, V., MELCHER, K. & XU, H. E. 2015. Crystal structure of rhodopsin bound to arrestin by femtosecond X-ray laser. *Nature* 523**,** 561-567.

KARIYA, K., KOYAMA, S., NAKASHIMA, S., OSHIRO, T., MORINAKA, K. & KIKUCHI, A. 2000. Regulation of complex formation of POB1/epsin/adaptor protein complex 2 by mitotic phosphorylation. *Journal of Biological Chemistry,* 275**,** 18399-18406.

KARLSSON, R. 1994. Real-Time Competitive Kinetic Analysis of Interactions between Low-Molecular-Weight-ligands in Solution and Surface-Immobilized Receptors. *Analytical Biochemistry,* 221.

KARLSSON, R. 2004. SPR for molecular interaction analysis: a review of emerging application areas. *J Mol Recognit.,* 17**,** 151-61.

KARLSSON, R., JENDEIERG, L., NILSSON, B., NILSSON, J. & NYGREN, P.-A. 1995. Direct and competitive kinetic analysis of the interaction between human IgGl and a one domain analogue of protein A. *Journal of Immunological Methods* 183**,** 43-49.

KARLSSON, R., KATSAMBA, P. S., NORDIN, H., POL, E. & MYSZKA, D. G. 2006. Analyzing a kinetic titration series using affinity biosensors. *Anal Biochem,* 349**,** 136-47.

KARNIK, R., LUDLOW, M. J., ABUARAB, N., SMITH, A. J., HARDY, M. E. L., ELLIOTT, D. J. S. & SIVAPRASADARAO, A. 2013. Endocytosis of hERG Is Clathrin-Independent and Involves Arf6. *PLoS ONE* 8.

KAVRAN, J. M. & LEAHY, D. J. 2014. Lysis of mammalian and Sf9 cells. *Methods Enzymol,* 536**,** 47-52.

KELLY, B. T., GRAHAM, S. C., LISKA, N., DANNHAUSER, P. N., HONING, S., UNGEWICKELL, E. J. & OWEN, D. J. 2014. Clathrin adaptors. AP2 controls clathrin polymerization with a membrane-activated switch. *Science,* 345**,** 459-63.

KELLY, B. T., MCCOY, A. J., SPAETE, K., MILLER, S. E., EVANS, P. R., HOENING, S. & OWEN, D. J. 2008. A structural explanation for the binding of endocytic dileucine motifs by the AP2 complex. *Nature,* 456**,** 976-981.

KEYEL, P., THIEMAN, J., ROTH, R., ERKAN, E., EVERETT, E., WATKINS, S., HEUSER, J. & TRAUB, L. 2008. The AP-2 adaptor beta2 appendage scaffolds alternate cargo endocytosis. *Molecular Biology of the Cell,* 19**,** 5309–5326.

KIM, Y. M. & BENOVIC, J. L. 2002. Differential roles of arrestin-2 interaction with clathrin and adaptor protein 2 in G protein-coupled receptor trafficking. *J Biol Chem,* 277**,** 30760-8.

KIRCHHAUSEN, T., OWEN, D. & HARRISON, S. C. 2014. Molecular structure, function, and dynamics of clathrin-mediated membrane traffic. *Cold Spring Harb Perspect Biol,* 6**,** a016725.

KNUEHL, C., CHEN, C. Y., MANALO, V., HWANG, P. K., OTA, N. & BRODSKY, F. M. 2006. Novel binding sites on clathrin and adaptors regulate distinct aspects of coat assembly. *Traffic,* 7**,** 1688-700.

KOPPEN, C. J. V. & JAKOBS, K. H. 2004. Arrestin-Independent Internalization of G Protein-Coupled Receptors. *Mol Pharmacol* 66**,** 365–367.

KOVTUN, O., TILLU, V. A., ARIOTTI, N., PARTON, R. G. & COLLINS, B. M. 2015. Cavin family proteins and the assembly of caveolae. *J Cell Sci.,* 7**,** 1269-78.

KUMARI, P., SRIVASTAVA, A., BANERJEE, R., GHOSH, E., GUPTA, P., RANJAN, R., CHEN, X., GUPTA, B., GUPTA, C., JAIMAN, D. & SHUKLA, A. K. 2016. Functional competence of a partially engaged GPCR–β-arrestin complex. *Nature Communications,* 7**,** 13416.

LADDS, G., GODDARD, A. & DAVEY, J. 2005. Functional analysis of heterologous GPCR signalling pathways in yeast. . *Trends in biotechnology,* 23**,** 367--373.

LAI, C. L., JAO, C. C., LYMAN, E., GALLOP, J. L., PETER, B. J., MCMAHON, H. T., LANGEN, R. & VOTH, G. A. 2012. Membrane Binding and Self- Association of the Epsin N-Terminal Homology Domain. *Journal of Molecular Biology,* 423**,** 800-817.

LANG, B. D., DELMAR, M. & COOMBS, W. 2005. Surface Plasmon Resonance as a Method to Study the Kinetics and Amplitude of Protein- Protein Binding. *In:* DHEIN, S., MOHR, F. W. & DELMAR, M. (eds.) *Practical Methods in Cardiovascular Research.* Berlin, Heidelberg: Springer Berlin Heidelberg.

LAPORTE, S. A., MILLER, W. E., KIM, K. M. & CARON, M. G. 2002. beta-Arrestin/AP-2 interaction in G protein-coupled receptor internalization: identification of a beta-arrestin binging site in beta 2-adaptin. *J Biol Chem,* 277**,** 9247-54.

LAPORTE, S. A., OAKLEY, R. H., HOLT, J. A., BARAK, L. S. & CARON, M. G. 2000. The interaction of beta-arrestin with the AP-2 adaptor is required for the clustering of beta 2-adrenergic receptor into clathrin-coated pits. *J Biol Chem,* 275**,** 23120-6.

LE CLAINCHE, C., PAULY, B. S., ZHANG, C. X., ENGQVIST-GOLDSTEIN, A. E. Y., CUNNINGHAM, K. & DRUBIN, D. G. 2007. A Hip1R-cortactin complex negatively regulates actin assembly associated with endocytosis. *Embo Journal,* 26**,** 1199-1210.

LEE, S. C., KNOWLES, T. J., POSTIS, V. L., JAMSHAD, M., PARSLOW, R. A., LIN, Y. P., GOLDMAN, A., SRIDHAR, P., OVERDUIN, M., MUENCH, S. P. & DAFFORN, T. R. 2016. A method for detergent-free isolation of membrane proteins in their local lipid environment. *Nat Protoc,* 11**,** 1149-62.

LEFKOWITZ, R., RAJAGOPAL, K. & WHALEN, E. 2006. New Roles for β-Arrestins in Cell Signaling: Not Just for Seven-Transmembrane Receptors. *Molecular Cell Biology,* 24**,** 643-652.

LEGENDRE-GUILLEMIN, V., METZLER, M., CHARBONNEAU, M., GAN, L., CHOPRA, V., PHILIE, J., HAYDEN, M. R. & MCPHERSON, P. S. 2002. HIP1 and HIP12 display differential binding to F-actin, AP2, and clathrin. Identification of a novel interaction with clathrin light chain. *J Biol Chem,* 277**,** 19897-904.

LEGENDRE-GUILLEMIN, V., WASIAK, S., HUSSAIN, N. K., ANGERS, A. & MCPHERSON, P. S. 2004. ENTH/ANTH proteins and clathrin-mediated membrane budding. *J Cell Sci,* 117**,** 9-18.

LEMMON, S. K. & TRAUB, L. M. 2012. Getting in touch with the clathrin terminal domain. *Traffic,* 13**,** 511-9.

LINDNER, R. & UNGEWICKELL, E. 1992. Clathrin-associated proteins of bovine brain coated vesicles. An analysis of their number and assembly-promoting activity. *J Biol Chem,* 15**,** 16567-73.

LIU, S., XIONG, X., ZHAO, X., YANG, X. & WANG, H. 2015. F-BAR family proteins, emerging regulators for cell membrane dynamic changes-from structure to human diseases. *J Hematol Oncol,* 8**,** 47.

LIU, S. H., WONG, M. L., CRAIK, C. S. & BRODSKY, F. M. 1995. Regulation of clathrin assembly and trimerization defined using recombinant triskelion hubs. *Cell,* 83**,** 257-267.

LOERKE, D., METTLEN, M., YARAR, D., JAQAMAN, K., JAQAMAN, H., DANUSER, G. & SCHMID, S. L. 2009. Cargo and Dynamin Regulate Clathrin-Coated Pit Maturation. *Plos Biology,* 7**,** 628-639.

MA, L., UMASANKAR, P. K., WROBEL, A. G., LYMAR, A., MCCOY, A. J., HOLKAR, S. S., JHA, A., PRADHAN-SUNDD, T., WATKINS, S. C., OWEN, D. J. & TRAUB, L. M. 2016. Transient Fcho1/2.Eps15/R.AP-2 Nanoclusters Prime the AP-2 Clathrin Adaptor for Cargo Binding. *Developmental Cell,* 37**,** 428-443.

MASSOL, R. H., BOLL, W., GRIFFIN, A. M. & KIRCHHAUSEN, T. 2006. A burst of auxilin recruitment determines the onset of clathrin-coated vesicle uncoating. *Proc Natl Acad Sci U S A,* 103**,** 10265-70.

MASSOTTE, D. 2003. G protein-coupled receptor overexpression with the baculovirus–insect cell system: a tool for structural and functional studies. *Biochimica et Biophysica Acta (BBA) - Biomembranes,* 1610**,** 77-89.

MATTHEYSES, A. L., ATKINSON, C. E. & SIMON, S. M. 2011. Imaging Single Endocytic Events Reveals Diversity in Clathrin, Dynamin and Vesicle Dynamics. *Traffic,* 12**,** 1394-1406.

MAYOR, S., PARTON, R. G. & DONALDSON, J. G. 2014. Clathrin-Independent Pathways of Endocytosis. *Cold Spring Harbor Perspectives in Biology,* 6.

MCMAHON, H. T. & BOUCROT, E. 2011. Molecular mechanism and physiological functions of clathrin-mediated endocytosis. *Nat Rev Mol Cell Biol,* 12**,** 517-33.

MELLMAN, I. & YOSEF, Y. 2013. Endocytosis and Cancer. *Cold Spring Harb Perspect Biol*

MERRIFIELD, C. J. & KAKSONEN, M. 2014. Endocytic accessory factors and regulation of clathrin-mediated endocytosis. *Cold Spring Harb Perspect Biol,* 6**,** a016733.

MESSA, M., FERNANDEZ-BUSNADIEGO, R., SUN, E. W., CHEN, H., CZAPLA, H., WRASMAN, K., WU, Y., KO, G., ROSS, T., WENDLAND, B. & DE CAMILLI, P. 2014. Epsin deficiency impairs endocytosis by stalling the actin-dependent invagination of endocytic clathrin-coated pits. *Elife,* 3**,** e03311.

METTLEN, M., LOERKE, D., YARAR, D., DANUSER, G. & SCHMID, S. L. 2010. Cargo- and adaptor-specific mechanisms regulate clathrin-mediated endocytosis. *J Cell Biol,* 188**,** 919-33.

METTLEN, M., STOEBER, M., LOERKE, D., ANTONESCU, C. N., DANUSER, G. & SCHMID, S. L. 2009. Endocytic Accessory Proteins Are Functionally Distinguished by Their Differential Effects on the Maturation of Clathrin- coated Pits. *Molecular Biology of the Cell,* 20**,** 3251-3260.

MIELE, A. E., WATSON, P. J., EVANS, P. R., TRAUB, L. M. & OWEN, D. J. 2004. Two distinct interaction motifs in amphiphysin bind two independent sites on the clathrin terminal domain beta-propeller. *Nat Struct Mol Biol,* 11**,** 242-8.

MILANO, S. K., PACE, H., KIM, Y., BRENNER, C. & BENOVIC, J. 2002. Scaffolding Functions of Arrestin-2 Revealed by Crystal Structure and Mutagenesis. *Biochemistry,* 41**,** 3321-3328

MILIC, D. & VEPRINTSEV, D. B. 2015. Large-scale production and protein engineering of G protein-coupled receptors for structural studies. *Front Pharmacol,* 6**,** 66.

MILLER, S. E., SAHLENDER, D. A., GRAHAM, S. C., HONING, S., ROBINSON, M. S., PEDEN, A. A. & OWEN, D. J. 2011. The molecular basis for the endocytosis of small R-SNAREs by the clathrin adaptor CALM. *Cell,* 147**,** 1118-31.

MILOSEVIC, I., GIOVEDI, S., LOU, X. L., RAIMONDI, A., COLLESI, C., SHEN, H. Y., PARADISE, S., O'TOOLE, E., FERGUSON, S., CREMONA, O. & DE CAMILLI, P. 2011. Recruitment of Endophilin to Clathrin-Coated Pit Necks Is Required for Efficient Vesicle Uncoating after Fission. *Neuron,* 72**,** 587- 601.

MISHRA, M., HUANG, J. & BALASUBRAMANIAN, M. K. 2014. The yeast actin cytoskeleton. *FEMS Microbiol Rev,* 38**,** 213-27.

MISHRA, S. K., AGOSTINELLI, N. R., BRETT, T. J., MIZUKAMI, I., ROSS, T. S. & TRAUB, L. M. 2001. Clathrin- and AP-2-binding sites in HIP1 uncover a general assembly role for endocytic accessory proteins. *J Biol Chem,* 276**,** 46230-6.

MOLLAY, C., VILAS, U. & KREIL, G. 1982. Cleavage of honeybee prepromelittin by an endoprotease from rat liver microsomes: identification of intact signal peptide. *Proc Natl Acad Sci U S A,* 79**,** 2260-2263.

MORELOCK, M. M., INGRAHAM, R. H., BETAGERI, R. & JAKESS, S. 1995. Determination of Receptor-Ligand Kinetic and Equilibrium Binding Constants using Surface Plasmon Resonance: Application to the Zck SH2Domain and Phosphotyrosyl Peptides. *J. Med. Chem. ,* 38**,** 1309-1318.

MORGAN, J. R., ZHAO, X., WOMACK, M., PRASAD, K., AUGUSTINE, G. J. & LAFER, E. M. 1999. A Role for the Clathrin Assembly Domain of AP180 in Synaptic Vesicle Endocytosis. *Journal of Neuroscience* 19**,** 10201-10212.

MORPHEW, M. K., O'TOOLE, E. T., PAGE, C. L., PAGRATIS, M., MEEHL, J., GIDDINGS, T., GARDNER, J. M., ACKERSON, C., JASPERSEN, S. L., WINEY, M., HOENGER, A. & MCINTOSH, J. R. 2015. Metallothionein as a clonable tag for protein localization by electron microscopy of cells. *J Microsc,* 260**,** 20-9.

MUENZNER, J., TRAUB, L. M., KELLY, B. T. & GRAHAM, S. C. 2017. Cellular and viral peptides bind multiple sites on the N-terminal domain of clathrin. *Traffic,* 18**,** 44-57.

NEUMANN, S. & SCHMID, S. L. 2013. Dual Role of BAR Domain-containing Proteins in Regulating Vesicle Release Catalyzed by the GTPase, Dynamin-2. *Journal of Biological Chemistry,* 288**,** 25119-25128.

NIU, Q. & YBE, J. A. 2008. Crystal structure at 2.8 A of Huntingtin-interacting protein 1 (HIP1) coiled-coil domain reveals a charged surface suitable for HIP1 protein interactor (HIPPI). *J Mol Biol,* 375**,** 1197-205.

NOBLES, K. N., GUAN, Z., XIAO, K., OAS, T. G. & LEFKOWITZ, R. J. 2007. The active conformation of beta-arrestin1: direct evidence for the phosphate sensor in the N-domain and conformational differences in the active states of beta-arrestins1 and -2. *J Biol Chem,* 282**,** 21370-81.

NUBER, S., ZABEL, U., LORENZ, K., NUBER, A., MILLIGAN, G., TOBIN, A. B., LOHSE, M. J. & HOFFMANN, C. 2016. beta-Arrestin biosensors reveal a rapid, receptor-dependent activation/deactivation cycle. *Nature,* 531**,** 661-4.

OLUSANYA, O., ANDREWS, P. D., SWEDLOW, J. R. & SMYTHE, E. 2001. Phosphorylation of threonine 156 of the mu 2 subunit of the AP2 complex is essential for endocytosis in vitro and in vivo. *Current Biology,* 11**,** 896-900.

OWEN, D. J. & EVANS, P. R. 1998. A structural explanation for the recognition of tyrosine-based endocytotic signals. *Science,* 282**,** 1327-1332.

OWEN, D. J., VALLIS, Y., PEARSE, B. M. F., MCMAHON, H. T. & EVANS, P. R. 2000. The structure and function of the beta 2-adaptin appendage domain. *The EMBO Journal,* 19**,** 4216-4227.

PACZKOWSKI, J. E., RICHARDSON, B. C. & FROMME, J. C. 2015. Cargo adaptors: structures illuminate mechanisms regulating vesicle biogenesis. *Trends Cell Biol,* 25**,** 408-16.

PARTON, R. G. & DEL POZO, M. A. 2013. Caveolae as plasma membrane sensors, protectors and organizers. *Nature Reviews Molecular Cell Biology,* 14**,** 98-112.

PEARSE, B. M. 1975. Coated vesicles from pig brain: purification and biochemical characterization. *J Mol Biol,* 97**,** 93-98.

PETTERSEN, E. F., GODDARD, T., HUANG, C., COUCH, G., GREENBLATT, D., MENG, E. & FERRIN, T. 2004. CSF Chimera – a

visualization system for exploratory research and analysis. *U J Comput Chem,* 25**,** 1605–1612.

PICCO, A., KUKULSKI, W., MANENSCHIJN, H. E., SPECHT, T., BRIGGS, J. A. G. & KAKSONEN, M. 2017. The contributions of the actin machinery to endocytic membrane bending and vesicle formation. *bioRxiv.*

PICHVAEE, B., COSTAGUTA, G., YEUNG BG, RYAZANTSEV S, GREENER T, GREENE L, EISENBERG E, MCCAFFERY JM & GS, P. 2000. A yeast DNA J protein required for clathrin-coated vesicle uncoating in vivo. *Nat Cell Biol,* 2**,** 958-963.

PIZARRO-CERDA, I., J., , BONAZZI, M. & COSSART, P. 2010. Clathrin-mediated endocytosis: What works for small, also works for big.32**,** 496- 504.

POPOVA, N.V., DEYER, I.E., PETRENKO, A.G. 2013. Clathrin-Mediated Endocytosis and Adaptor Proteins. *ACTA NATURE*, 5, 62-73

POSTIS, V., RAWSON, S., MITCHELL, J. K., LEE, S. C., PARSLOW, R. A., DAFFORN, T. R., BALDWIN, S. A. & MUENCH, S. P. 2015. The use of SMALPs as a novel membrane protein scaffold for structure study by negative stain electron microscopy. *Biochim Biophys Acta,* 1848**,** 496-501.

PRAEFCKE, G. J. K., FORD, M. G. J., SCHMID, E. M., OLESEN, L. E., GALLOP, J. L., PEAK-CHEW, S. Y., VALLIS, Y., BABU, M. M., MILLS, I. G. & MCMAHON, H. T. 2004. Evolving nature of the AP2 alpha-appendage hub during clathrin-coated vesicle endocytosis. *The EMBO Journal,* 23**,** 4371-4383.

RAHMEH, R., DAMIAN, M., COTTET, M., ORCEL, H., MENDRE, C., DURROUX, T., SHARMA, K., DURAND, G., PUCCI, B., TRINQUET, E., ZWIER, J., DEUPI, X., BRON, P., BANÈRES , J., MOUILLAC, B. & GRANIER, S. 2012. Structural insights into biased G protein-coupled receptor signaling revealed by fluorescence spectroscopy. *PNAS,* 109**,** 6733–6738.

RANJAN, R., DWIVEDI, H., BAIDYA, M., KUMAR, M. & SHUKLA, A. K. 2017. Novel Structural Insights into GPCR-beta-Arrestin Interaction and Signaling. *Trends Cell Biol*, 30087-9.

RAPOPORT, I., BOLL, W., YU, A., BOCKING, T. & KIRCHHAUSEN, T. 2008. A motif in the clathrin heavy chain required for the Hsc70/auxilin uncoating reaction. *Molecular Biology of the Cell,* 19, 405-413.

RAPPOPORT, J. Z., KEMAL, S., BENMERAH, A. & SIMON, S. M. 2006. Dynamics of clathrin and adaptor proteins during endocytosis. *Am J Physiol Cell Physiol,* 291, 1072-81.

REITER, E., AYOUB, M. A., PELLISSIER, L. P., LANDOMIEL, F., MUSNIER, A., TREFIER, A., GANDIA, J., DE PASCALI, F., TAHIR, S., YVINEC, R., BRUNEAU, G., POUPON, A. & CREPIEUX, P. 2017. beta-arrestin signalling and bias in hormone-responsive GPCRs. *Mol Cell Endocrinol,* 449, 28-41.

REN, X. R., REITER, E., AHN, S., KIM, J., CHEN, W. & LEFKOWITZ, R. J. 2005. Different G protein-coupled receptor kinases govern G protein and beta-arrestin-mediated signaling of V2 vasopressin receptor. *Proc Natl Acad Sci U S A,* 102, 1448-53.

RICOTTA, D., CONNER, S. D., SCHMID, S. L., VON FIGURA, K. & HONING, S. 2002. Phosphorylation of the AP2 mu subunit by AAK1 mediates high affinity binding to membrane protein sorting signals. *Journal of Cell Biology,* 156, 791-795.

ROSENTHAL, J. A., CHEN, H., SLEPNEV, V. I., PELLEGRINI, L., SALCINI, A. E., DI FIORE, P. P. & DE CAMILLI, P. 1999. The epsins define a family of proteins that interact with components of the clathrin coat and contain a new protein module. *Journal of Biological Chemistry,* 274, 33959-33965.

ROTHNIE, A., CLARKE, A., KUZMIC, P., CAMERON, A. & SMITH, C. 2011. A sequential mechanism for clathrin cage disassembly by 70-kDa heat-shock cognate protein (Hsc70) and auxilin. *Proceedings of the National Academy of Sciences,* 108, 6927-6932.

SAFFARIAN, S., COCUCCI, E. & KIRCHHAUSEN, T. 2009. Distinct dynamics of endocytic clathrin-coated pits and coated plaques. *PLoS Biol,* 7**,** e1000191.

SCHEELE, U., ALVES, R., FRANK, R., DUWEL, M., KALTHOFF, C. & UNGEWICKELL, E. 2003. Molecular and functional characterization of clathrin- and AP-2-binding determinants within a disordered domain of auxilin. *Journal of Biological Chemistry,* 278**,** 25357-25368.

SCHEELE, U., KALTHOFF, C. & UNGEWICKELL, E. 2001. Multiple interactions of auxilin 1 with clathrin and the AP-2 adaptor complex. *J Biol Chem,* 276**,** 36131-8.

SCHEERER, P. & SOMMER, M. E. 2017. Structural mechanism of arrestin activation. *Curr Opin Struct Biol,* 45**,** 160-169.

SCHMID, E. M., FORD, M. G., BURTEY, A., PRAEFCKE, G. J., PEAK-CHEW, S. Y., MILLS, I. G., BENMERAH, A. & MCMAHON, H. T. 2006. Role of the AP2 beta-appendage hub in recruiting partners for clathrin-coated vesicle assembly. *PLoS Biol,* 4**,** e262.

SCOTTI, P. 1977. End-point dilution and plaque assay methods for titration of cricket paralysis virus in cultured Drosophila cells. *J Gen Virol,* 35**,** 393-396.

SHENOY, S. K. & LEFKOWITZ, R. J. 2011. beta-Arrestin-mediated receptor trafficking and signal transduction. *Trends Pharmacol Sci,* 32**,** 521-33.

SHIH, W., GALLUSSER, A. & KIRCHHAUSEN, T. 1995. A clathrin-binding site in the hinge of the beta 2 chain of mammalian AP-2 complexes. *Journal of Biological Chemistry,* 270**,** 31083-31090.

SHUKLA, A. K., MANGLIK, A., KRUSE, A. C., XIAO, K., REIS, R. I., TSENG, W. C., STAUS, D. P., HILGER, D., UYSAL, S., HUANG, L. Y., PADUCH, M., TRIPATHI-SHUKLA, P., KOIDE, A., KOIDE, S., WEIS, W. I., KOSSIAKOFF, A. A., KOBILKA, B. K. & LEFKOWITZ, R. J. 2013. Structure of active beta-arrestin-1 bound to a G-protein-coupled receptor phosphopeptide. *Nature,* 497**,** 137-41.

SHUKLA, A. K., WESTFIELD, G. H., XIAO, K., REIS, R. I., HUANG, L. Y., TRIPATHI-SHUKLA, P., QIAN, J., LI, S., BLANC, A., OLESKIE, A. N.,

DOSEY, A. M., SU, M., LIANG, C. R., GU, L. L., SHAN, J. M., CHEN, X., HANNA, R., CHOI, M., YAO, X. J., KLINK, B. U., KAHSAI, A. W., SIDHU, S. S., KOIDE, S., PENCZEK, P. A., KOSSIAKOFF, A. A., JR, V. L. W., KOBILKA, B. K., SKINIOTIS, G. & LEFKOWITZ, R. J. 2014. Visualization of arrestin recruitment by a G-protein-coupled receptor. *Nature,* 512**,** 218-222.

SKRUZNY, M., DESFOSSES, A., PRINZ, S., DODONOVA, S. O., GIERAS, A., UETRECHT, C., JAKOBI, A. J., ABELLA, M., HAGEN, W. J., SCHULZ, J., MEIJERS, R., RYBIN, V., BRIGGS, J. A., SACHSE, C. & KAKSONEN, M. 2015. An organized co-assembly of clathrin adaptors is essential for endocytosis. *Dev Cell,* 33**,** 150-62.

SMITH, C. J., DAFFORN, T. R., KENT, H., SIMS, C. A., KHUBCHANDANI-ASWANI, K., ZHANG, L., SAIBIL, H. R. & PEARSE, B. M. F. 2004. Location of Auxilin Within a Clathrin Cage. *Journal of Molecular Biology,* 336**,** 461-471.

SMITH, C. J., GRIGORIEFF, N. & PEARSE, B. M. F. 1998. Clathrin coats at 21 angstrom resolution: a cellular assembly designed to recycle multiple membrane receptors. . *Embo Journal,* 17.

SMITH, C. M. & CHIRCOP, M. 2012. Clathrin-Mediated Endocytic Proteins are Involved in Regulating Mitotic Progression and Completion. *Traffic,* 13**,** 1628- 1641.

SMITH, J. S. & RAJAGOPAL, S. 2016. The beta-Arrestins: Multifunctional Regulators of G Protein-coupled Receptors. *J Biol Chem,* 291**,** 8969-77.

SMITH, S. M., BAKER, M., HALEBIAN, M. & SMITH, C. J. 2017. Weak Molecular Interactions Implicated in Clathrin-Mediated Endocytosis. *In:* WARWICK, U. O. (ed.). Frontiers: .

SNOPOK, B., YURCHENKO, M., SZEKELY, L., KLEIN, G. & KASHUBA, E. 2006. SPR-based immunocapture approach to creating an interfacial sensing architecture: mapping of the MRS18-2 binding site on retinoblastoma protein. *Anal Bioanal Chem,* 386**,** 2063–2073.

SOUSA, R., LIAO, H. S., CUELLAR, J., JIN, S., VALPUESTA, J. M., JIN, A. J. & LAFER, E. M. 2016. Clathrin-coat disassembly illuminates the mechanisms of Hsp70 force generation. *Nat Struct Mol Biol,* 23**,** 821-9.

STEFAN, C. J., AUDHYA, A. & EMR, S. D. 2002. The yeast synaptojanin-like proteins control the cellular distribution of phosphatidylinositol (4,5)-bisphosphate. *Molecular Biology of the Cell,* 13**,** 542-557.

STEFAN, C. J., PADILLA, S. M., AUDHYA, A. & EMR, S. D. 2005. The phosphoinositide phosphatase Sjl2 is recruited to cortical actin patches in the control of vesicle formation and fission during endocytosis. *Molecular and Cellular Biology,* 25**,** 2910-2923.

SULEYMANOVA, N., CRUDDEN, C., SHIBANO, T., WORRALL, C., OPREA, I., TICA, A., CALIN, G. A., GIRNITA, A. & GIRNITA, L. 2017. Functional antagonism of beta-arrestin isoforms balance IGF-1R expression and signalling with distinct cancer-related biological outcomes. *Oncogene***,** 1-11.

TAYLOR, M. J., PERRAIS, D. & MERRIFIELD, C. J. 2011. A High Precision Survey of the Molecular Dynamics of Mammalian Clathrin-Mediated Endocytosis. *Plos Biology,* 9.

TER HAAR, E., HARRISON, S. C. & KIRCHHAUSEN, T. 2000. Peptide-in-groove interactions link target proteins to the β-propeller of clathrin. *Proceedings of the National Academy of Sciences,* 97**,** 1096-1100.

TER HAAR, E., MUSACCHIO, A., HARRISON, S. C. & KIRCHHAUSEN, T. 1998. Atomic structure of clathrin: A beta propeller terminal domain joins an alpha zigzag linker. *Cell,* 95**,** 563-573.

TERRILLON, S., BARBERIS, C. & BOUVIER, M. 2004. Heterodimerization of V1a and V2 vasopressin receptors determines the interaction with beta-arrestin and their trafficking patterns. *Proc Natl Acad Sci U S A,* 101**,** 1548-53.

THOMSEN, A. R., PLOUFFE, B., CAHILL, T. J., 3RD, SHUKLA, A. K., TARRASCH, J. T., DOSEY, A. M., KAHSAI, A. W., STRACHAN, R. T., PANI, B., MAHONEY, J. P., HUANG, L., BRETON, B.,

HEYDENREICH, F. M., SUNAHARA, R. K., SKINIOTIS, G., BOUVIER, M. & LEFKOWITZ, R. J. 2016. GPCR-G Protein-beta-Arrestin Super-Complex Mediates Sustained G Protein Signaling. *Cell,* 166**,** 907-19.

TIAN, X., KANG, D. S. & BENOVIC, J. L. 2014. beta-arrestins and G protein-coupled receptor trafficking. *Handb Exp Pharmacol,* 219**,** 173-86.

TRAUB, L. M. 2005. Common principles in clathrin-mediated sorting at the Golgi and the plasma membrane. *Biochim Biophys Acta,* 1744**,** 415-37.

TRAUB, L. M. 2009. Tickets to ride: selecting cargo for clathrin-regulated internalization. *Nat Rev Mol Cell Biol,* 10**,** 583-96.

TRAUB, L. M. 2011. Regarding the amazing choreography of clathrin coats. *PLoS Biol,* 9**,** e1001037.

TRAUB, L. M. & BONIFACINO, J. S. 2013. Cargo recognition in clathrin-mediated endocytosis. *Cold Spring Harb Perspect Biol,* 5**,** a016790.

UMEDA, A., MEYERHOLZ, A. & UNGEWICKELL, E. 2000. Identification of the universal cofactor (auxilin 2) in clathrin coat dissociation. *European Journal of Cell Biology,,* 79**,** 336-342.

UNGEWICKELL, E. & BRANTON, D. 1981. Assembly units of clathrin coats. *Nature,* 289**,** 420-422.

UNGEWICKELL, E., UNGEWICKELL, H., HOLSTEIN, S. E. H., LINDNER, R., PRASAD, K., BAROUCH, W., MARTIN, B., GREENE, L. E. & EISENBERG, E. 1995. Role of auxilin in uncoating clathrin-coated vesicles. *Nature,* 378**,** 632-635.

UNGEWICKELL, E. J. & HINRICHSEN, L. 2007. Endocytosis: clathrin-mediated membrane budding. *Curr Opin Cell Biol. ,* 19**,** 417-25.

VAN DER MERWE, P. A. 2001. Surface Plasmon Resonance. *In:* HARDING, E. E. & CHOWDHRY, B. Z. (eds.) *Protein-Ligand Interaction: Hydrodynamics and Calorimetry.*

VANLANDINGHAM, P. A., FORE, T. R., CHASTAIN, L. R., ROYER, S. M., BAO, H., REIST, N. E. & ZHANG, B. 2013. Epsin 1 Promotes

Synaptic Growth by Enhancing BMP Signal Levels in Motoneuron Nuclei. *PLoS One,* 8**,** e65997.

VASSILOPOULOS, S., ESK, C., HOSHINO, S., FUNKE, B. H., CHEN, C. Y., PLOCIK, A. M., WRIGHT, W. E., KUCHERLAPATI, R. & BRODSKY, F. M. 2009. A Role for the CHC22 Clathrin Heavy-Chain Isoform in Human Glucose Metabolism. *Science,* 324**,** 1192-1196.

VERSTREKEN, P., KOH, T. W., SCHULZE, K. L., ZHAI, R. G., HIESINGER, P. R., ZHOU, Y., MEHTA, S. Q., CAO, Y., ROOS, J. & BELLEN, H. J. 2003. Synaptojanin is recruited by Endophilin to promote synaptic vesicle uncoating. *Neuron,* 40**,** 733-748.

VIGERS, G. P. A., CROWTHER RA & PEARSE, B. M. F. 1986. Three-dimensional structure of clathrin cages in ice. *The EMBO Journal,* 5**,** 529–534.

WAELTER, S., SCHERZINGER, E., HASENBANK, R., NORDHOFF, E., LURZ, R., GOEHLER, H., GAUSS, C., SA THASIV AM, K., BA TES, G. P., LEHRACH, H. & WANKER, E. E. 2001. The huntingtin interacting protein HIP1 is a clathrin and alpha-adaptin-binding protein involved in receptor- mediated endocytosis. *Human Molecular Genetics,* 10**,** 1807-1817.

WHALEN, E. J., RAJAGOPAL, S. & LEFKOWITZ, R. J. 2011. Therapeutic potential of beta-arrestin- and G protein-biased agonists. *Trends Mol Med,* 17**,** 126-39.

WHEATLEY, M., CHARLTON, J., JAMSHAD, M., ROUTLEDGE, S. J., BAILEY, S., LA-BORDE, P. J., AZAM, M. T., LOGAN, R. T., BILL, R. M., DAFFORN, T. R. & POYNER, D. R. 2016. GPCR-styrene maleic acid lipid particles (GPCR-SMALPs): their nature and potential. *Biochem Soc Trans,* 44**,** 619-23.

WILBUR, J. D., CHEN, C. Y., MANALO, V., HWANG, P. K., FLETTERICK, R. J. & BRODSKY, F. M. 2008. Actin Binding by Hip1 (Huntingtin-interacting Protein 1) and Hip1R (Hip1-related Protein) Is Regulated by Clathrin Light Chain. *Journal of Biological Chemistry,* 283**,** 32870-32879.

WILBUR, J. D., HWANG, P. K., YBE, J. A., LANE, M., SELLERS, B. D., JACOBSON, M. P., FLETTERICK, R. J. & BRODSKY, F. M. 2010. Conformation switching of clathrin light chain regulates clathrin lattice assembly. *Dev Cell,* 18**,** 841-8.

WILLOX, A. K. & ROYLE, S. J. 2012. Functional analysis of interaction sites on the N-terminal domain of clathrin heavy chain. *Traffic,* 13**,** 70-81.

WINKLER, F. & STANLEY, K. K. 1983. Clathrin heavy chain, light chain interactions. *The EMBO Journal,* 2**,** 1393–1400.

WU, F. & YAO, P. J. 2009. Clathrin-mediated endocytosis and Alzheimer's disease: an update. *Ageing Res Rev,* 8**,** 147-9.

XING, Y., BOCKING, T., WOLF, M., GRIGORIEFF, N., KIRCHHAUSEN, T. & HARRISON, S. C. 2010. Structure of clathrin coat with bound Hsc70 and auxilin: mechanism of Hsc70-facilitated disassembly. *EMBO J,* 29**,** 655-65.

YANG, F., YU, X., LIU, C., QU, C. X., GONG, Z., LIU, H. D., LI, F. H., WANG, H. M., HE, D. F., YI, F., SONG, C., TIAN, C. L., XIAO, K. H., WANG, J. Y. & SUN, J. P. 2015. Phospho-selective mechanisms of arrestin conformations and functions revealed by unnatural amino acid incorporation and (19)F-NMR. *Nat Commun,* 6**,** 8202.

YBE, J. A., BRODSKY, F. M., HOFMANN, K., LIN, K., LIU, S. H., CHEN, L., EARNEST, T. N., FLETTERICK, R. J. & HWANG, P. K. 1999. Clathrin self- assembly is mediated by a tandemly repeated superhelix. *Nature,* 399**,** 371- 375.

YBE, J. A., CLEGG, M. E., ILLINGWORTH, M., GONZALEZ, C. & NIU, Q. 2009. Two Distantly Spaced Basic Patches in the Flexible Domain of Huntingtin-Interacting Protein 1 (HIP1) Are Essential for the Binding of Clathrin Light Chain. *Res Lett Biochem,* 2009**,** 256124.

YBE, J. A., GREENE, B., LIU, S. H., PLEY, U., PARHAM, P. & BRODSKY, F. M. 1998. Clathrin self-assembly is regulated by three light-chain residues controlling the formation of critical salt bridges. *Embo Journal,* 17**,** 1297- 1303.

YBE, J. A., MISHRA, S., HELMS, S. & NIX, J. 2007. Crystal structure at 2.8 A of the DLLRKN-containing coiled-coil domain of huntingtin-interacting protein 1 (HIP1) reveals a surface suitable for clathrin light chain binding. *J Mol Biol,* 367**,** 8-15.

YOUNG, A., STOILOVA-MCPHIE, S., ROTHNIE, A., VALLIS, Y., HARVEY-SMITH, P., RANSON, N., KENT, H., BRODSKY, F. M., PEARSE, B. M., ROSEMAN, A. & SMITH, C. J. 2013. Hsc70-induced changes in clathrin-auxilin cage structure suggest a role for clathrin light chains in cage disassembly. *Traffic,* 14**,** 987-96.

ZHANG, C. X., ENGQVIST-GOLDSTEIN, A. E., CARRENO, S., OWEN, D. J., SMYTHE, E. & DRUBIN, D. G. 2005. Multiple roles for cyclin G-associated kinase in clathrin-mediated sorting events. *Traffic,* 6**,** 1103-13.

ZHUO, Y., CANO, K. E., WANG, L., ILANGOVAN, U., HINCK, A. P., SOUSA, R. & LAFER, E. M. 2015. Nuclear Magnetic Resonance Structural Mapping Reveals Promiscuous Interactions between Clathrin-Box Motif Sequences and the N-Terminal Domain of the Clathrin Heavy Chain. *Biochemistry,* 54**,** 2571-80.